NASA/CP—2001-211164

Twentieth International Microgravity Measurements Group Meeting

December 2001

The NASA STI Program Office . . . in Profile

Since its founding, NASA has been dedicated to the advancement of aeronautics and space science. The NASA Scientific and Technical Information (STI) Program Office plays a key part in helping NASA maintain this important role.

The NASA STI Program Office is operated by Langley Research Center, the Lead Center for NASA's scientific and technical information. The NASA STI Program Office provides access to the NASA STI Database, the largest collection of aeronautical and space science STI in the world. The Program Office is also NASA's institutional mechanism for disseminating the results of its research and development activities. These results are published by NASA in the NASA STI Report Series, which includes the following report types:

- TECHNICAL PUBLICATION. Reports of completed research or a major significant phase of research that present the results of NASA programs and include extensive data or theoretical analysis. Includes compilations of significant scientific and technical data and information deemed to be of continuing reference value. NASA's counterpart of peer-reviewed formal professional papers but has less stringent limitations on manuscript length and extent of graphic presentations.

- TECHNICAL MEMORANDUM. Scientific and technical findings that are preliminary or of specialized interest, e.g., quick release reports, working papers, and bibliographies that contain minimal annotation. Does not contain extensive analysis.

- CONTRACTOR REPORT. Scientific and technical findings by NASA-sponsored contractors and grantees.

- CONFERENCE PUBLICATION. Collected papers from scientific and technical conferences, symposia, seminars, or other meetings sponsored or cosponsored by NASA.

- SPECIAL PUBLICATION. Scientific, technical, or historical information from NASA programs, projects, and missions, often concerned with subjects having substantial public interest.

- TECHNICAL TRANSLATION. English-language translations of foreign scientific and technical material pertinent to NASA's mission.

Specialized services that complement the STI Program Office's diverse offerings include creating custom thesauri, building customized data bases, organizing and publishing research results . . . even providing videos.

For more information about the NASA STI Program Office, see the following:

- Access the NASA STI Program Home Page at ***http://www.sti.nasa.gov***

- E-mail your question via the Internet to help@sti.nasa.gov

- Fax your question to the NASA Access Help Desk at 301–621–0134

- Telephone the NASA Access Help Desk at 301–621–0390

- Write to:
  NASA Access Help Desk
  NASA Center for AeroSpace Information
  7121 Standard Drive
  Hanover, MD 21076

NASA/CP—2001-211164

Twentieth International Microgravity Measurements Group Meeting

Proceedings of a conference sponsored by the Microgravity Science Division,
NASA Glenn Research Center
and held at the Sheraton Airport Hotel, Cleveland, Ohio
August 7–9, 2001

National Aeronautics and
Space Administration

Glenn Research Center

December 2001

Available from

NASA Center for Aerospace Information
7121 Standard Drive
Hanover, MD 21076

National Technical Information Service
5285 Port Royal Road
Springfield, VA 22100

Available electronically at http://gltrs.grc.nasa.gov/GLTRS

Preface

The International Microgravity Measurements Group (MGMG) annual meetings have been held since 1988 to provide a forum for an exchange of information and ideas about various aspects of microgravity acceleration research in international microgravity research programs. These meetings are sponsored by the Principal Investigator Microgravity Services (PIMS) project at the NASA Glenn Research Center for the NASA Microgravity Research Program and cooperating international microgravity research programs.

The 20th MGMG meeting was held 7–9 August 2001 at the Hilton Garden Inn Hotel in Cleveland, Ohio. The 35 attendees represented NASA and other space agencies, universities, and commercial companies; eight of the attendees were international representatives from Canada, Germany, Italy, Japan, and Russia.

Seventeen presentations were made on a variety of microgravity environment topics including the International Space Station (ISS), acceleration measurement and analysis results, science effects from microgravity accelerations, vibration isolation, free flyer satellites, ground testing, and microgravity outreach. Two working sessions were included in which a demonstration of ISS acceleration data processing and analyses were performed with audience participation.

One paper was submitted by one of the Russian authors but was not presented at the meeting. The paper is an analytical derivation of the Russian segment quasi-steady acceleration environment based on vehicle orbit data. This paper is included in the minutes.

The 21st MGMG annual meeting will most likely be held in mid-year 2002 at a site not yet determined. Bjarni Tryggvason has offered that the Canadian Space Agency could host a future MGMG meeting in either Montreal or in Toronto.

The regular topics of sensors, accelerometer systems, analysis results, vibration isolation, microgravity environment, and science effects will continue to be included.

Table of Contents

Tuesday, August 7, 2001

start	*end*	*Title*	*Presenter*	*Paper #*
9:00 AM	9:15 AM	Welcoming remarks & logistics	R. DeLombard (NASA GRC)	
Session A		**PROGRAMMATICS**		
9:15 AM	9:25 AM	Microgravity Environment Program	David Francisco (NASA GRC)	1
9:25 AM	10:10 AM	Overview of Microgravity Environment Interpretation Tutorial (MEIT)	Kevin McPherson (NASA GRC)	2
10:10 AM	10:25 AM	Introduction of MGMG attendees		
10:25 AM	10:50 AM	BREAK		
10:50 AM	11:30 AM	NASDA's Activities for "Microgravity" in JEM	Toshitami Ikeda (NASDA)	3
11:30 AM	12:45 PM	LUNCH		
Session B		**ISS ENVIRONMENT - PART 1**		
12:49 PM	1:30 PM	Payload Microgravity Verification	Fred Henderson (TBE/Boeing @ JSC)	4
1:30 PM	1:44 PM	BREAK		
1:44 PM	2:00 PM	SSUAS microgravity status chart	Craig Schafer (SAIC @ JSC)	5
2:00 PM	4:30 PM	ISS Vibratory Acceleration Environment	Ken Hrovat (ZIN Technologies @ GRC)	6

Wednesday, August 8 2001

start	*end*	*Title*	*Presenter*	*Paper #*
Session B		**ISS ENVIRONMENT - PART 1 (con'td)**		
9:05a	9:45 AM	Space Station Multi-Rigid Body Simulation (SSMRBS) Runs Comparison to On-Orbit MAMS Data	Michael R. Laible (Boeing ISS)	7
Session C		**FREE-FLYER ENVIRONMENT**		
9:45 AM	10:10 AM	Features of space microacceleration measurement program SINUS for FOTON type satellites	Oleg Mumin (CSRI Electropribor, St. Petersburg, Russia) & Valentin Agarkov (CSDB, Samara, Russia)	8
10:10 AM	10:30 AM	BREAK		
Session D		**ISS ENVIRONMENT - PART 3**		
10:30 AM	10:56 AM	An instrument for measuring the quasi steady acceleration vector on board of the ISS	Giulio Poletti (University of Milan, Milan, Italy)	9
10:58 AM	11:30 AM	Initial ARIS Performance Assessment for the Fluids & Combustion Facility (FCF)	Marcus Just (ZIN Technologies @ GRC)	10
11:30 AM	1:05 PM	LUNCH		
1:05 PM	1:40 PM	Light Microscopy Module: An Optical Payload in a Microgravity Environment	Tony Haecker (Logicon @ GRC)	11
1:40 PM	1:50 PM	BREAK		
1:50 PM	4:00 PM	ISS Quasi-Steady Acceleration Environment	Eric Kelly (ZIN Technologies @ GRC)	12

Thursday, August 9, 2001

start	end	Title	Presenter	Paper #
Session E		**OUTREACH**		
9:02 AM	9:32 AM	Demonstration of microgravity outreach devices	Richard DeLombard (NASA GRC)	13
Session F		**GROUND TESTING**		
9:32 AM	10:05 AM	Microgravity Emissions Laboratory (MEL) Testing of the Experiment of Physics of Colloids in Space (EXPPCS)	Anne McNelis (NASA GRC)	14
10:05 AM	10:20 AM	BREAK		
10:20 AM	11:10 AM	Working Session for AAA Fan Retesting	Tom Goodnight, Mark McNelis (NASA GRC), Roy Christoffersen (SAIC @ JSC)	15
11:10 AM	11:25 AM	IBC in Microgravity Environment	Scott Spearing (Morgan Research @ MSFC))	16
11:25 AM	11:45 AM	Microgravity Vibration Isolation Systems that CSA is developing for ISS	Bjarni Tryggvason (CSA)	17
MEETING SUMMARY				
11:45 AM	12:00 PM	Summary discussion of MGMG #20 and plans for MGMG #21	Richard DeLombard (NASA GRC)	
PAPER SUBMITTED BUT NOT PRESENTED				
		Preliminary review of microgravity environment in Service Module of ISS	E.V.Babkin, M.Yu.Belyaev, A.Yu.Kaleri, V.M.Stazhkov, O.N.Volkov (Rocket and Space Corporation Energiya) and V.V.Sazonov (Keldysh Institute of Applied Mathematics, RAS)	18

Microgravity Environment Program

David Francisco
NASA GRC
Cleveland, Ohio

The Microgravity Environment Program is managed by the Microgravity Science Division at the NASA Glenn Research Center in Cleveland, Ohio. The program which is funded by Code U and M at headquarters includes the development and operations of acceleration measurement systems, and the analysis, interpretation, and correlation of the data. The program also supports the development of microgravity verification facilities for the ISS Fluids and Combustion Facility (FCF) along with support for the ARIS integration activities for FCF.

The program operated the SAMS, SAMS-FF, and OARE instruments on the Shuttle from 1991 through 1999. SAMS and SAMS-FF supported operations on the KC-135 and on sounding rockets. A SAMS unit supported the NASA-Mir Science program from 1994 through 1998.

Presently, SAMS and MAMS instruments are on the ISS to support the early science experiments as well as to characterize the microgravity environment of ISS as it is being assembled on-orbit. Data downlinked from the ISS is automatically processed and disseminated to users via the World Wide Web.

NASA/CP—2001-211164

Glenn Research Center

Microgravity Science Division

Space Directorate

20th Microgravity Measurement Group Meeting

Microgravity Environment Program

Dave Francisco

NASA Glenn Research Center

(216) 433-2653

david.francisco@grc.nasa.gov

Microgravity Science Division
Acceleration Measurement Program
Glenn Research Center

SAMS

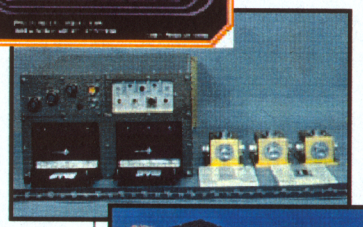

OARE
MMAP

Microgravity Emission Lab

PIMS
μg
PRINCIPAL INVESTIGATOR MICROGRAVITY SERVICES

Science Supported

- Combustion
- Fluid Physics
- Materials
- Fundamental Physics
- Vehicle Dynamics
- Biotechnology

SAMS - FF

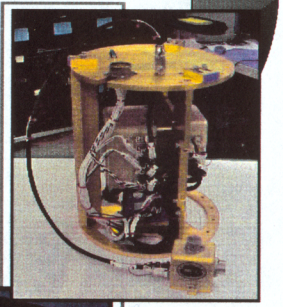

SAMS-II

Glenn Research Center

Microgravity Science Division

Space Directorate

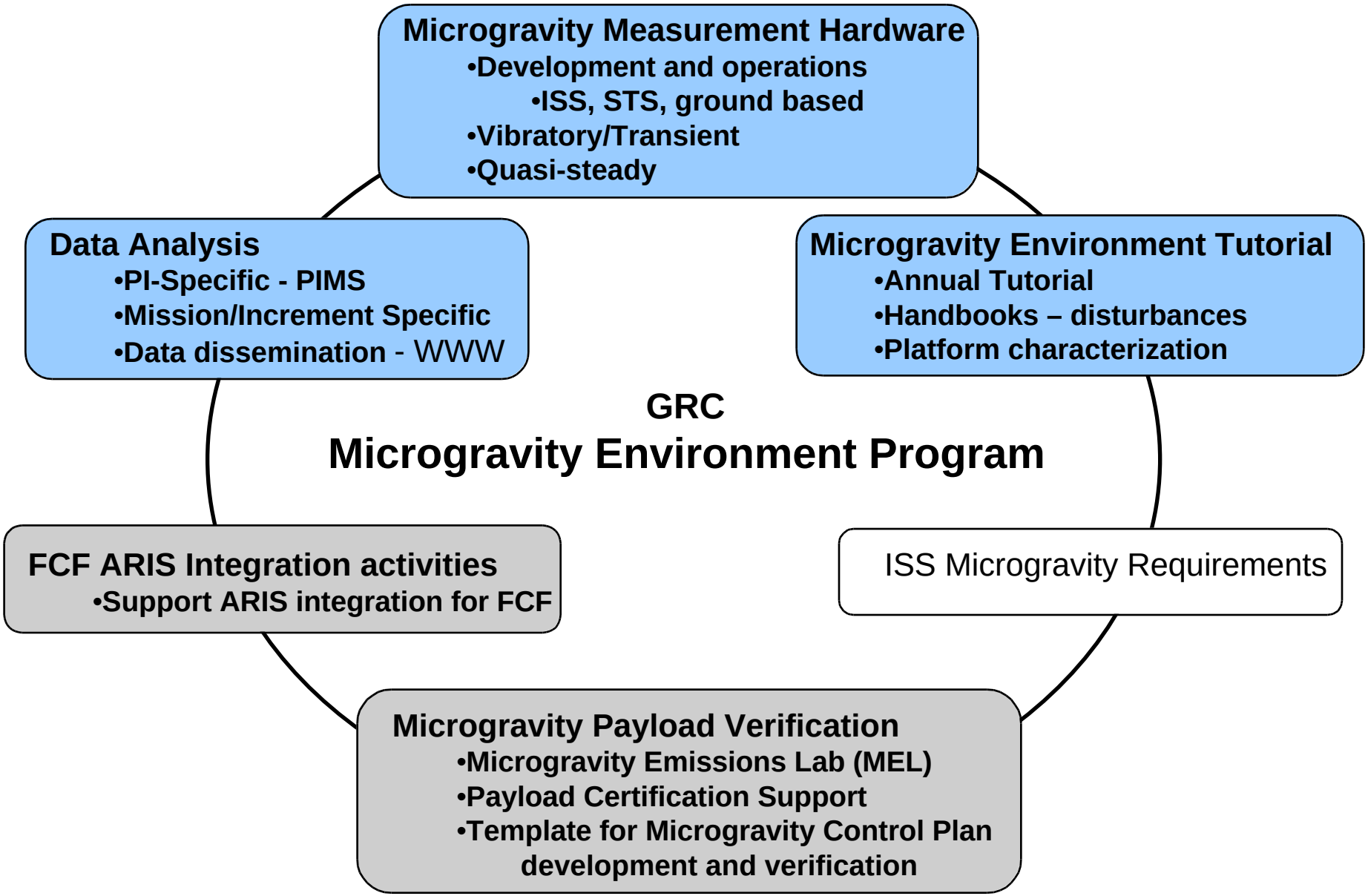

Microgravity Environment Program

•**Funding:** From the Office of Biological and Physical Research, NASA Code U and ISS Code M

•**History:** GRC has developed, integrated and flown instruments on 20+ missions with the SAMS, OARE, and SAMS-FF since 1991. Analyzed and distributed data from these missions.

•Instruments have flown on the Shuttle, MIR, sounding rockets, KC-135 and in ground based facilities (drop towers).

•**Present Status:** Operating the SAMS-II and MAMS instruments on ISS since June 2001 (launched on 6A)
•Quick look report published and Increment 2 report complete

•**Supporting:** PCS, ARIS-ICE and PIMS

NASA/CP—2001-211164

NASA/CP—2001-211164

Contacts List:

PIMS
Kevin McPherson
(216) 433-6182
Kevin.M.McPherson@grc.nasa.gov

SAMS Hardware
Bill Foster
(216) 433-2368
William.M.Foster@grc.nasa.gov

Science/MEIT
Kenol Jules
(216) 977-7016
Kenol.Jules@grc.nasa.gov

Science/Requirements
Richard DeLombard
(216) 433-5285
Richard.DeLombard@grc.nasa.gov

ARIS Integration
Kathy Shepherd
(216) 433-3665
Kathleen.A.Shepherd@grc.nasa.gov

Microgravity Testing
Anne McNelis
(216) 433-8880
Anne.M.McNelis@grc.nasa.gov

Overview of Microgravity Environment Interpretation Tutorial (MEIT)

Kevin McPherson
NASA GRC
Cleveland, Ohio

The Microgravity Environment Interpretation Tutorial (MEIT) conveys significant features of the microgravity acceleration environment to the microgravity Principal Investigator teams and other interested parties.

Typical contents include

* Acceleration Measurement Systems
* Basics of Signal Processing
* Analysis Techniques for Quasi-Steady Data
* Analysis Techniques for Vibratory Data
* Microgravity Environment of Non-orbital Platforms
* Highlights of the Microgravity Environment of the Orbiters, Mir, and ISS
* Implications for Microgravity Experimenters
* ISS Acceleration Environment Predictions
* PIMS Space Station Operations
* Vibration Isolation Techniques
* Predicting Residual Acceleration Effects on Space Experiments
* Impact of the Microgravity Environment on Experiments

NASA/CP—2001-211164

Overview of Microgravity Environment Interpretation Tutorial

Kenol Jules
PIMS Project Scientist
NASA Glenn Research Center

Microgravity Measurements Group Meeting #20

August 7th, 2001

PIMS' Responsibilities are:

- To assist PI teams in understanding different aspects of measuring and interpreting the microgravity environment of various platforms and ground-based facilities.

- To provide interpretation of the microgravity environment and perform detailed analyses for general and specialized characterization.

- To educate PIs, Project scientists and associates about the microgravity environment through the Microgravity Environment Interpretation Tutorial (MEIT) and the MicroGravity Measurements Group (MGMG) gatherings.

- To acquire and archive acceleration data for accelerometer systems.

Principal Investigator Microgravity Services (PIMS)

- PIMS performs the project scientist role for the accelerometer instruments
  - PIMS works with the science experiment principal investigators, project scientists, and other program participants to assist in the understanding and use of the acceleration data and information
  - PIMS products include general and specific analyses, vehicle characterization, and mission summary reports
  - PIMS conducts the Microgravity Measurements Group (MGMG) meetings to foster interchange of data and information within the microgravity environment community and to the microgravity science community
  - PIMS conducts the Microgravity Environment & Interpretation Tutorial (MEIT) to convey significant features of the microgravity acceleration environment to the microgravity Principal Investigator teams and other interested parties

Principal Investigator Microgravity Services (PIMS)

Support NASA's Microgravity Research Program Principal Investigators (PIs) by providing acceleration data processing, analysis, and interpretation for a variety of reduced gravity carriers and ground-based facilities, such as:

- **Space Shuttle**
- **Parabolic Flight Aircraft (KC-135)**
- **Sounding Rockets**
- **Drop Towers**
- **ISS**
- **Ground Testing**
- **Microgravity Emission Lab (MEL)**

Principal Investigator Microgravity Services (PIMS)

Analyze acceleration data from a number of acceleration measurement systems, such as:

- **Space Acceleration Measurement System (SAMS)**
- **Space Acceleration Measurement System for Free-Flyers (SAMS-FF)**
- **Microgravity Acceleration Measurement System (MAMS)**
  - **MAMS-0SS**
  - **MAMS-HiRAP**

Principal Investigator Microgravity Services (PIMS)

Support the following areas:

- **Biotechnology**
- **Combustion Science**
- **Fluid Physics**
- **Materials Science**
- **Fundamental Physics**
- **Astronaut Office**
- **International Partners**
- **Vehicle Dynamics**
- **Payload Developers**

Overview of Microgravity Environment Interpretation Tutorial

PIMS Functions During Experiment Life Cycle

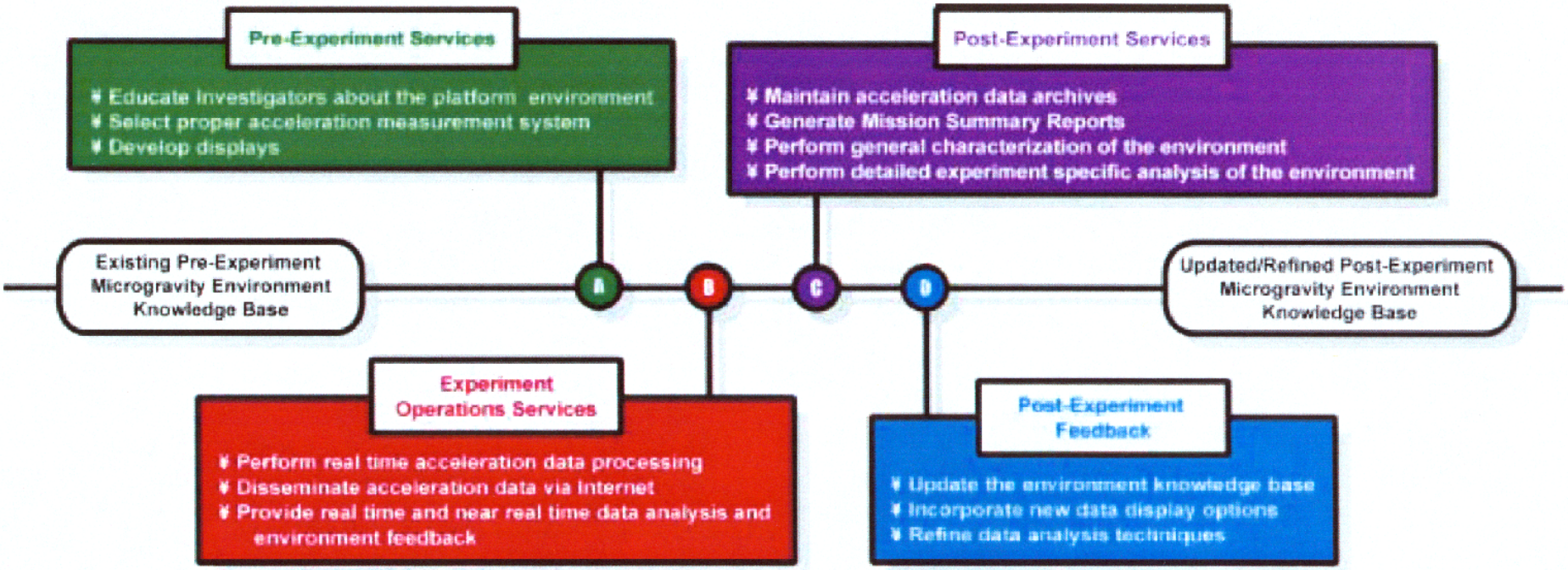

Overview of Microgravity Environment Interpretation Tutorial

MEIT 2001 Content

- Acceleration Measurement Systems
- Basics of Signal Processing
- Analysis Techniques for Quasi-Steady Data
- Analysis Techniques for Vibratory Data
- Microgravity Environment of Non-Orbital Platforms
- Highlights of the Microgravity Environment of the Orbiters, Mir, and ISS
- Implications for Microgravity Experimenters
- ISS Acceleration Environment Predictions
- PIMS Space Station Operations
- Vibration Isolation Techniques
- Predicting Residual Acceleration Effects on Space Experiments
- Impact of the Microgravity Environment on Experiments

PIMS' support to PIs includes the following:

- Receive, Process, Analyze, and Interpret Accelerometer Data to Characterize the Microgravity Environment of Various Platforms for the Investigative Teams.

ANALYSIS SUPPORT:

- Monitor the Microgravity Environment in Real Time to Support Their Operation (when needed)
- Provide Real Time Displays
- Provide Near Real Time Support
- Provide Post Mission Support
- Provide a Near Real Time ISS Microgravity Environment Monitoring System (ISS MEMS) Via WWW

PIMS' support to PIs includes the following:

DATA SUPPORT:

- Provide easy access to plots of acceleration data via WWW
- Provide customized format plots to PI teams based on pre-mission inputs
- Publish Summary Report of Mission Acceleration Measurements

EDUCATIONAL:

- Annual Microgravity Environment Interpretation Tutorial (MEIT)
- Annual MicroGravity Measurements Group (MGMG) gatherings

PIMS Plotted Data Options

Display Format	Regime(s)	Notes
Acceleration versus Time	Transient, Quasi-Steady, Vibratory	• precise accounting of measured data with respect to time; best temporal resolution
Interval Min/Max Acceleration versus Time	Vibratory, Quasi-Steady	• displays upper and lower bounds of peak-to-peak excursions of measured data • good display approximation for time histories on output devices with resolution insufficient to display all data in time frame of interest
Interval Average Acceleration versus Time	Vibratory, Quasi-Steady	• provides a measure of net acceleration of duration greater than or equal to interval parameter
Interval RMS Acceleration versus Time	Vibratory	• provides a measure of peak amplitude for pure sinusoids
Trimmed Mean Filtered Acceleration versus Time	Quasi-Steady	• removes infrequent, large amplitude outlier data
Quasi-Steady Mapped Acceleration versus Time	Quasi-Steady	• use rigid body assumption and vehicle rates and angles to compute acceleration at any point in the vehicle
Quasi-Steady Three-Dimensional Histogram (QTH)	Quasi-Steady	• summarize acceleration magnitude and direction for a long period of time • indication of acceleration "center-of-time" via projections onto three orthogonal planes

PIMS Plot Options

Display Format	Regime(s)	Notes
Power Spectral Density (PSD) versus Frequency	Vibratory	• displays distribution of power with respect to frequency
Spectrogram (PSD versus Frequency versus Time)	Vibratory	• displays power spectral density variations with time • identify structure and boundaries in time and frequency
Cumulative RMS Acceleration versus Frequency	Vibratory	• quantifies RMS contribution at and below a given frequency
Frequency Band(s) RMS Acceleration versus Time	Vibratory	• quantify RMS contribution over selected frequency band(s) as a function of time
RMS Acceleration versus One-Third Frequency Bands	Vibratory	• quantify RMS contribution over proportional frequency bands • compare measured data to ISS vibratory requirements
Principal Component Spectral Analysis (PCSA)	Vibratory	• summarize magnitude and frequency excursions for key spectral contributors over a long period of time • results typically have finer frequency resolution and high PSD magnitude resolution relative to a spectrogram at the expense of poor temporal resolution

Overview of Microgravity Environment Interpretation Tutorial

Example Figures

- Figure 1 – Nominal Environment Plot (STS-78)
- Figure 2 - Principal Component Spectral Analysis (STS-78)
- Figure 3 – Flight 7A Docking (STS-104)
- Figure 4 – Progress Docking Acceleration vs. Time (ISS)
- Figure 5 – EXPPCS Mixing Operations Spectrogram (ISS)
- Figure 6 - EXPPCS Mixing Operations Minimum/Maximum Acceleration vs. Time (ISS)
- Figure 7 – Quasi-Steady Three Dimensional Histogram During Crew Sleep (ISS)
- Figure 8 - Quasi-Steady Three Dimensional Histogram During Crew Wake Periods (ISS)
- Figure 9 – Cabin Depressurization (STS-87)
- Figure 10 - OARE vs. SOFBALL Radiometry Data (STS-94)

Principal Investigator Microgravity Services

Acceleration Measurement WWW links

- Microgravity Science Division at NASA Glenn Research Center
  - http://microgravity.grc.nasa.gov
- NASA Glenn Acceleration Measurement Program
  - http://microgravity.grc.nasa.gov/MSD/MSD_htmls/acceleration.html
- Principal Investigator Microgravity Services Home Page
  - http://microgravity.grc.nasa.gov/MSD/MSD_htmls/PIMS.html

Microgravity Environment References

- Microgravity Environment Description Handbook TM
  - Compilation of major microgravity environment disturbances, their sources, and their effects as measured on the Shuttle Orbiters and the Mir Space Station
  - NASA TM-107486 July 1997
  - http://www.grc.nasa.gov/WWW/MMAP/PIMS/HTMLS/Micro-descpt.html
- Acceleration Data Analysis and Presentation Techniques TM
  - Detailed description of acceleration data analysis techniques
  - http:// www.grc.nasa.gov/WWW/MMAP/PIMS/HTMLS/adapt.html
- Mission Summary Reports
  - Mission specific characterizations for various Shuttle and Mir missions
  - http:// www.grc.nasa.gov/WWW/MMAP/PIMS/HTMLS/reportlist.html

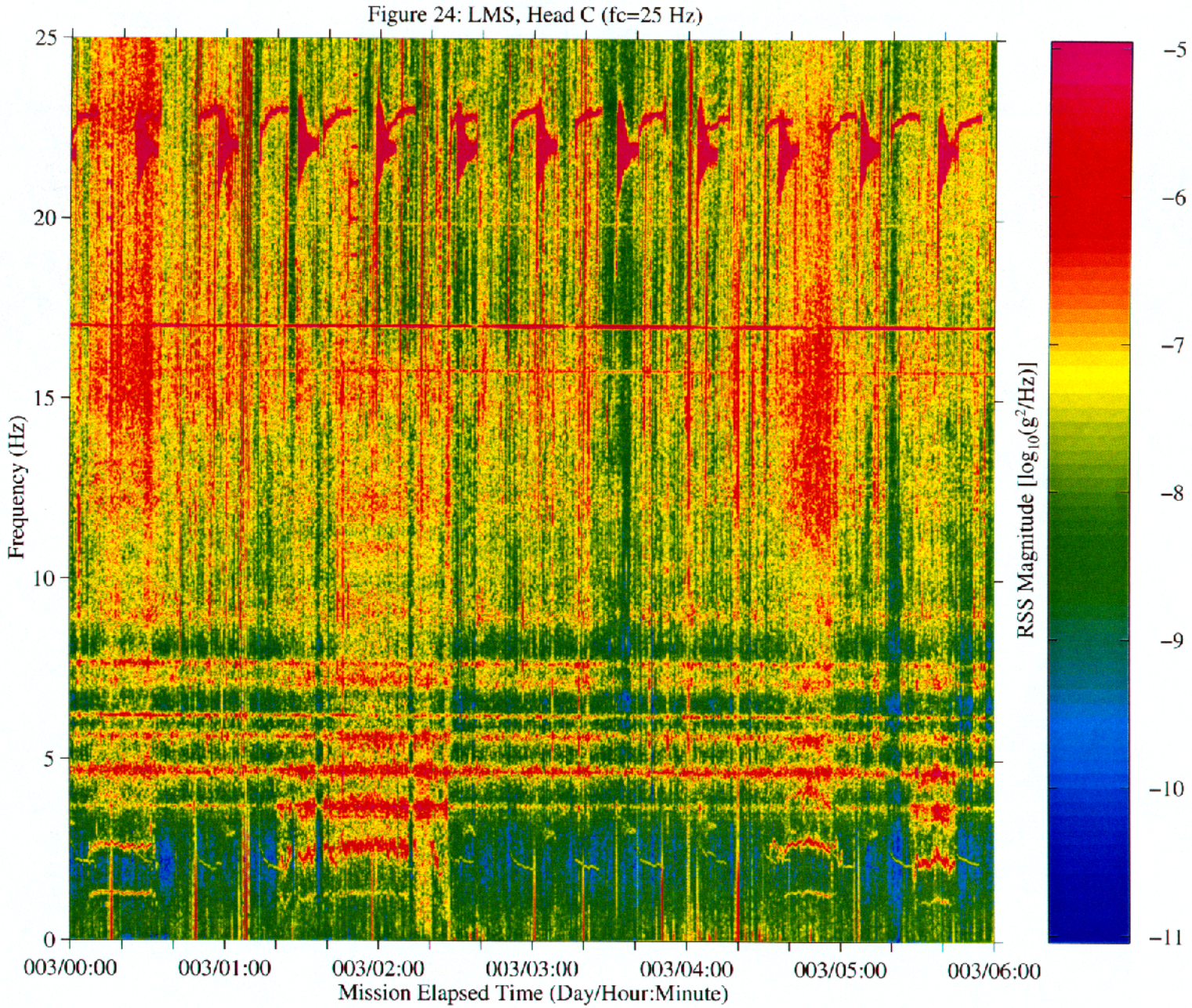

Figure 1. Nominal Environment Plot (STS-78)

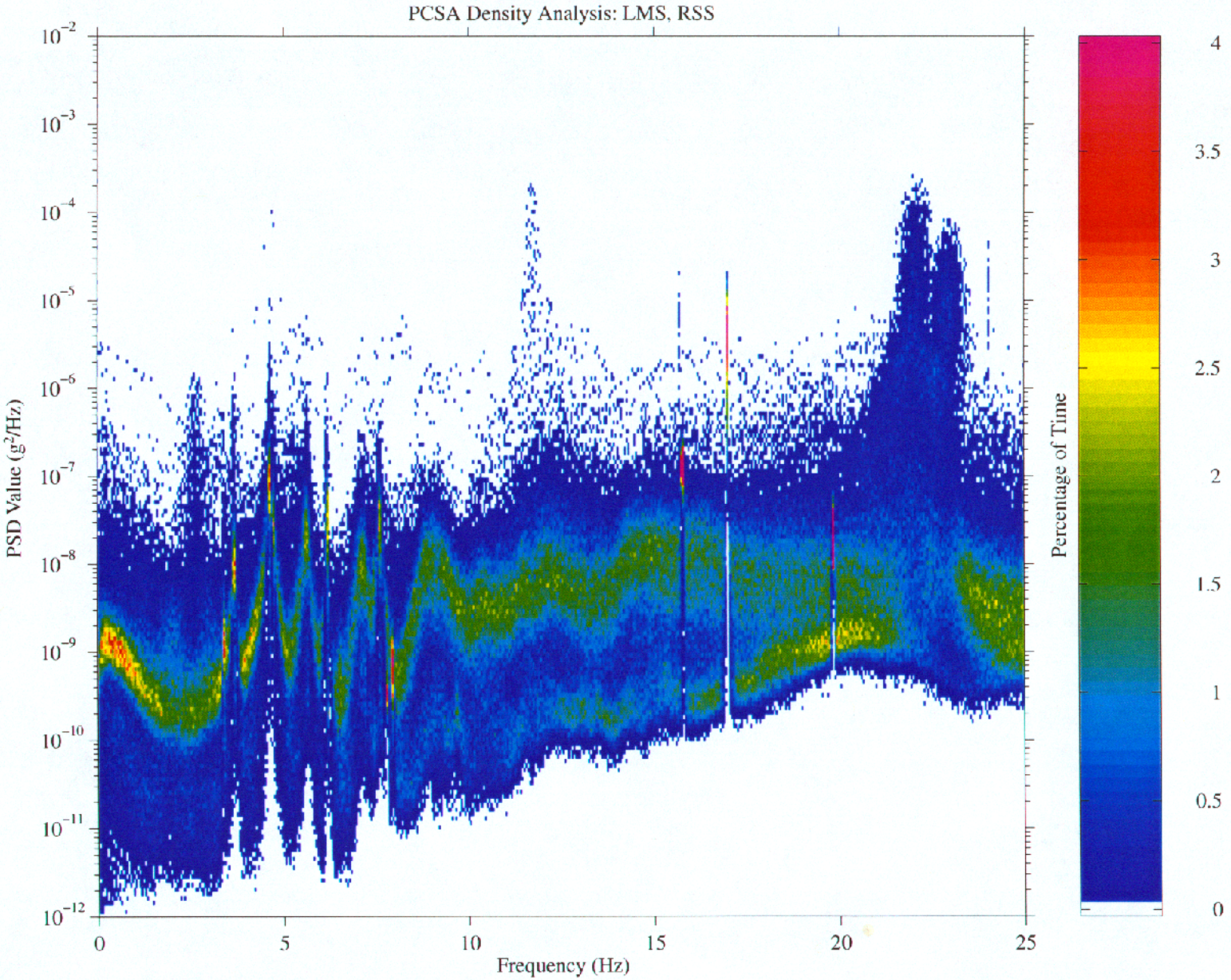

Figure 2. Principal Component Spectral Analysis (STS-78)

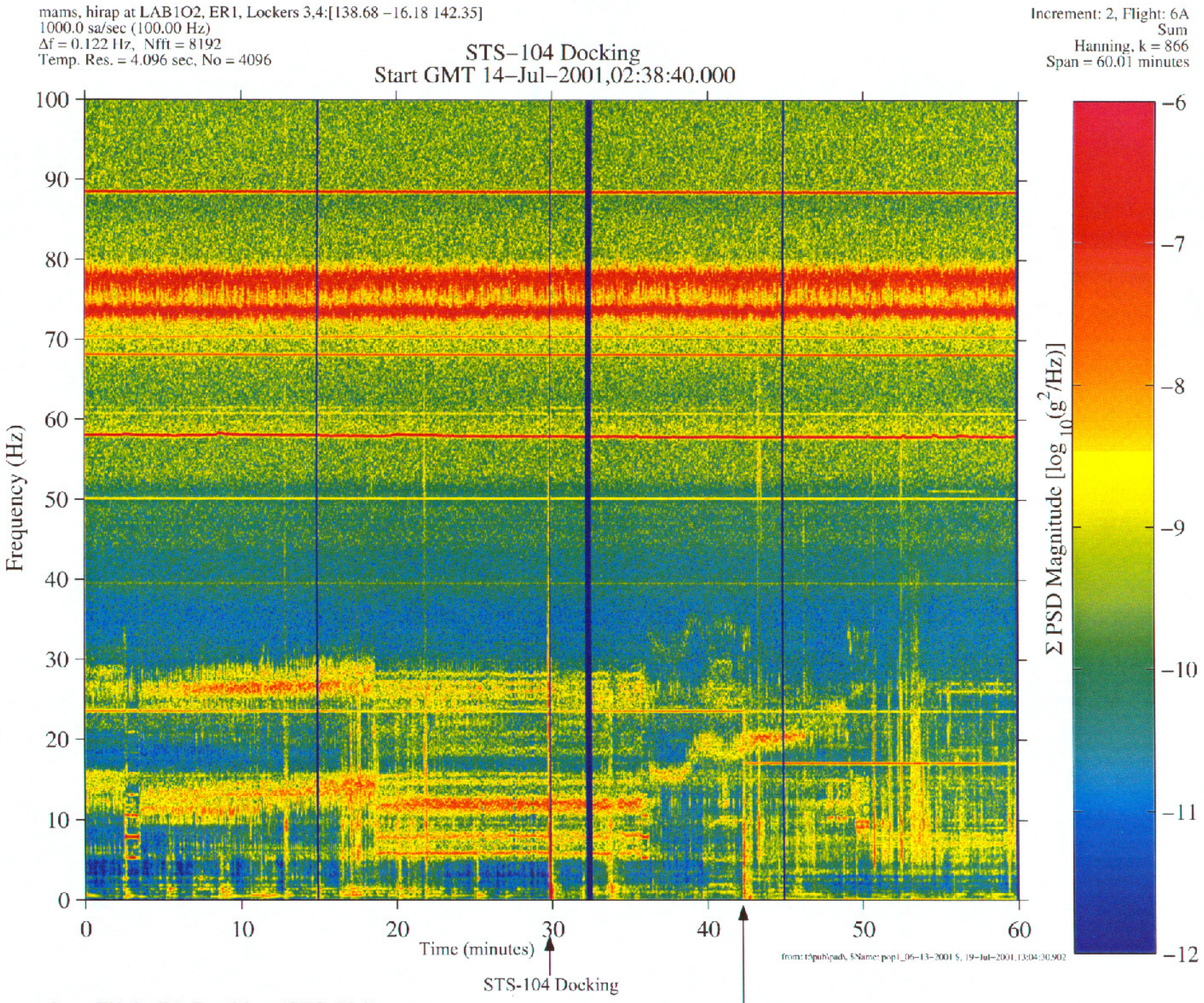

Figure 3 — Flight 7A Docking (STS-104)

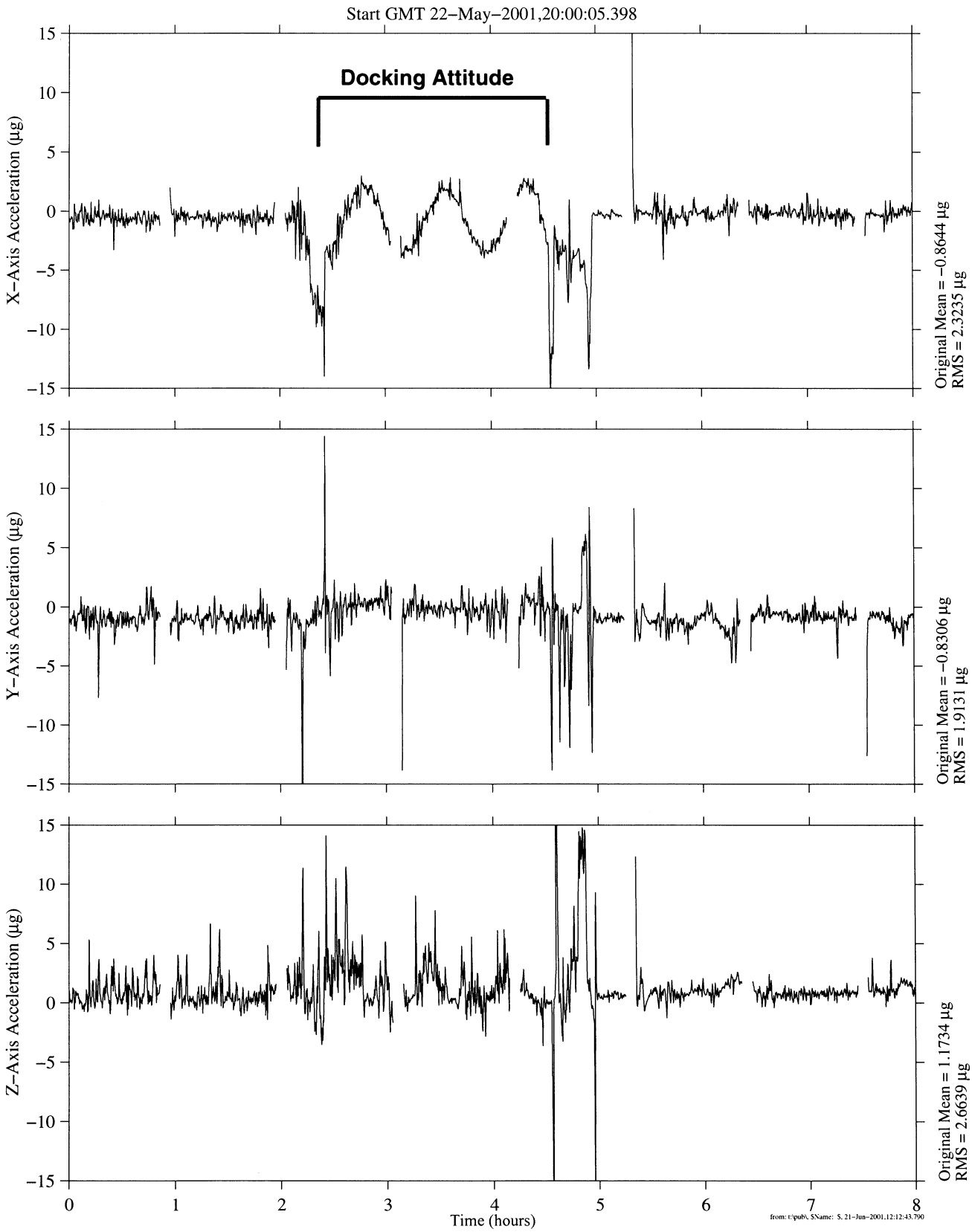

Figure 4 — Progress Docking Acceleration vs. Time (ISS)

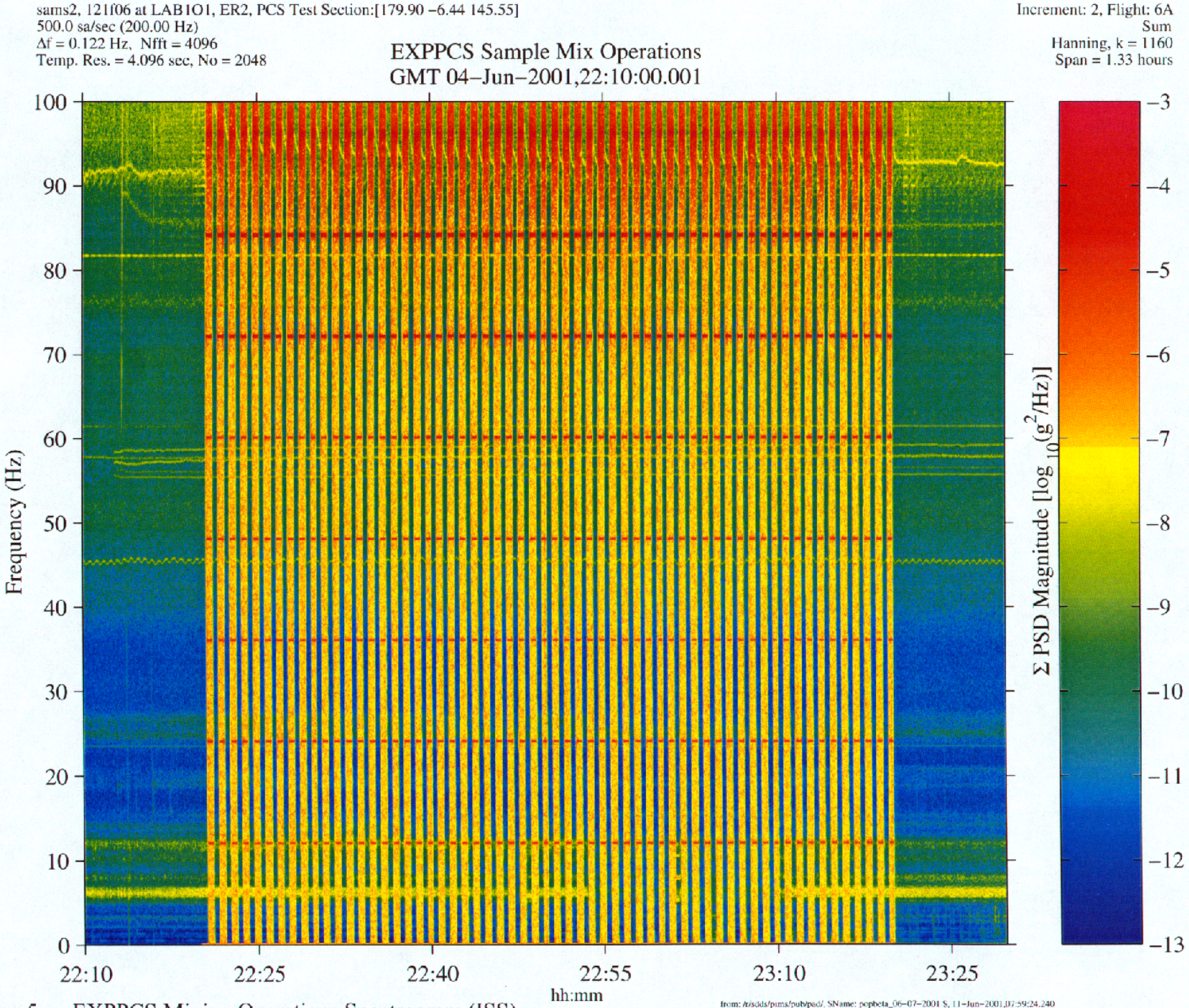

Figure 5 — EXPPCS Mixing Operations Spectrogram (ISS)

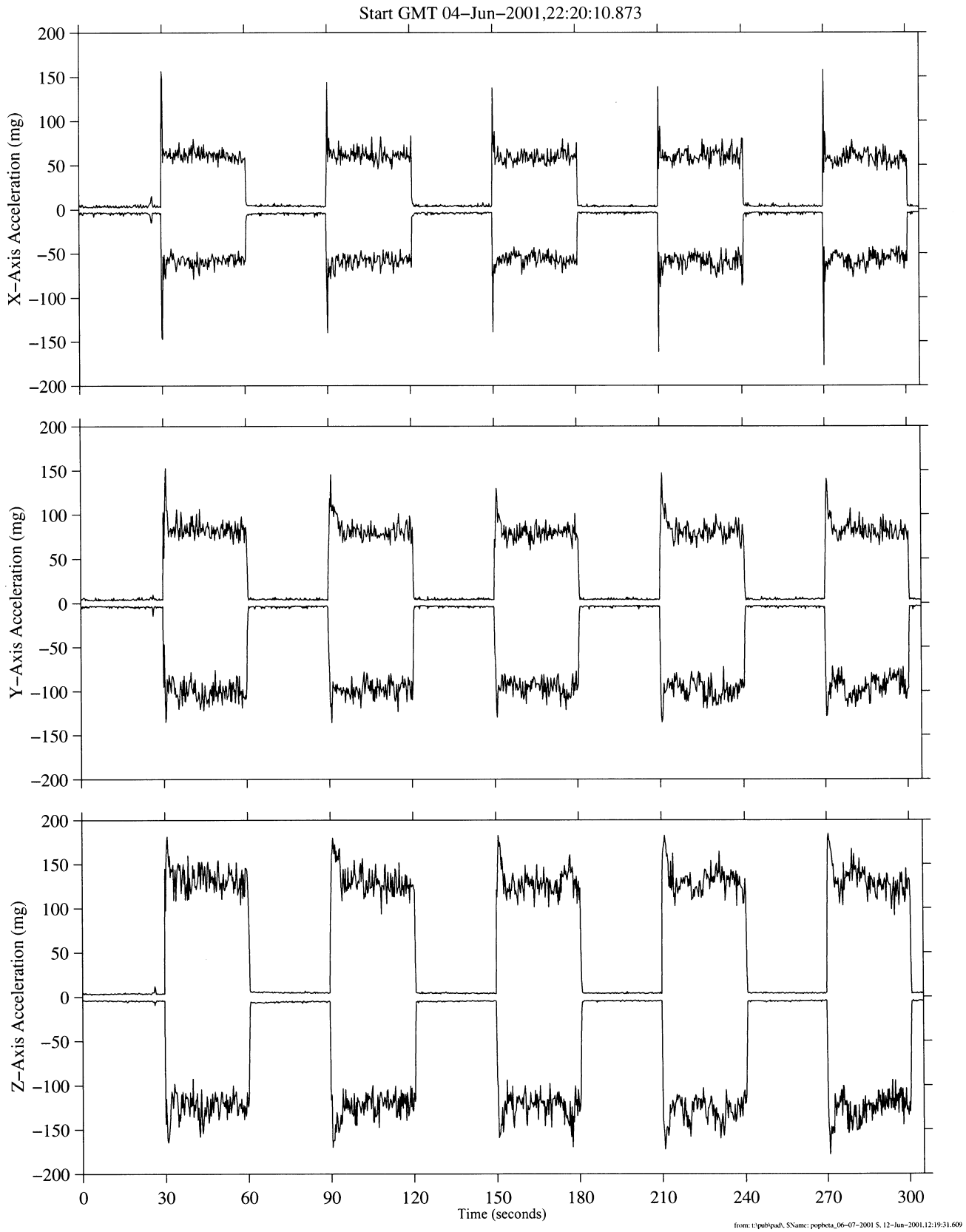

Figure 6 - EXPPCS Mixing Operations Minimum/Maximum Acceleration vs. Time (ISS)

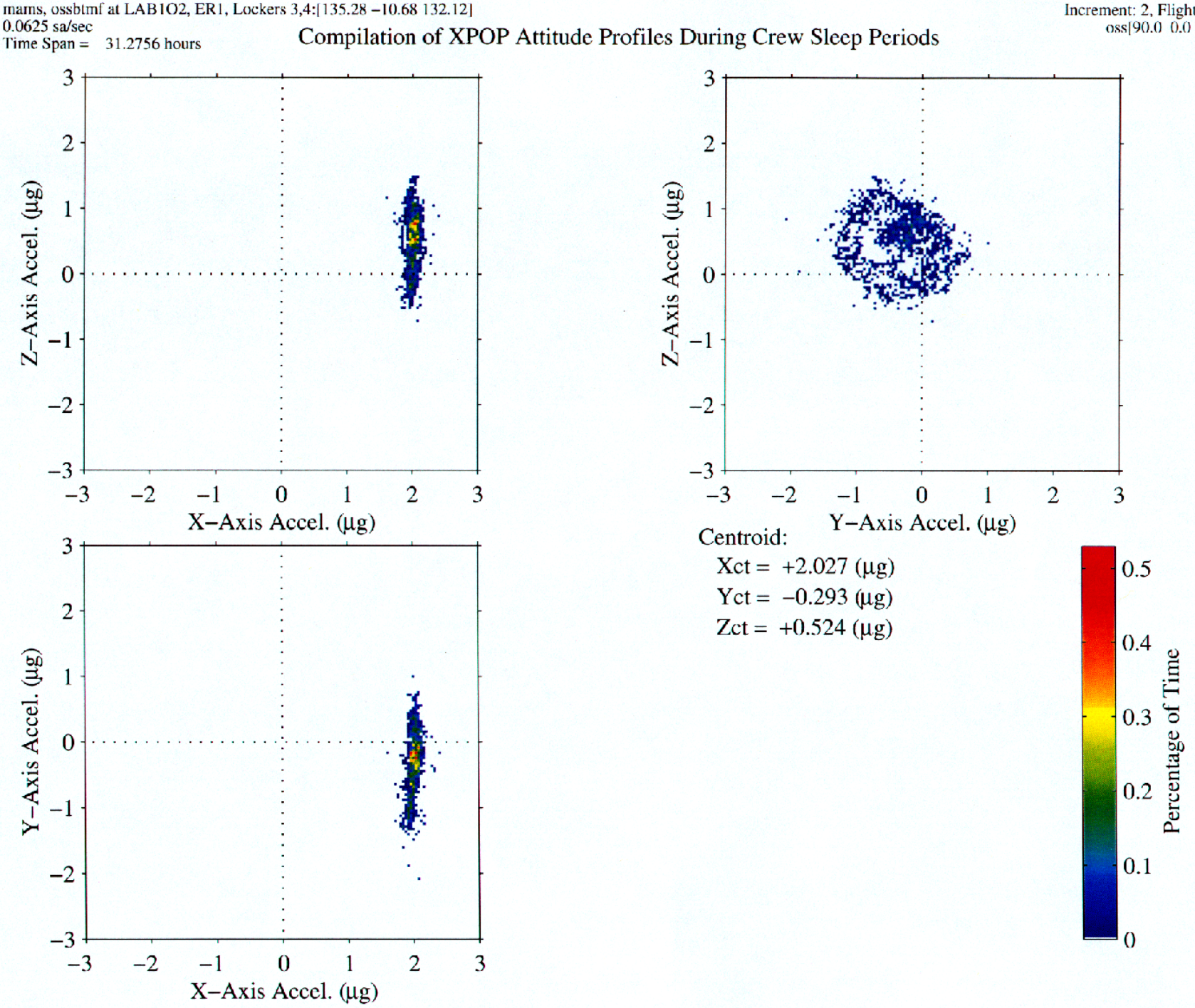

Figure 7 Quasi-Steady Three Dimensional Histogram During Crew Sleep (ISS)

from t:\pub\, $Name: , 20-Jun-2001.13:15:37.550

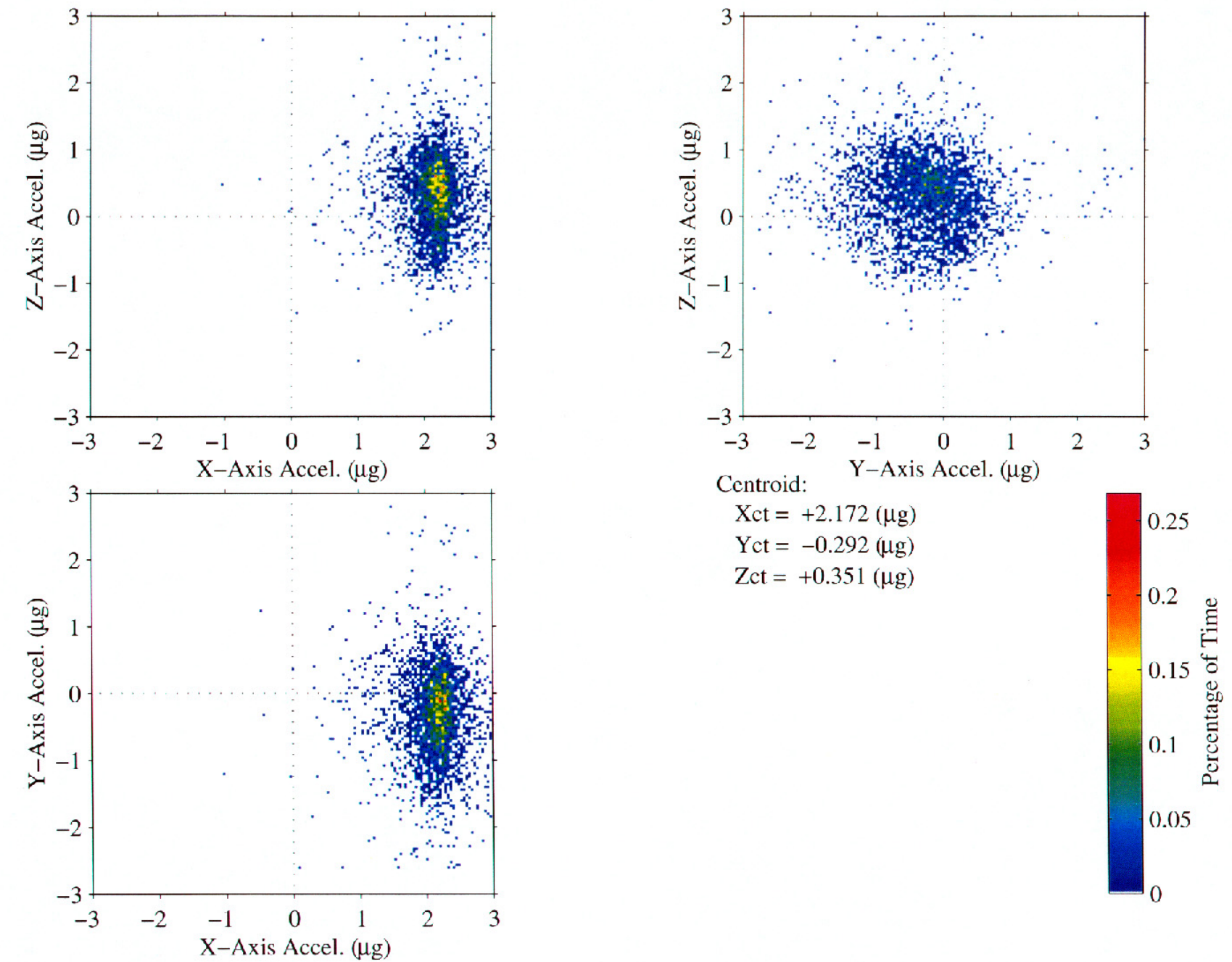

Figure 8 - Quasi-Steady Three Dimensional Histogram During Crew Wake Periods (ISS)

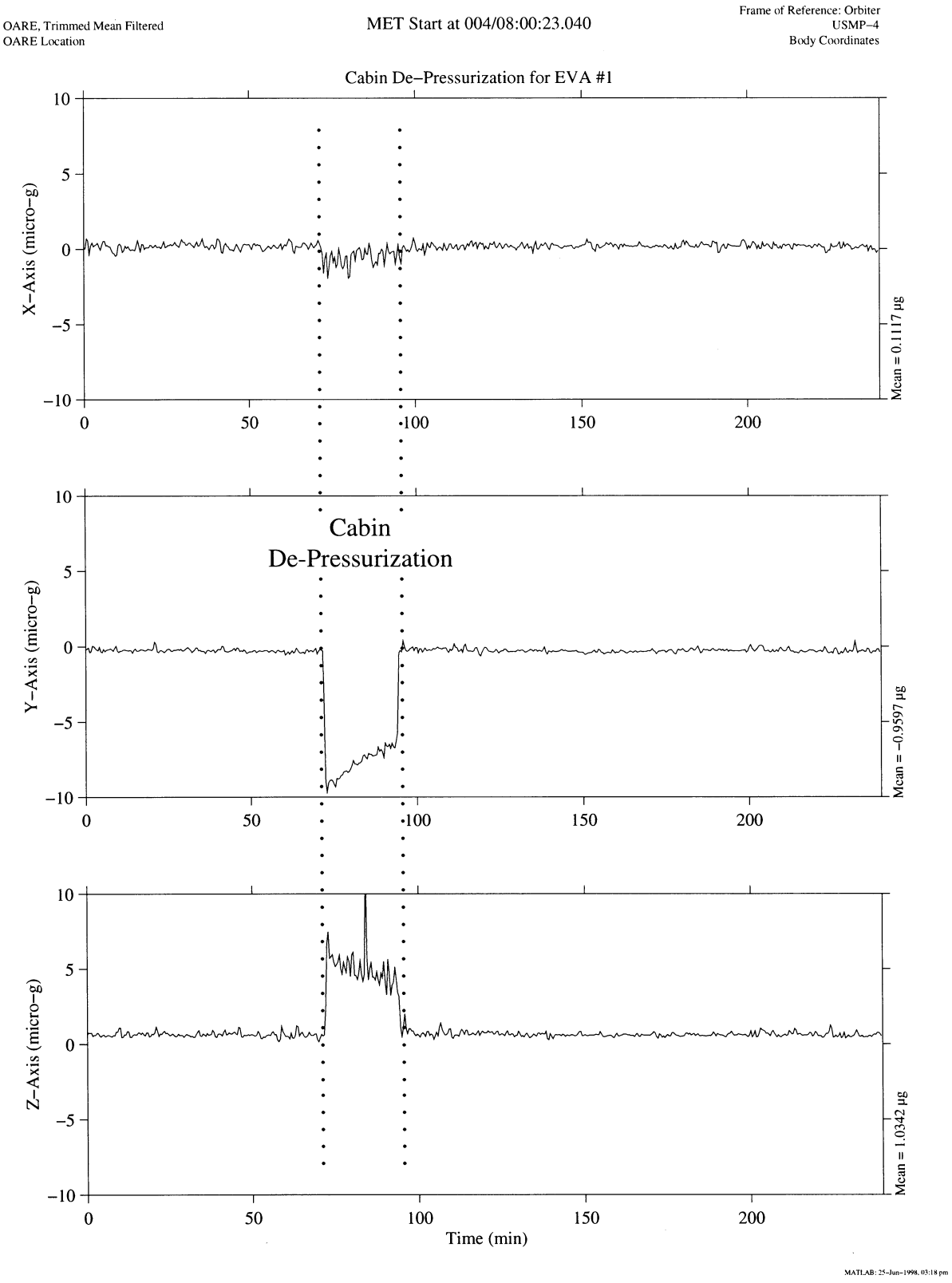

Figure 9. Cabin De-pressurization (STS-87)

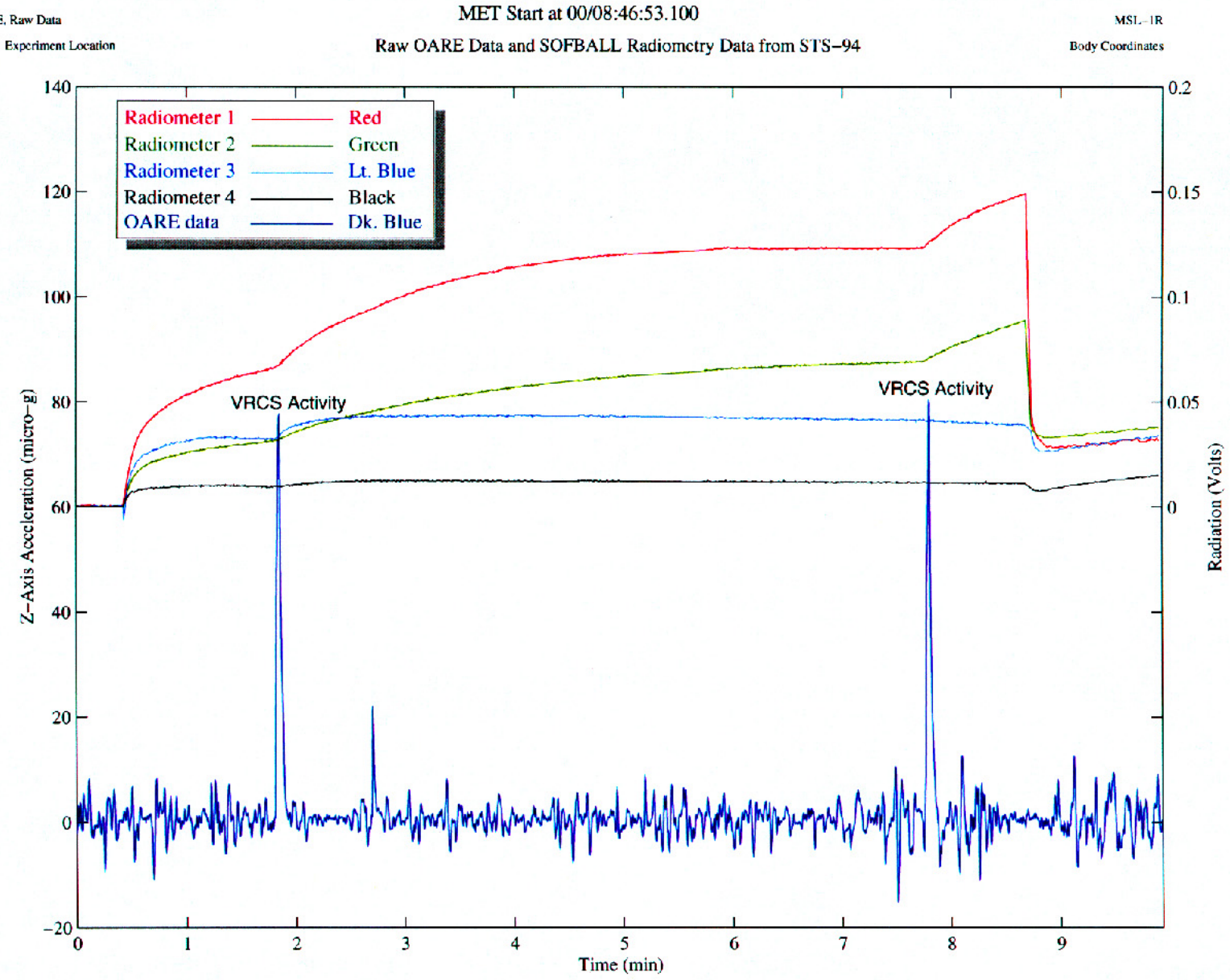

Figure 10. OARE vs. SOFBALL Radiometry Data (STS-94)

NASDA's Activities for "Microgravity" in JEM

Toshitami Ikeda and Keiji Murakami
Space Utilization Research Center
National Space Development Agency of Japan (NASDA)

In this presentation, NASDA's activities for microgravity acceleration measurements, vibration isolation, and microgravity control plan in JEM will be shown. First, NASDA has been developing a microgravity measurement apparatus (MMA) to be installed in the JEM. The Critical Design Review (CDR) #1 was held in February 2001 and CDR#2 (system CDR) will be held in this autumn. Second, we will show our approach concerning vibration isolation in JEM. And finally, situation of establishing a JEM payloads microgravity control plan and a test plan for measurements of acceleration disturbances from ISPRs will be informed.

NASA/CP—2001-211164

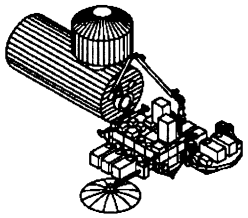

NASDA's Activities for "Microgravity" in JEM

20th Microgravity Measurement Group

August 7-9, 2001

Toshitami IKEDA and Keiji MURAKAMI
Space Utilization Research Center,
NASDA

NASDA

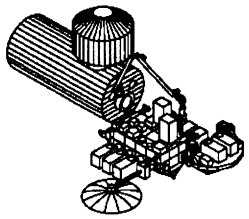

Topics

- **JEM-Microgravity Measurement Apparatus (MMA)**
  - System Description
  - Development Status
- **Vibration Isolation in JEM**
  - NASDA's approach of vibration isolation in JEM
- **Acceleration Disturbances from NASDA Payloads in JEM**
  - Payload Microgravity Constraints in JEM
  - Measurement of Payload's Disturbances

NASDA

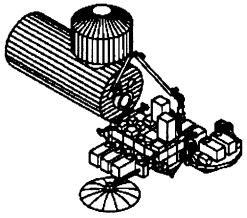

Introduction

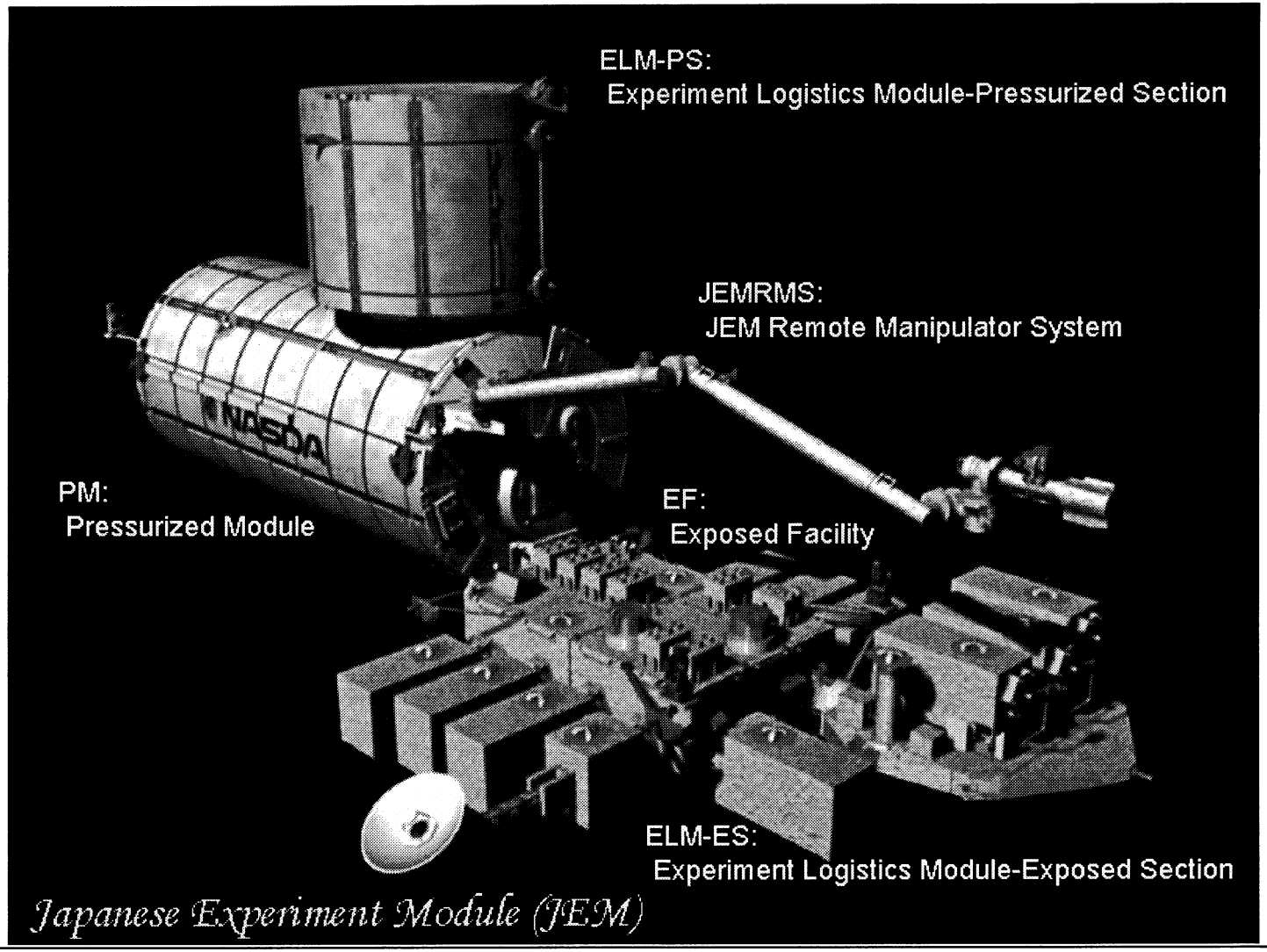

NASDA

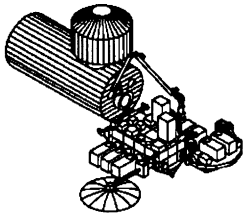

JEM-Microgravity Measurement Apparatus (1/6)

Purpose of the MMA

(1) To provide measurement data for investigators to analyze their experiment results.

(2) To reflect the equipment design of payloads for the next generation.

(3) As a future plan, to validate the JEM-PM structural analysis models, by measuring microgravity accelerations.

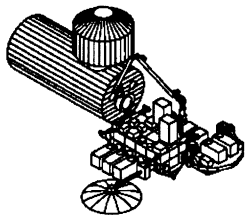

JEM-Microgravity Measurement Apparatus (2/6)

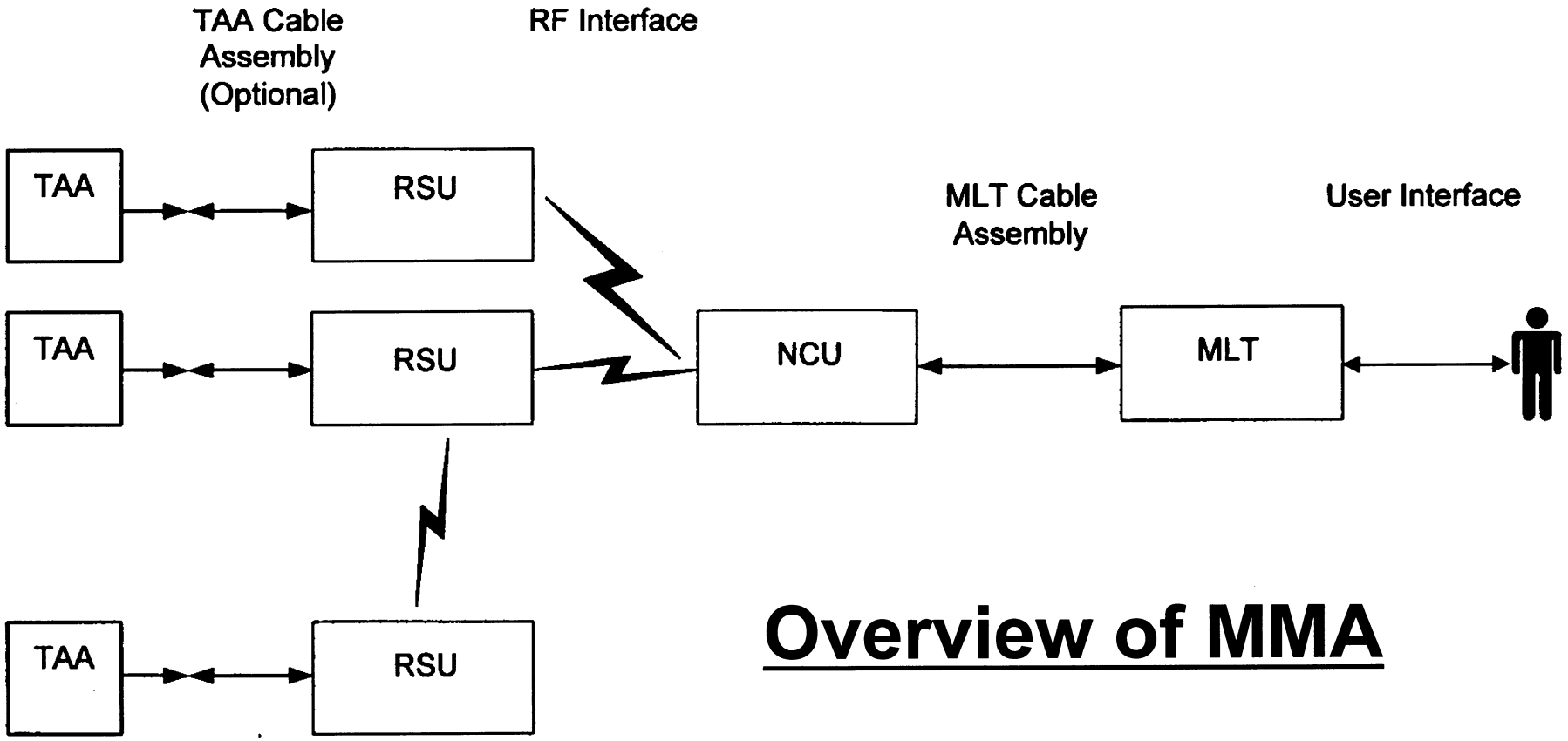

Overview of MMA

TAA: Honeywell QA-2000s are assembled.

NASDA

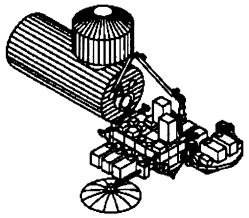

JEM-Microgravity Measurement Apparatus (3/6)

The MMA measures accelerations at the following five equipment in JEM-PM.

a) Gradient Heating Furnace (GHF)
b) Fluid Physics Experiment Facility (FPEF)
c) Advanced Furnace for Microgravity Experiment with X-ray Radiography (AFEX)
d) Solution/Protein Crystal Growth Facility (SPCF)
e) Cell Biology Experiment Facility (CBEF)

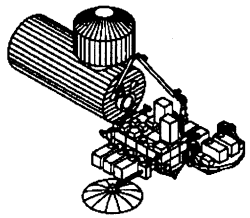

JEM-Microgravity Measurement Apparatus (4/6)

Over Head	O1 Data Management System 2	O2 System Stowage 1	O3 User Stowage 1	O4 Inter-Orbit Communication System	O5 Data Management System 1	Experiment Logistic Module Pressurized Section Hatch
Aft	A1 (Life Science) TBD	A2 (Life Science) **CB/CBEF**	A3 (Material) **SPCF/FPEF/ IPU**	A4 (Material) **AFEX**	A5 (Material) TBD	A6 Remote Manipulator System Equipment
Deck	D1 *ECLSS/ TCS1	D2 Electric Power System 1	D3 (User Stowage) MELFI	D4 System Stowage 2	D5 Electric Power System 2	D6 *ECLSS/ TCS2
Forward	F1 (Life Science) TBD	F2 (Life Science) TBD	F3 (Material) **GHF**	F4 Workstation	F5 (Material) TBD	F6 (Material) TBD

Connection to the Space Station Core

Air Lock to the Exposed Facilities

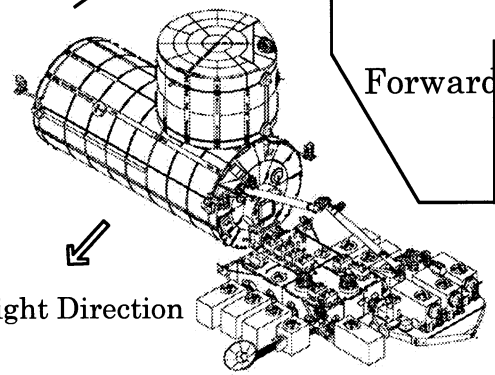

Flight Direction

Flight Direction

* ECLSS : Environment Control and Life Support System
TCS : Thermal Control System

ISPR layout in JEM-PM

NASDA

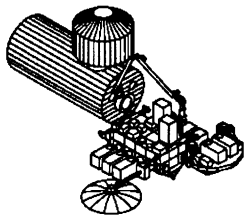

JEM-Microgravity Measurement Apparatus (5/6)

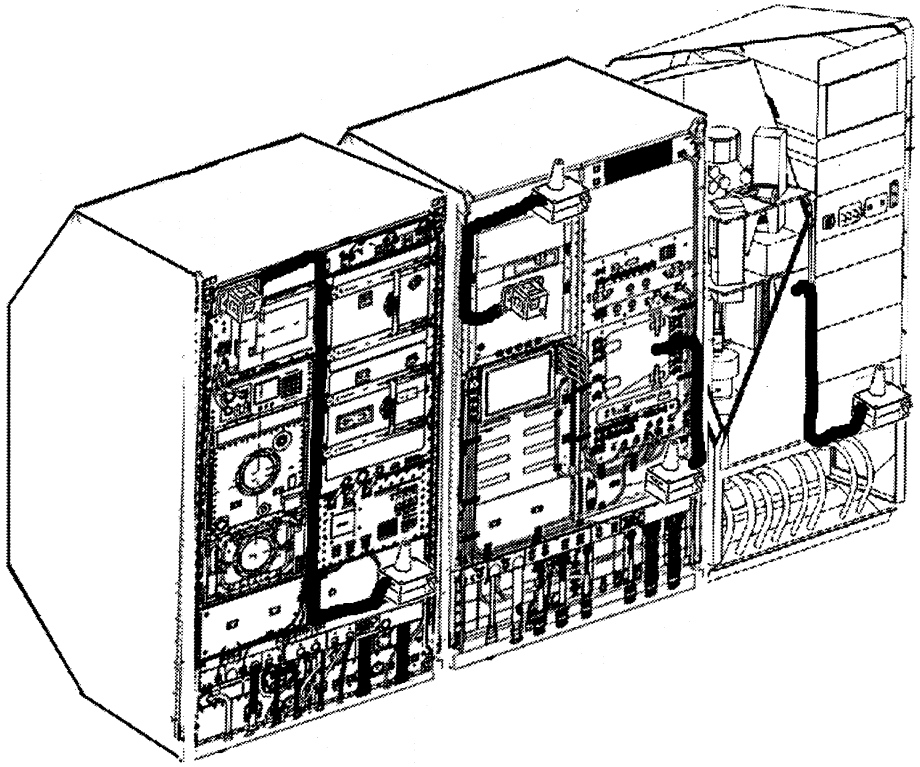

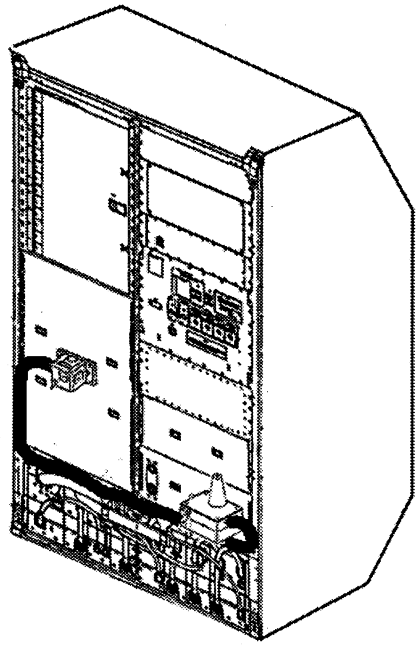

TAAs & RSUs locations

NASDA

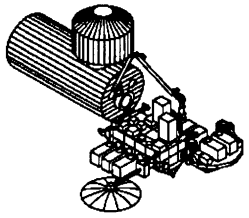

JEM-Microgravity Measurement Apparatus (6/6)

Microgravity Measurement Apparatus (MMA) Development Schedule (draft)

	1998	1999	2000	2001	2002	2003	2004
Milestone				CDR#1 ▽ CDR#2 ▽	PQR/PSR ▽		UF-3
design phase	Basic Design			Critical Design / Design Change		Sustaining Design	
Proto-Flight Model							
Rack Integration Test							
Overall System Test & Launch Site Operation							

NASDA

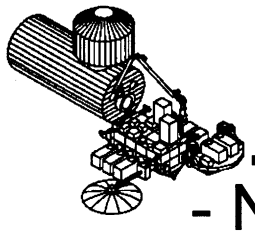

Vibration Isolation in JEM (1/3)

- NASDA's approach of vibration isolation in JEM

Predicted
Microgravity Environment
(DAC output, NIRA)

NASDA studied what type of isolation system was proper for JEM.

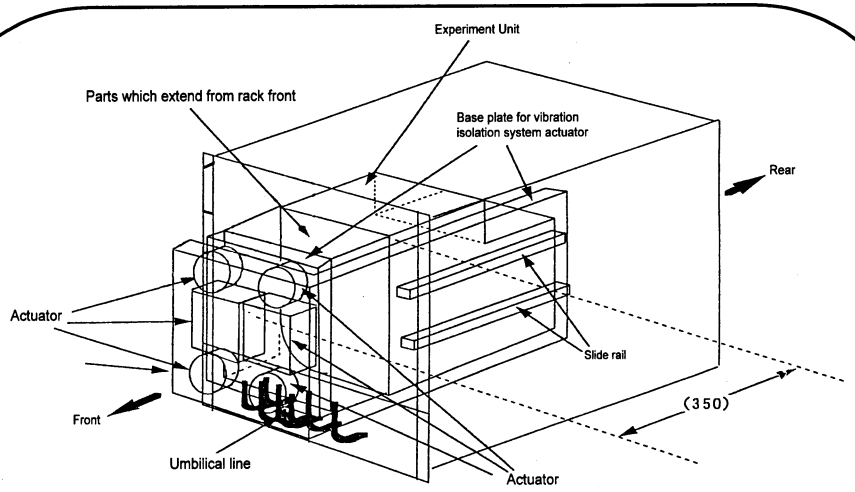

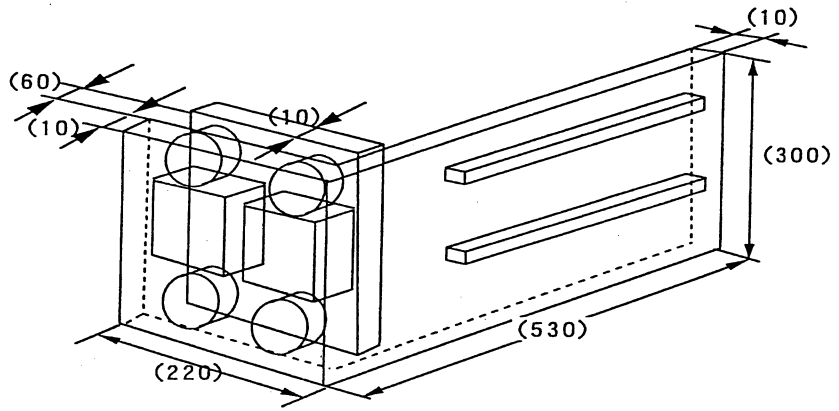

AVICS: February 1997

NASDA

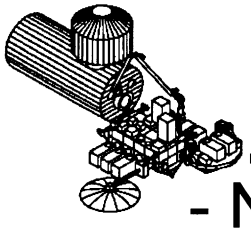

Vibration Isolation in JEM (2/3)

- NASDA's approach of vibration isolation in JEM

- DAC8
- NIRA99

According to NIRA99, the predicted environment in JEM was worse than the requirement. But NIRA was the worst case analysis and the deviation from the requirement below 50Hz are not so much in JEM.

Microgravity Environment in JEM Primary Module
NIRA 99

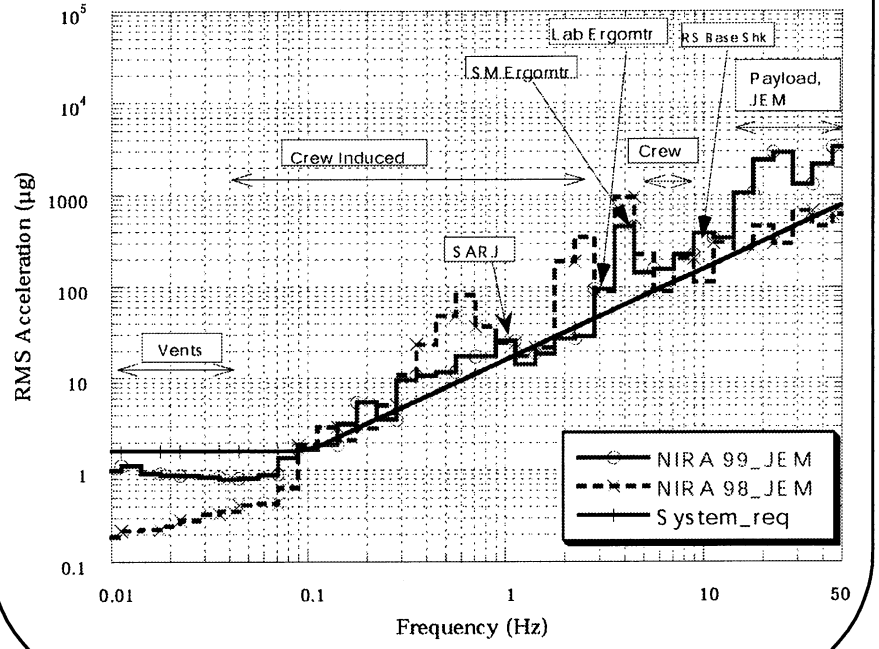

NASDA

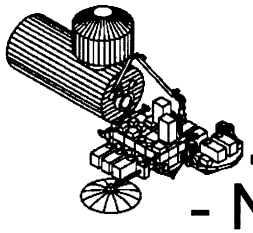

Vibration Isolation in JEM (3/3)

- NASDA's approach of vibration isolation in JEM

For the first generation payloads
- No Active vibration isolation system
- Acceleration measurement by JEM-MMA

< Output >
- Actual
  Microgravity Environment
- Experiment Results

NASDA will study whether to employ active vibration isolation systems to the next generation payloads or not.

What type of isolation system should be used?
--- ARIS? MIM? G-LIMIT? etc… ---

NASDA

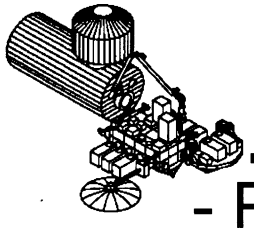

Acceleration Disturbances from NASDA Payloads in JEM (1/5)

- Payload Microgravity Constraints in JEM

Quasi-steady

Transient

Quasi-steady and Transient requirements to JEM payloads are the same level as that to US-lab payloads specified in PIRN57000NA110H.

Vibratory

Vibratory requirement of PIRN57000NA110H is based on ARIS attenuation performance. But NASDA's ISPRs don't have active vibration systems. Therefore, acceleration disturbances from payloads in JEM have to be lower than that from US-lab payloads.

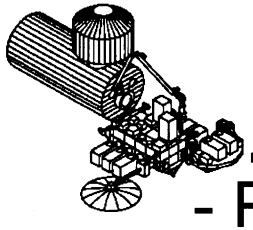

Acceleration Disturbances from NASDA Payloads in JEM (2/5)

- Payload Microgravity Constraints in JEM

Microgravity Environment in US Lab Module
NIRA 99

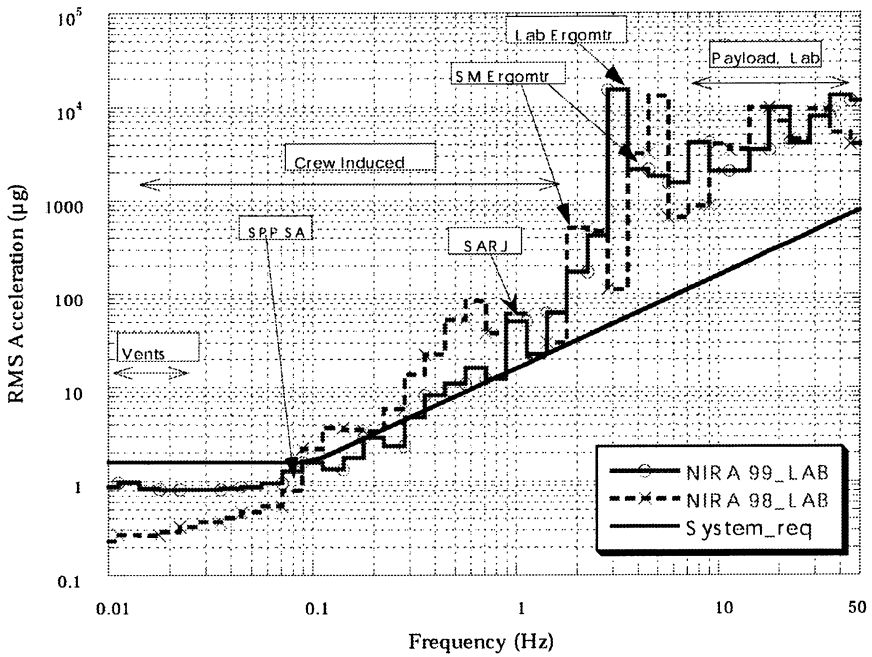

Microgravity Environment in JEM Primary Module
NIRA 99

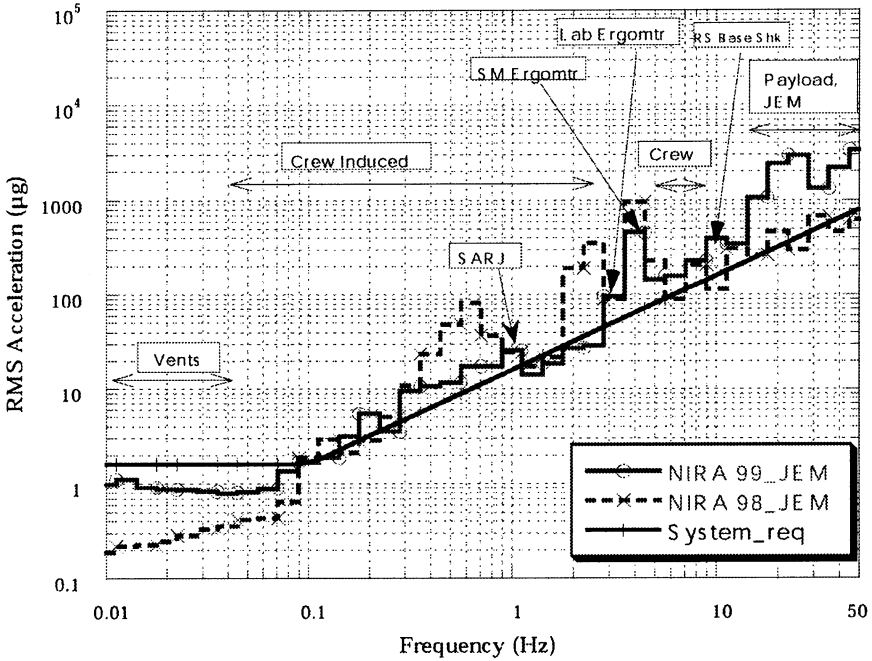

According to NIRA99, microgravity environment below 50Hz in JEM will be better than that in US lab.

NASDA

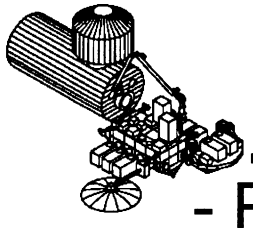

Acceleration Disturbances from NASDA Payloads in JEM (3/5)

- Payload Microgravity Constraints in JEM

Vibratory requirement in US-lab (PIRN57000NA110H)

Microgravity Acceleration Limit + ARIS attenuation

⇒ US Payload Disturbance Force Limit

Vibratory requirement in JEM (under construction)

NIRA in JEM (to be available in this autumn)

⇒ JEM Payload Disturbance Force Limit

NASDA

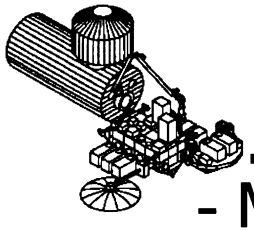

Acceleration Disturbances from NASDA Payloads in JEM (4/5)

- Measurement of Payload's Disturbances

Experiment Equipment level

Payload Developers measure acceleration or force disturbances at the interface point between equipment and the rack structure, and the obtained data are reviewed by the Rack Integrator.

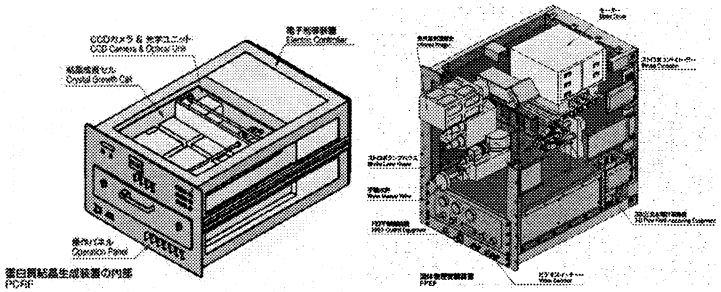

Integrated Rack level

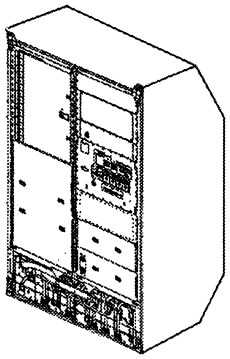

Rack Integrator measure acceleration disturbances at the interface point between ISPR and JEM module, and the obtained data are converted to force disturbances and they are reviewed by Element Integrator.

NASDA

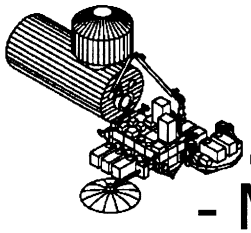

Acceleration Disturbances from NASDA Payloads in JEM (5/5)

- Measurement of Payload's Disturbances

Acceleration disturbance measurement test configuration (Rack level)

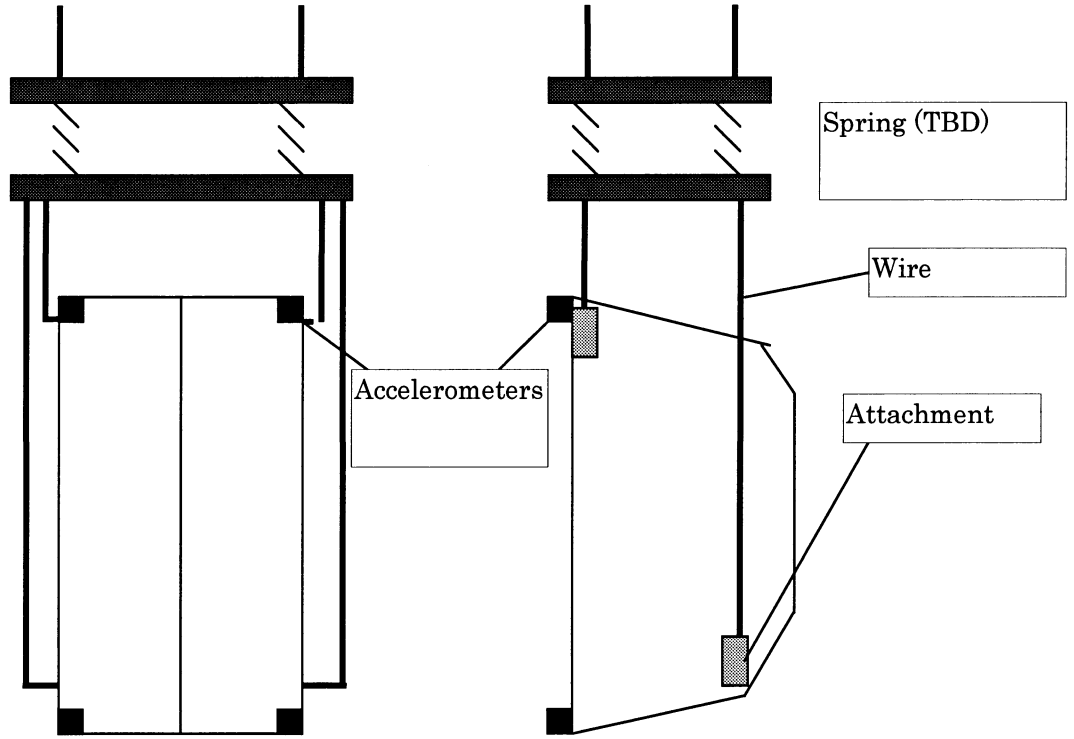

NASDA

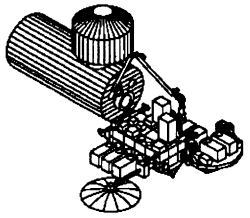

Summary

Microgravity Measurement in JEM

- Microgravity accelerations on the ISPRs are measured by JEM-MMA.

Vibration Isolation in JEM

- For the first generation payloads, we don't use any active vibration isolation system. Actual microgravity environment in JEM will be measured by MMA and NASDA will study the isolation systems for the next generation payloads.

Payload Microgravity Constraints in JEM

- PIRN57000NA110H is based on the ARIS attenuation performances and looks just lax for JEM payloads. NASDA is waiting for the next NIRA and plans to prepare the JEM payload Microgravity Control Plan based on it.

Payload Microgravity Verification

Fred Henderson
ISS Payloads Engineering and Integration
Teledyne Brown Engineering / Boeing

With the implementation of specific payload microgravity requirements for pressurized and attached payloads over the last two years, the new emphasis is for efficient means of ISS payload microgravity verification. Spreadsheets containing embedded Visual Basic code are to be used to ease payload data submittal and comparison with requirements. These spreadsheets will feed additional calculations for Element level and ISS level verification and provide inputs to payload operations planners. Output formats will also summarize microgravity impacts in support of waiver request evaluation. The presentation concludes with suggestions of how SAMS should be used to ease payload microgravity requirements by updating NIRA, identifying exact modal frequencies with associated damping and determination of complete (embedded impedance) transfer functions.

NASA/CP—2001-211164

Payload Microgravity Verification

MGMG #20

August 7, 2001

Fred Henderson

TBE /Boeing / ISS PEI

(281) 336-4256

fred.h.henderson@boeing.com

Purpose

Discuss the role of ISS Payload Engineering and Integration, progress toward developing standardized verification report data, and tools complementary to the Generic Payload Microgravity Control Plan.

Recommend SAMS microgravity measurements to improve ease of payload verification.

Overview

- **Payload Engineering and Integration Functions**
- **Tools to support verification**
- **Suggest on-orbit measurements to support verification**

The Role of ISS Payloads Engineering and Integration (PEI)

Payload Engineering and Integration (PEI) Functions

- **Develop/Maintain the Payload Interface Requirements Document(IRD)**
- **Coordinate Development of US Payload Interface Control Documents (ICDs)**
- **Collect and Screen Verification Data. Close Exceptions for CoFR.**
- **Report ISS Available Resources and Operational Constraints to Payload Operations and NASA OZ**

PEI Analysis Example - Stage UF-1
Channel 2B Payload Power

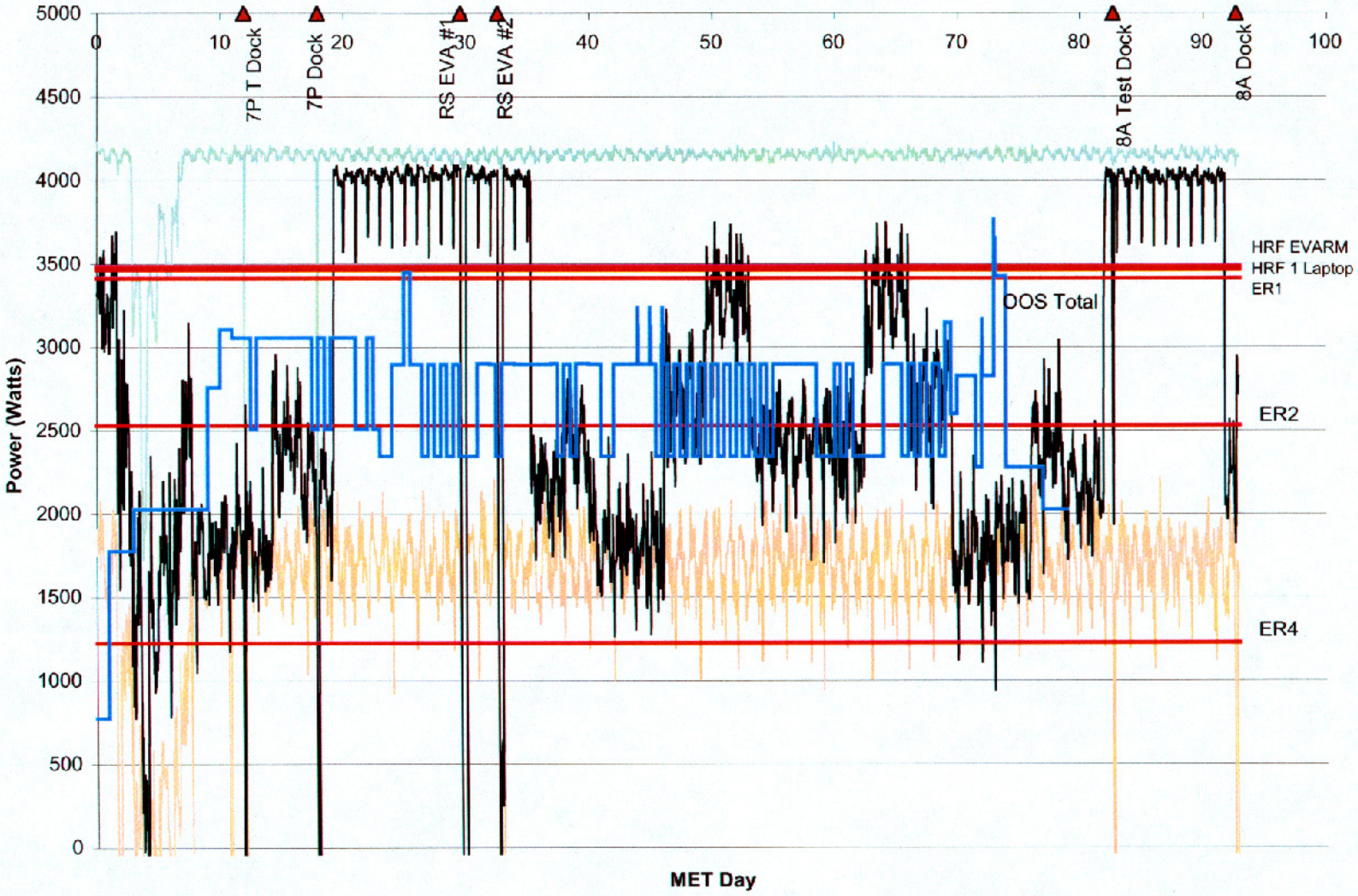

As performed for electrical, thermal, acoustic and C&DH for each stage

Standardized Tools for Payload Verification

- Test Data Collection Setup
- FFT Program for Disturbance Power Spectrum
- FEM and SEA Setup Instructions
- Standardized Narrow-Band Log-F Report Program
- Standardized 1/3 Octave Report Program
- RSS Summation per IRD Requirement Program

Narrow-Band Peak Reporting for Payloads

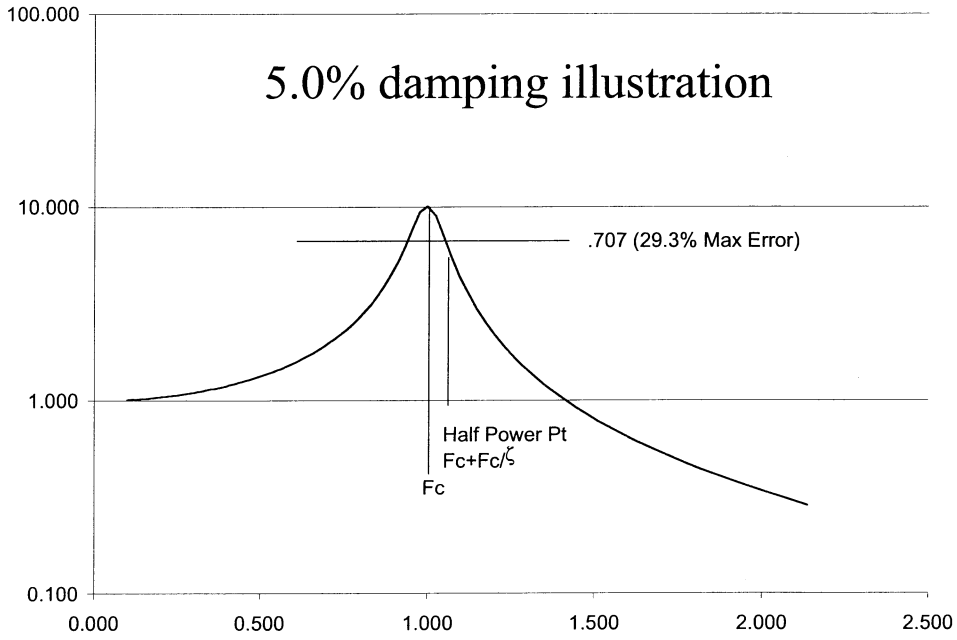

0.5% Damping Trades

Freq Ratio	Max Err	Nsamp Decade	Nsamp 0.01-300 Hz
1.01	29.80%	231	1036
1.005	11.00%	462	2067
1.0025	3.20%	922	4129
1.0012	0.45%	1920	8596
1.001	0.30%	2304	10314

- **Accuracy vs Volume of Information Tradeoff**
  - **Number of Samples to Acquire and Process**
  - **Payload Integration Interpretation**

- **Recommend 1.0025 frequency ratio separation**
  - **3.2% Max Error**
  - **4129 Frequency Intervals for FEM, SEA and Measured Data**

Test Data Collection Setup

Range (Hz)	SPS	Time	Samples**	Analysis or Test
0.01 to .1	0.4	11.4 h	16384	Analysis Recommended
0.1 to 1	4 SPS	1.1 h	16384	Analysis or Test
1 to 10	40 SPS	7m	16384	Test Recommended
10 to 100	400 SPS	41 s	16384	Test Recommended
100-300	1200 SPS	14 s	16384*	Test Recommended

* 8 Freq Domain sets to be rms averaged to span 100 sec

** Time Domain Samples Needed for 922 Narrow-band, log-frequency bins per decade
(Total log-frequency bins for 0.01 to 300 Hz Range is 4129)

Narrow-Band Reporting by Payloads

- **Useful to Show Modal and Disturbance Frequency Spectrum**
  - **Damping coefficients**
  - **Modal Avoidance**
  - **Narrow-band Vs Wide-Band Criteria**
- **Provides manageable data set consistent with 0.5% lowest modal damping and 4% accuracy**
- **Reduces 81,920 Data Points to 4130**
- **Similar to Using FREQ2 Output Specification with NASTRAN**
  - **F1=0.01, F2=300, NF=4130**

1	0.010000
2	0.010025
3	0.010050
...	...
922	0.099954
923	0.100204
...	...
1845	0.999077
1846	1.001575
...	...
2766	9.986163
2767	10.01113
...	...
3690	99.81555
3691	100.0651
...	...
4129	299.4511
4130	300.1998

1/3 Octave Reporting by Payloads

- **EXCEL worksheet provides requirement and calculation of margin for each one-third octave band. (First rows shown below)**
- **May choose either force or acceleration method allowed by PIRN 110H**
- **Narrow-band vs Wideband calculation for force method calculated separately**

Frequency (Hz)	Wide Band (lb or N)		Narrow Band (lb or N)		Peak (Hz)	Accleration (microg)		Margin
	Limit	Actual	Limit	Actual		Limit	Actual	
0.0101	0.0896	0.0000	0.0626			0.159		0.0000
0.0127	0.0732	0.0000	0.0626			0.185		0.0000
0.0160	0.0847	0.0020	0.0682			0.213		0.0236
0.0201	0.0975	0.0020	0.0792			0.244		0.0205
0.0253	0.1130	0.1000	0.0914			0.281		0.8852
0.0318	0.1331	0.0000	0.1056			0.325		0.0000
0.0401	0.1611		0.1237	0.0850		0.383		0.6869
0.0505	0.2055	0.0015	0.1345			0.458		0.0073
0.0635	0.2214	0.0012	0.0427			0.556		0.0054
0.0800	0.1589	0.5210	0.0427			0.682		3.2784
0.1007	0.2093	0.3200	0.0427			0.843		1.5289
0.1268	0.3731	0.3600	0.0302			1.322		0.9649
0.1596	0.1460	0.0052	0.0173			2.079		0.0356
0.2009	0.0834	0.0280	0.0218			3.280		0.3356
0.2529	0.2471	0.0143	0.0274			5.180		0.0579
0.3183	0.2248	0.0110	0.0615			8.190		0.0489
0.4008	0.3788	0.0110	0.0309			12.970		0.0290
0.5045	0.1389	0.0230	0.0389			20.530		0.1656
0.6351	0.2746		0.0490	0.0490		32.490		1.0000
0.7996	0.2226		0.0692	0.0702	0.7150	51.420		1.0144
1.0067	0.4047	0.2100	0.0872			81.330		0.5189

Payload Microgravity Compatibility

- **Contribution Identified by Payload, Element and ISS Effect**
- **Payload Allocations Adjusted if ISS Contribution is Known**
- **Unused Allocations May Provide Margin for Some Deviations**

Fraction of PIRN 110H Limit, by 1/3 Octave Band
If number of payloads exceeds N allocation, greatest N combination RSS/N is given
Simulated Data - for Discussion Purposes Only

N Alloc:	*17.000*	7.000	4.000	4.000	2.000	*(Allocations may be fixed for a stage or dynamic)*								Attached Payloads		
TOB freq.	ISS	USL	COF	JEM	Attach.	USL						COF	JEM			
(Hz)	RSS/N	RSS/N	RSS/N	RSS/N	RSS/N	RSS	ER1	ER2	ER5	ER8	HRF1	RSS	RSS	RSS	S4-1	S4-2
0.010																
0.013																
0.016																
0.020	0.194			0.400									0.800			
0.025	0.229		0.250	0.400								0.500	0.800			
0.032	1.295	1.978	0.300	0.400	0.220	5.235		5.200		0.600		0.600	0.800	0.311	0.220	0.220
0.040	0.298		0.300	0.400	0.506							0.600	0.800	0.716	0.420	0.580
0.050	0.146		0.300									0.600				
0.063	0.121		0.250									0.500				
0.079																
0.100																
0.126	0.024	0.038				0.100	0.100									
0.158	0.150				0.438									0.620		0.620
0.200	0.038	0.059				0.157		0.121			0.100					
0.251	0.220	0.156			0.573	0.412	0.150	0.250	0.150	0.150	0.200			0.810	0.810	
0.316	0.376	0.585				1.549	0.150	0.251	1.500	0.150	0.200					
0.398	0.101	0.158				0.417	0.150	0.258	0.150	0.150	0.200					
0.501	0.100	0.156				0.413	0.150	0.251	0.150	0.150	0.200					
0.631	0.038	0.059				0.155		0.155								
0.794																
1.000																

Payload Compatibility-Detail

Fraction of PIRN 110H Limit, by 1/3 Octave Band
If number of payloads exceeds N allocation, greatest N combination RSS/N is given
Simulated Data - for Discussion Purposes Only

N Alloc:	*17.000*	7.000	4.000	4.000	2.000		*(Allocations may be fixed for a stage or dynamic)*					
TOB freq.	ISS	USL	COF	JEM	Attach.		USL					
(Hz)	RSS/N	RSS/N	RSS/N	RSS/N	RSS/N		RSS	ER1	ER2	ER5	ER8	HRF1
0.010												
0.013												
0.016												
0.020	0.194			0.400								
0.025	0.229		0.250	0.400								
0.032	1.295	1.978	0.300	0.400	0.220		5.235		5.200		0.600	
0.040	0.298		0.300	0.400	0.506							
0.050	0.146		0.300									
0.063	0.121		0.250									
0.079												
0.100												
0.126	0.024	0.038					0.100	0.100				
0.158	0.150				0.438							
0.200	0.038	0.059					0.157		0.121			0.100
0.251	0.220	0.156			0.573		0.412	0.150	0.250	0.150	0.150	0.200
0.316	0.518	0.807					2.135	0.150	0.251	2.100	0.150	0.200
0.398	0.101	0.158					0.417	0.150	0.258	0.150	0.150	0.200
0.501	0.100	0.156					0.413	0.150	0.251	0.150	0.150	0.200
0.631	0.038	0.059					0.155		0.155			
0.794												
1.000												

Potential Method for Analysis of Transient and Quasi-Steady Disturbances

#1	ISS	USL					COF	JEM	Attached Payloads		
	DJP	ER1	ER2	ER5	ER8	HRF1	DJP	DJP	DJP	S4-1	S4-2
Impulse											
lb-sec		5								2	2.5
Duration (sec)		1								0.5	7.5
N per Day		0.1								5	1.5
Quasi-Steady											
ug-sec				8							
Duration (sec)				180							
Transient Vib											
ug RMS		200			1000						
Frequency (Hz)		10			50						
Duration (sec)		3			20						
N per Day		0.1			5						

Notes:
Payload Entry Required only if greater than 10% of Limit
Daily Joint Probability (DJP) Method TBD

All data is simulated

NASA/CP—2001-211164

Suggested On-Orbit Microgravity Measurements

On-Orbit Microgravity Measurement Needs

- **Information that may enable reduction of probable conservatism of IRD Requirements**
  - **0.5% damping applied only to appropriate ISS modes (A change to 2% damping for key frequencies could allow payloads a factor of 4 greater vibration allowance at that frequency)**
  - **High modal frequency identification accuracy will permit disturbances to lie closer to known modal frequencies than 15% without assuming possible coincidence (Permitting possible factors of 5 or 6 greater disturbances)**
- **Information that would permit greater accuracy of ISS assessments**
  - **Few NIRA sources are measured**
  - **Loss Factors with Distance are not available in FEM Models**
  - **Rack to ISS transfer function gap and sliding stiction effects may greatly reduce vibration transfer**

Suggested Areas of SAMS Emphasis

- Identify Principal Lab Modes and Damping Coefficients
- Identify Principal Lab Subsystem and Payload Disturbances
- Perform Interface Impedance Test of a Non-ARIS rack (ER1?)
- Perform USL to Node Impedance Test
- Rack Attenuation with Position Measurement
- Attached Payload Site Transfer Function Measurement

SSUAS Microgravity Status Charts

Craig Schafer
SAIC / Code OZ
NASA Johnson Space Center
Houston, Texas

Several microgravity environment status charts from the recent SSUAS meeting were presented and discussed.

Comparison of Modeled Acceleration Environment to On-Orbit Measurements

Craig Schafer

JSC/ISS Payloads Office

SAIC-Houston

8/22/01

Abstract

In 1999, Boeing used Finite Element Analyses to produce a predicted U.S. Lab (Destiny) acceleration environment of ISS Stage 6A at the LAB1O1 ARIS Rack. The model results are compared to the environment measured by the Space Acceleration Measurement System (SAMS II). The models appear to be conservative compared to the measured environment. However, the on-orbit results are of a single 100 second measurement sample,and a larger sampling of acceleration environment is necessary in order to positively establish the degree of conservation in the FEA model.

Acknowledgements

My thanks to John-David Bartoe of NASA Johnson Space Center (ISS Research Manager) for collaborating on this presentation, Steve DelBasso and April Steelman of The Boeing Company (Microgravity Analysis and Integration Team) for their valuable input on the analytical model, and to Kenol Jules of Principal Investigator Microgravity Services (PIMS) of the NASA Glenn Research Center for retrieving and processing SAMS data for me.

Introduction

Finite Element Analysis has been used to predict the microgravity environment of the International Space Station's Destiny Module. Some of the greatest questions are what is the degree of conservatism in the FEA models, and are the models adequately capturing the characteristics of the individual disturbance sources and the structures? Boeing produced a Finite Element Model (FEM) of the ISS at Stage 6A in 1999 and predicted the microgravity environment for the research community. The Space Acceleration Measurement System-II (SAMS-II) was aboard and operating during the stage covered by the FEM. Two time periods were selected for comparison: a sleep period, and a time period during a test involving the Treadmill with Vibration Isolation System (TVIS).

Times of Interest

- Sleep period- Supposedly, the crew makes no appreciable vibrations while they are asleep, leaving only station systems. A sleep period was of interest to see what the vehicle reaction was to system disturbances only.

- TVIS SDTO- A Station Detailed Test Objective (SDTO) was scheduled to test the effect of use of the Treadmill with Vibration Isolation System (TVIS) on the station structure. Its effect on the microgravity environment was detected by SAMS-II. One crewmember was to walk or jog on the TVIS while the other two remained motionless. TVIS's isolation system was damaged during Increment 1, and a temporary fix was in place at the time of this test. Bungee cords were used in the place of damaged passive isolator cables, so the accelerations induced by the TVIS are not reflective of the isolation system's true performance.

6A Non-Isolated Acceleration Environment

- Boeing used Finite Element Analysis to model ISS Stage 6A acceleration environment in 1999.
- Results were enveloped over several points at the U.S. Lab LAB1O1 Rack and presented in an enveloped, 1/3 octave band format in acceleration as a function of frequency.
- The model used in this study was the 6A Environment Prediction with the following modifications:
  - Sleep period: All crew-induced accelerations were removed to simulate a sleep period.
  - TVIS operation: All crew-induced accelerations removed except TVIS and crew push-off/landing.

6A Environment

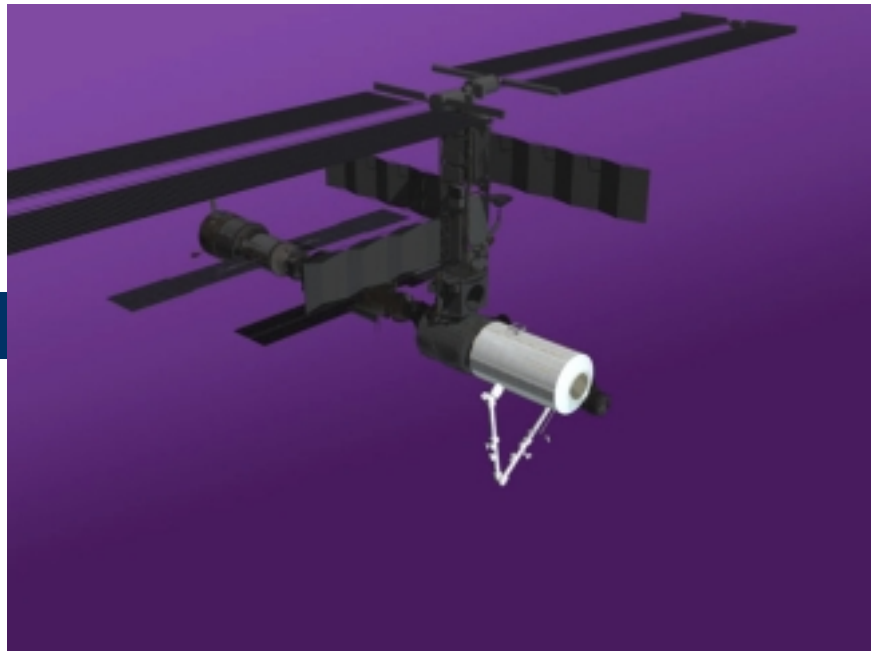

Modeled Vehicle Disturbances

Verified Components:	**P6 Truss Segment**	**U. S . Lab**	**Transient Disturbances**
Model Correlation for standard shuttle launch configuration: • FGB Zarya • Z1 Truss • PV Arrays • SM Zvezda • Progress • Node 1 Unity • U. S. Lab Shell/ Standoffs • System Racks • Express Rack #1	• Stick Slip • Beta Gimbal **Service Module** • High Gain Antenna • Fans (VS, TCS, Hygiene) • Pump (TCS, WSS, Hygiene) • TCS Compressor • **Treadmill Walking/ Jogging • Solar Arrays	• 45 Coldplates • **Crew Push- Off/ Landing • Fans (AAA, IMV, THC) • Pumps (CDRA, MCA, Water Sep.) **Node 1** • Fans (CCAV, IMV) **Z1 Segment** • Ku- Band • CMG	•P6 Beta Gimbal •SM High Gain Antenna •SM Solar Arrays •**Crew Push- Off/ Landing **Removed to simulate sleep period

SAMS-II Sensor Locations

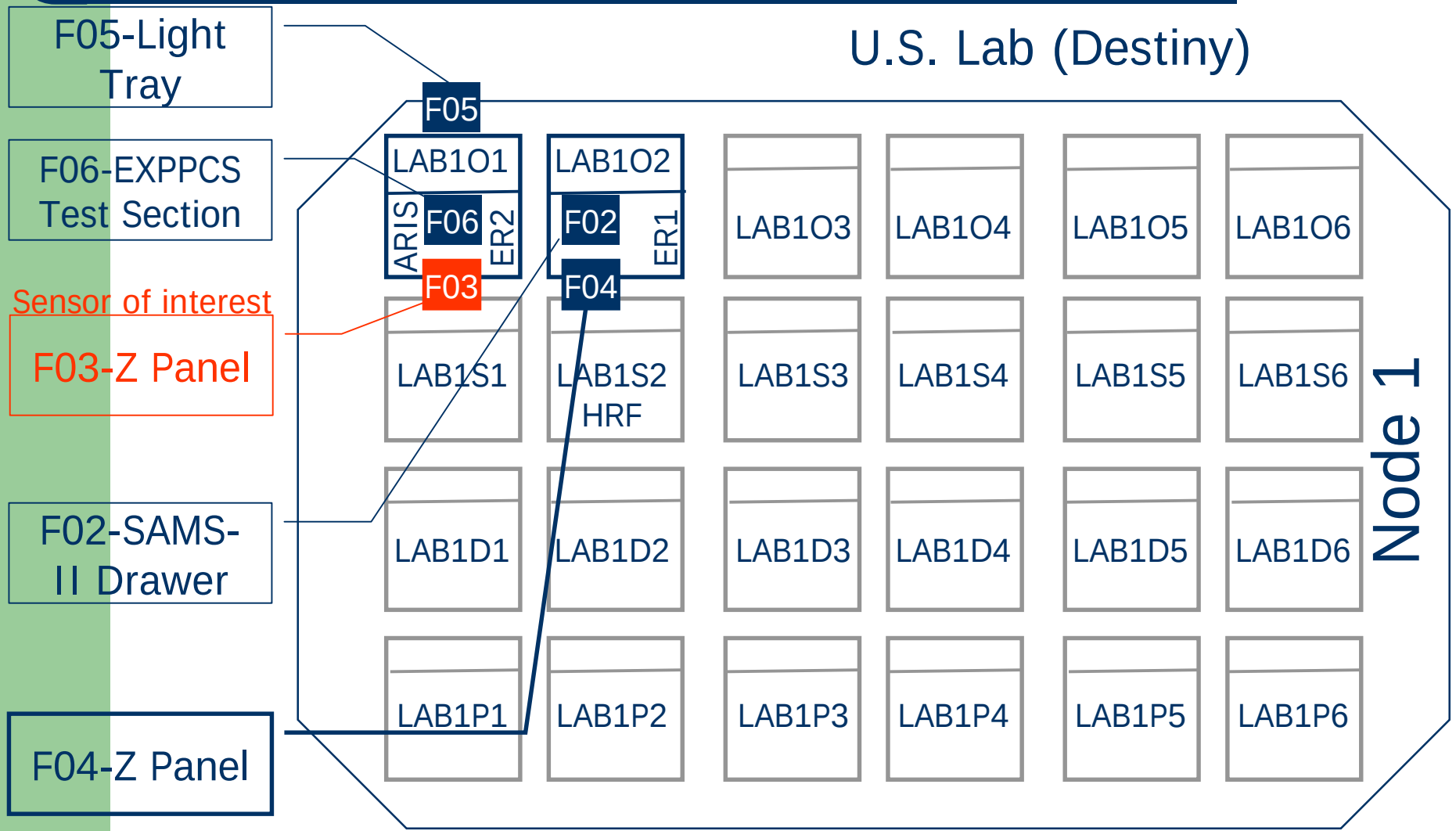

On-Orbit Picture of SAMS-II RTS F03

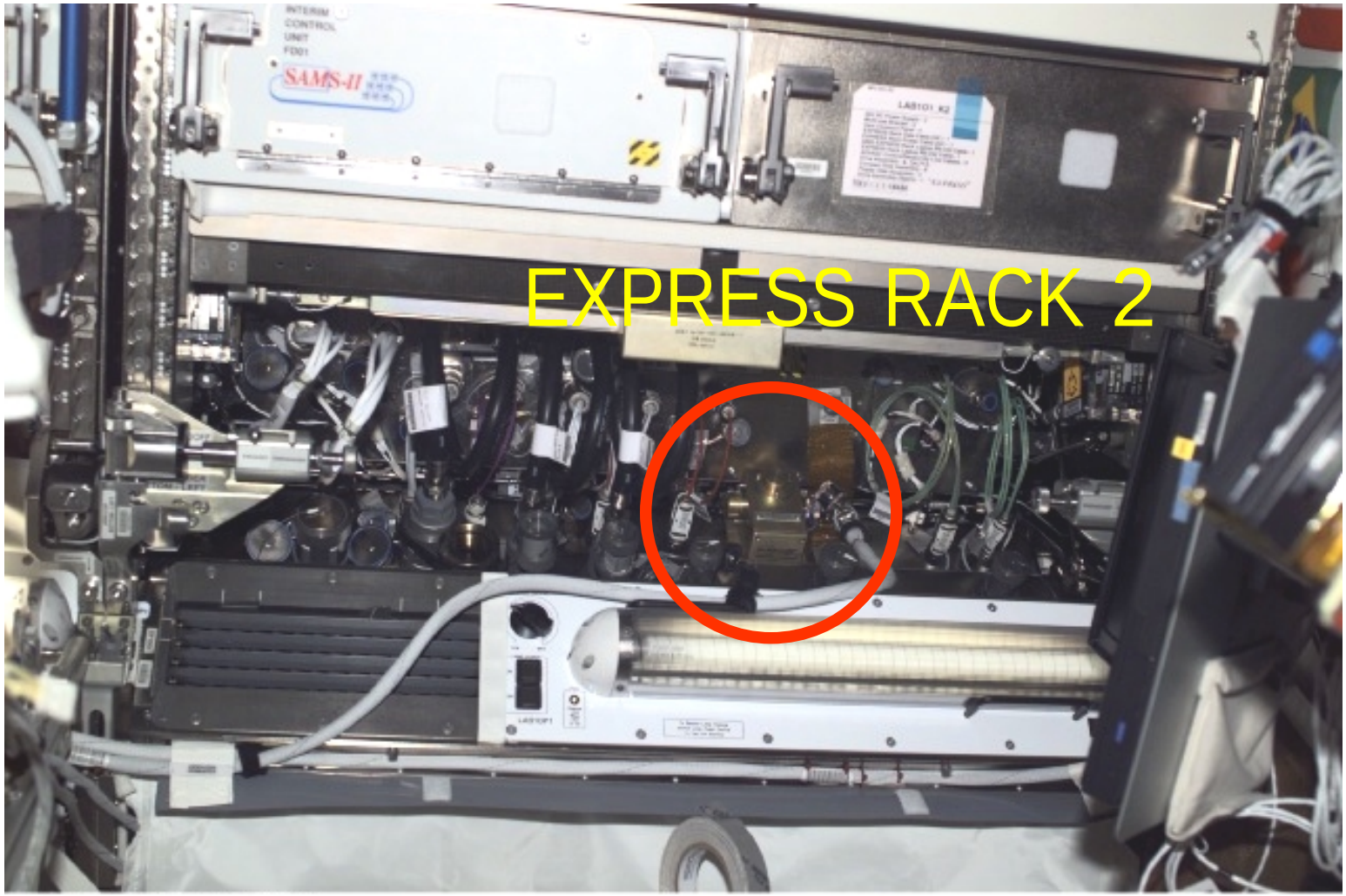

ISS002E7513 2001/06/22 11:20:15

Comparisons

- Sleep Period
  - 6A Prediction: All crew-induced accelerations were removed to simulate a sleep period.
  - SAMS-II data: Sleep period, 6/29/01, 100 second interval starting at 00:00 GMT.
- TVIS SDTO
  - 6A Prediction: Only crew-induced accelerations were TVIS operation (walking) and one crew push-off/landing.
  - SAMS-II data: TVIS SDTO period 6/28/01, 100 second interval starting at 10:29:10 GMT.

Predicted and Measured Stage 6A Microgravity Environment of EXPRESS Rack 2 Z-Panel During Crew Sleep Period

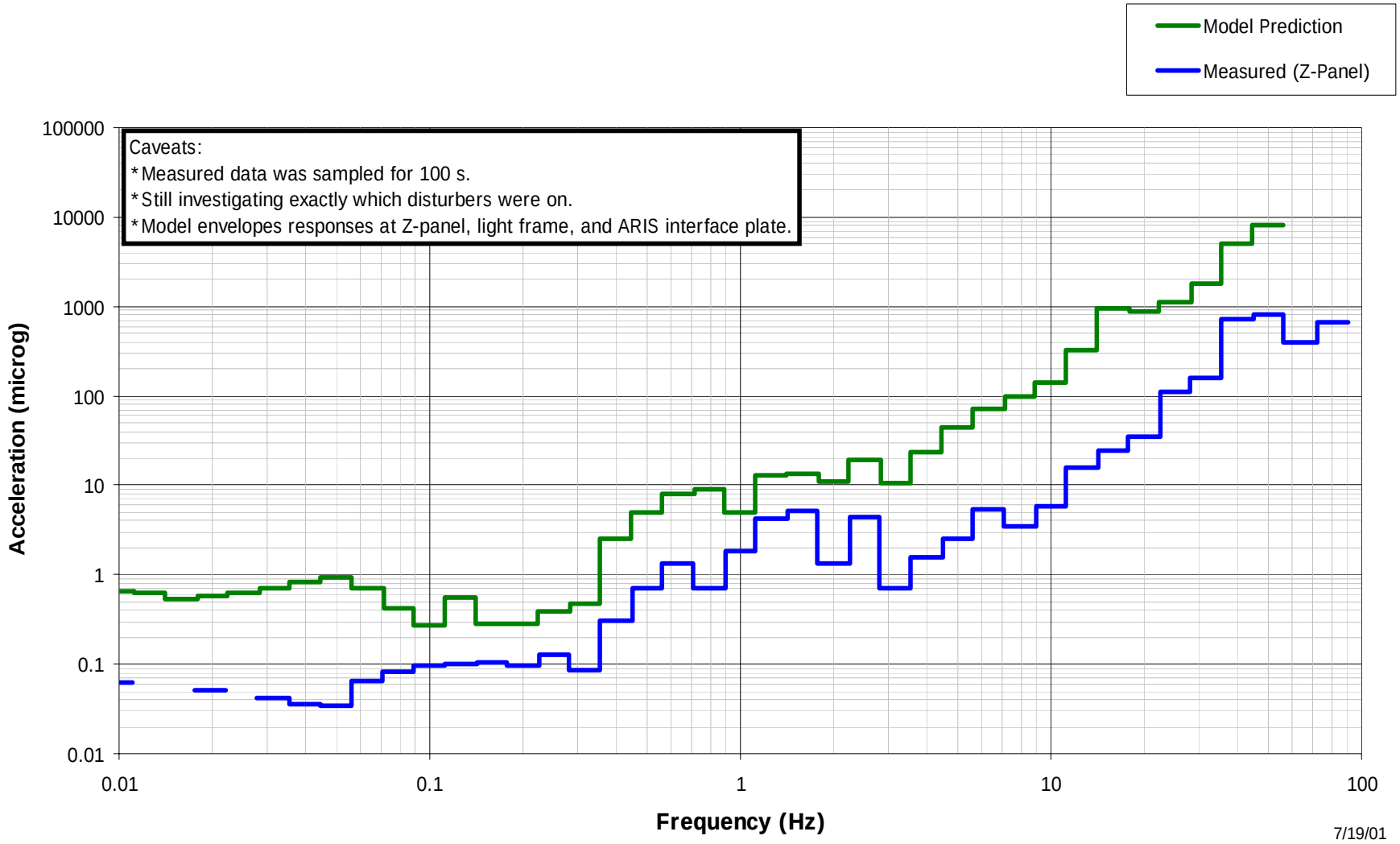

7/19/01

Sleep Period Discussion

- Caveats
  - Measured data was sampled for 100 s.
  - Still investigating exactly which disturbers were on.
  - Model envelopes responses at the LAB1O1 Z-panel, light frame, and ARIS interface plate.
- Observations
  - The model appears conservative throughout the frequency range (0.01-50 Hz). Considerable margin exists (3X-15X, depending on frequency).
  - The general shape of the model data agrees with the measured data.
  - In some frequency regions, the detailed shape of model data agrees with the measured data.

Predicted and Measured Stage 6A Microgravity Environment of EXPRESS Rack 2 Z-Panel During Treadmill Testing Period

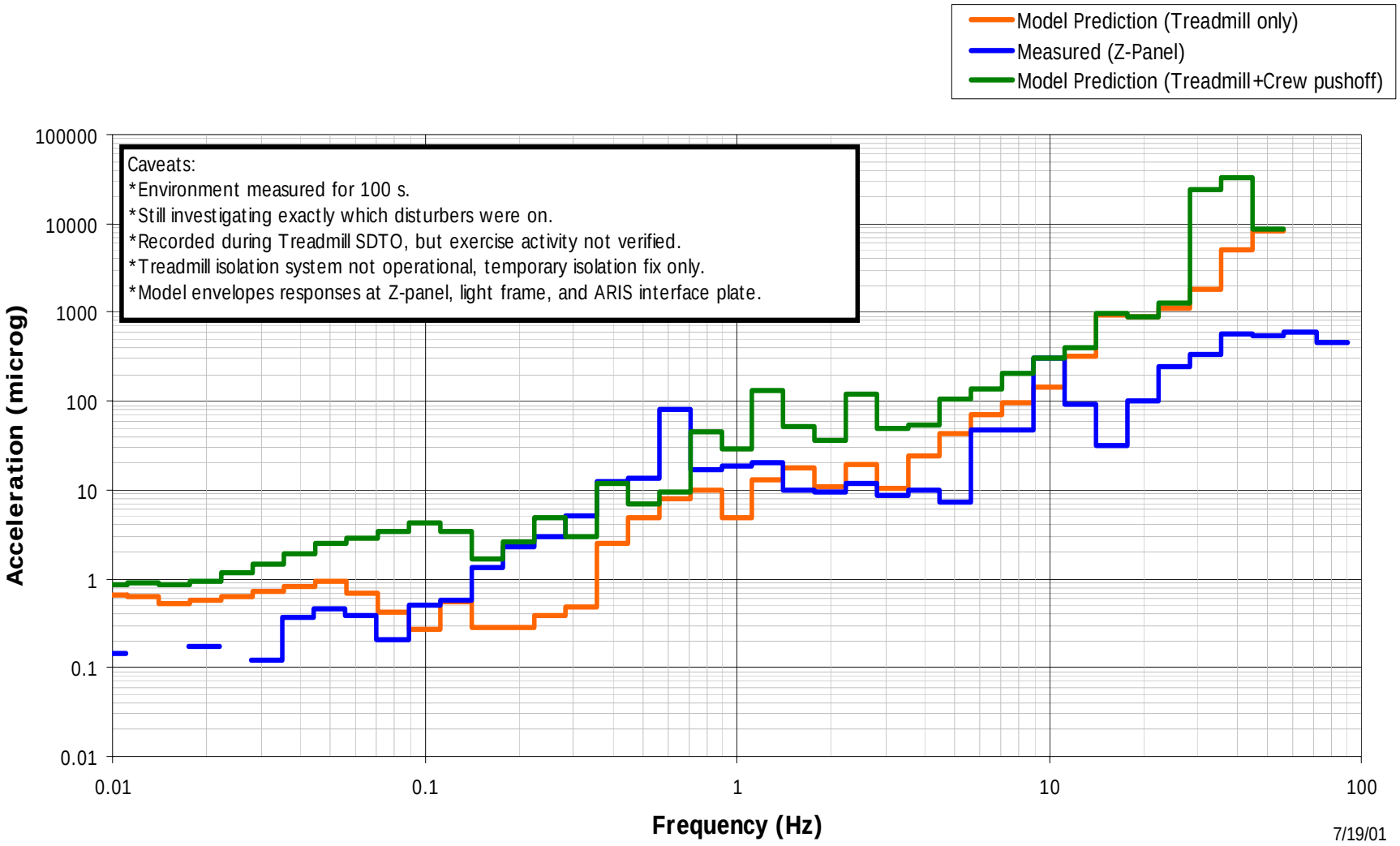

7/19/01

TVIS SDTO Period Discussion

- Caveats
  - Environment measured for 100 s.
  - Still investigating exactly which disturbers were on.
  - Recorded during Treadmill SDTO, but exact exercise activity (run, jog, walk) not verified.
  - Treadmill isolation system not operational, temporary isolation fix only.
  - Model envelopes responses at the LAB1O1 Z-panel, light frame, and ARIS interface plate.
  - Modeled crew pushoff is a worst case (9.34 lb push off followed by a 186.5 lb + 4476 in-lb landing). This pushoff dominates the 0.1-10 Hz range.
  - The treadmill was modeled as a superposition of five sinusoids, which does not sufficiently bring out the broadband nature of the true disturbance.

- Observations
  - Conservatisms not as obvious as in the sleep period comparison.
  - The general shape of the model data agrees with the measured data, except in the 0.1-1 Hz range, where the treadmill effects are dominant.
  - Except for the 0.1-1 Hz range, and one point at 10 Hz, the model data are below the Treadmill Only measured data.

Conclusions

The data presented here are only a cursory comparison between predicted and measured acceleration environment. It may be beneficial to accumulate many more periods and compare the average to the predicted environment. This forward work will be conducted by the PIMS and the Microgravity Integrated Products Team (MIPT). A possible benefit of continuing the study is to feed the results back into the Finite Element Model to improve its accuracy. It may also help find margin in the microgravity requirement that could be used by the payloads.

References

- Steelman, April, “Flight 6A Microgravity Analysis”, July 30, 1999.
- Steelman, April, email and teleconferences, 7/12, 18, 20/01.
- Steelman, April, “Flight 6A Environment Predictions for 2001 SSUAS Presentation" (AG-J32-STN-M-AMS-2001-0110), 8/21/01.

ISS Vibratory Acceleration Environment

Kenneth Hrovat
ZIN Technologies
Cleveland, Ohio

A computer will be available in the meeting room for access to the SAMS and MAMS data from the ISS. This will be a working session and a time for MGMG attendees to interact with PIMS project analysts and software engineers about data and data processing actions.

Discussion points about PCSA plots:

* It was pointed out that the PCSA plot is rather arcane so PIMS offered to develop a more complete explanation for the PCSA plot
* Eddie Snell (MSFC - PCG) commented that the PCSA type of plot is of particular use for crystal growers
  + PCG researchers have correlated the microgravity environment from these plots to success of crystal growth under various conditions on several Shuttle missions
* A request was received to include PCSA plots in the PIMS increment reports

ISS Vibratory Acceleration Environment

MGMG #20

7-Aug-2001

Kenneth Hrovat

ZIN Technologies

Brookpark, Ohio

Outline

- How much?
- Browse roadmap (bottom-up)
- Top-down correlation
- Demo
- Some findings
- Feedback

How much?

Acceleration Data Archive Through July 2001			
System	Sensor	Bytes	Gigabytes
SAMS-2	121f02	3,737,256,560	3.48
SAMS-2	121f03	12,818,314,800	11.94
SAMS-2	121f04	9,173,064,208	8.54
SAMS-2	121f05	5,773,426,784	5.38
SAMS-2	121f06	15,809,513,792	14.72
		SAMS-2:	**44.06**
MAMS	hirap	30,716,455,936	28.61
MAMS	ossraw	1,191,210,240	1.11
		MAMS:	**29.72**
		NASA GRC:	**73.78**

How much?

Percentage of July Recorded (744 Hours)			
System	Sensor	Hours	
MAMS	OSS raw	646.5	86.9%
MAMS	OSS btmf	408.2	54.9%
MAMS	hirap	295.9	39.8%
MAMS Total:		942.4	hours
SAMS	121f02	440.4	59.2%
SAMS	121f03	437.2	58.8%
SAMS	121f04	439.8	59.1%
SAMS	121f05	437.5	58.8%
SAMS	121f06	496.1	66.7%
SAMS Total:		2251.1	hours
NASA GRC Total:		3193.4	hours

How much?

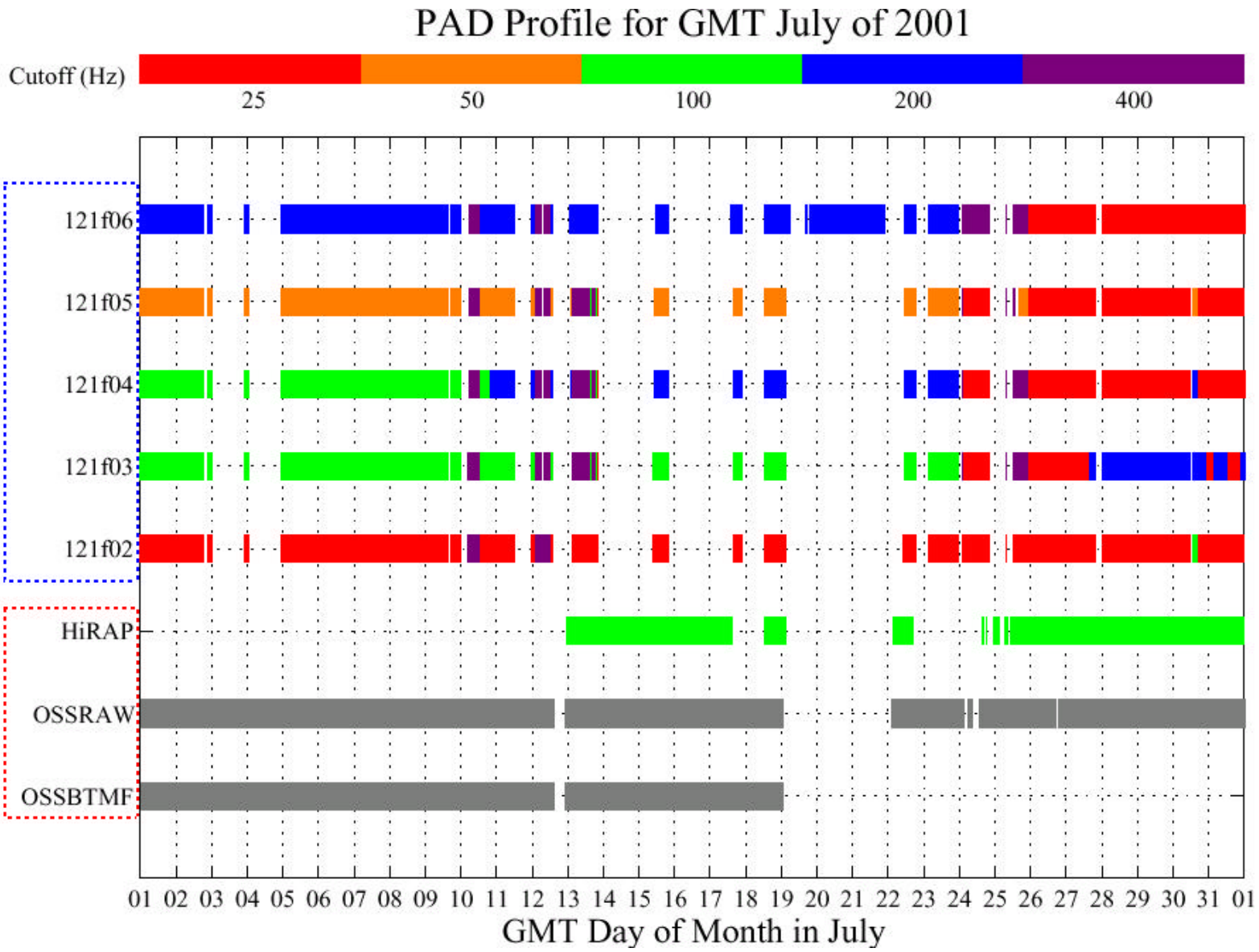
PAD Profile for GMT July of 2001
Cutoff (Hz)
25
50
100
200
400
121f06
121f05
121f04
121f03
121f02
HiRAP
OSSRAW
OSSBTMF
01 02 03 04 05 06 07 08 09 10 11 12 13 14 15 16 17 18 19 20 21 22 23 24 25 26 27 28 29 30 31 01
GMT Day of Month in July

Browse roadmap

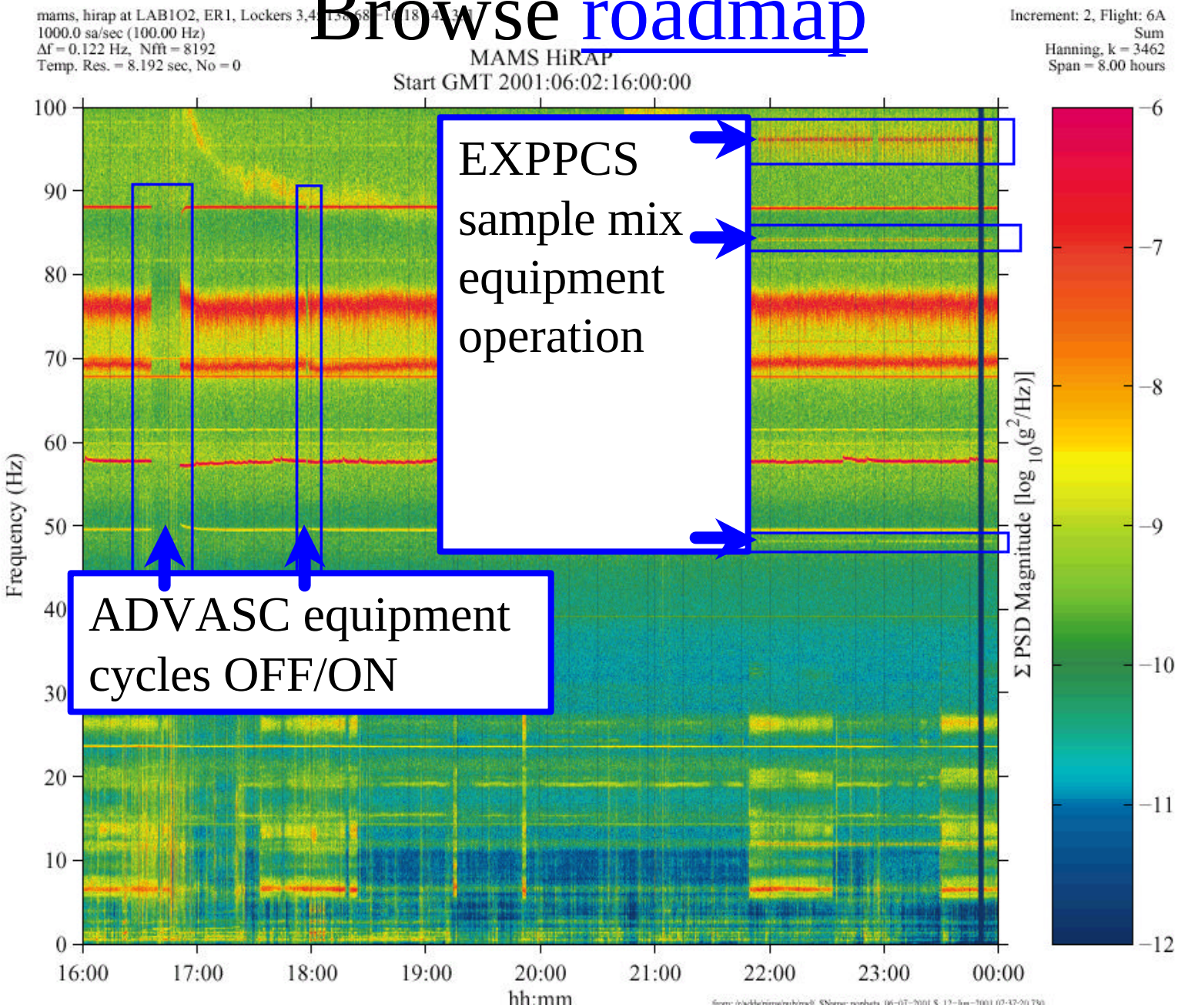

Top-Down Correlation

Key sources of information:

- As-flown attitude timelines & Short-term *plans*.
- Voice loops at Telescience Support Center - monitor & log communications between: cadre at MSFC, MCC at JSC, crew at ISS, and PIs.
- E-mail & telephone correspondence with experiment teams, payload developers (ARIS-ICE, EXPPCS, ADVASC), and MGMG people like you.
- Near real-time telemetry playback (vehicle state).
- ODRC database at JSC (cannot get through GRC firewall yet).

Outline

- How much?
- Browse roadmap (bottom-up)
- Top-down correlation
- Demo
- Some findings
- **Feedback**

Space Station Multi-Rigid Body Simulation (SSMRBS) Runs Comparison to On-Orbit MAMS Data

Michael R. Laible
Boeing, International Space Station
502 Gemini
Houston, TX 77058

One of the tasks that the microgravity sustaining engineering will have is to verify and predict the quasi-steady environment of the ISS. To accomplish this task the microgravity group will need tools to predict and verify the existing environment. The main tool currently used for quasi-steady analysis is the Space Station Multi-Rigid Body Simulator (SSMRBS), developed and maintained by the Johnson Space Center Engineering Directorate. To gain experience and knowledge of the simulation correlation with actual flight data, a state vector of the ISS stage 6A, was recorded and SSMRBS runs were performed to match the actual flight data from the Micro Acceleration Measurement System (MAMS). This presentation will document the inputs, runs performed, and findings of the comparison.

The procedures used for this study are outlined below:

1. Get actual vectors of stage 6A (ephemeris data).
2. Run a baseline version of SSMRBS, using atmosphere file with NOAA Solar Flux data and appropriate state vector.
3. Compare SSMRBS attitude with actual ISS attitude — adjust accordingly.
4. Compare simulation results with actual MAMS acceleration and ISS attitude values.
5. Perform additional runs changing simulation environment parameters to match actual flight attitude (ephemeris data) and MAMS acceleration values.
6. Compare results and summarize findings.

The MAMS data of interest was recorded between a GMT of 2001 / 127:22:00:00.072 and 128:07:00:00.072. All simulations and real-time data was gathered for this particular time frame.

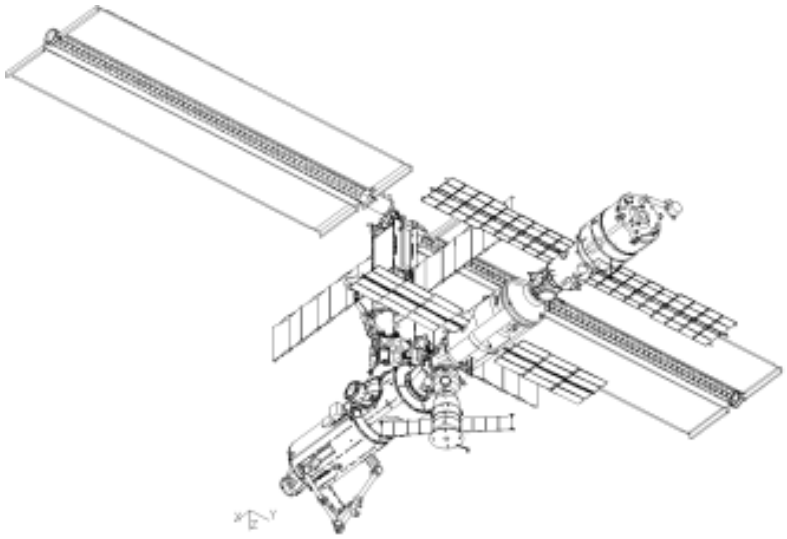

Figure 1 — 6A, Post 2R Relocation, ISS Configuration

NASA/CP—2001-211164

6A QUASI-STEADY MICROGRAVITY SSMRBS ANALYSIS AND MAMS REALTIME DATA COMPARISON

Structural Analysis Microgravity
Michael Laible
Boeing
281-853-1604

August 8, 2001

METHOD

- Received Draft report from PIMS concentrating on 9 hours of data during one sleep period
  - Begin GMT 2001/127:22:00:00.00 (May 7, 2001)
  - Acquire digital MAMS data
- Acquire ISS State vector during time of interest (On-orbit Data Retrieval Collection - ODRC)
- Acquire Solar Flux data during time of interest (NOAA Webpage - gopher://sec.noaa.gov/)
- Acquire appropriate configuration and mass properties (ODRC and Mass Properties Databook)
- Make SSMRBS comparison run and review deltas
- Converge by modifying initial conditions to SSMRBS

Michael.Laible@SW.boeing.com, 281-853-1604, Boeing

INITIAL CONDITIONS

- **Flight Dynamics weekly ISS Trajectory Report**
  - **http://spaceflight.nasa.gov/realdata/elements/**
- **Use ODRC real-time data**

LADP06MD2395H X Position J2K (m)
LADP06MD2396H Y Position J2K (m)
LADP06MD2397H Z Position J2K (m)
LADP06MD2399R X Velocity J2K (m/s)
LADP06MD2400R Y Velocity J2K (m/s)
LADP06MD2401R Z Velocity J2K (m/s)
LADP06MD7466U Attitude quaternion q1
LADP06MD7467U Attitude quaternion q2
LADP06MD7468U Attitude quaternion q3
LADP06MD7469U Attitude quaternion q4

On-orbit computation from RSA computers,
Vector update at least once a day
Data output once per second

LADP06MD2281H X ISS CM Vector (ref. Frame in m)
LADP06MD2282H Y ISS CM Vector (ref. Frame in m)
LADP06MD2283H Z ISS CM Vector (ref. Frame in m)

Ground Computed and uplinked

- **Quaternion Conversion**

Yaw = ATAN{[2*(q2*q3 + q1*q4)] / [q1^2 + q2^2 – q3^2 – q4^2] }*180/PI
Pitch = ATAN{[-2*(q2*q4 - q1*q3] / SQRT[1 - (2*(q2*q4-q1*q3))^2] }*180/PI
Roll = ATAN{[2*(q1*q2 + q3*q4)] / [q1^2 - q2^2 -q3^2 + q4^2] }*180/PI

Michael.Laible@SW.boeing.com, 281-853-1604, Boeing

INITIAL CONDITIONS (Cont.)

- **Stage 2r**

Sign Convention:
ISS x = MAMS x
ISSy = -MAMSz
ISSz = MAMSy

Mass Properties:

	SSMRBS	VIPeR	ODRC
ISSx CM (ft)	-36.8	-37.15	-38.58
ISSy CM (ft)	-0.10	-.07	-.07
ISSz CM (ft)	8.52	8.57	8.33
Mass (lbs.)	250,651.5	251,086.7	250,651.0

State Vectors:

	MOD-TOPO	ODRC
J2Kx (m)	4555272.46	4527442.00
J2Ky (m)	-3944756.64	-4038246.25
J2Kz (m)	3049891.45	2967785.75
J2Kxd (m/s)	1621.18	1718.66
J2Kyd (m/s)	5684.40	5598.92
J2Kzd (m/s)	4922.27	4987.01

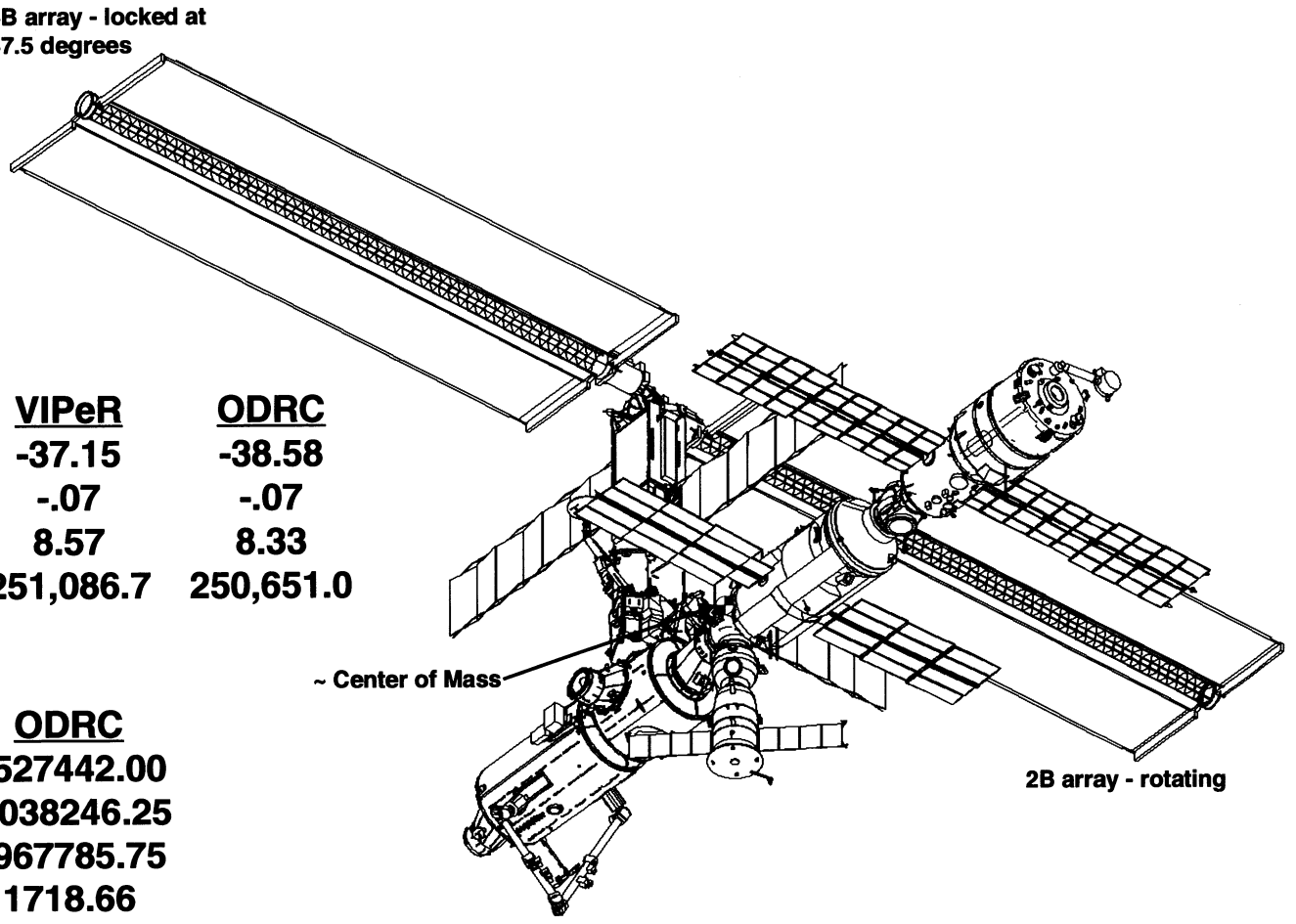

Michael.Laible@SW.boeing.com, 281-853-1604, Boeing

INITIAL CONDITIONS (Cont.)

- **Use Solar Flux conditions as reported on May 7, 2001, NOAA Webpage**
  - **Solar Flux affects the atmospheric density, thus ISS drag**
  - **SSMRBS uses Marshall Engineering Thermosphere (MET) Model**
- **Drag is calculated as flow across flat plates**
  - **Where** $f_D = \rho V^2 S C_D / 2$
- **Simulations performed using flat plate areas as shown**
  - **.5sm runs used half the sm_pva**

Body Flat Plate Area

X (ft^2)	y (ft^2)	z (ft^2)	Body Name
1566.2	3515.7	1875.0	core
25.8	16.7	732.0	fgb_pva
32.4	10.5	957.8	sm_pva
16.2	5.25	478.9	.5 sm_pva
83.4	70.5	3255.1	popv_aft
83.4	70.5	3255.1	popv_fwd

- **MAMS Location from PIMS:**
  - **ISS: x=11.27 ft, y=-.89 ft, z=11.01 ft**
  - **LVLH: x=48.10 ft, y=-9.46 ft, z=9.47 ft**

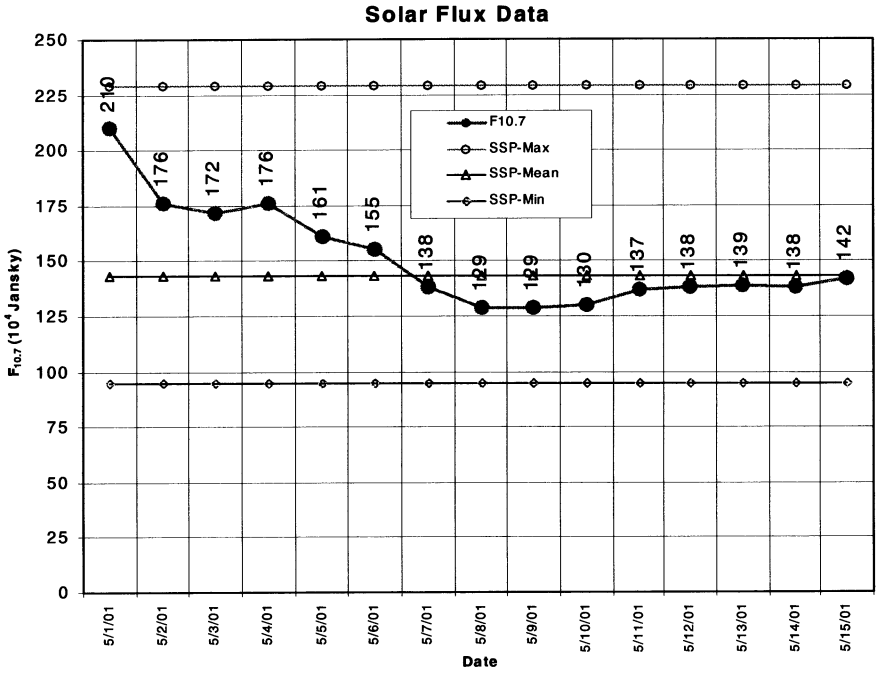

Michael.Laible@SW.boeing.com, 281-853-1604, Boeing

ANALYTICAL CHECK

USNG: $a_x = 0,\ a_y = -\mu\left(\frac{\Delta y}{r_g^3}\right),\ a_z = \mu\left(\frac{3\Delta z}{r_g^3}\right)$

Initial Parameters:

r (ft)	alt(ft)	mu	mu/(r+alt)^3
20925672.57	1263862	1.41E+16	1.29E-06

Using a mean attitude of y,p,r = -10.01, -8.16, 0.07:

	CG to iss	Iss to MAMS	cg to MAMS	LVLH(cg) to MAMS
x	-38.58	11.27	49.85	LVLHx=48.10
y	-0.07	-0.89	-0.82	LVLHy=-9.46
z	8.33	11.01	2.68	LVLHz=9.4

Now compute acceleration:

Ax=0+drag

Ay=-[(LVLHy)*mu/(r+alt)^3]/(32.174*10^{-6}) = -[(-9.46)*1.29E-06]/(32.174*10^{-6})= .379 μg

Az=[(LVLHz*3)*mu/(r+alt)^3]/(32.174*10^{-6}) = [(9.47)*1.29E-06]/(32.174*10^{-6})= 1.14 μg

Michael.Laible@SW.boeing.com, 281-853-1604, Boeing

RESULTS - ATTITUDE COMPARISON

- **LVLH Attitude comparison**

Three sets of curves:
1 - "Yaw, etc." - ODRC data
2 - "Ivy_.5sm_j2k, etc." - SSMRBS run, ODRC Mass properties, ODRC state vector, 1/2 SM array flat plate area
3 - "Ivy_nom, etc." - SSMRBS run, using mg control plan

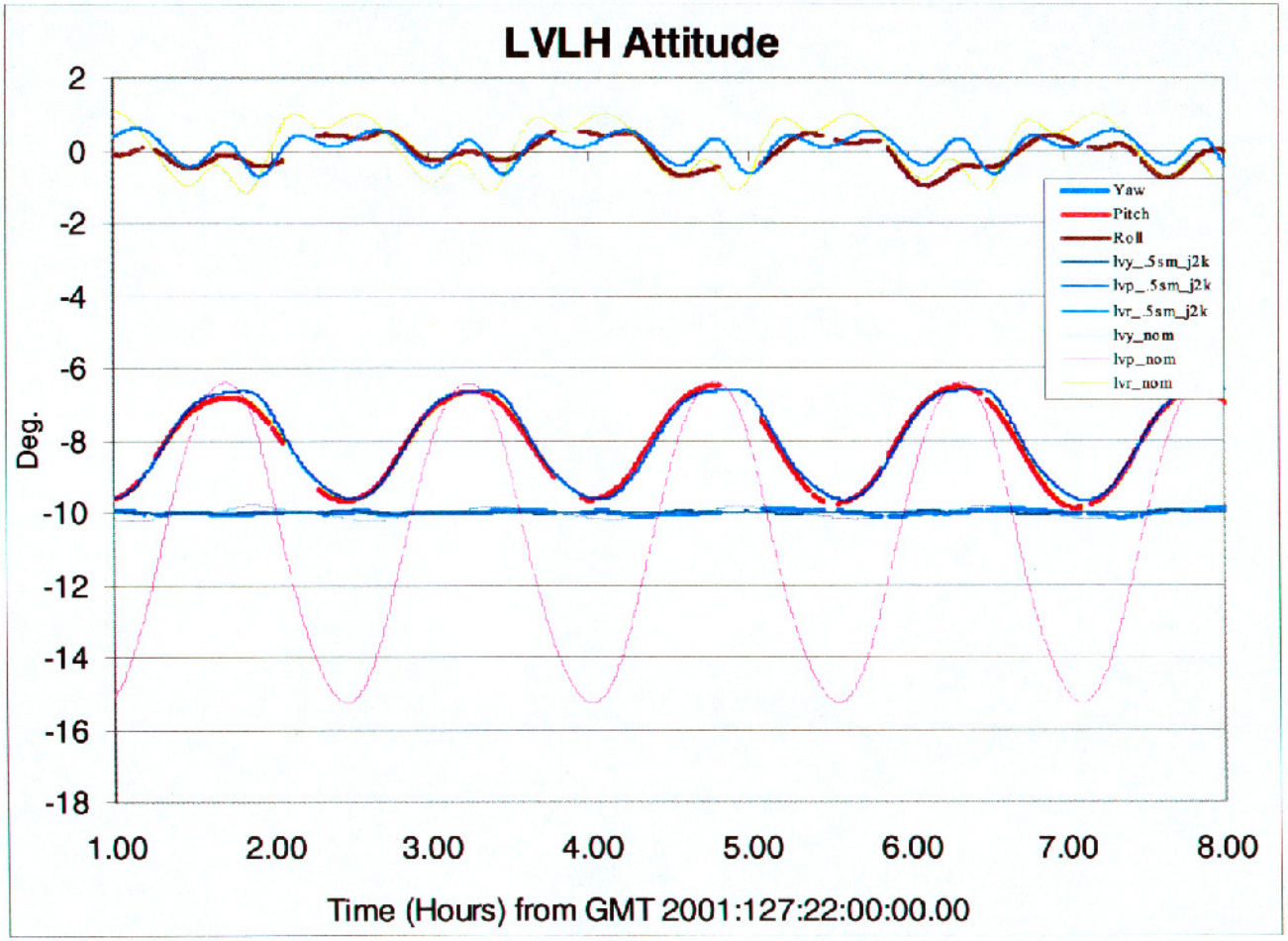

Michael.Laible@SW.boeing.com, 281-853-1604, Boeing

RESULTS - MAMS COMPARISON

- **Quasi-Steady x,y,z in μG**

Three sets of curves:

1 - "lssx, etc." - MAMS Real-time data, GMT 2001:127:22:00:00.00

2 - "lvy_.5sm_j2k, etc." - SSMRBS run, ODRC Mass properties, ODRC state vector, 1/2 SM array flat plate area

3 - "lvy_nom, etc." - SSMRBS run, using mg control plan

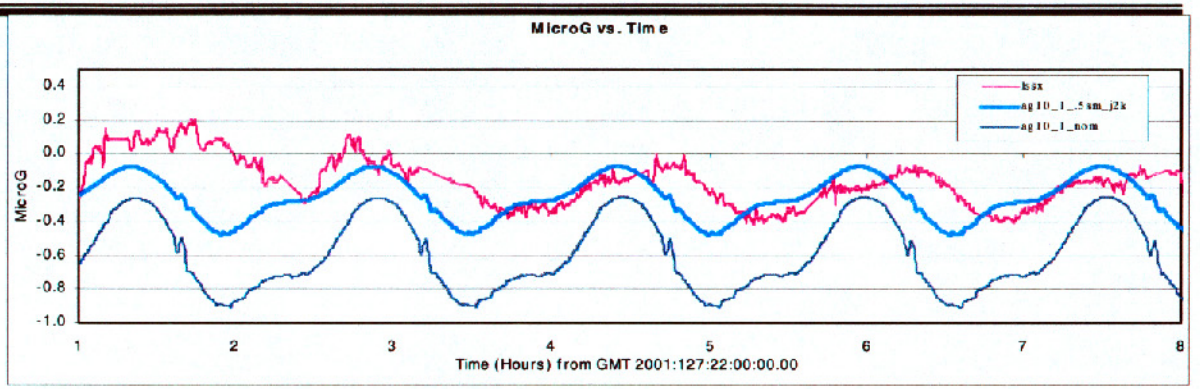

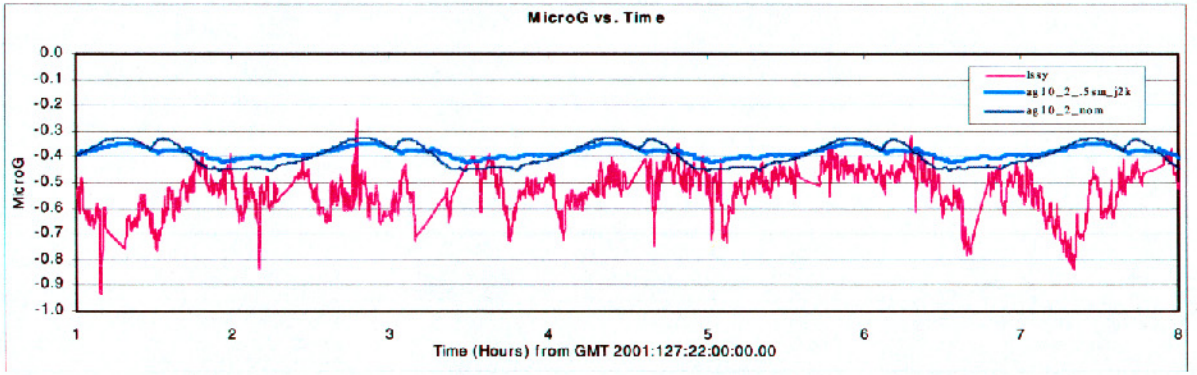

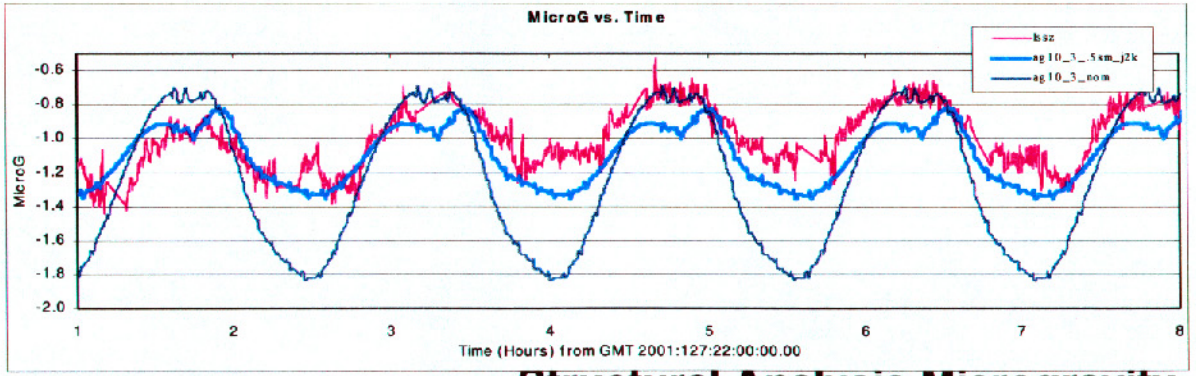

Michael.Laible@SW.boeing.com, 281-853-1604, Boeing

RESULTS - MAMS COMPARISON (Cont.)

- **Quasi-Steady Magnitude Comparison**

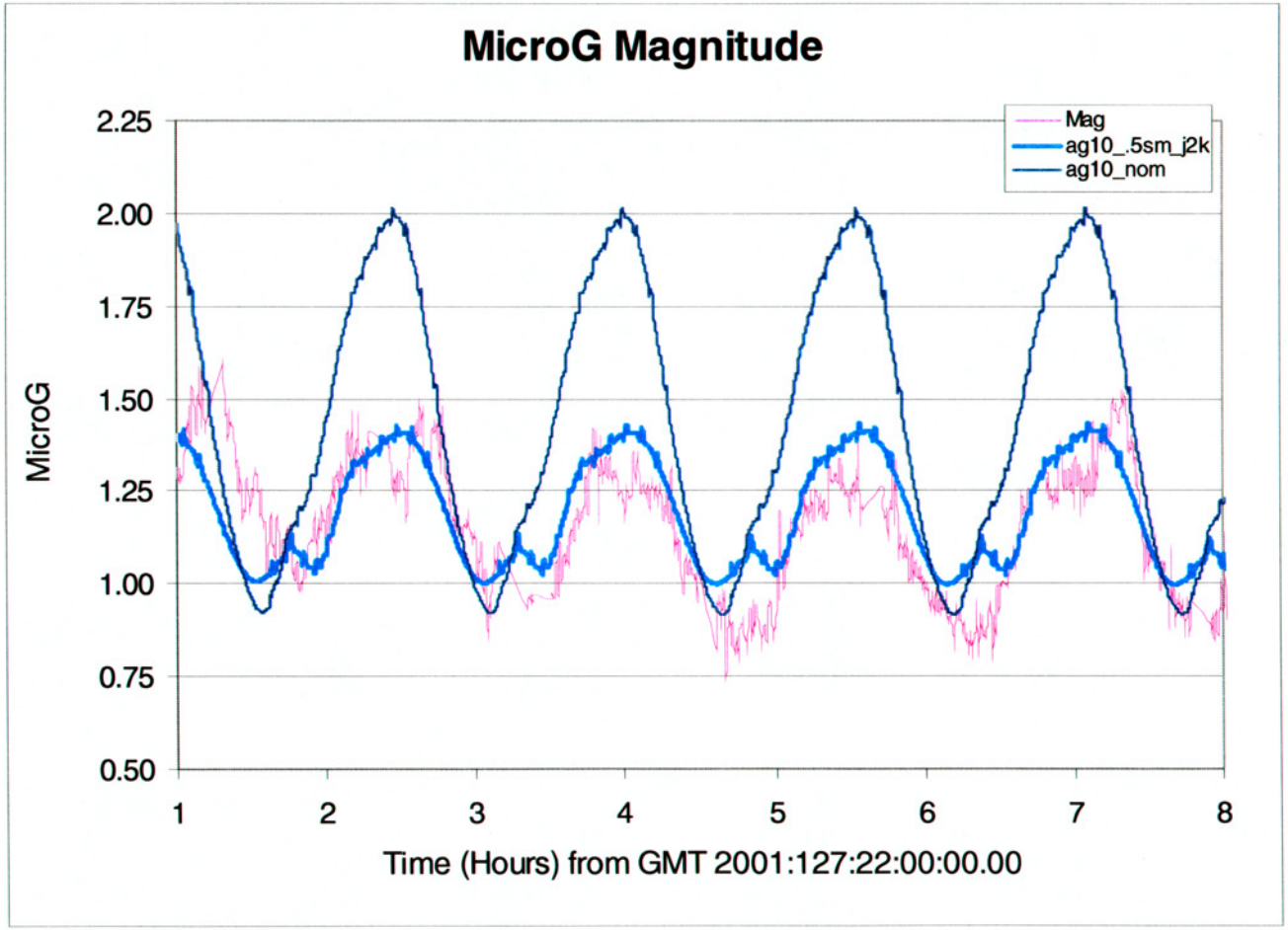

Michael.Laible@SW.boeing.com, 281-853-1604, Boeing

RESULTS - PREVIOUS ANALYSIS COMPARISON

- 6A Parametric Study produced July, 1999
- Baseline case is mxsf_lwalt
- MAMS Location similar to USLC2
- MAMS Maximum value is approximately 1.5 μg

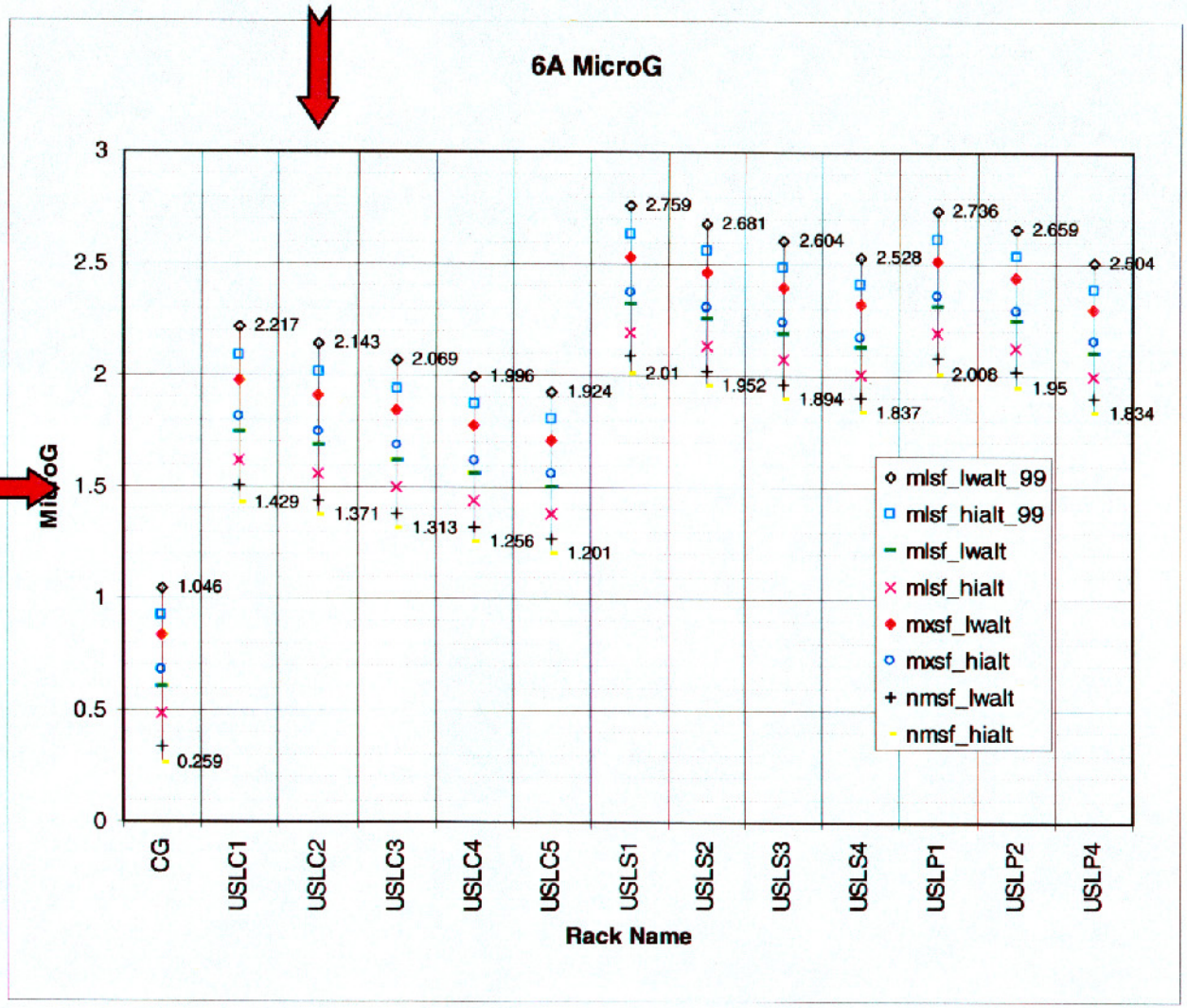

Michael.Laible@SW.boeing.com, 281-853-1604, Boeing

SUMMARY

- Comparison of SSMRBS and MAMS exhibit similar trends
- Using ODRC State Vector produced similar attitude profiles
- Slight modifications to Flat Plate area and mass properties produced good results
- Slight deltas could be difficult to mitigate - various
  - Center of Mass delta
  - MAMS location delta
  - CMG torque output
  - Atmospheric density
- Percent deltas from Mean and RMS:

	ISSx	ISSy	ISSz	Magnitude
MAMS Mean	-0.1591 μG	-0.5344 μG	-0.9988 μG	1.1558 μG
MAMS RMS	0.2140 μG	0.5414 μG	1.0134 μG	1.1687 μG
.5SM SSMRBS Mean	-0.2710 μG	-0.3848 μG	-1.0960 μG	1.2024 μG
.5SM SSMRBS RMS	0.2970 μG	0.3852 μG	1.1089 μG	1.2109 μG
% diff. of MAMS Mean	70.3 %	-28.0 %	9.7 %	4.0 %
% diff. of MAMS RMS	38.8 %	-28.8 %	9.4 %	3.6 %
NOM SSMRBS Mean	-0.6180 μG	-0.3948 μG	-1.2506 μG	1.4763 μG
NOM SSMRBS RMS	0.6517 μG	0.3972 μG	1.3144 μG	1.5199 μG
% diff. of MAMS Mean	288.4%	-26.1%	25.2%	27.7%
% diff. of MAMS RMS	204.6%	-26.6%	29.7%	30.0%
Analytical Value	N/A	.379 μG	1.14 μG	N/A

Michael.Laible@SW.boeing.com, 281-853-1604, Boeing

ADDENDUM

- **To converge on a solution, several μg points of interest were designed to envelop the MAMS location.**

```
11.27     -0.89     11.01     !BASELINE MAMS_1_02_RACK_GRC
11.27     -1.89     11.01     !01 MAMS_1_02_RACK_GRC
11.27     -2.89     11.01     !02 MAMS_1_02_RACK_GRC
11.27     -3.89     11.01     !03 MAMS_1_02_RACK_GRC
11.27     -4.89     11.01     !04 MAMS_1_02_RACK_GRC
11.27     -1.89     10.01     !05 MAMS_1_02_RACK_GRC
11.27     -2.89     10.01     !06 MAMS_1_02_RACK_GRC
11.27     -3.89     10.01     !07 MAMS_1_02_RACK_GRC
11.27     -4.89     10.01     !08 MAMS_1_02_RACK_GRC
11.27     -1.89      9.01     !09 MAMS_1_02_RACK_GRC
11.27     -2.89      9.01     !10 MAMS_1_02_RACK_GRC
```

- **Run was the same as .5sm_j2k**
- **The points were compared to MAMS flight data and best fit used**
  - **Delta position used is ISSy = +2 feet, ISSz = -1 foot, noted as ag21 on plots**

	ISSx	ISSy	ISSz	Magnitude
MAMS Mean	-0.1591 μG	-0.5344 μG	-0.9988 μG	1.1558 μG
MAMS RMS	0.2140 μG	0.5414 μG	1.0134 μG	1.1687 μG
.5SM SSMRBS Mean	-0.2710 μG	-0.3848 μG	-1.0960 μG	1.2024 μG
.5SM SSMRBS RMS	0.2970 μG	0.3852 μG	1.1089 μG	1.2109 μG
% diff. of MAMS Mean	51.6 %	-13.3 %	-1.8 %	-2.9 %
% diff. of MAMS RMS	26.1 %	-14.4 %	-1.8 %	-3.2 %

Michael.Laible@SW.boeing.com, 281-853-1604, Boeing

ADDENDUM (Cont.)

- **Quasi-Steady Magnitude Comparison of baseline MAMS position and new position of ISSy = +2 feet, ISSz = -1 foot**

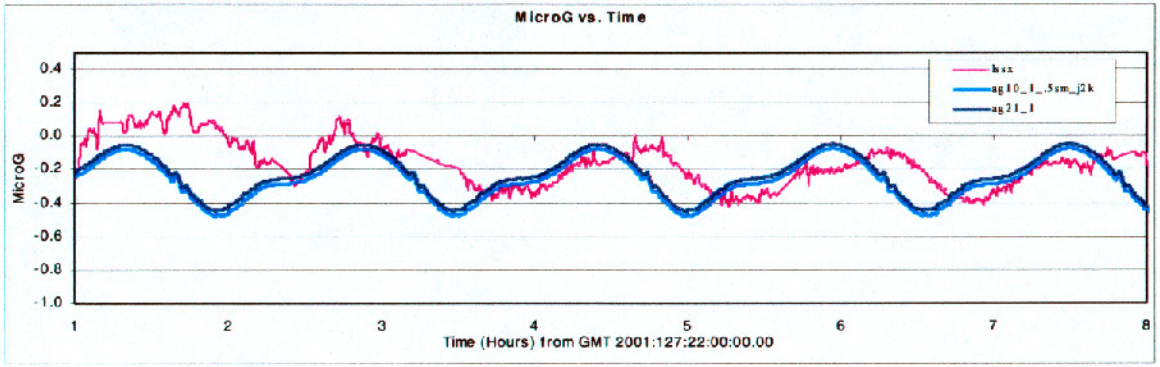

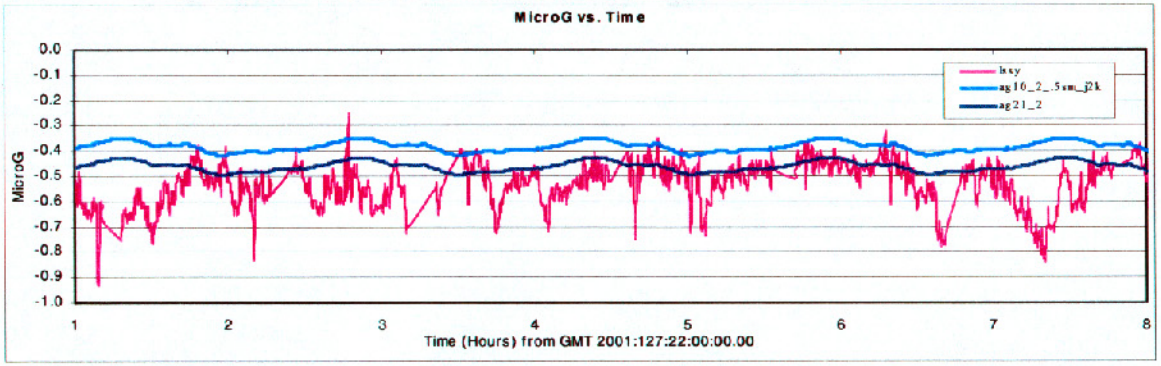

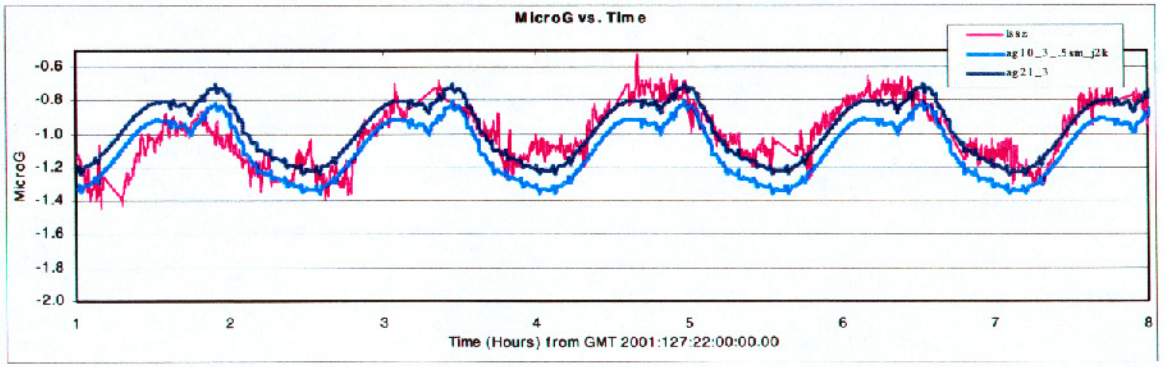

Michael.Laible@SW.boeing.com, 281-853-1604, Boeing

ADDENDUM (Cont)

- **Quasi-Steady Magnitude Comparison of baseline MAMS position and new position of ISSy = +2 feet, ISSz = -1 foot**

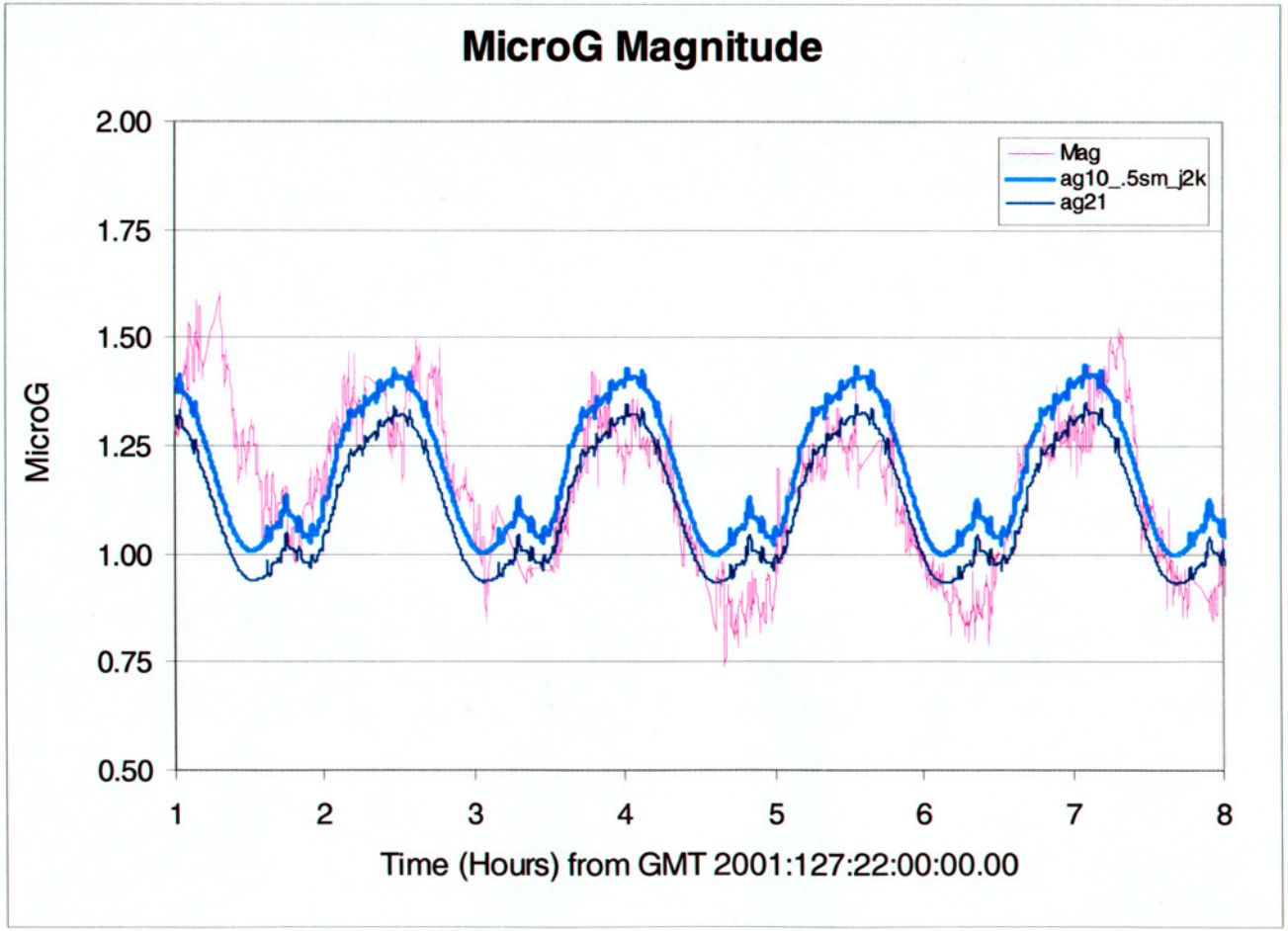

Michael.Laible@SW.boeing.com, 281-853-1604, Boeing

Features of space microacceleration measurement program SINUS for FOTON type satellites

Oleg L. Mumin, CSRI Elektropribor, St. Petersburg, Russia
Vladimir G. Peshekhonov, CSRI Elektropribor, St. Petersburg, Russia
Gennady P. Anshakov, CSDB, Samara, Russia
Valentin F. Agarkov, CSDB, Samara, Russia

SINUS is a program of developing and using a system for measuring nano- and microaccelerations to ensure the flights of "technological" satellites designed by the Central Specialised Design Bureau in Samara. The program SINUS is founded on the microacceleration measuring systems Sinus type, developing of the CSRI Elektropribor, St.Petersburg, Russia.

The purpose of the program SINUS is to integrate partial problems aimed at providing microgravitational conditions aboard process spacecrafts. The program includes the following problem issues:

1. Measuring accelerations aboard spacecrafts during the orbital flight;
2. Measuring microaccelerations aboard spacecrafts during pre-flight ground preparation;
3. Reducing the influence of on-board and research equipment on the level of microaccelerations;
4. Development of facilities for measuring microaccelerations aboard spacecrafts;
5. Development of data processes programs;
6. Statement of requirements to microgravitational conditions aboard process spacecrafts.

This paper discusses some aspects of developing and using of microacceleration measuring systems Sinus type. It also discusses some results of Photon12 spaceflight (system Sinus12K was installed and worked aboard this spacecraft) and prospects for the future space missions of microgravitational platform FOTON-M#1, that will launch in the next year.

Features of space microacceleration measurement program SINUS for FOTON type satellites

results and prospects

Oleg L. Mumin, Vladimir G. Peshekhonov, St.Petersburg, Russia.
Gennady P. Anshakov, Valentin F. Agarkov, Samara, Russia.

Key words: space, microgravitation, measuring, accelerometer, spacecraft.

Abstract

The paper deals with the results of developing facilities and methods used aboard spacecrafts to provide the required microgravity conditions for manufacturing and research work under weightlessness conditions. The prospects for employing various spacecrafts for performing different operations under microgravity conditions are discussed. **SINUS**, *the program that specifies the main lines in developing and refining microgravity technologies, is considered.*

Space investigations are one of the most expensive types of scientific and industrial work, and hence the recoupment of capital investment has always been of vital importance. The employment of orbital spacecrafts for unique technologies that can only be realized successfully under weightlessness conditions is rather promising and profitable. That is the reason that the problem of using "microgravity" technologies for manufacturing materials and compounds of unique properties is given much attention to practically by all the leading countries: the USA, Russia, France, Germany, Japan, Canada, Italy, Brazil [1].

The basic investigations on the possibilities to use microgravity conditions have been conducted and are in progress now aboard the spacecrafts *Photon, Bion,Mir* (Russia), *Space Shuttle* (USA). Multiple experiments on manned (*Mir, Space Shuttle*) and unmanned spacecrafts (*Photon, Bion)* showed that the quality of the materials produced on unmanned spacecrafts is much higher. First of all, this is due to the fact that the microaccelerations aboard *Photon* and *Bion* are an order of magnitude lower as compared to the other spacecrafts where it would be possible to perform manufacturing and research work.

At present some of potential customers orients to employing special modules of the International Space Station (INSS). The Russian developers consider specialized spacecrafts *Photon* and *Nika* more promising. The possibilities for creating proper conditions aboard the INSS seem to be problematic.This opinion is based on the analysis of the construction and operational conditions of the INSS. The construction of the station is characterized by large dimensions and low stiffness. Misalignment of the center of mass and the center of aerodynamic pressure in the presence of significant aerodynamic resistance (orbital altitude of 385 km) will cause, under the conditions of low damping, angular oscillations of the station. Microaccelerations aboard the INSS will most likely be at the level more than 10^{-6}g, which is supported by the theoretical research done in the Central Specialized Design Bureau (CSDB) in Samara [2]. The microgravity conditions aboard *Photon* are favorably distinguished from those on the INSS due to the fact that *Photon* has compact rigid structure, does not contain solar panels and its center of mass is practically aligned with the center of aerodynamic pressure [3].

At the moment extensive manufacturing and research work is being and is supposed to be conducted under weightlessness conditions: semiconductor crystal growth, organic crystal growth (interferons, and the like), research on growth and functioning of biological objects, etc.

Generally speaking, the requirements of the users to the microgravity conditions necessary for successful realization of the program today are not systematized as yet, but they are the same in the main parameters [4]. Tentatively, they are as follows in Table 1.

Table 1

Frequency range	*Microacceleration range*
10 – 300 Hz	$10^{-4} - 10^{-3}$g
0.1 – 10 Hz	$10^{-5} - 10^{-4}$g
0.001 – 0.1 Hz	$10^{-6} - 10^{-5}$g
0.0 – 0.001 Hz	$10^{-7} - 10^{-6}$g

A number of firms and governmental organizations in the USA, France, Germany and the European Community employ *Photon* and *Bion* designed in the Samara CSDB for their manufacturing and research work under weightlessness conditions. "Weightlessness" is generally understood as conditions under which gravitational and inertia forces are lacking. However, "absolute" weightlessness aboard any spacecraft is unavailable. In a free uncontrollable flight of a spacecraft in space the effect of gravitational and inertia forces is considerably (1000 and more times) less than on the Earth. "Fine" investigations and technologies call for tight control (inspection certification) of the residual gravitation (microgravitation) and microacceleration effects. The equipment for performing inspection certification aboard the spacecraft is developed by many firms, however the following systems are known to be the leaders: *SAMS* designed by Glenn Research Center, NASA, USA, *SINUS* designed by the CSRI *Elektropribor*, St.Petersburg, Russia [5], and *BETA* designed by *CNES*, France.

At present it is considered that these systems are of similar accuracy and reliability, but *SINUS* is thought to be the most promising among them, as it allows for further perfection. It is connected with great potentialities of the accelerometers MSTA and ESTA, developed in the CSRI *Elektropribor* exclusively for space microacceleration measuring.

The accelerometer MSTA (magnetic spherical triaxial accelerometer) [5] is an accelerometer with a contactless magnetic suspension of a levitating spherical rotor. The characteristics of the accelerometer may vary in a wide range due to possibility to change standard electronic components only. The accelerometer ESTA (electrostatic spherical triaxial accelerometer) presents a spherical rotor that levitates in the electrical field of the suspension. ESTA has capabilities to reach a sensitivity of up to 10^{-10}g.

The system *Sinus6K* was first used to measure microaccelerations aboard *Photon11* in October 1997. The main microacceleration measurement results obtained by *Sinus6K* were reported at the 18th MGMG [5].

The next modification of *SINUS – Sinus 12K* was designed for *Photon12*. The main peculiarities of *Sinus12K* as compared to *Sinus6K* are the increase of the number of measuring channels from 6 to 12, improvement of accelerometer sensitivity to 10^{-7}g and extension of the time period over which it is possible to measure microaccelerations from 32 to 400 hours [5]. *Photon12* was launched in September 1999. 12 sets of measurements were performed during the flight in the frequency ranges of 0 –0.1Hz, 0.2 – 10 Hz and 10 – 300 Hz. The measurement results in the ranges

of 10 – 300 Hz and 0.2 – 10 Hz are close to the similar results obtained on *Photon11*. The measurement results in the range of 0 – 0.1 Hz show that the values of the so-called "quasi-constant accelerations" do not exceed several units of micro-g (10^{-6}g). Fig.1 and Fig.2 represent results of measurements of quasi-steady accelerationes in 7th set (19.09.99 – 20.09.99).

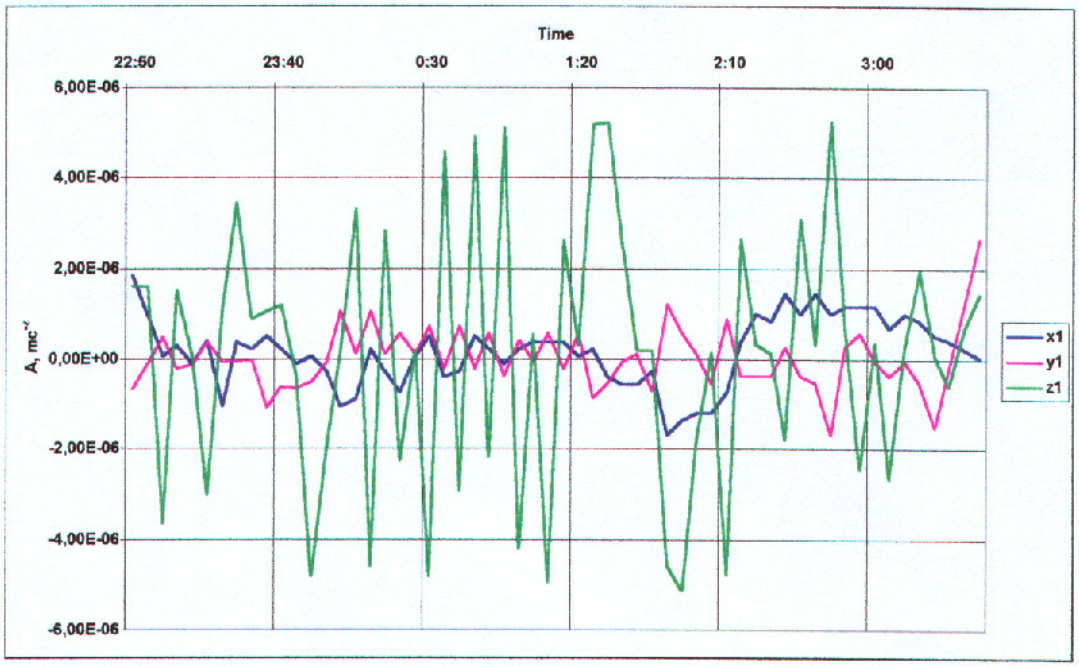

Fig.1 (MSTA N1)

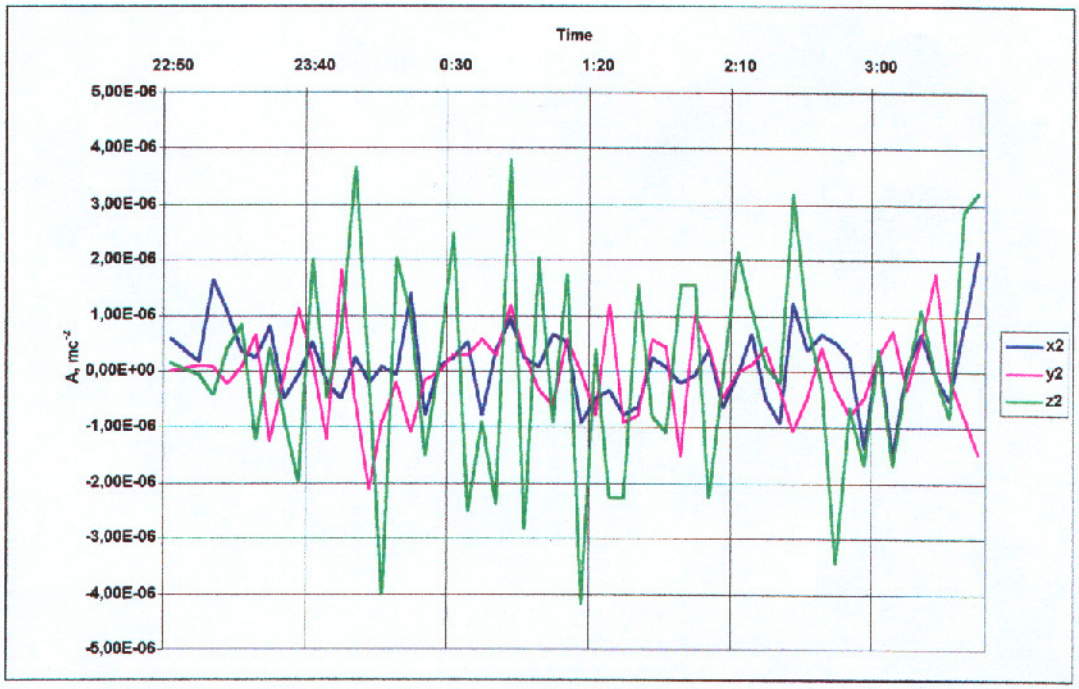

Fig.2 (MSTA N2)

One of the features of the *Photon12* flight program was using Sinus12K to measure motion parameters of *Photon12*. Fig.3 – 6 represent the results of an acceleration measuring by Sinus12K when *Photon12* was braking for landing from the orbit 24.09.99.

Here: Fig.3 – changing of the *Photon12* velocity in the orbital velocity direction (axis X of the accelerometer), Fig.4 – acceleration in the orbital velocity direction, Fig.5,7 and Fig.6,8 – velocity and acceleration in the direction perpendicular to the orbital velocity (axis Y and Z of the accelerometer.

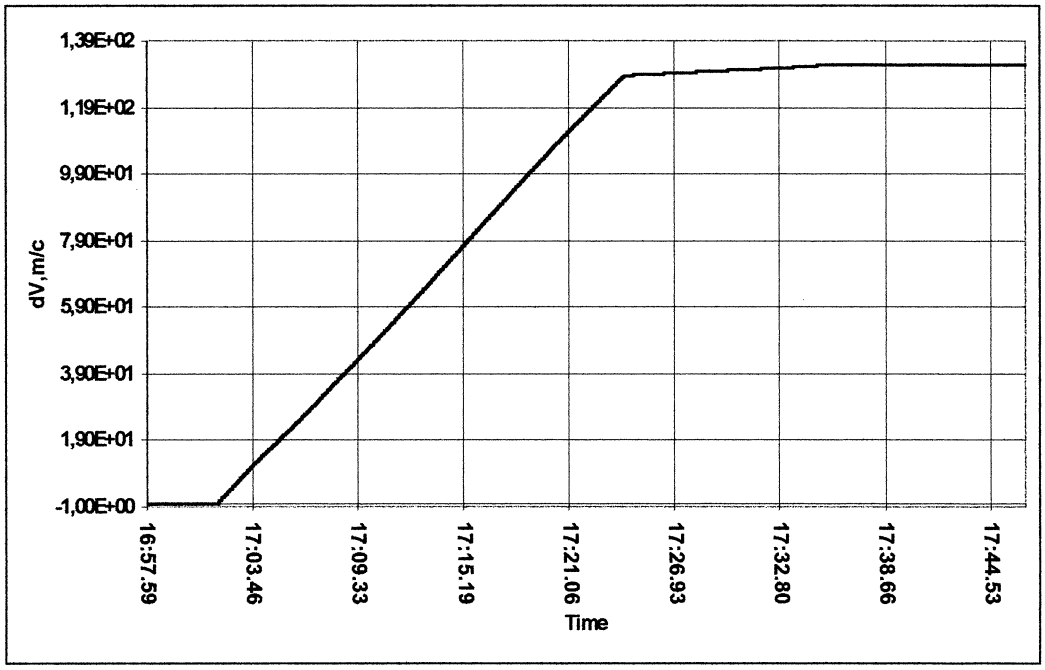

Fig.3 (axis X)

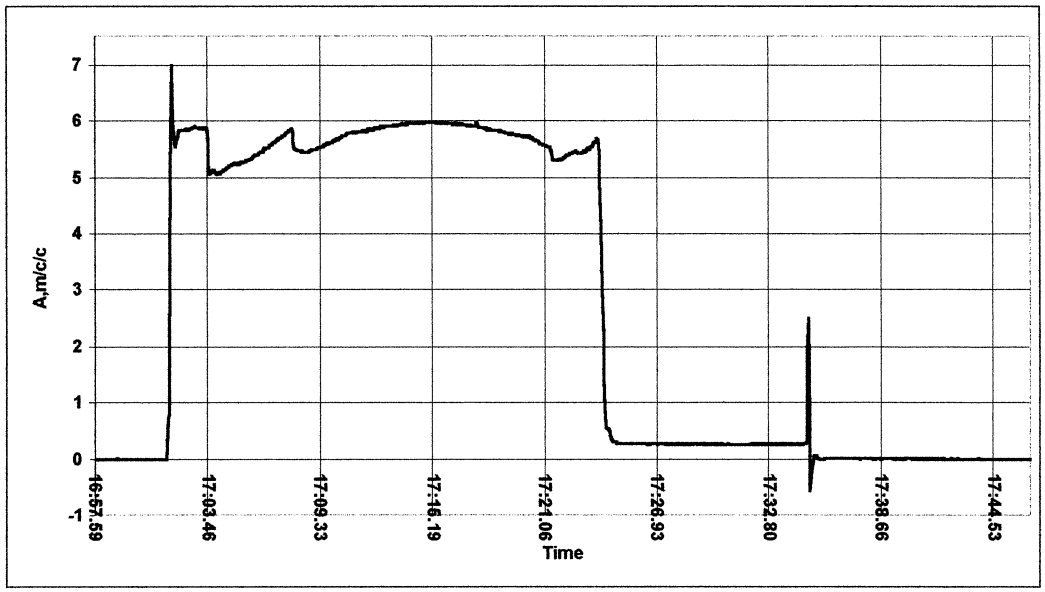

Fig.4 (axis X)

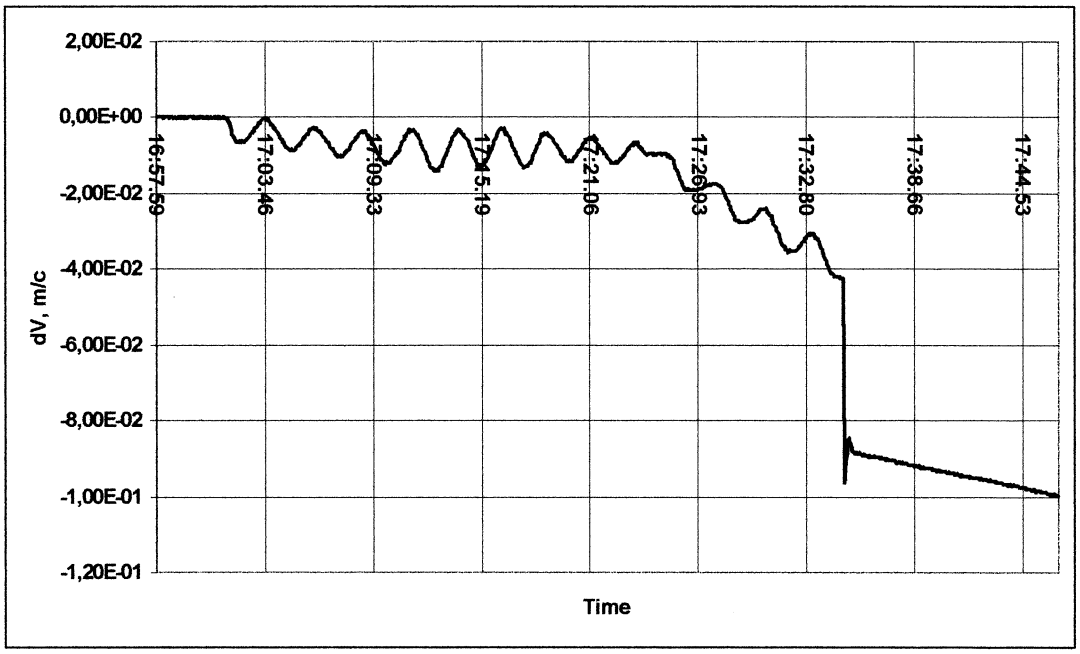

Fig.5 (axis Y)

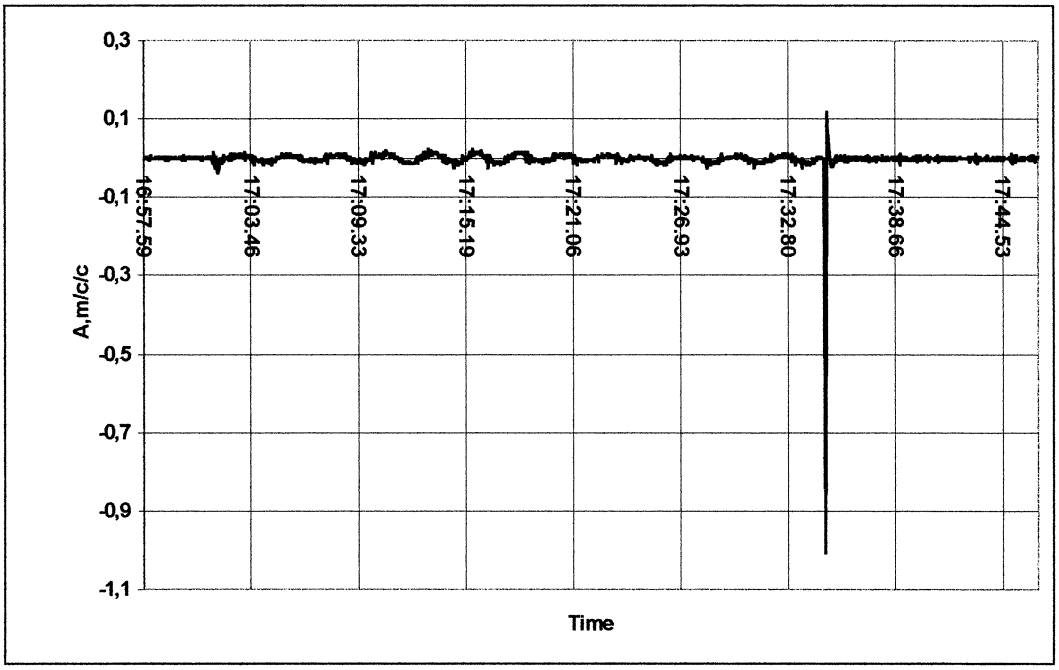

Fig.6 (axis Y)

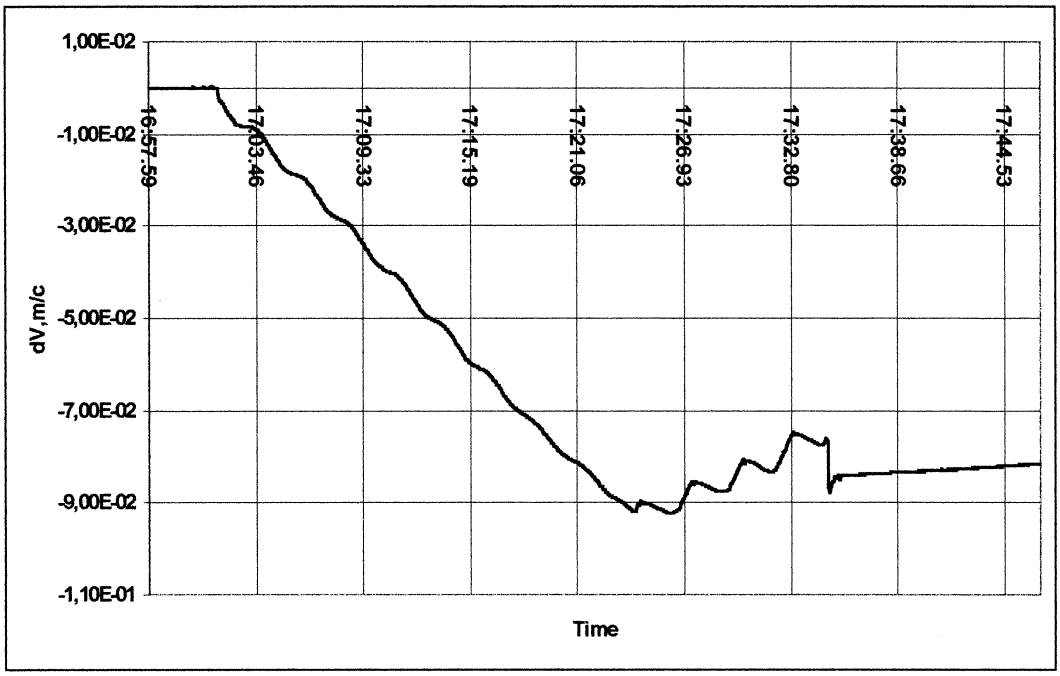

Fig.7 (axis Z)

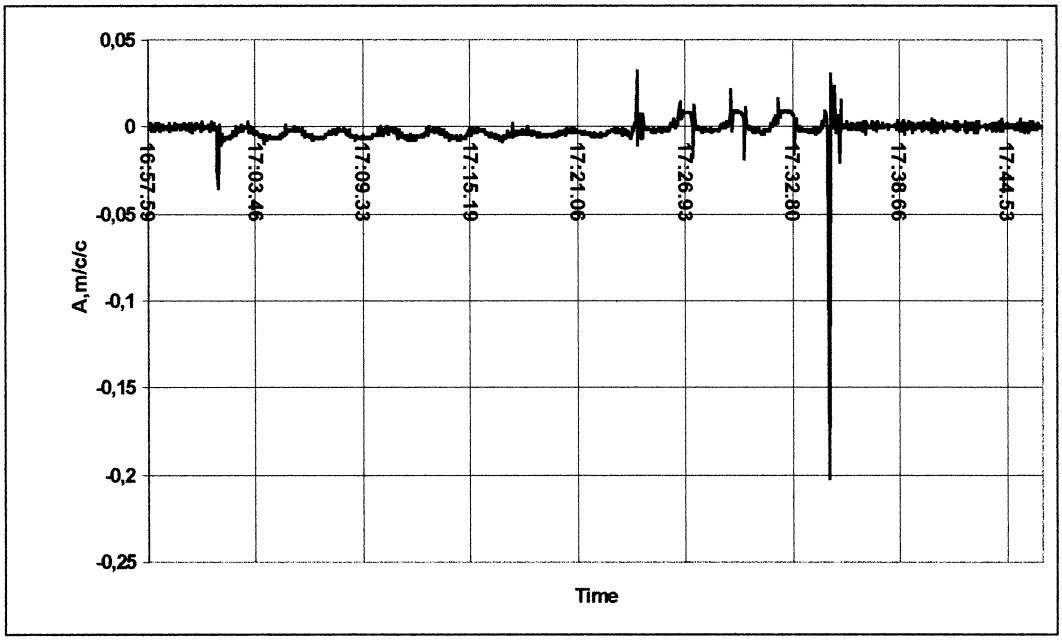

Fig.8 (axis Z)

The test results demonstrate of the capability of Sinus12K to measure accelerations for the satellite motion control. It is one of the tasks of the "Program **SINUS**", see below (lines 4.4, 4.5).

The next Photon is expected to be launched in 2001. For this, a system *Sinus 15K* has been designed and is now being adjusted and tested under terrestrial conditions. *Sinus 15K* includes 5 three-axis accelerometers. Two of them have the sensitivity of 10^{-8}g, the other two – 10^{-7}g, and one accelerometer – 10^{-6}g. The information obtained by *Sinus 15K* during the flight is transmitted to the ground-based flight control center, thus allowing operative decisions about the organization of experiments and manufacturing and research work aboard *Photon*. Besides this the *Sinus15K* is significantly lighter than *Sinus12K*.

Step-by-step extension of the *Sinus* potentialities described above is provided by the program **SINUS**, which enables integrated development of the facilities used to ensure the required microgravity conditions aboard spacecrafts.

The program **SINUS** involves the following main problems that are to be solved:

1. Measuring accelerations aboard the spacecraft during the orbital flight.

1.1 High-frequency components of microaccelerations.
1.2 Low-frequency components of microaccelerations.
1.3 Quasi-constant components of microaccelerations.
1.4 Angular rates.

2. Measuring microaccelerations aboard the spacecraft during the ground-based preflight preparation.

2.1 Checking the influence of the onboard equipment on the level of microaccelerations.
2.2 Checking the influence of the experimental and manufacturing equipment to be mounted onboard the spacecraft on the level of microaccelerations.

3. Decreasing the influence of the onboard and experimental equipment on the level of microaccelerations.

3.1 Specifying the requirements to the onboard and experimental equipment.
3.2 Developing flight programs, optimal for ensuring microacceleration and microgravitation conditions for specific experimental and manufacturing equipment.
3.3 Developing low-noise onboard and experimental equipment.

4. Developing instrumentation to measure microaccelerations aboard the spacecraft.

4.1 Developing measuring instrumentation for ground-based operation.
4.2 Developing measuring instrumentation for orbital operation.
4.3 Developing programs for interaction with the spacecraft telemeter channel.
4.4 Developing programs for interaction with the spacecraft motion control systems.
4.5 Developing universal measuring instrumentation allowing measuring both microgravity conditions aboard the spacecraft and motion parameters needed for the spacecraft motion control systems.

5. Specifying the requirements to microgravity conditions aboard the spacecraft.

5.1 Systematization of the requirements of the designers of experimental and manufacturing equipment to microgravity conditions aboard the spacecraft.

5.2 Specifying standard (typical) requirements to microgravity conditions aboard the spacecraft designed for experimental and manufacturing work.

Conclusion

The Samara *CSDB* and CSRI *Elektropribor* work in close contact to perfect step by step the equipment and techniques in order to provide by the program SINUS specified microgravity conditions aboard the spacecrafts. In 2002 the FotonM1 with the Sinus15 abord will be launched. And we expect to get more exact date about microgravity conditions on board.

.

REFERENCES

[1] Richard DeLombard, Meeting summary, Proceedings of 17th International Microgravity Measurements Group Meeting, Brook Park, OH, US, March 1998.

[2] V. F. Agarkov, V. D. Kozlov, Yu. N. Gorelov and S. B. Danilov, Theoretical microgravity field and the numerical calculation methods of microgravity levels in flight. Proceedings of 18th International Microgravity Measurements Group Meeting, Cocoa Beach, Fl, US, June 1999.

[3] Designing unmanned spacecrafts /D.I.Kozlov, G.P.Anshakov. Mashinostroiyenie, 1966. (In Russian)

[4] Space material authority/ ed. V.S.Avduyevsky, M., Mir, 1989.

[5] G. Anshakov, O. Mumin, V. Peshekhonov, Features of acceleration measurement system SINUS, Proceedings of 18th International Microgravity Measurements Group Meeting, Cocoa Beach, Fl, US, June 1999.

NASA/CP—2001-211164

QUASI-CONSTANT ACCELERATION

RESULTS OF FLIGHT OF

FOTON12

09.09.1999 - 24.09.1999

System Sinus12K was install aboard of Foton12 (free- flyer), developed by SamaraCSDB(Russia) and launched from the Cosmodrom-Plesetsk in 09.09.1999.
Sinus12K was measuring microacceleration in range 0 - 300Hz.
In this presentations amplitude of quasisteady microacceleration vector presents.
Time of averaging on following plots is 300c (5 min).

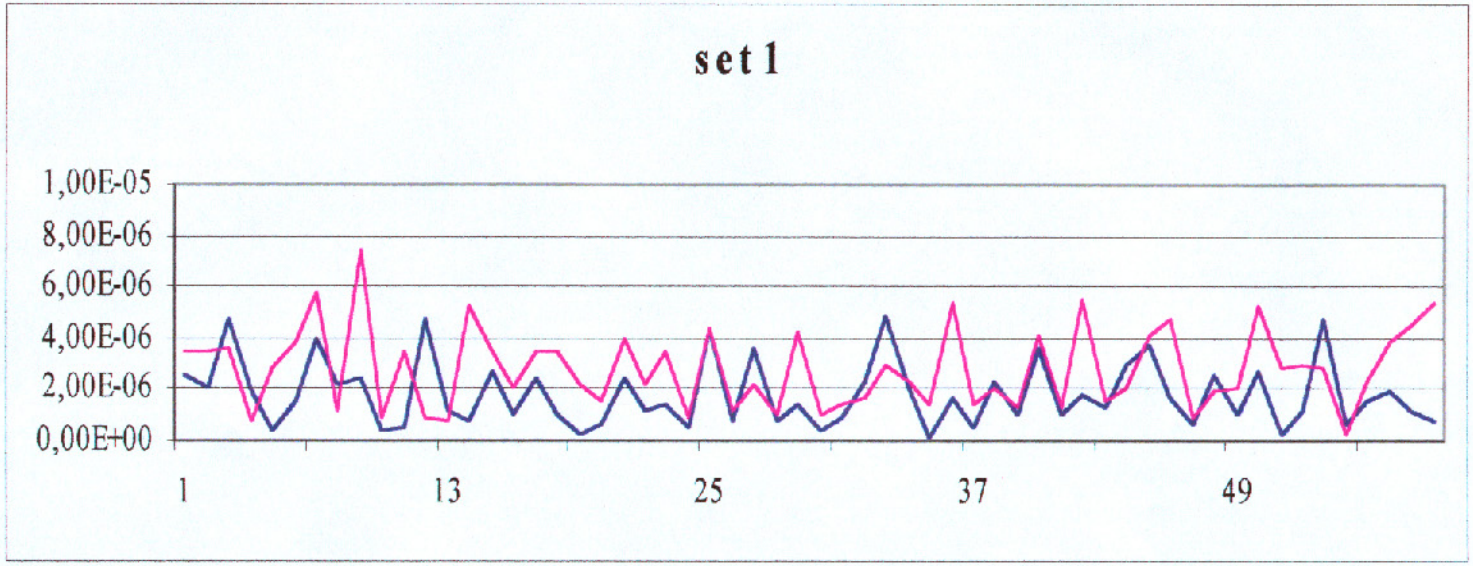

X – axis - time in 5min intervals (1unit – 5min), Y- axis – vector of acceleration in m/c/c

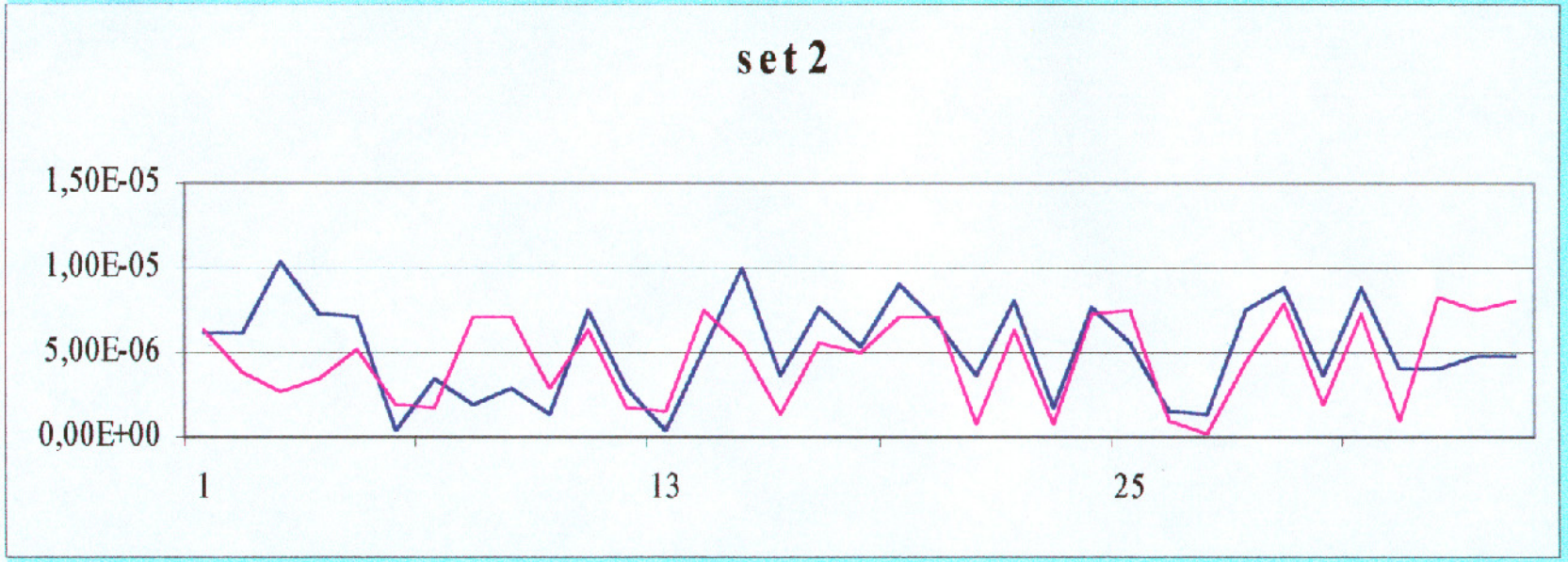

X – axis - time in 5min intervals (1unit – 5min), Y- axis – vector of acceleration in m/c/c

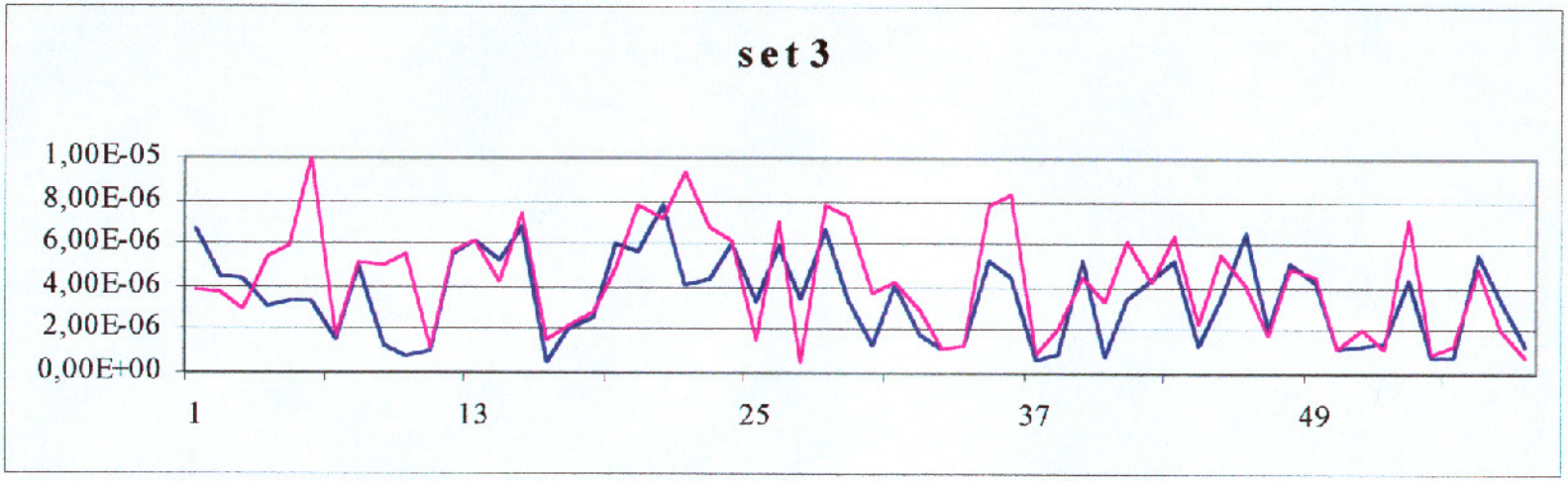

X – axis - time in 5min intervals (1unit – 5min), Y- axis – vector of acceleration in m/c/c

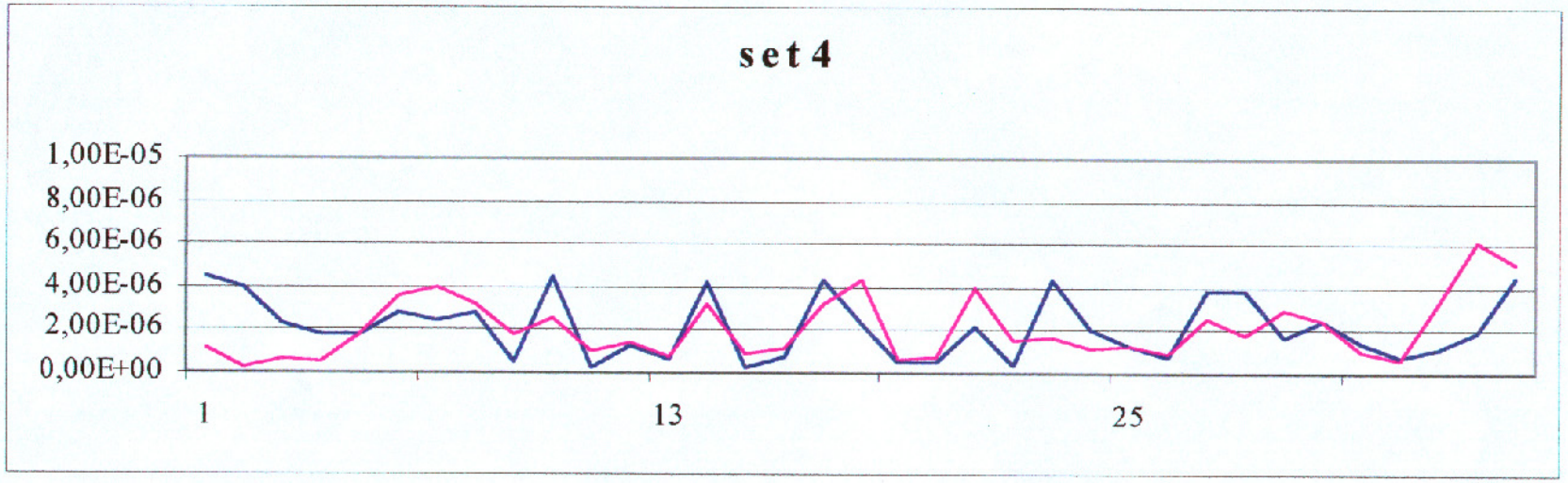

X – axis - time in 5min intervals (1unit – 5min), Y- axis – vector of acceleration in m/c/c

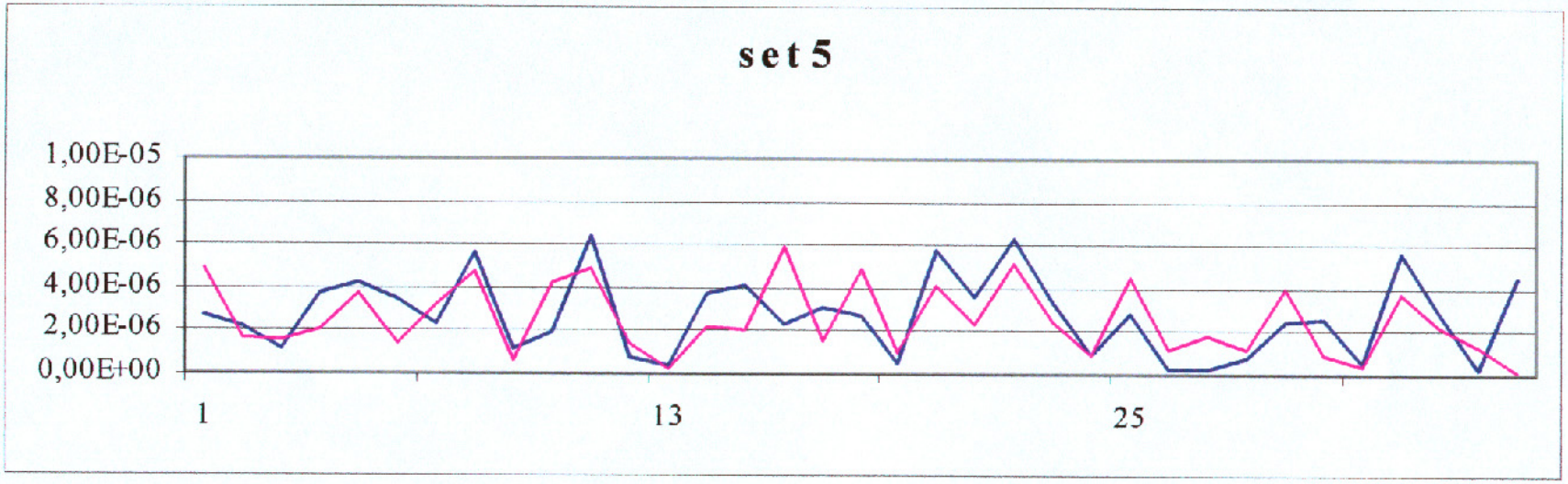

X – axis - time in 5min intervals (1unit – 5min), Y- axis – vector of acceleration in m/c/c

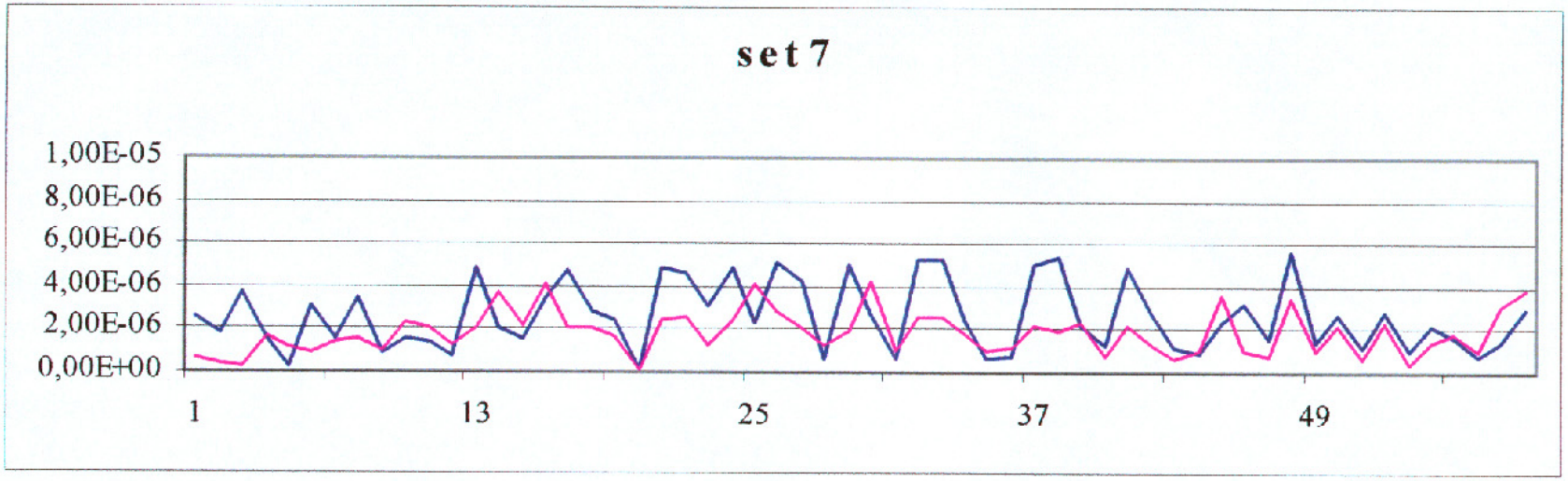

X – axis - time in 5min intervals (1unit – 5min), Y- axis – vector of acceleration in m/c/c

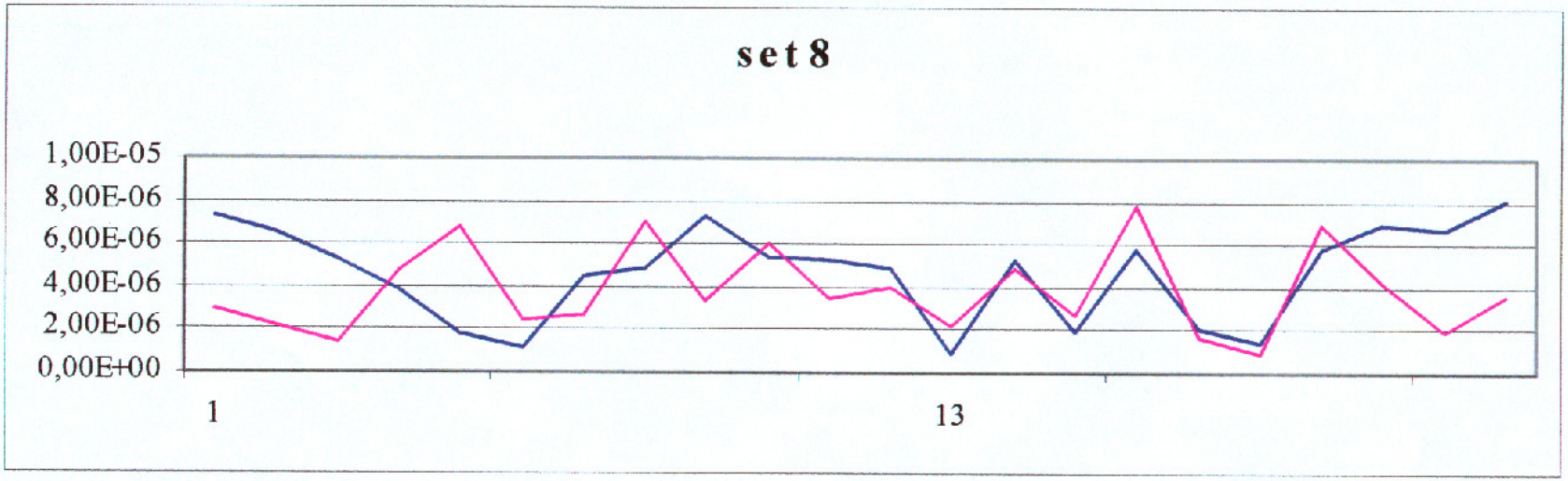

X – axis - time in 5min intervals (1unit – 5min), Y- axis – vector of acceleration in m/c/c

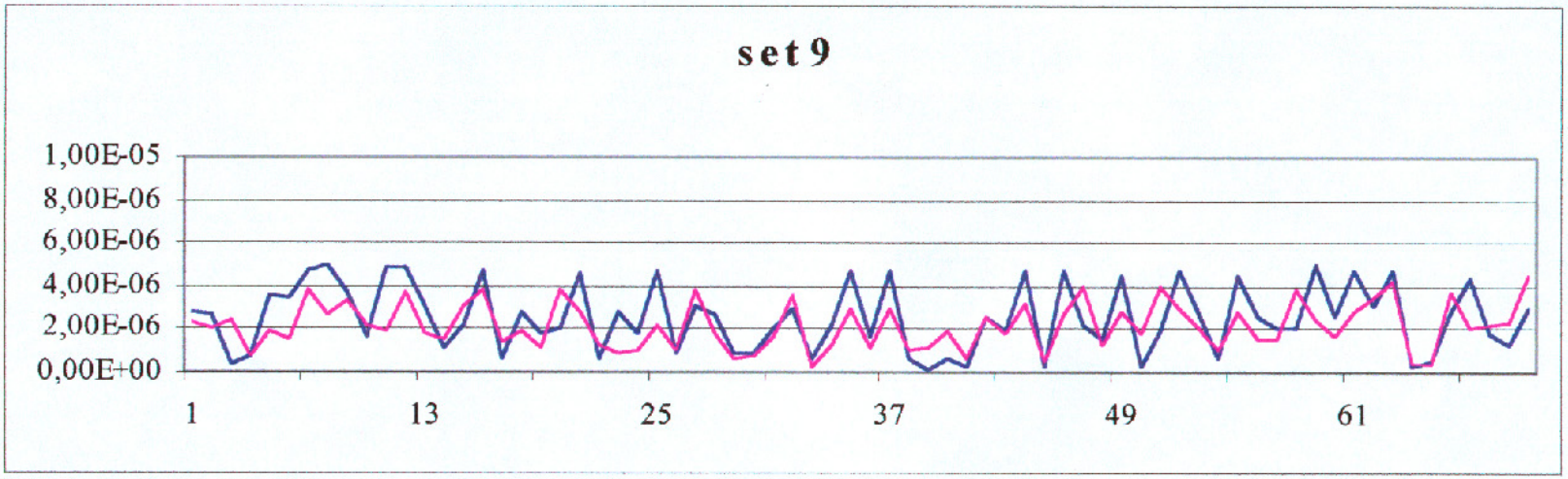

X – axis - time in 5min intervals (1unit – 5min), Y- axis – vector of acceleration in m/c/c

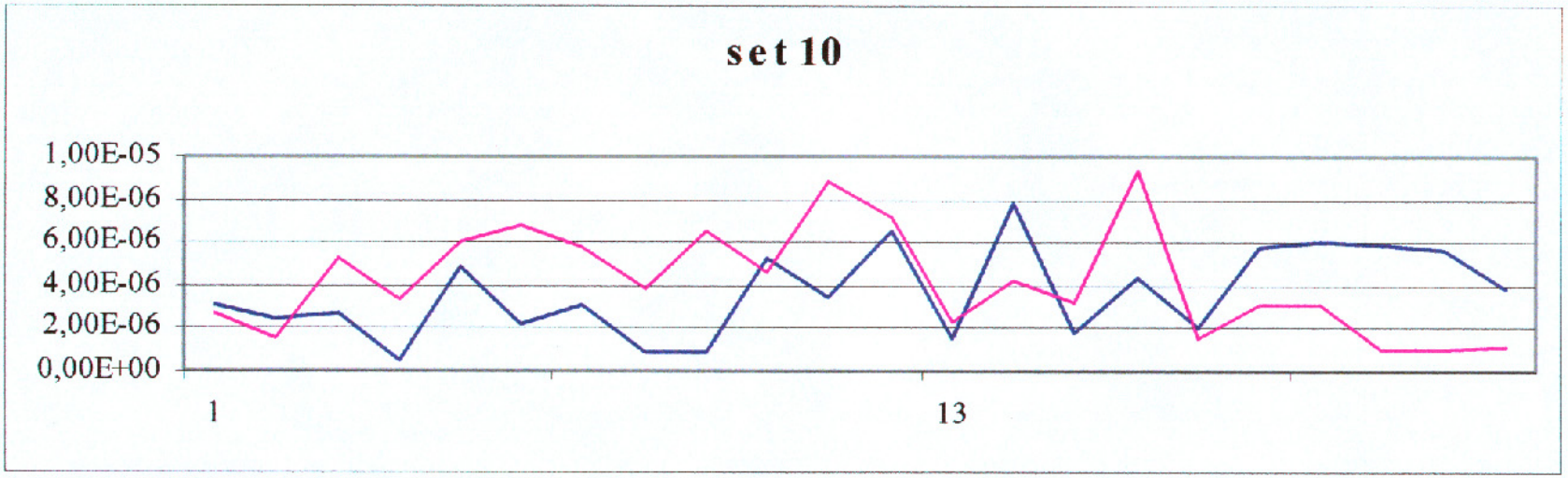

X – axis - time in 5min intervals (1unit – 5min), Y- axis – vector of acceleration in m/c/c

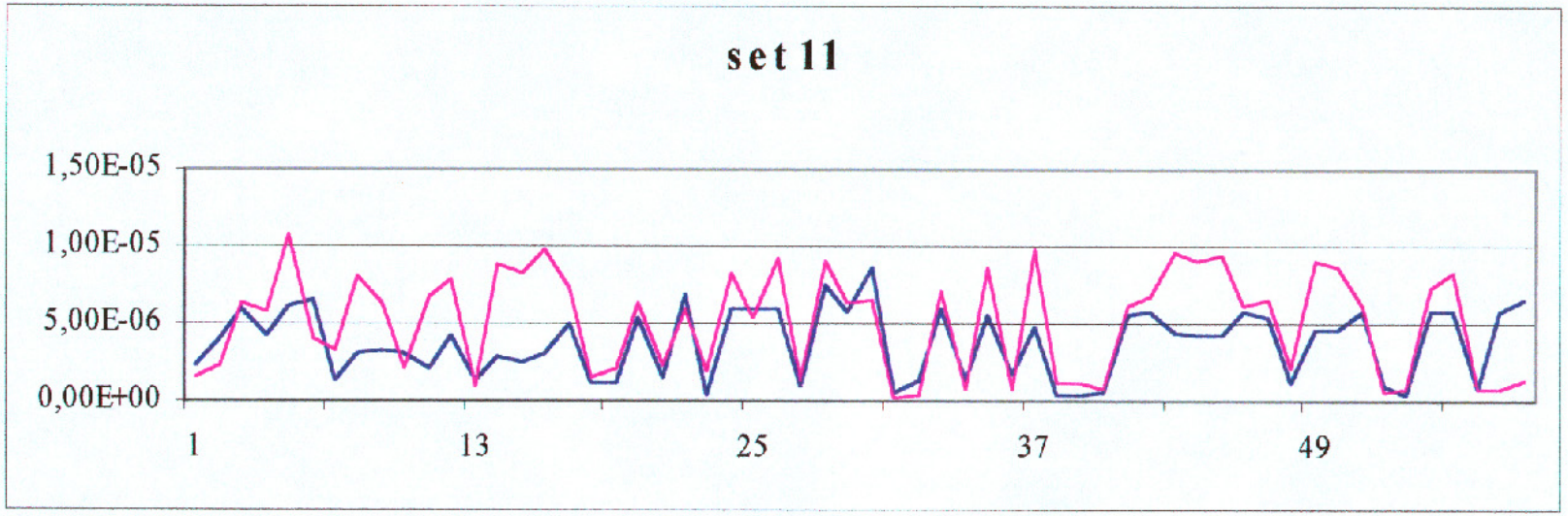

X – axis - time in 5min intervals (1unit – 5min), Y- axis – vector of acceleration in m/c/c

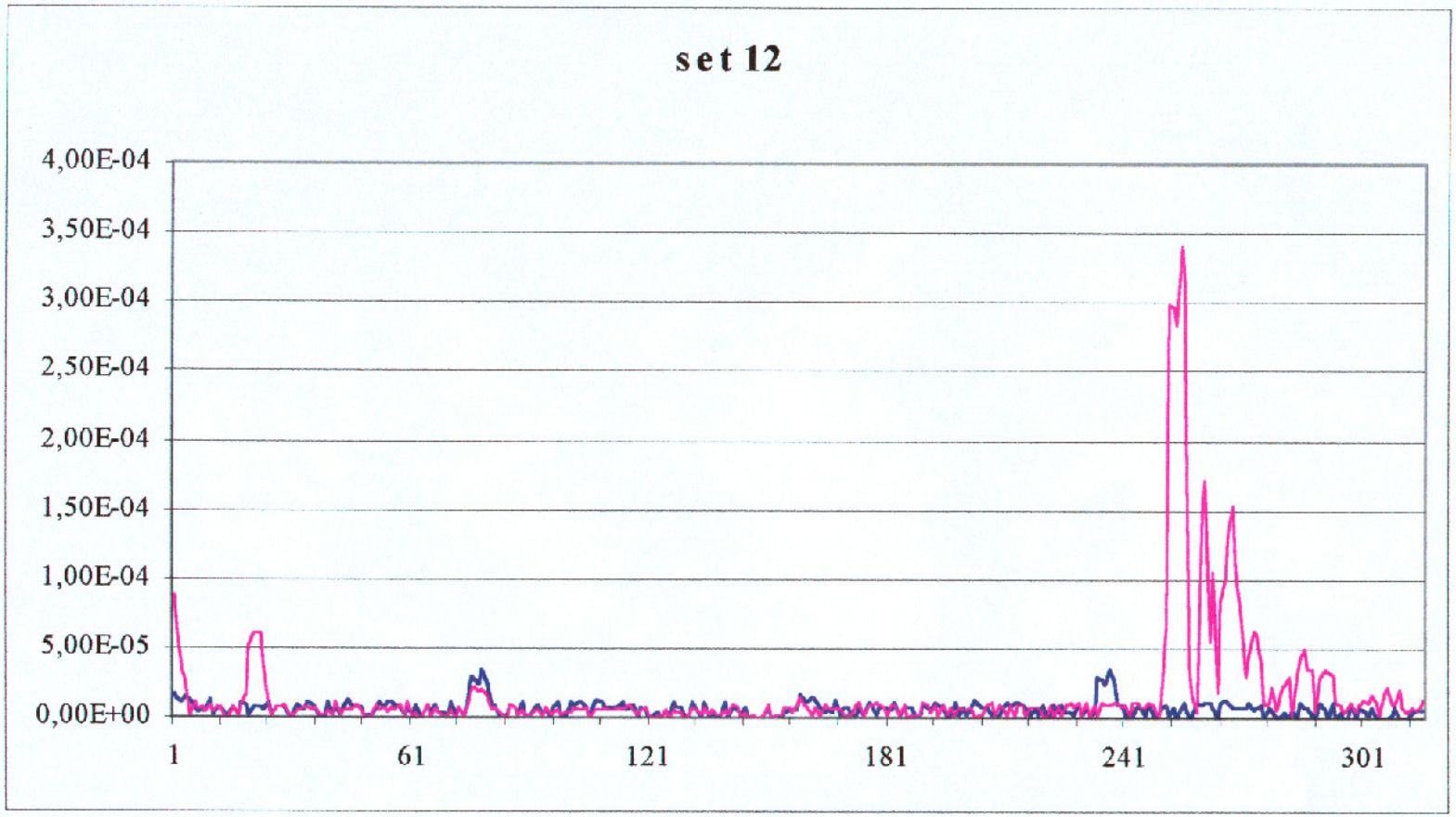

X – axis - time in 5min intervals (1unit – 5min), Y- axis – vector of acceleration in m/c/c

An instrument for measuring the quasi steady acceleration vector on board of the ISS

Giulio Poletti
University of Milan
via Trentacoste 2
20134 Milan
Italy

It is by now ascertained that for most of the experiments of material processing and fluid science the quality of the experimental conditions is mainly determined by the low frequency microgravity value.Really these experiments can tolerate acceleration disturbances much greater if they are short lasting or at high frequency. Therefore the measurement of the residual quasi steady g-vector comes out to be the most important. Furthermore it has been argued that in fluid physics experiments aligning the cell in the residual g-vector direction can reduce the effects of the microgravity on the experiment.

A new conception accelerometer is presented that overcomes some of the problems of the simple mass-spring units that have been commonly used as the basis for most accelerometer systems.The basic idea is to measure the law of motion of a small sphere free floating in a vacuum cell integral with the ISS.The optical devices recording the position of the sphere as a function of time are integral with the cell and therefore suffer the same accelerations of the ISS while the small sphere is by definition in free fall.From the recorded data the magnitude and the direction of the quasi steady g-vector are easily calculated with good accuracy.Sensitivities better than 0.1 micro-g can easily be achieved.In addition the system does not react to relatively high (above 0.5 Hz approx.) frequency g-jitter making easier the interpretation of the experimental data.

The device will be located inside the GLAD facility that will be taken on board of the ISS by the UF#3 flight of NASA.The overall envisaged configuration of the facility is illustrated. The expected performances of the device are discussed on the basis of the results of numerical computer simulations of the experiment based on the calculations performed by Boeing concerning the quasi steady accelerations inside the US Lab.

An instrument for measuring the quasi steady acceleration vector on board of the ISS

Giulio Poletti

University of Milan

Presented to the

Microgravity Measurements Group

Cleveland

August 7-9 , 2001

An instrument for measuring the quasi steady acceleration vector on board of the ISS

Giulio Poletti

University of Milan

Abstract

A new conception accelerometer is presented that overcomes many of the problems of the commonly used simple mass-spring units.The basic idea is to measure the law of motion of a small sphere free floating in a vacuum cell integral with the ISS.The system does not react in practice to relatively high (above 0.1 Hz approximately) frequency oscillatory accelerations making easier the interpretation of the experimental data.The expected performaces of the device are discussed.The results of the numerical simulations point out that the measurement of the magnitude and of the direction of the quasi steady acceleration vector can be achieved and that in addition it is possible to discriminate the g-jitter from the quasi steady acceleration.

Introduction

For many microgravity experiments in which individual trial extend over relatively long period of time the knowledge of the small quasi-steady residual acceleration is essential to interpret the results and is the most critical acceleration measurement. In fact it is well known that many experiments in material processing and in fluid science can often tolerate much larger acceleration disturbances if they are of short duration or of high frequency, but the very small (in general less than or of the order of 1 microg) quasi-steady background is a determining factor in the quality of the experimental conditions.
Furthermore it is conceivable that the direction of this quasi-steady acceleration can be nearly constant for limited but significant period of time.

And it has been shown theoretically that aligning the experiments with this privileged direction could result in a better understanding of the experimental results and possibly in a better control of the effects of the overall microgravity on the experiments.
It is therefore evident that the measurement of the quasi-steady acceleration and particularly of the orientation of the acceleration vector as a function of time can be of outmost importance to characterize the microgravity environment in which the experiments are performed and to establish the effects of these accelerations on the experiments.
In addition if the possibility of separating the g-jitter from the quasi-steady accelerations could be accomplished,it could allow to separate their effects on the experiments giving rise to a better understanding of the experimental results.
Unfortunately any attempt to get the intensity and particularly the orientation of the residual acceleration vector as a function of time from the measurement of the x,y and z components of the acceleration performed with the low frequency triaxial accelerometers packages at present in use is prevented.The utmost difficulty of manufacturing accelerometers showing the extremely high required thermal stability and the very complicated process of filtering the output signal that is very noisy due to the presence of the g-jitter are the main reason.
The present work concerns a new conception device to measure the quasi-steady accelerations on board of the ISS.The device is called PAU (Passive Acceleration Unit) and is included in the Italian GLAD drawer that will be launched within the UF#3 Mission of NASA and located inside a rack on board of the ISS possibly within the US Lab.

Outline of the experiment

A small sphere is launched with very low velocity along a given direction inside a vacuum cell that is integral with the ISS.The sphere is free floating while the cell suffers the accelerations of the ISS.Two optical systems integral with the cell and located on two planes orthogonal each other measure the trajectories of the sphere position as a function of time.From the recorded data the law of motion is inferred and from this the magnitude and the direction of the quasi steady component of the residual acceleration are calculated at the position of the cell.
The cell dimensions will be limited to a few centimetres (10 cm in the performed simulations) so that during its motion the sphere impacts against the walls.Although the performed numerical simulations (see in the following) seems to show that it is conceivable to follow the trajectory of the sphere for periods of time encompassing many rebounds,it is to be envisaged, due to

many possible events,the need to stop the measurements after one/several/many rebounds and to recover the sphere in a way suitable to allow a new launch.
But in any case the need to recover the sphere and to launch it again exists really.
The main consequence of this fact is that a continuous measurement of the trajectories is only possible for limited periods of time that probably will range from 2-3 minutes to several minutes,depending also on the dimensions of the experimental cell and on the launch velocity of the sphere.The time necessary to recover the sphere and to perform another launch is evaluated as 1 minute approximately.Due to the expected very slow variation of the acceleration vector during the orbit this fact is not judged to be really detrimental to the experiment.
In any case the experiment would allow to determine with good accuracy the behaviour of the magnitude and of the direction of the quasi steady acceleration as a function of time during the orbit.

The UF#3 Mission scenario and the reference environment

To evaluate if the proposed device is able to measure the quasi steady acceleration on board of the ISS and to design properly the facility numerical simulations of the experiment have been performed in a well defined microgravity environment.
Since the experiment is included in the payload of the UF#3 Mission of Nasa reference is made to the envisaged ISS configuration at the time of that Mission.At present it is not known for sure where the GLAD drawer will be located but it is likely that it will be put inside a rack within the US Lab.
A sketch of the US Lab and a table showing the ISPR rack locations together with the used reference coordinate system is shown in Fig.1.
For the present purpose it is enough to state that the positive direction of the x axis in the used coordinate system is in the opposite direction of the atmospheric drag.
To perform numerical simulation of the experiment reference has been made to the S1 rack inside the US Lab and to the calculations of the quasi steady microgravity (see Fig.2 and 3) made by M.Laible (private communication) concerning the situation foreseen for the ISS at the time of the UF#3 Mission.

Numerical simulation of the experiment

The above data have been used as input for the numerical simulation of the experiment. As discussed in the preceding it is assumed that a small sphere

is launched in a given direction with assigned velocity inside a cubic cell under vacuum and that the motion of the sphere is monitored by means of two optical detectors (PSDs) located in two planes orthogonal each other and integral with the cell.The sphere is by definition in free fall while the detectors undergo the same acceleration of the cell and therefore of the ISS itself.
A first calculation program has been worked out that allows to calculate the position of the sphere as a function of time and the trajectory of the motion as it can be seen by two detectors located in two planes normal each other.
This program refers to a situation very simple where the g-jitter is neglected and the only considered acceleration sources are the atmospheric drag and the gravity gradient,that otherwise make up the most important contributions to the value of the quasi steady component of the microgravity.
The equations of motion of the sphere are very simple

$$X = -\frac{1}{2} A_{ad\,x} \cdot t^2 + v_{0x} \cdot t$$

$$Y = \frac{1}{2} A_{gg\,y} \cdot t^2$$

$$Z = \frac{1}{2} A_{gg\,z} \cdot t^2$$

and allow to calculate the behaviour of the functions X = X (t) ,Y = Y (t) and Z = Z (t) and the trajectories Y = Y (X) and Z = Z (X) as seen by the above mentioned detectors (PSD)
The program requires as input the values of the acceleration along the x,y and z directions,the direction and the value of the launch velocity of the sphere and the starting position of the sphere inside the vacuum cell.
In the simulations the launch velocity of the sphere is assumed in general to be equal to 0.3 mm/s and to be in the direction opposite to the atmospheric drag (the x axis in the above reference system).In fact this direction is the only one in which the acceleration is known a priori independently of the position of the facility in respect of the ISS center of mass.It has to be stressed that the launch velocity can be changed within a wide range to optimize the output of the experiment.
For simplicity the present simulations are restricted to the time of flight of the sphere that is the time elapsed between the launch and the impact against one of the wall of the cell that has a cubic shape with an edge of 100 mm. During the time of flight the accelerations are supposed to be constant and the initial position of the sphere is taken in one corner of the cubic cell.
Fig. 4 shows the results of a numerical simulation where the magnitude of the quasi steady accelerations due to the atmospheric drag and to the gravity gradient are assumed according the calculations of Laible and the coordinate

system has been chosen according to that used by NASA in the reference document for the ISS [1].
Namely the input parameters have been

$A_{ad\,x} = 3\ 10^{-7}$ g

$A_{gg\,y} = 4.2\ 10^{-7}$ g

$A_{gg\,z} = 7\ 10^{-7}$ g

$v_{0_x} = 0.3$ mm/s

As mentioned in the preceding the simulation stops when the sphere impacts against one of the walls of the cell,in the present case the (x,y) plane.
To complete the analysis the effect of changing the launch velocity of the sphere has to be investigated.The change of the launch velocity gives rise to a change in the sphere trajectories and in the sphere time of flight).This can be seen in Fig.5 relative to a launch velocity equal to 0.4 mm/s.In general a change in the launch velocity can be useful to make the flight time longer or to make easier the recording of details of the trajectories,that means to optimize the experiment conditions.
Later on to investigate how the unavoidable presence of the g-jitter affects the measurements,a second issue of the program has been developed that includes in addition oscillatory accelerations of given amplitudes at given frequencies.This program has been developed under the same above mentioned simplifying hypothesis and does not take into consideration the relative phase of the oscillatory accelerations.
The calculations have started taking into consideration one only oscillatory acceleration at a time,supposing that its magnitude had the maximum value compatible with the well known disturbance limits for ISS shown in Table 1.

Frequency Range	Disturbance Limit
0.01 Hz < F < 0.1 Hz	1.8 μg
0.1 Hz < F < 100 Hz	18 μg F [Hz]
100 Hz <F <300 Hz	1800 μg

This set of simulations show that the curves in which oscillatory accelerations are present having the above quoted magnitude and frequencies above 0.2 Hz approximately are indistinguishable from those in which only the quasi steady accelerations are present.
Therefore simulations have been performed taking into account simultaneously several oscillatory accelerations at different frequencies having the maximum magnitude compatible with the disturbance limits in

Table 1.The considered frequency range started from 0.01 Hz (the limit below which accelerations are considered to be quasi steady) and 0.3 Hz approximately (the frequency above which absolutely no effect is observed).
In this case the equations of motion of the sphere become

$$X = -\frac{1}{2} A_{ad\,x} \cdot t^2 + v_{0x} \cdot t + \sum_i \frac{A_{osc\,x}}{\omega_i^2} \cdot sin\omega_i t$$

$$Y = \frac{1}{2} A_{gg\,y} \cdot t^2 + \sum_i \frac{A_{osc\,y}}{\omega_i^2} \cdot sin\omega_i t$$

$$Z = \frac{1}{2} A_{gg\,z} \cdot t^2 + \sum_i \frac{A_{osc\,z}}{\omega_i^2} \cdot sin\omega_i t$$

where

A_{osc} = magnitude of the oscillatory acceleration

ω_i = angular frequency

Of course the values of the $A_{ad\,x}$, $A_{gg\,y}$, $A_{gg\,z}$ and v_{0_x} parameters are the same used for the previous simulations.Six oscillatory accelerations at frequencies in the quoted range have been selected,namely 0.3 – 0.2 – 0.1 – 0.075 – 0.05 – 0.025 Hz.
The results are collected in the figures from 6 to 14 in which the trajectories of the sphere as seen by the two PSD devices are shown.
The magnitudes of the oscillatory accelerations are always the maximum magnitude compatible with the disturbance limits (see Table 1).
The Fig. 6 shows the trajectories in the presence of the atmospheric drag, gravity gradient and three oscillatory frequencies 0.3 Hz – 0.2 Hz – 0.1 Hz. These curves are indistinguishable from the curves in which only the atmospheric drag and the gravity gradient are present.
The Fig. 7 shows the trajectories in the presence of the atmospheric drag,gravity gradient,the three preceding oscillatory frequencies and another frequency equal to 0.075 Hz.These curves are a little bit different from those in which only the atmospheric drag and the gravity gradient are present since a small oscillation comes out.The difference between the two cases is shown in Fig.8 and appears to be really very small but surely detectable.
The Fig. 9 shows the trajectories in the presence of the atmospheric drag,gravity gradient,the four preceding oscillatory frequencies and another frequency equal to 0.05 Hz.The difference of these curves from those in which only the atmospheric drag and the gravity gradient are present is

bigger than before and quite detectable as shown by the comparison in Fig.10.
The Fig. 11 shows the trajectories in the presence of the atmospheric drag,gravity gradient,the five preceding oscillatory frequencies and another frequency equal to 0.025 Hz.The difference of these curves from those in which only the atmospheric drag and the gravity gradient are present is great as attested by the comparison in Fig. 12.
As it was expected the influence of the oscillatory accelerations becomes bigger and bigger as the frequency becomes lower and lower.
But only oscillatory acceleration having very low frequency less than 0.05 Hz approximately and magnitude very close to the disturbance limit for the ISS modify the shape of the trajectories in a remarkable way,
But if the magnitude of the oscillatory acceleration for frequencies in the range 0.01 –0.1 Hz is taken according the forseen environment for ISS the trajectories are very similar to those recorded in the absence of oscillatory accelerations.This is shown in the Fig. 13 and 14 that display the trajectories of the sphere that take into account the atmospheric drag,the gravity gradient and one only oscillatory acceleration at 0.075 Hz having amplitude according the disturbance limit (Fig.13) and according to the foreseen environment for ISS (Fig.14),that as shown in Fig. 15.
In the preceding the last type of accelerations that occur on board of the ISS,namely the transient accelerations,are not taken into consideration.The reason is evident since they are seen as spikes superimposed on the sphere trajectories.

Comments

Two extremely important comments must be done immediately.
First of all the system is able to measure the quasi steady acceleration with good accuracy.
Secondly the system behaves as a low pass filter with a cut-off frequency for oscillatory accelerations around 0.1 Hz.
In this respect it seems to be the complement to the commonly used accelerometers packages that behave like a high pass filter.
The preceding simulations have been limited to the period of time between the launch of the sphere and the collision against a wall of the cell,that depend critically from the dimensions of the cell within which the sphere moves.But the collision with the wall gives rise only to a change in the direction and possibly in the value of the sphere velocity.Therefore it is enough to measure the sphere velocity after the impact to go back to the above discussed situation and it conceivable to go on with the measurements till a situation is reached in which the reliable measurements cannot be performed,e.g. for example the sphere stops or reaches a velocity too high

due to a transient disturbance.When this occurs it is necessary to recover the sphere and to launch it again.
As a consequence the measurements are not continuous during the orbit but will be performed during periods of say a few/several minutes alternating with periods lasting 1 minute approximately,necessary to recover the sphere and launch it again. Due to the expected very slow variation of the acceleration vector during the orbit this fact is not judged to be really detrimental to the experiment.
All the systems that can be used to record the trajectory of the sphere (Position Sensing Device,CCD arrays) can monitor the position of the sphere with precision greater than 10 microns and rate greater than 10 Hz that are approximately the performance required for the measurement.
The limit resolution of the overall system depends of course on many factors but it is adequate to the measurement of quasi steady accelerations down to 10^{-8} g.

Conclusions

Due above all to the mentioned filter effect getting the quasi steady acceleration vector from the experimental data would not be a difficult task so as it seems possible to discriminate the g-jitter from the quasi steady acceleration.
Really the problem of getting the law of motion from the trajectories in the presence of many oscillatory accelerations and transient accelerations have not been faced at present as it is the problem of getting the quasi steady acceleration vector and the information concerning the g-jitter from the recorded trajectories.In principle the problem seems not to be difficult but only a simulation of a real situation where many oscillatory accelerations are present at the same time can prove the sentence.
In any case it is important to point out the output signals of the present device are much simpler to be interpreted that the output signals of a classic triaxial mass-spring accelerometer.This is also due to the fact that the present device behaves as a low pass filter able to cut off all the oscillatory accelerations having frequency greater than 0.1 Hz approximately and magnitude equal to the disturbance limits set by NASA for the ISS.
On the grounds of the results of the numerical simulations it can be concluded that the proposed device is able to measure the quasi steady acceleration on board of the ISS.
In particular it is possible to measure the direction of the quasi steady acceleration vector as a function of time and therefore to evaluate its stability during the orbit,information that has never been obtained and that is extremely important to design experiments particularly in fluid physics.

In addition due again to the ability of the system to behave as a low-pass filter it seems possible to discriminate the g-jitter from the quasi steady acceleration.

References

[1].Laible,M (1999)Quasi-steady microgravity analysis,18thInternational Microgravity Measurements Group Meeting,June 15-17,Cocoa Beach (Florida) pag.369-390).

Acknowledgments

The experiment is financed by ASI (Agenzia Spaziale Italiana)

BACKGROUND
COORDINATE FRAMES USED

Station Analysis Coordinate Frame

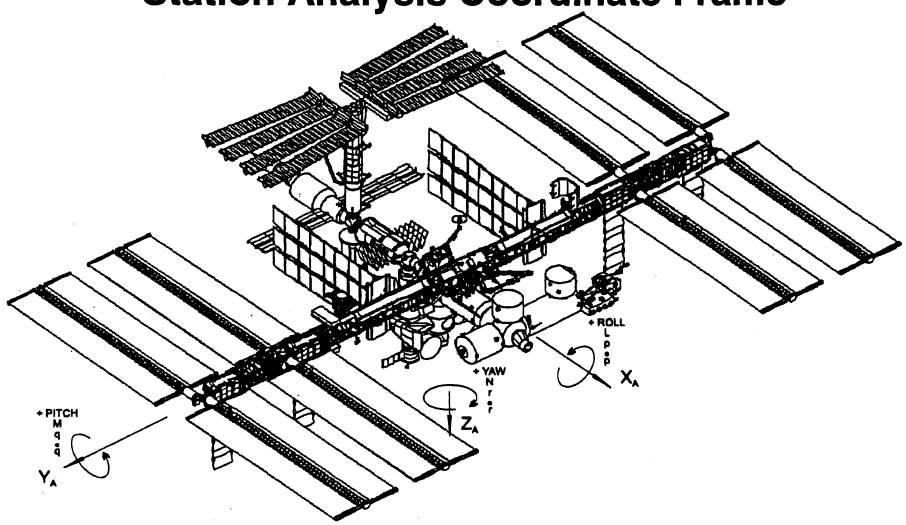

ORIGIN: The origin is located at the geometric center of Integrated Truss Segment (ITS) S0 and is coincident with the S0 Coordinate frame. See figure 5.0-12, SO coordinate frame for a more detailed description of the S0 geometric center.

ORIENTATION:

X_A The X-axis is parallel to the longitudinal axis of the module cluster. The positive X-axis is in the forward direction.

Y_A The Y axis is identical with the SO axis. The nominal alpha joint rotational axis is parallel with Y_A. The positive Y-axis is in the starboard direction.

Z_A The positive Z-axis is in the direction of nadir and completes the right-handed Cartesian system.

ISPR Locations

ISPR RACK LOCATIONS				ISPR RACK LOCATIONS			
X	Y	Z	Description	X	Y	Z	Description
15.55	0.00	11.26	USL-C1	29.66	-17.82	15.92	JPM5-A3
12.05	0.00	11.26	USL-C2	40.00	-17.82	15.92	JPM6-F3
8.55	0.00	11.26	USL-C3	29.66	-21.32	15.92	JPM7-A4
5.05	0.00	11.26	USL-C4	29.66	-24.82	15.92	JPM8-A5
1.55	0.00	11.26	USL-C5	40.00	-24.82	15.92	JPM9-P5
15.55	4.84	16.11	USL-S1	40.00	-28.32	15.92	JPM10-P6
12.05	4.84	16.11	USL-S2	34.84	14.39	10.74	APM-CLG1
8.55	4.84	16.11	USL-S3	34.84	18.33	10.74	APM-CLG2
5.05	4.84	16.11	USL-S4	40.00	14.39	15.91	APM-FWD1
15.55	-4.84	16.11	USL-P1	40.00	18.33	15.91	APM-FWD2
12.05	-4.84	16.11	USL-P2	40.00	22.26	15.91	APM-FWD3
5.00	-4.84	16.11	USL-P4	40.00	26.19	15.91	APM-FWD4
29.66	-10.82	15.92	JPM1-A1	29.67	14.39	15.91	APM-AFT1
40.00	-10.82	15.92	JPM2-F1	29.67	18.33	15.91	APM-AFT2
29.66	-14.32	15.92	JPM3-A2	29.67	22.26	15.91	APM-AFT3
40.00	-14.32	15.92	JPM4-F2	29.67	26.19	15.91	APM-AFT4

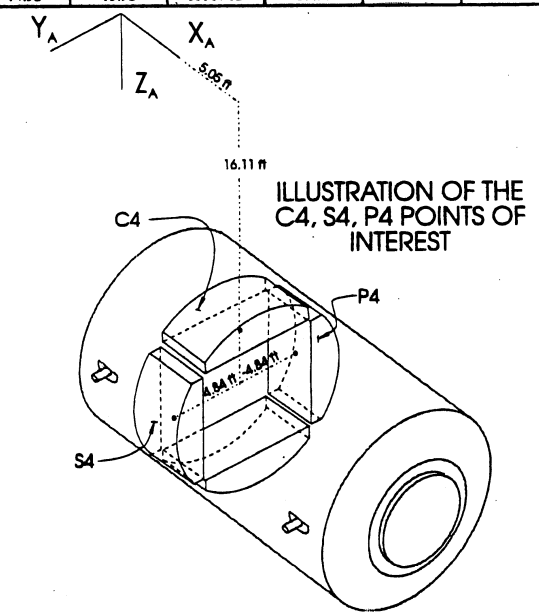

ILLUSTRATION OF THE C4, S4, P4 POINTS OF INTEREST

Analytical Integration

Michael Laible, Microgravity Team

Fig. 1

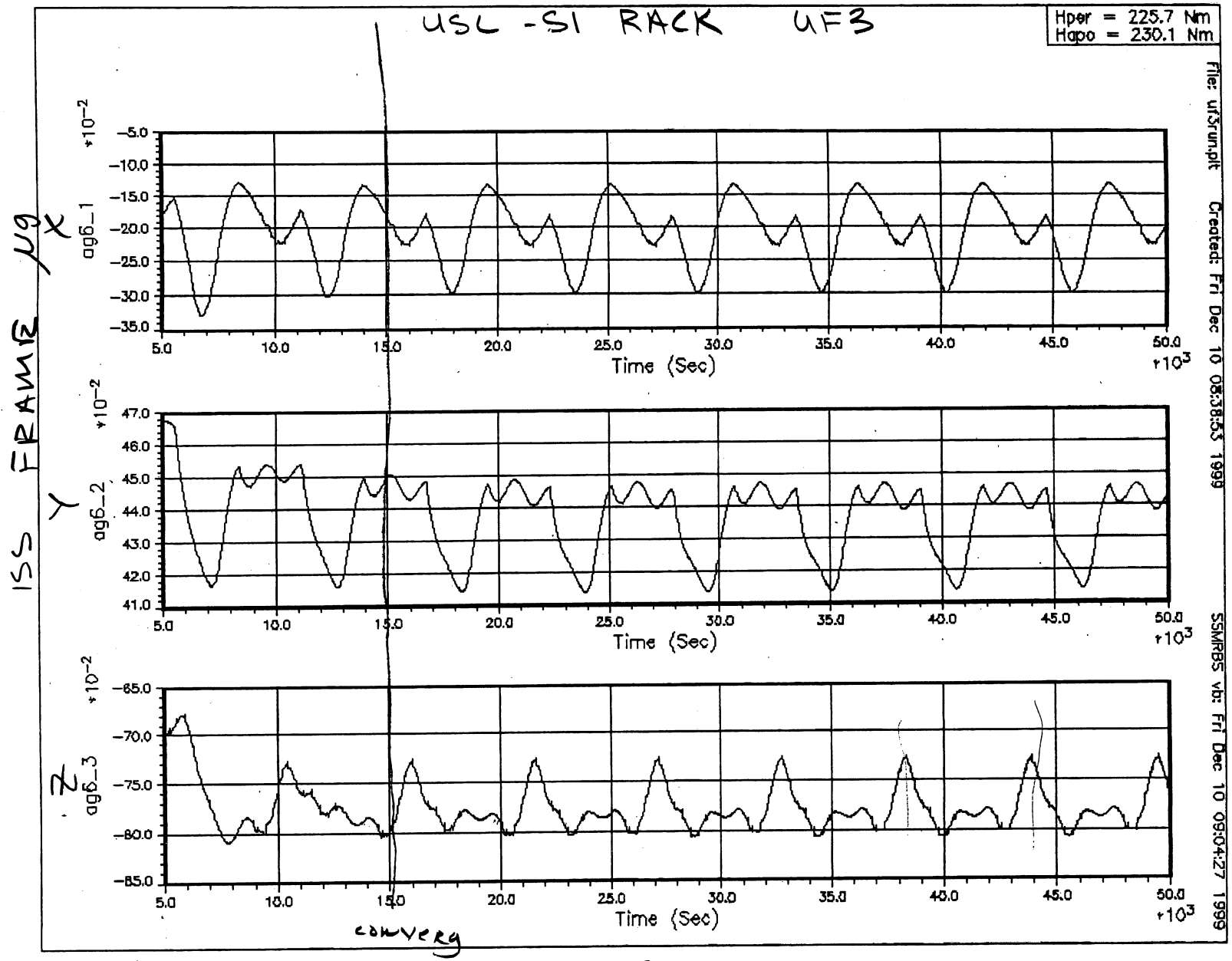
USL -SI RACK UF3
Hper = 225.7 Nm
Hapo = 230.1 Nm
ISS FRAME μg
X
Y
Z
ag6_1
ag6_2
ag6_3
*10^-2
Time (Sec)
*10^3
File: uf3run.plt Created: Fri Dec 10 08:38:53 1999
SSMRBS vb: Fri Dec 10 09:04:27 1999
convert
CMG

Fig. 2

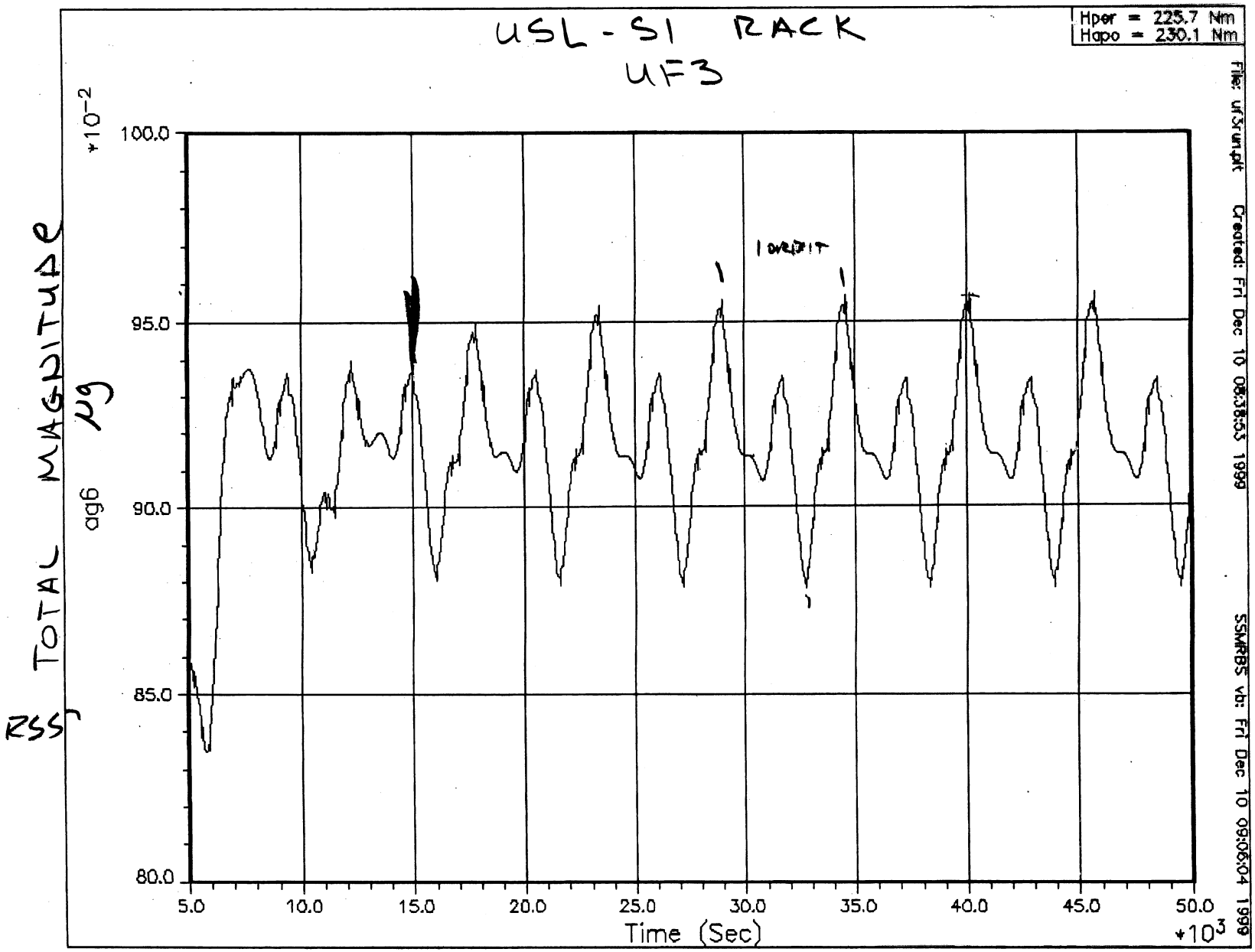
USL-SI RACK
UF3
Hper = 225.7 Nm
Hapo = 230.1 Nm
File: uf3rum.plt Created: Fri Dec 10 08:38:53 1999
SSMRBS vb: Fri Dec 10 09:06:04 1999
TOTAL MAGNITUDE
RSS
agб μg
+10⁻²
100.0
95.0
90.0
85.0
80.0
5.0
10.0
15.0
20.0
25.0
30.0
35.0
40.0
45.0
50.0
Time (Sec)
+10³

Fig. 3

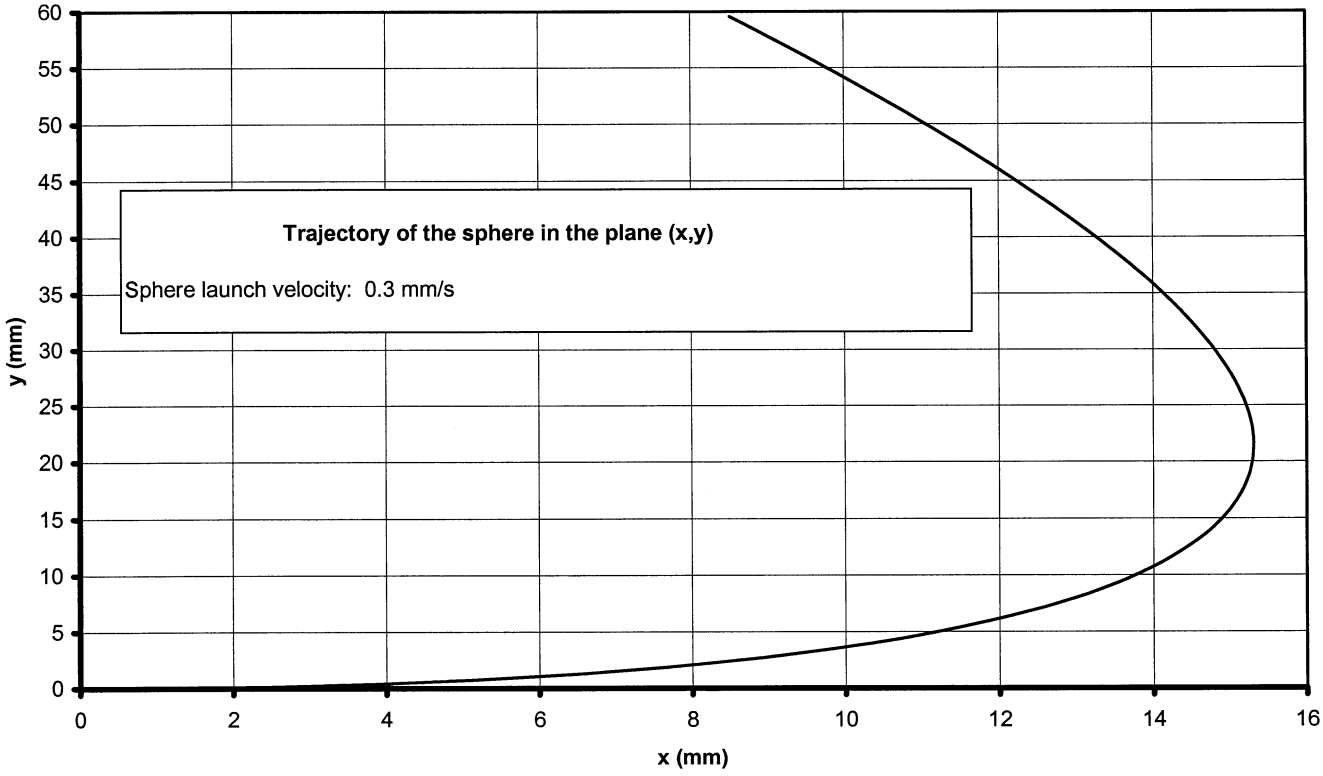

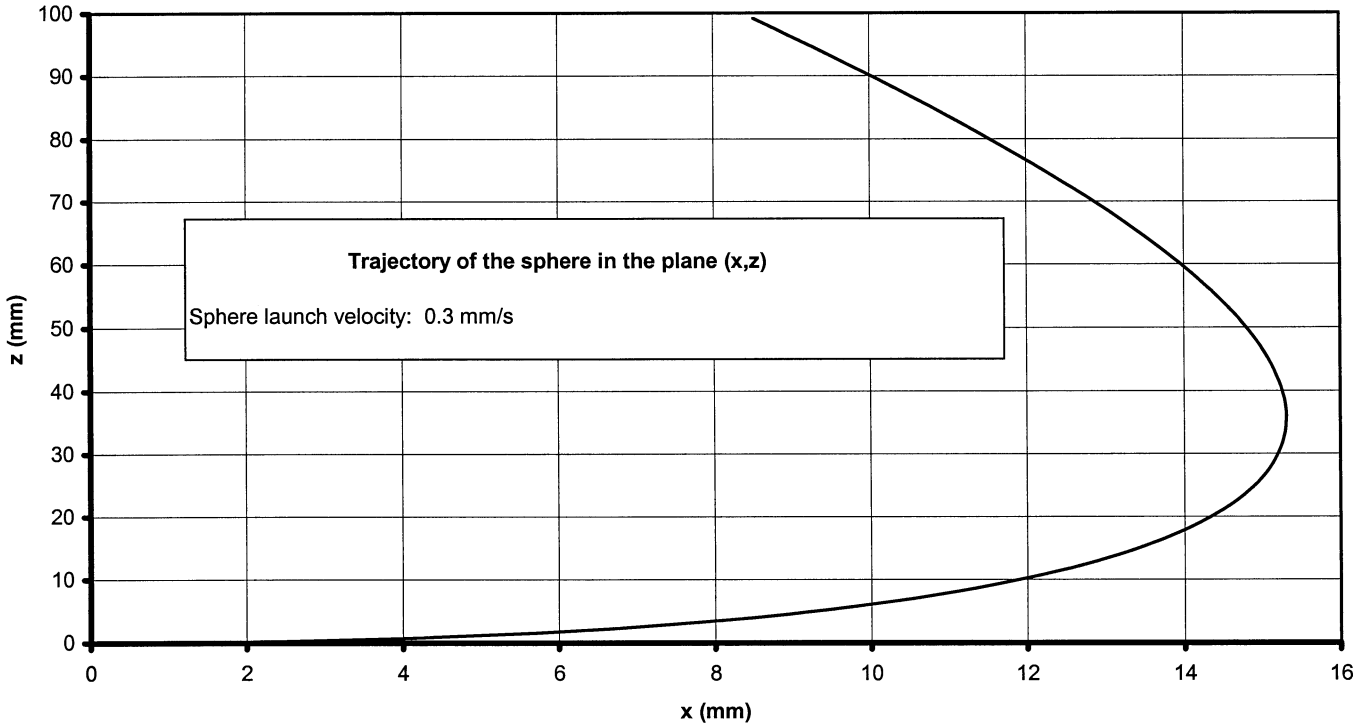

Figure 4

Giulio Poletti
University of Milan

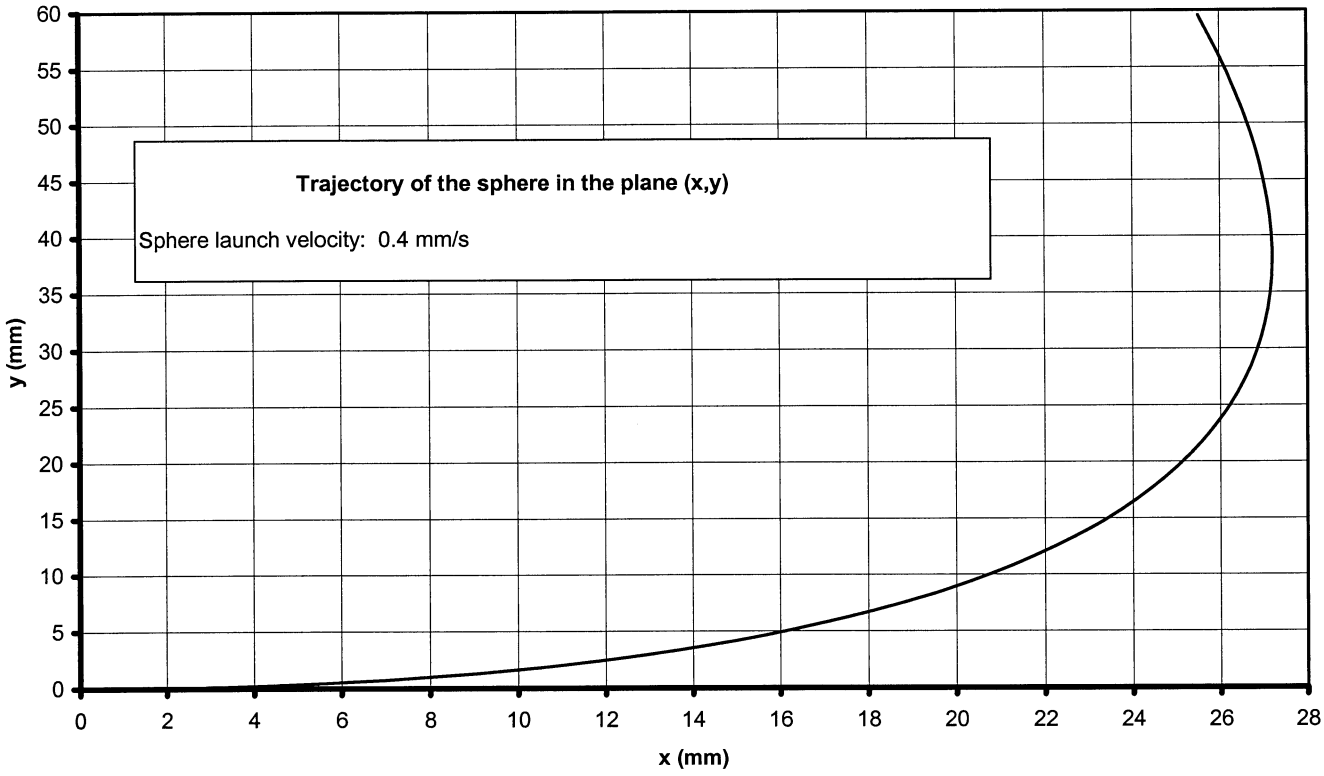

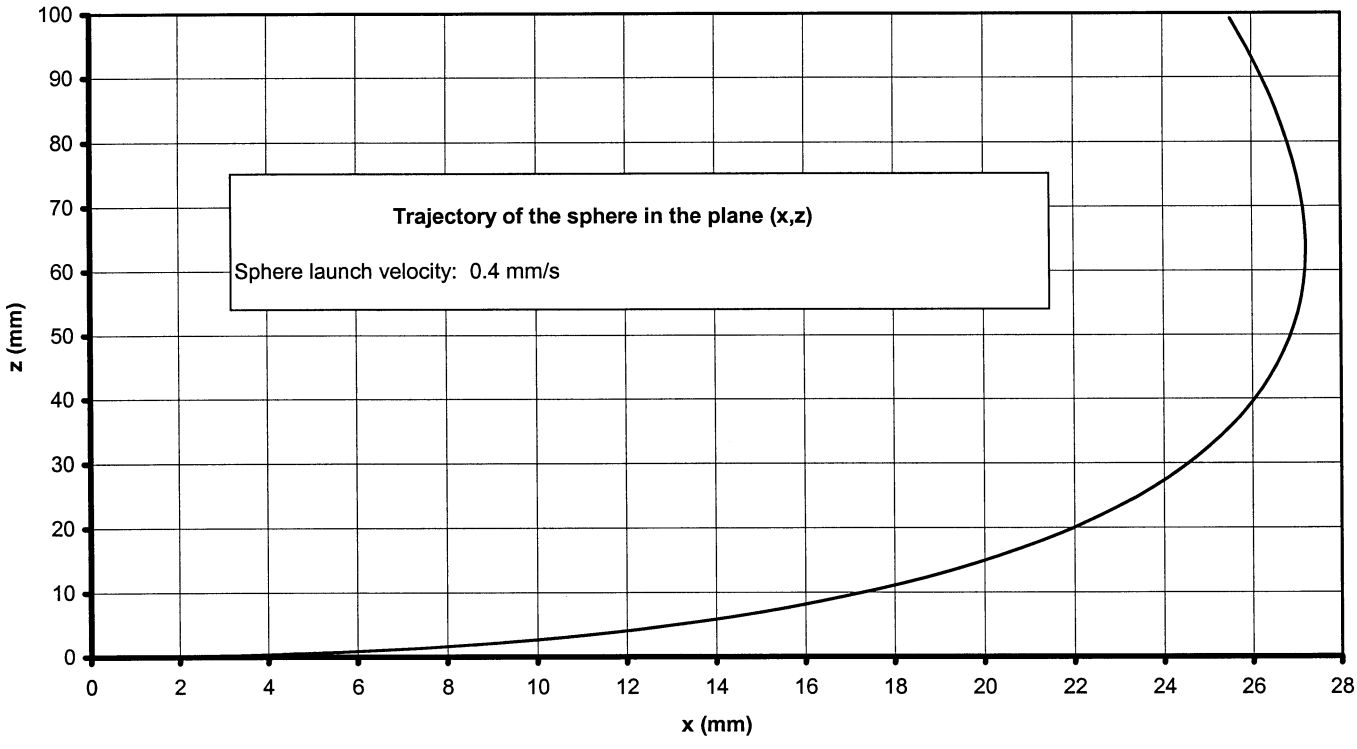

Figure 5

Giulio Poletti
University of Milan

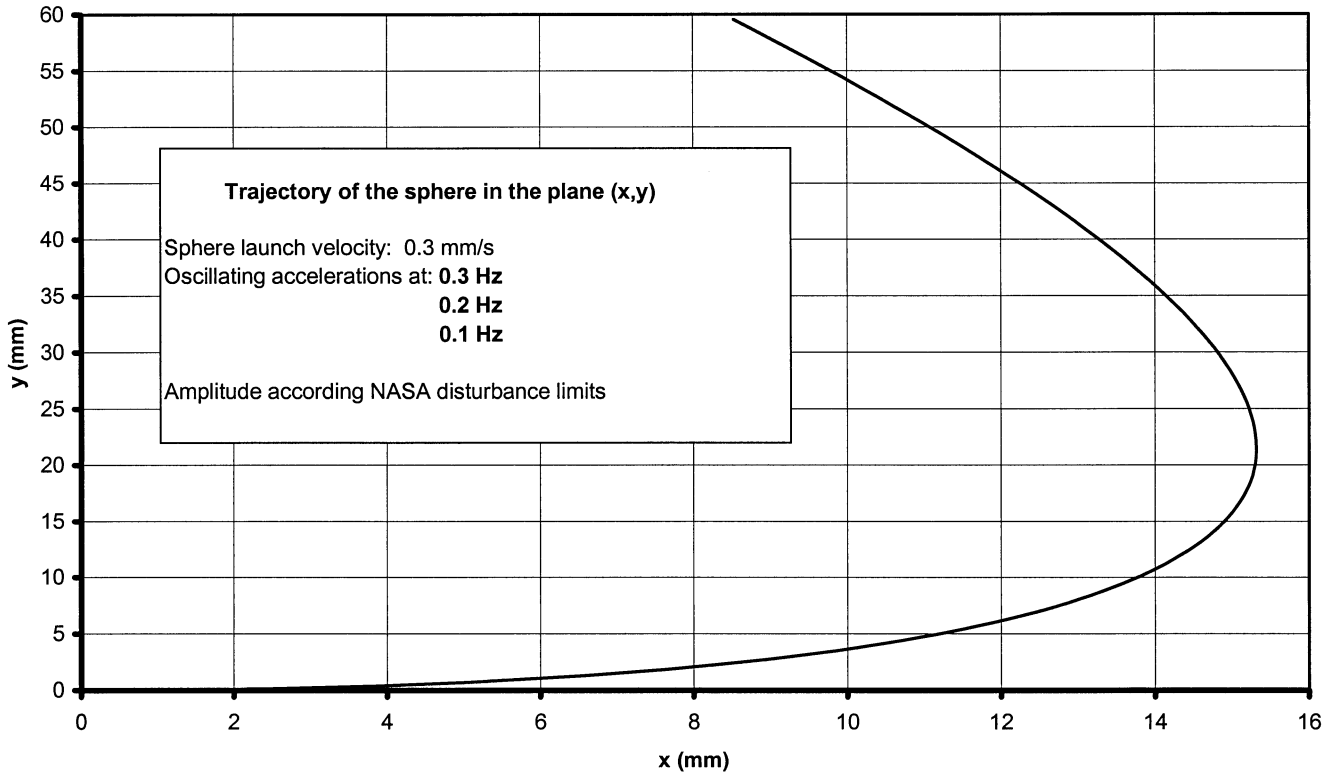

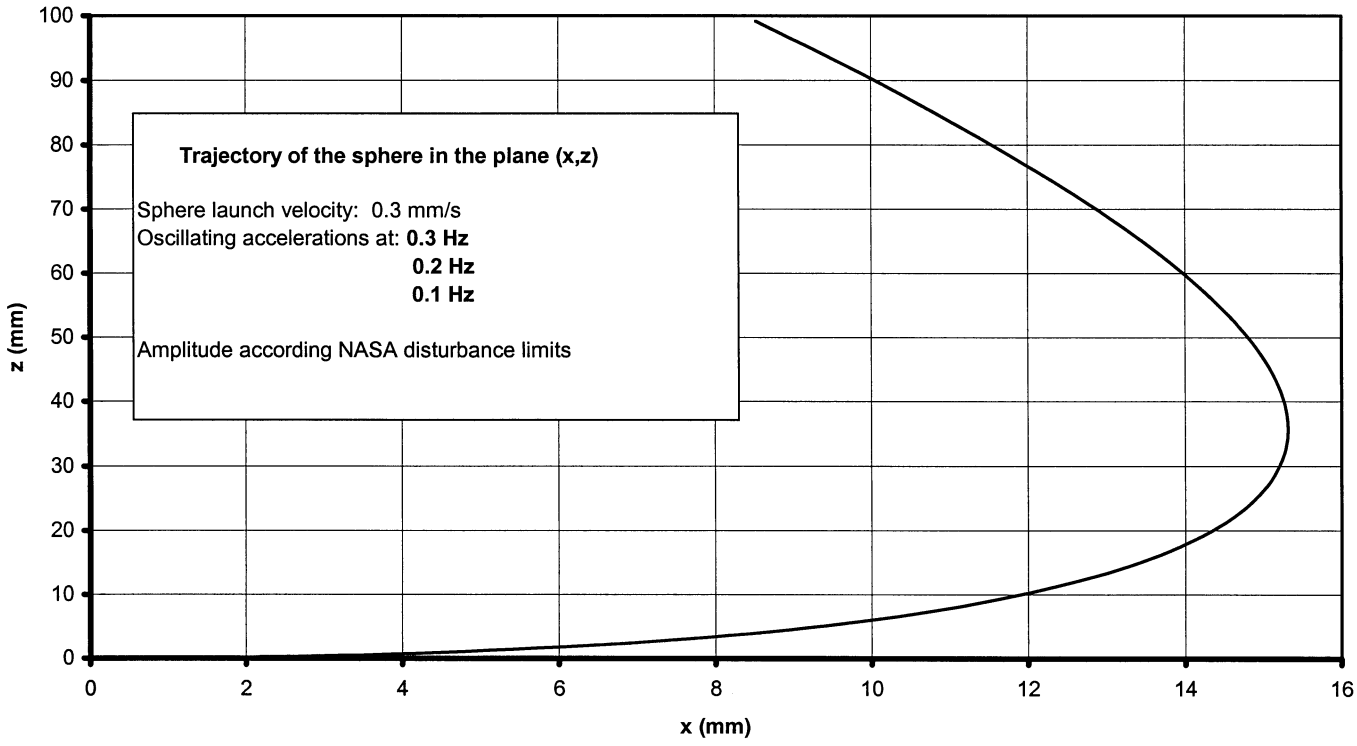

Figure 6

Giulio Poletti
University of Milan

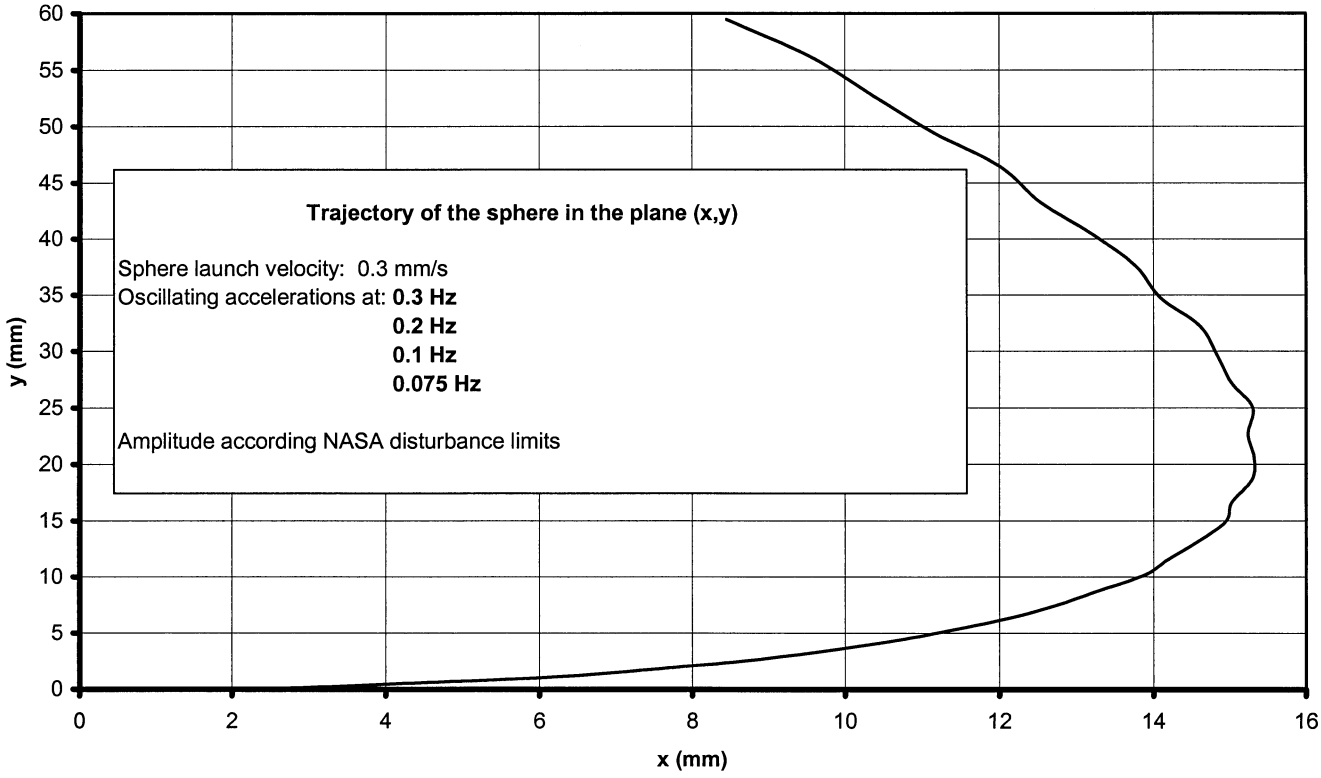

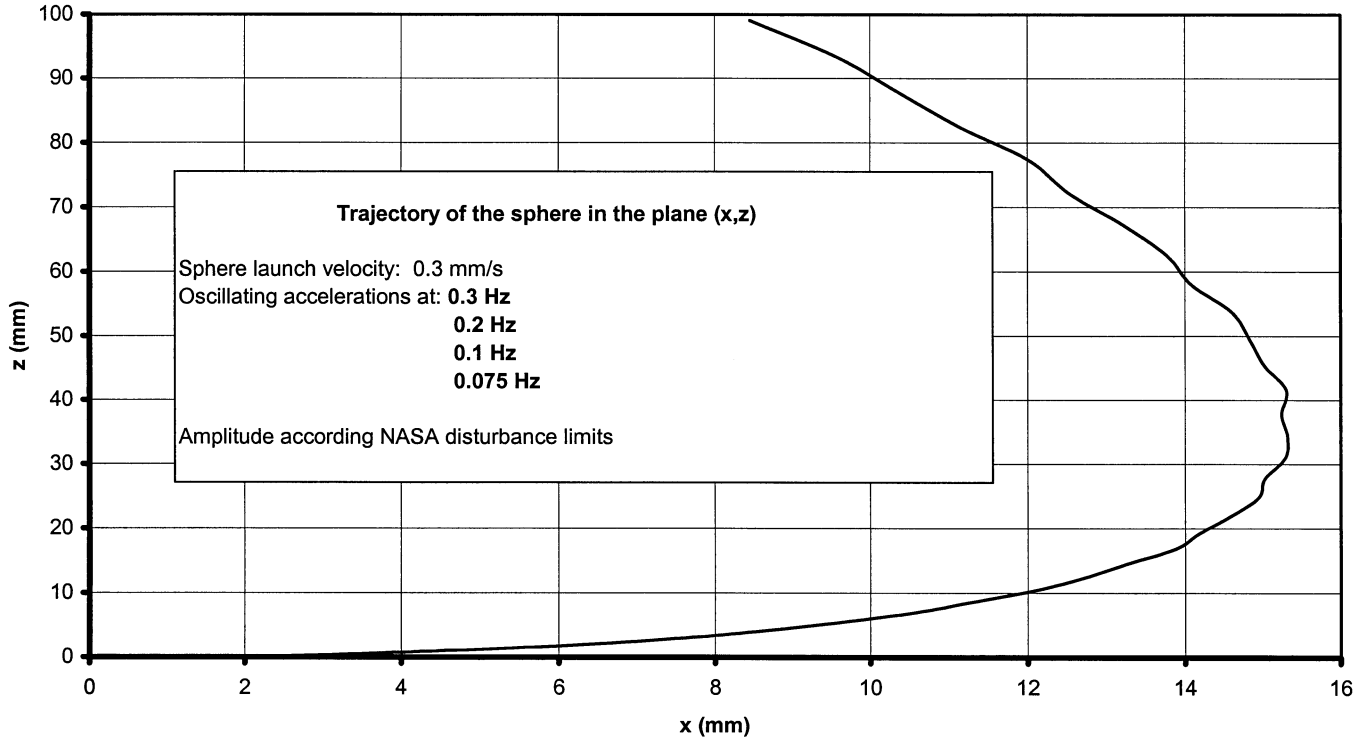

Figure 7

Giulio Poletti
University of Milan

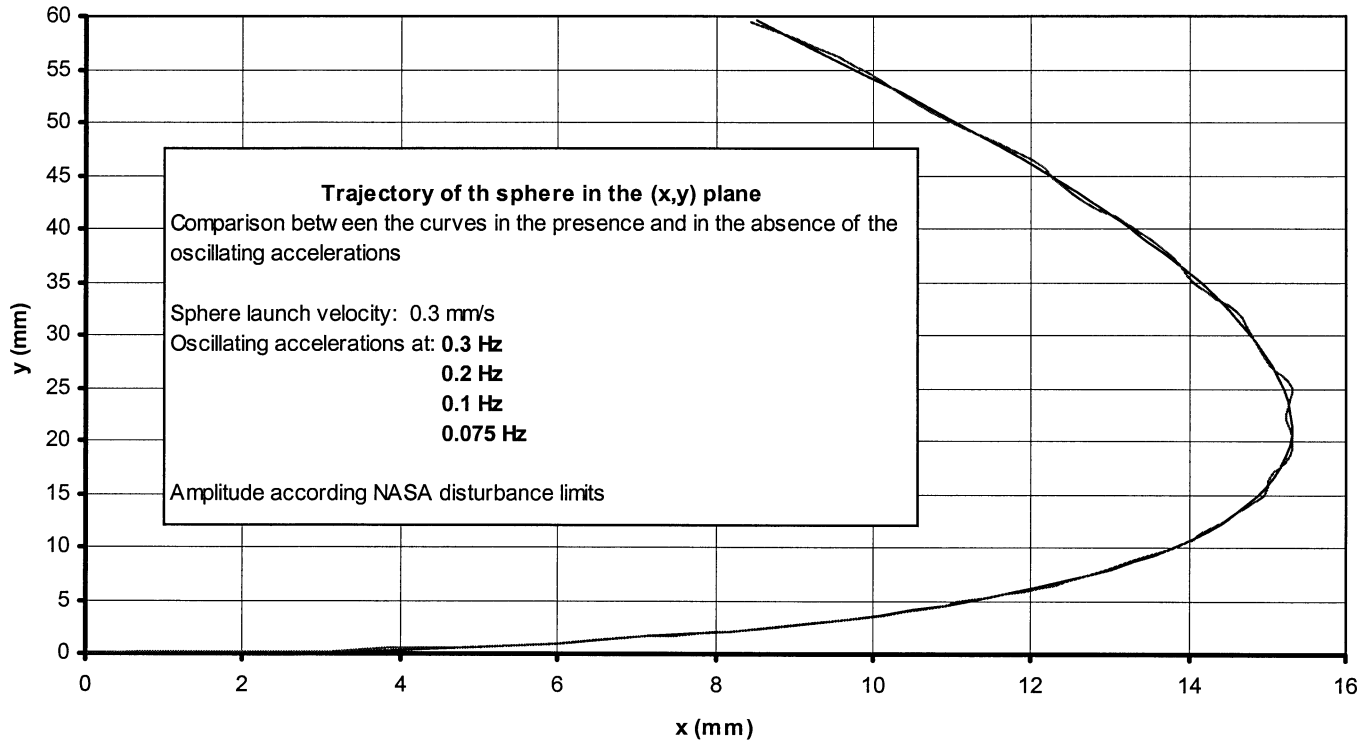

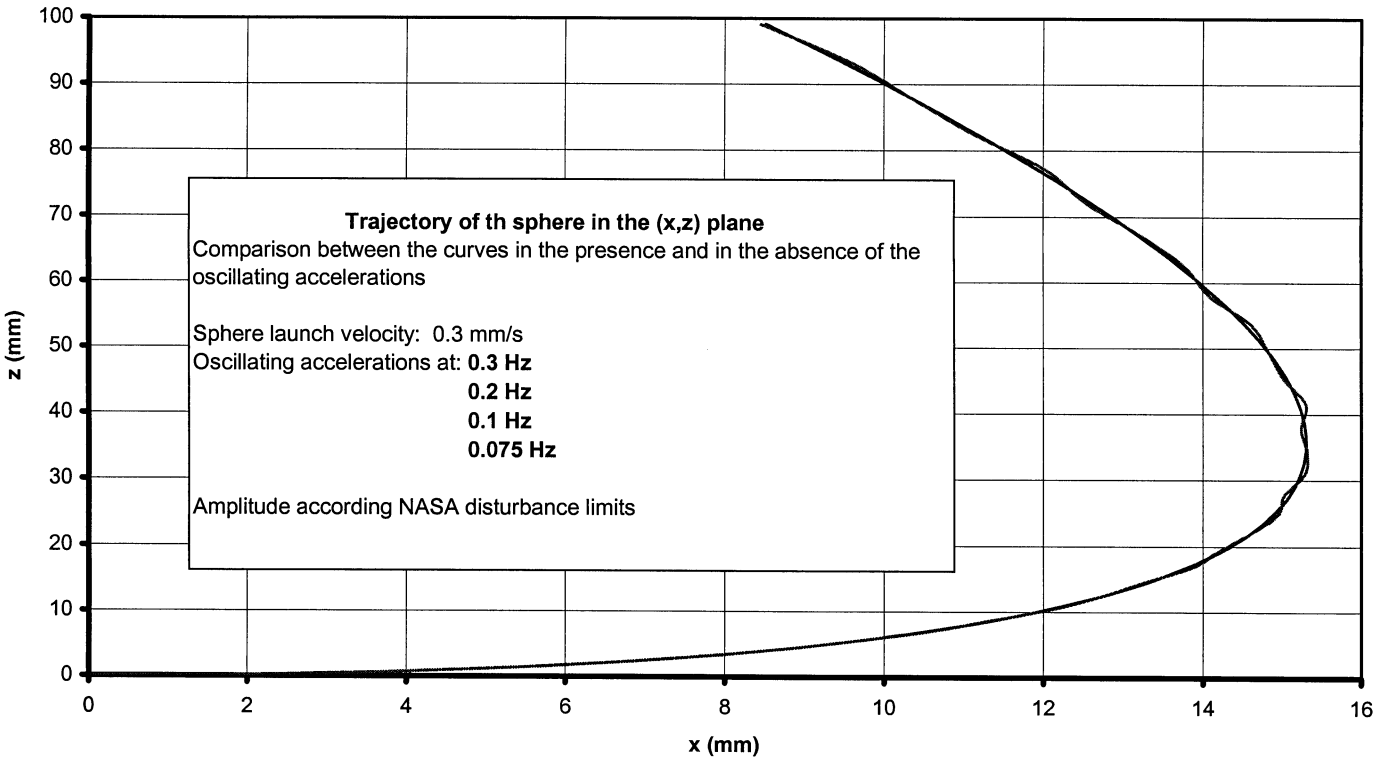

Figure 8

Giulio Poletti
University of Milan

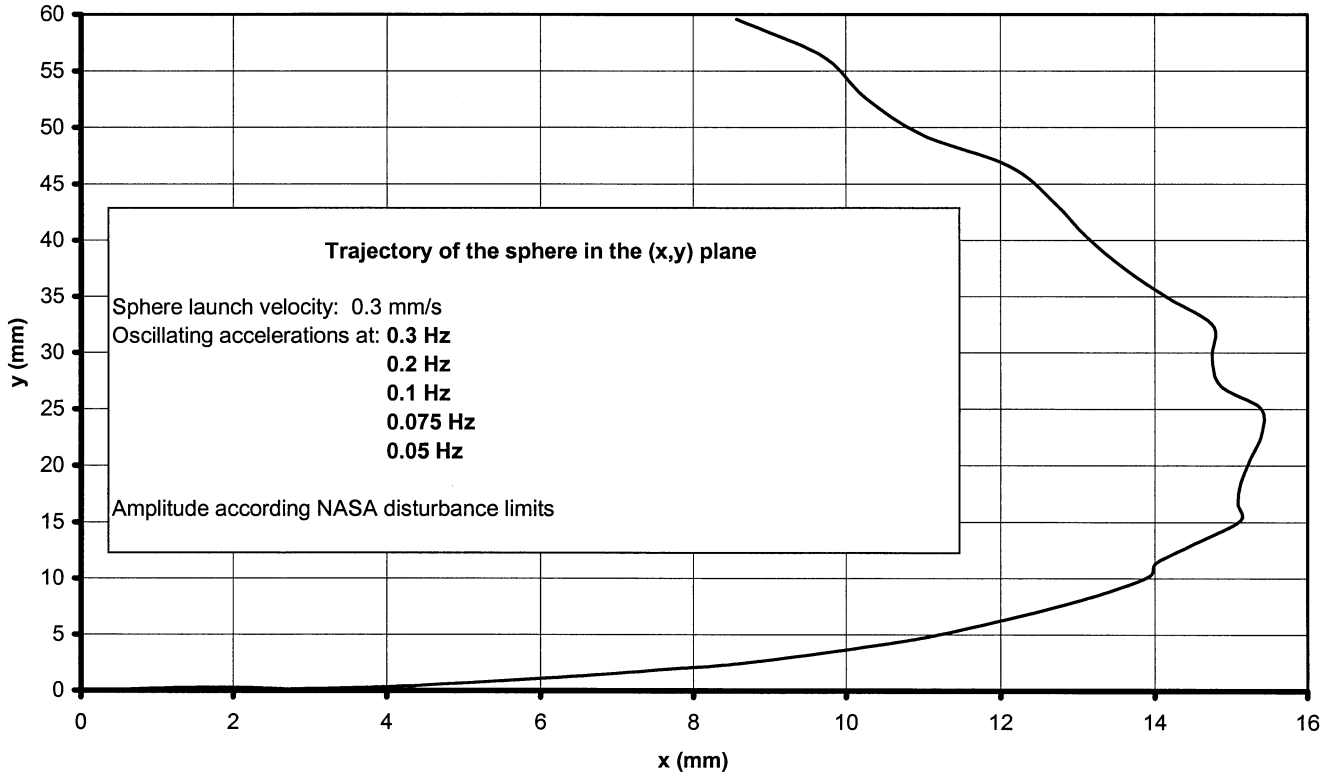

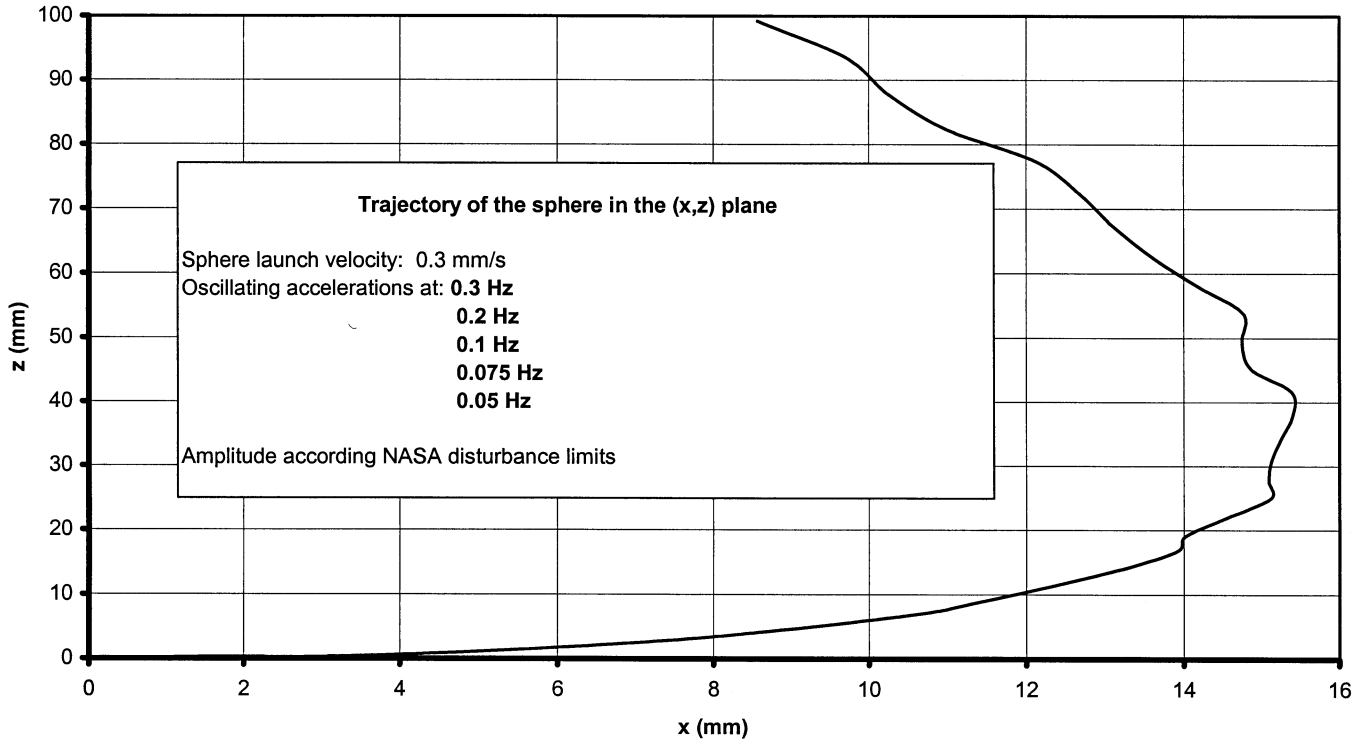

Figure 9

Giulio Poletti
University of Milan

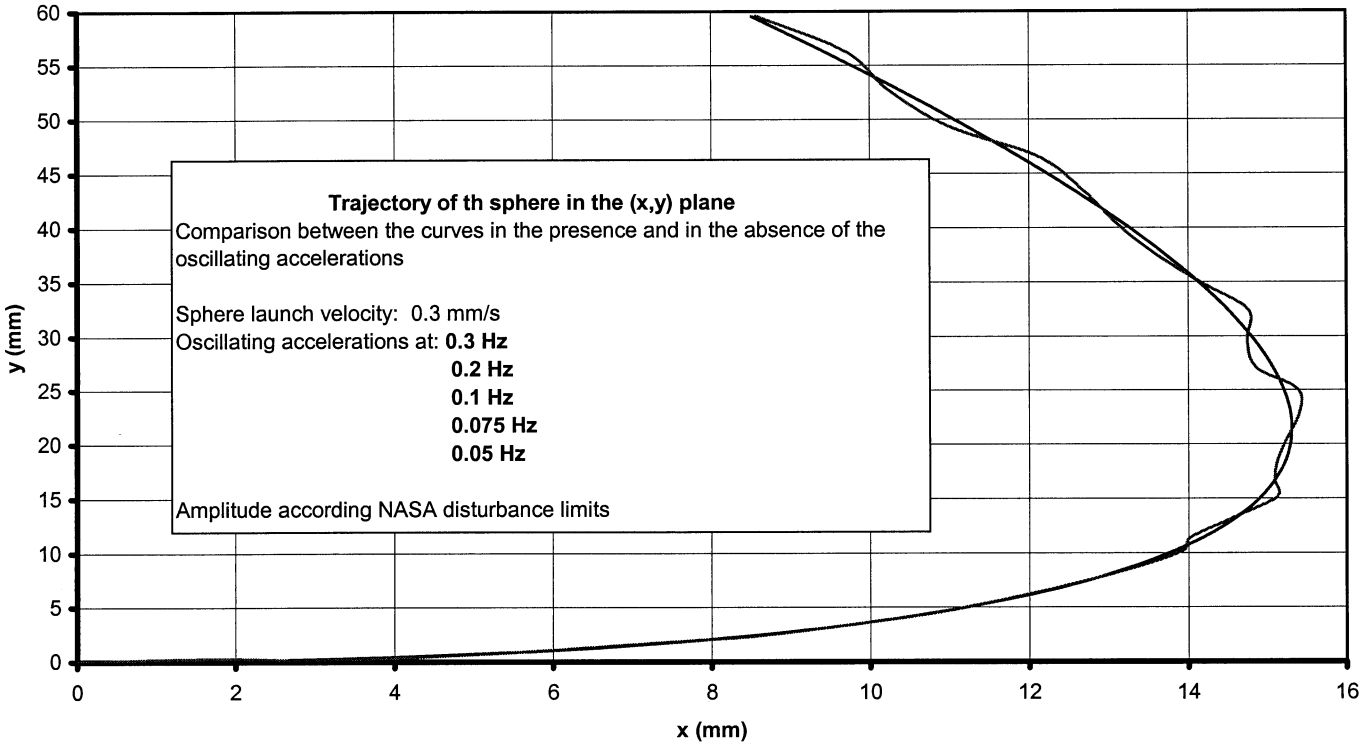

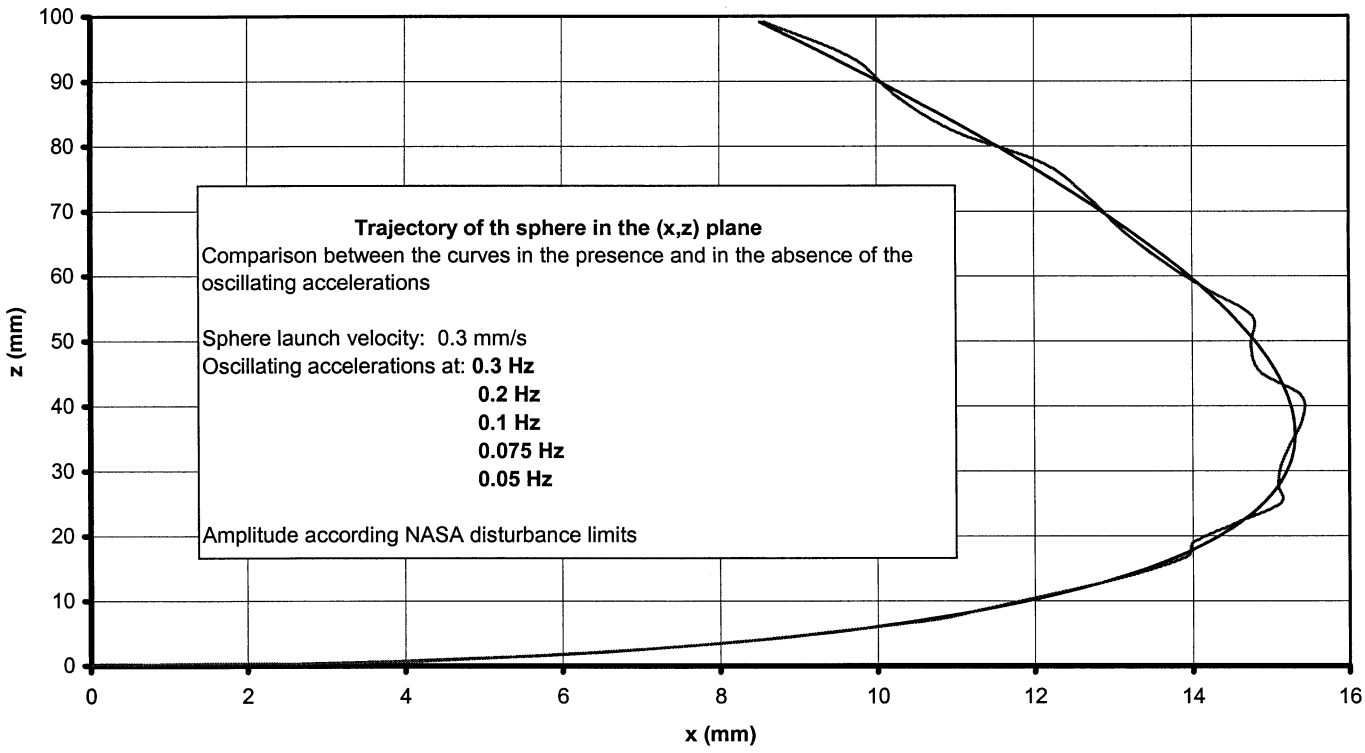

Figure 10

Giulio Poletti
University of Milan

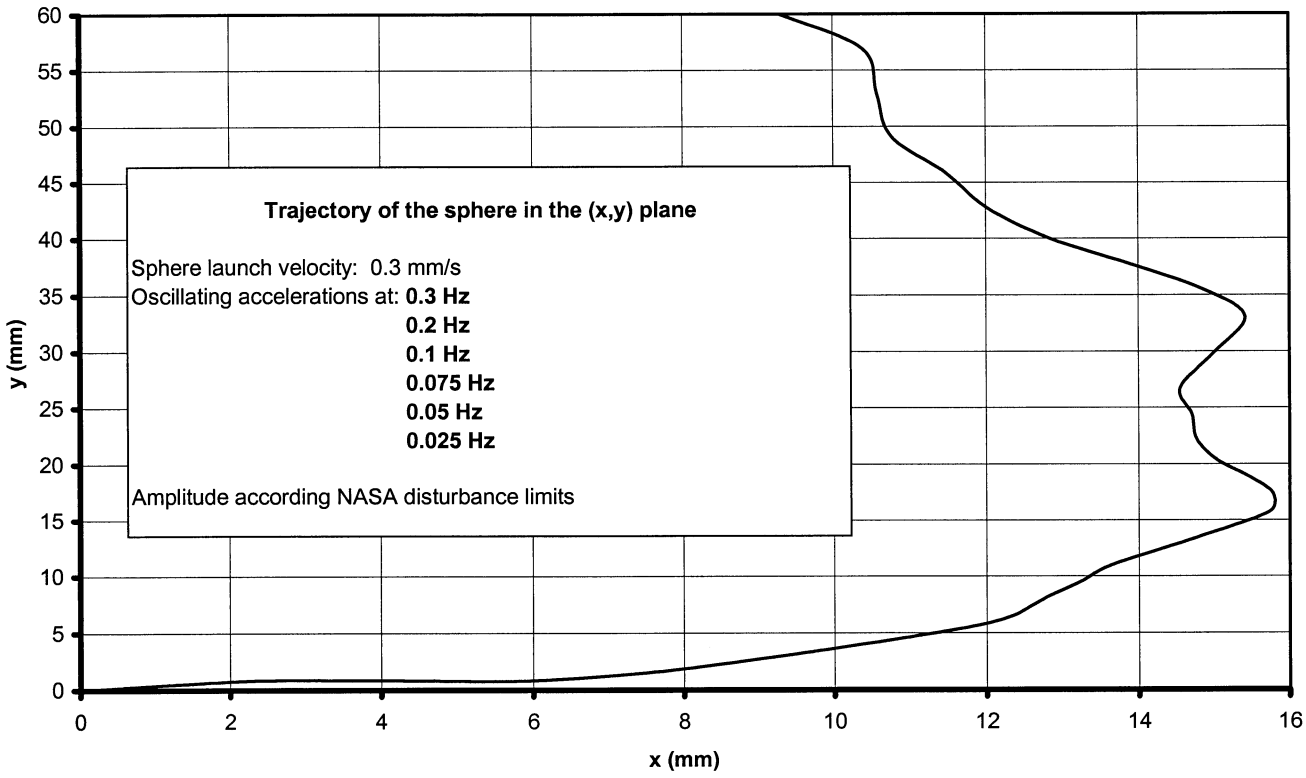

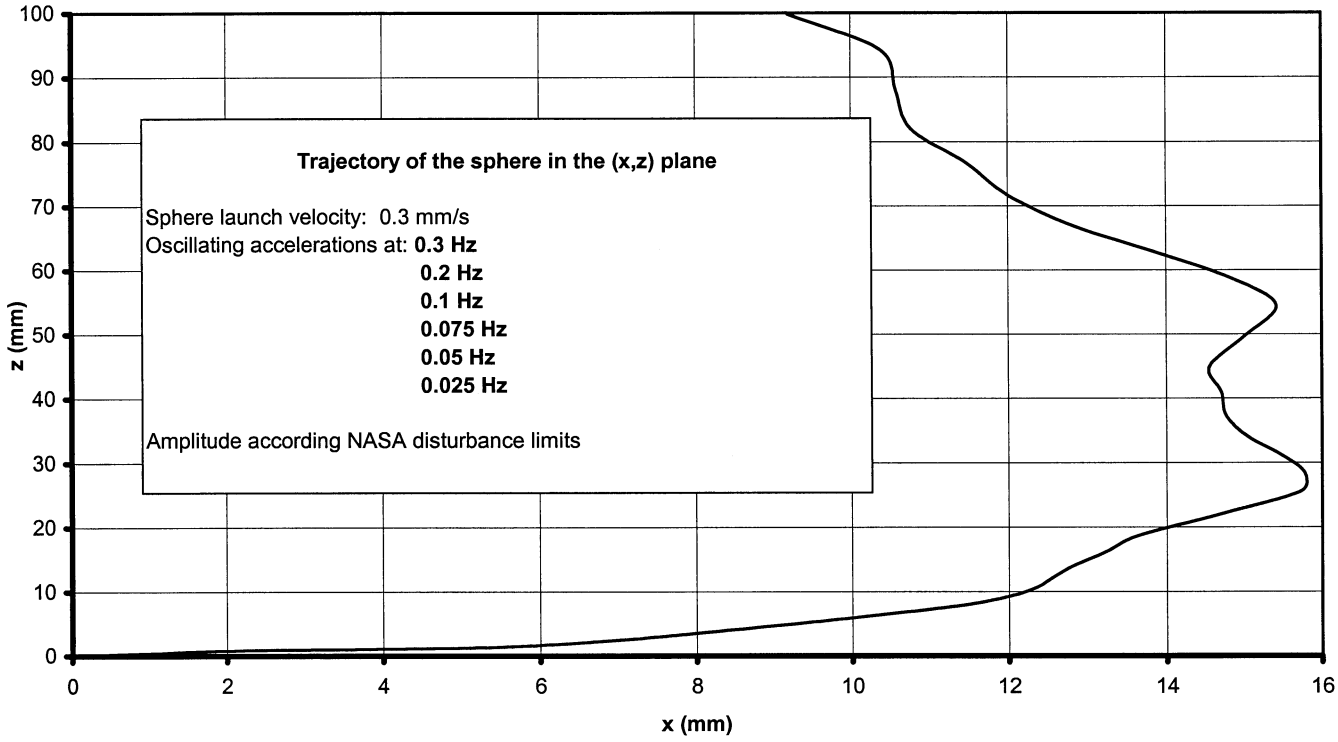

Figure 11

Giulio Poletti
University of Milan

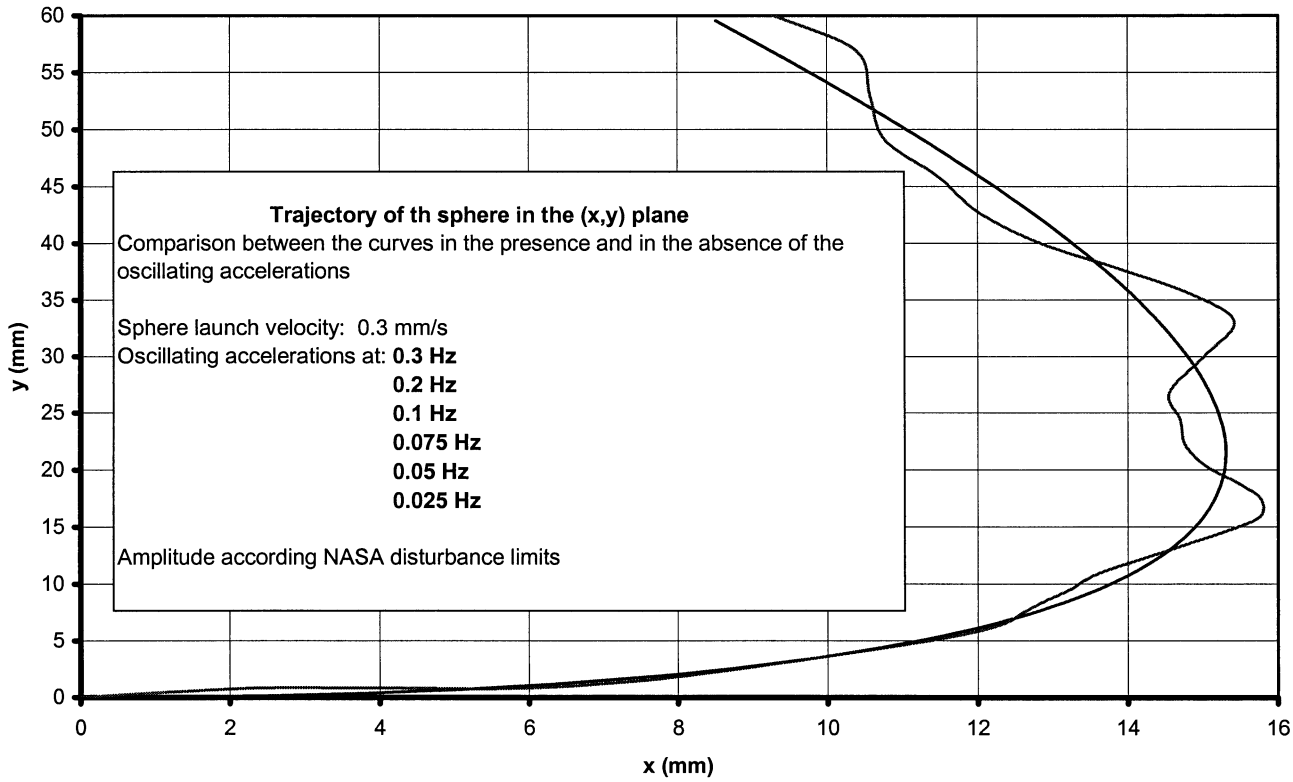

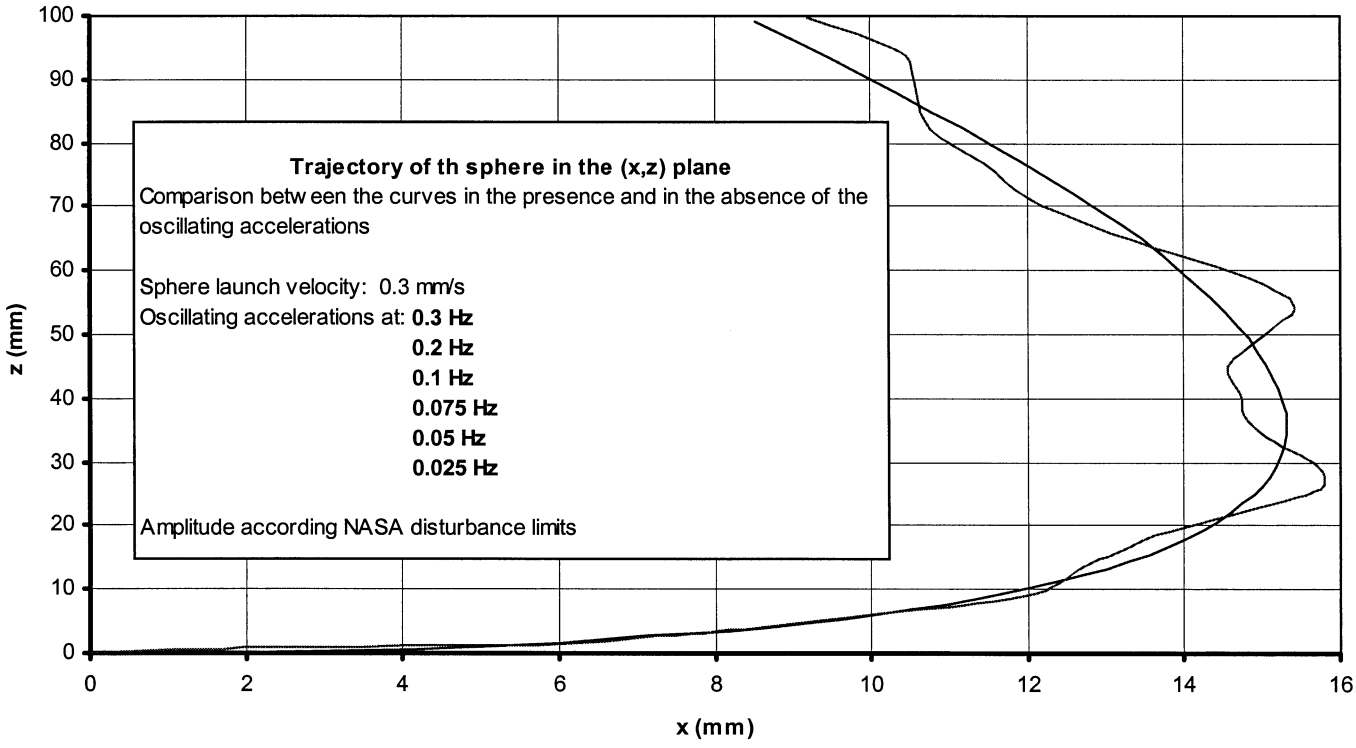

Figure 12

Giulio Poletti
University of Milan

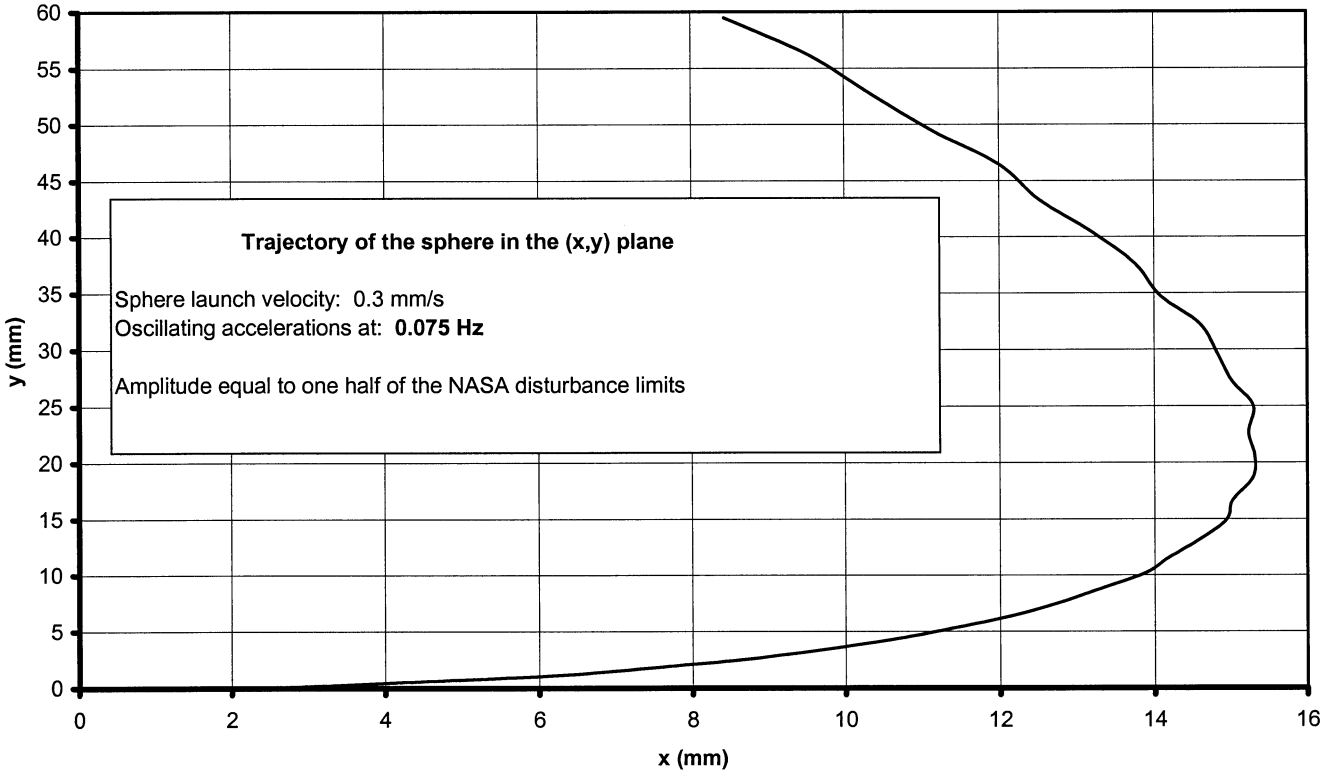

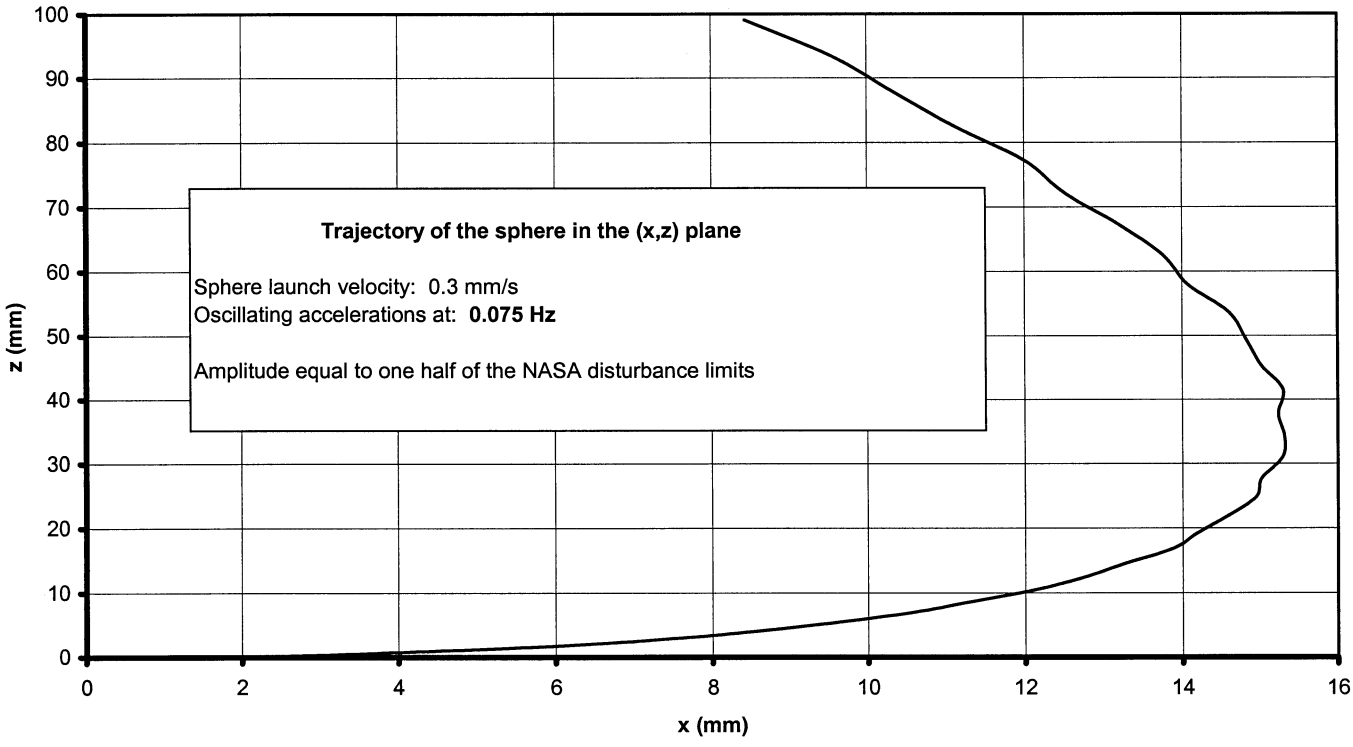

Figure 13

Giulio Poletti
University of Milan

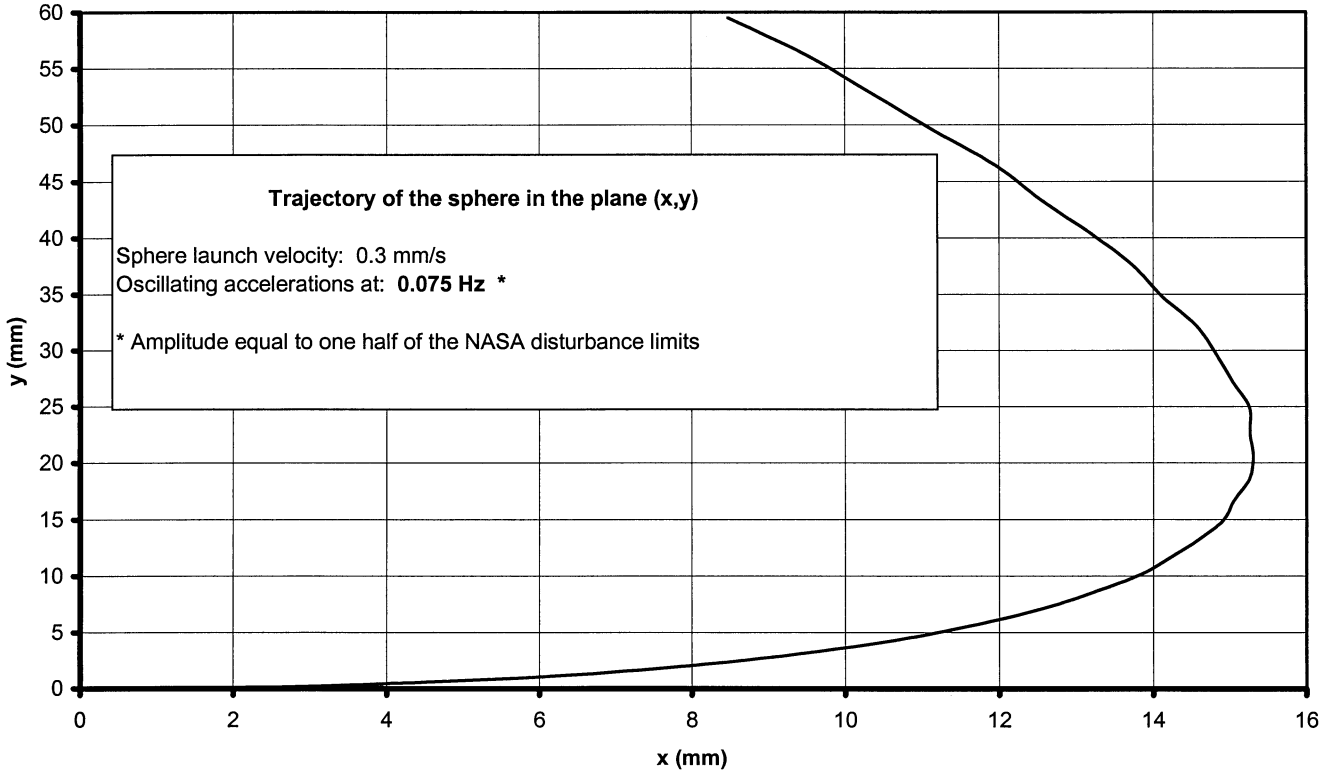

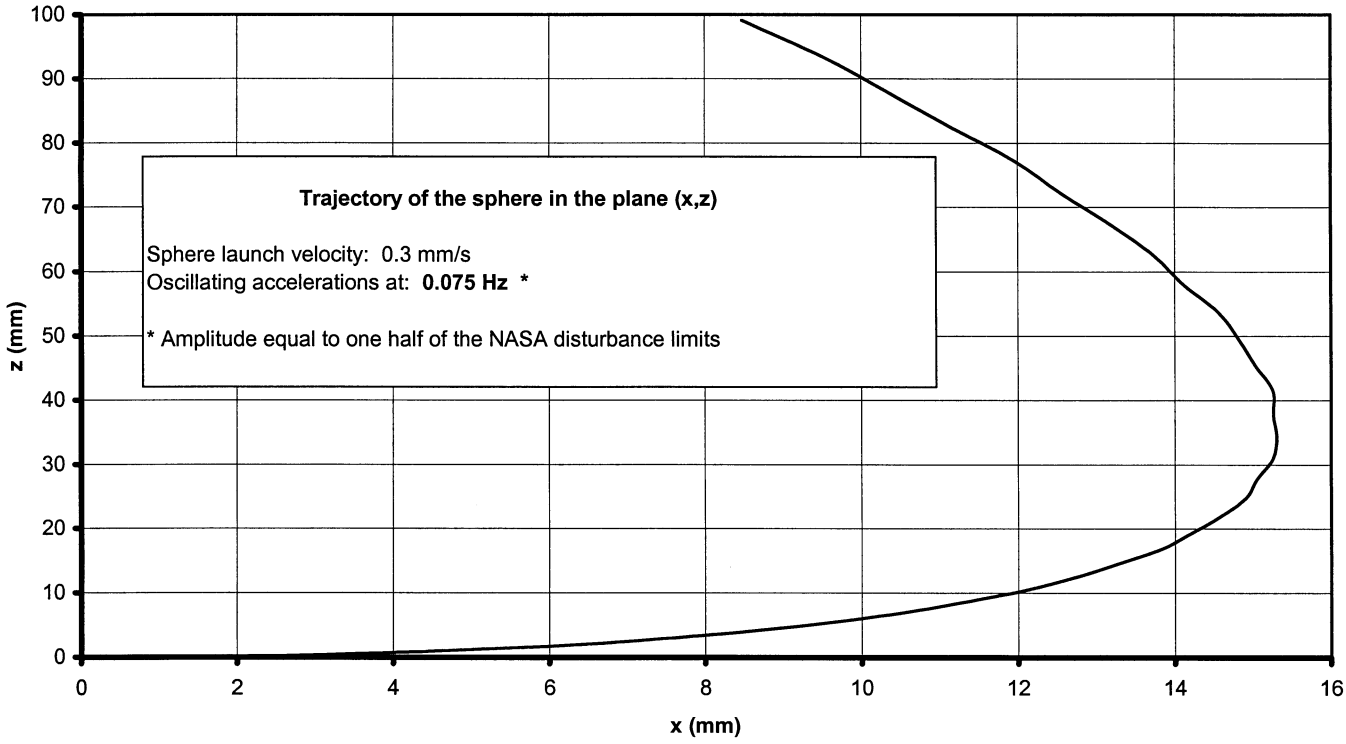

Figure 14

Giulio Poletti
University of Milan

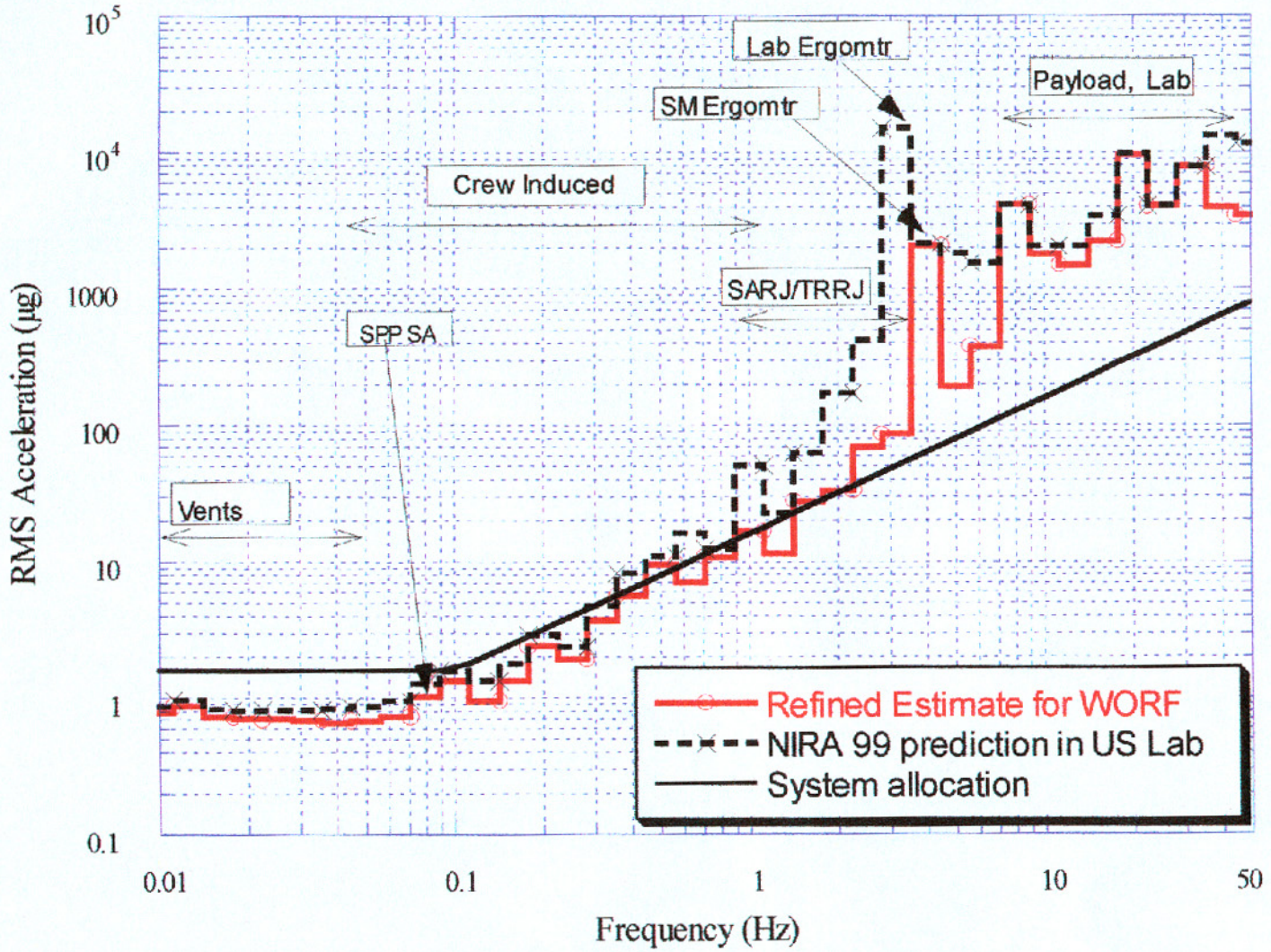

Figure 15
DAC-8 Isolated Microgravity Environment Prediction

Initial ARIS Performance Assessment for the Fluids & Combustion Facility (FCF)

Marcus Just
ZIN Technologies
Cleveland, Ohio

ZIN Technologies is working with the FCF project team to integrate ARIS with the FCF racks. ARIS will be used with multiple ISPRs in the U.S. Laboratory module, including the Combustion Integrated Rack (CIR) and the Fluids Integrated Rack (FIR). The current focus of this work is the CIR due to its modeling maturity.

Methods and procedures are being developed for the ARIS predicted performance. The resulting microgravity environment for CIR configurations are being studied. The environment will then be compared against the CIR & FIR Science Requirements Envelope Documents (SREDs) for verification, operational and facility design purposes.

NASA/CP—2001-211164

Glenn Research Center

ZIN Technologies Inc.
ARIS Integration Support

ARIS Feasibility Presentation to MGMG #20

Initial Microgravity and Performance Assessment

Marcus Just

August 8, 2001

Glenn Research Center

ZIN Technologies Inc.

ARIS Integration Support

Agenda

Active Rack Isolation System (ARIS)

- ARIS Overview
- Previous Work
- FCF-ARIS Integration Task
- Process Summary
- Initial Performance Analysis
- Process Verification
- Process Modifications
- NASTRAN Modeling
- Early ARIS-ICE Data
- Updates and Completion

NASA/CP—2001-211164

ZIN Technologies Inc.
ARIS Integration Support

ARIS Overview - Design

- ARIS Controller (Control & input/output): Decoupling implemented in controller allows freedom to place actuators and sensors. Payloads have extensive command, data acquisition, and control options.
- 3 Remote Electronic Units : Programmable analog filters & gains & 16 bit analog-to-digital converters.
- 3 Tri-axial Accelerometer Heads : Built small to fit in rack corners
- 1 Actuator Driver : Pulse width modulation used to reduce power consumption
- 8 Actuators : Voice coil rotary actuator used to reduce profile and power consumption.

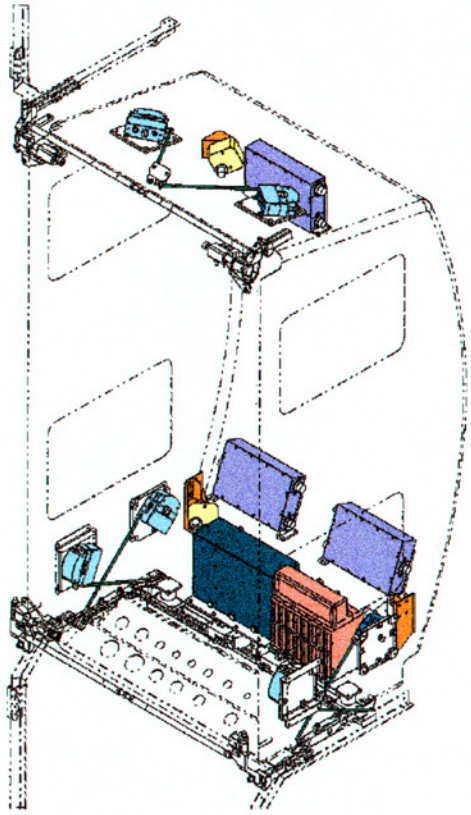

Glenn Research Center

ZIN Technologies Inc.
ARIS Integration Support

ARIS Overview- Specs

- Active Isolation 0.01-2 Hz
- Passive Isolation > 2 Hz
- Communication With User: 1553B Data Bus
- Operational States:
  - * Idle (passive)
  - * Active Built In Test
  - * Hold (rack centered)
  - * Power Off (emergency only)
  - * Initialize
  - * NoGo (Idle after error)
  - * Active
- Requirements:
  - * ISS Microgravity
  - * "Good Neighbor"
  - * Sway Space < ±0.5"

Glenn Research Center

ZIN Technologies Inc.
ARIS Integration Support

Previous Work

- 6 DOF Demonstrations: Learjet Missions
- RME1313: STS-79 Mission to Mir
- ARIS -ISS Characterization Experiment (ARIS-ICE)
  - Currently in US Lab
  - 5 SAMS accelerometer heads utilized
  - Assessing actual ARIS performance for EXPRESS Rack #2
  - On-orbit data verifying ARIS performance
  - Currently behind their original test matrix and working with reduced actuator set
  - Also awaiting soft looped umbilical set-scheduled to be launched for 7A.1 operations

Glenn Research Center

ZIN Technologies Inc.
ARIS Integration Support

FCF-ARIS Integration Task

- ARIS to be used for 6 to 10 experiment US Lab ISPRs
- Current focus on CIR due to modeling maturity
- Establish analytical methods and procedures for ARIS predicted performance
- Characterize science microgravity environment for various CIR configurations:
  - ARIS Active
  - ARIS Idle (Passive)
  - Hard Mounted (No ARIS or ARIS in "Hold" state)

Glenn Research Center

ZIN Technologies Inc.
ARIS Integration Support

Process Summary

- Supplied with Boeing ARIS Simulink Model used for EXPRESS Rack #2
- Test runs conducted for benchmark process
  - simple lumped mass-damper-spring model
  - simple plate suspended with corner springs model
  - verifications with NASTRAN and theory
- Implemented modifications to Simulink model
- Developed CIR on-orbit NASTRAN model with temporary umbilical representation
- Extracted eigenvector info from FEM
- Input CIR eigenvectors into Simulink model
- Conducted verifications with NASTRAN
- Conducted initial performance assessment

Glenn Research Center

ZIN Technologies Inc.
ARIS Integration Support

ARIS Integration Analytical Process Flow –Rev 1.2 (June 5, 2001)

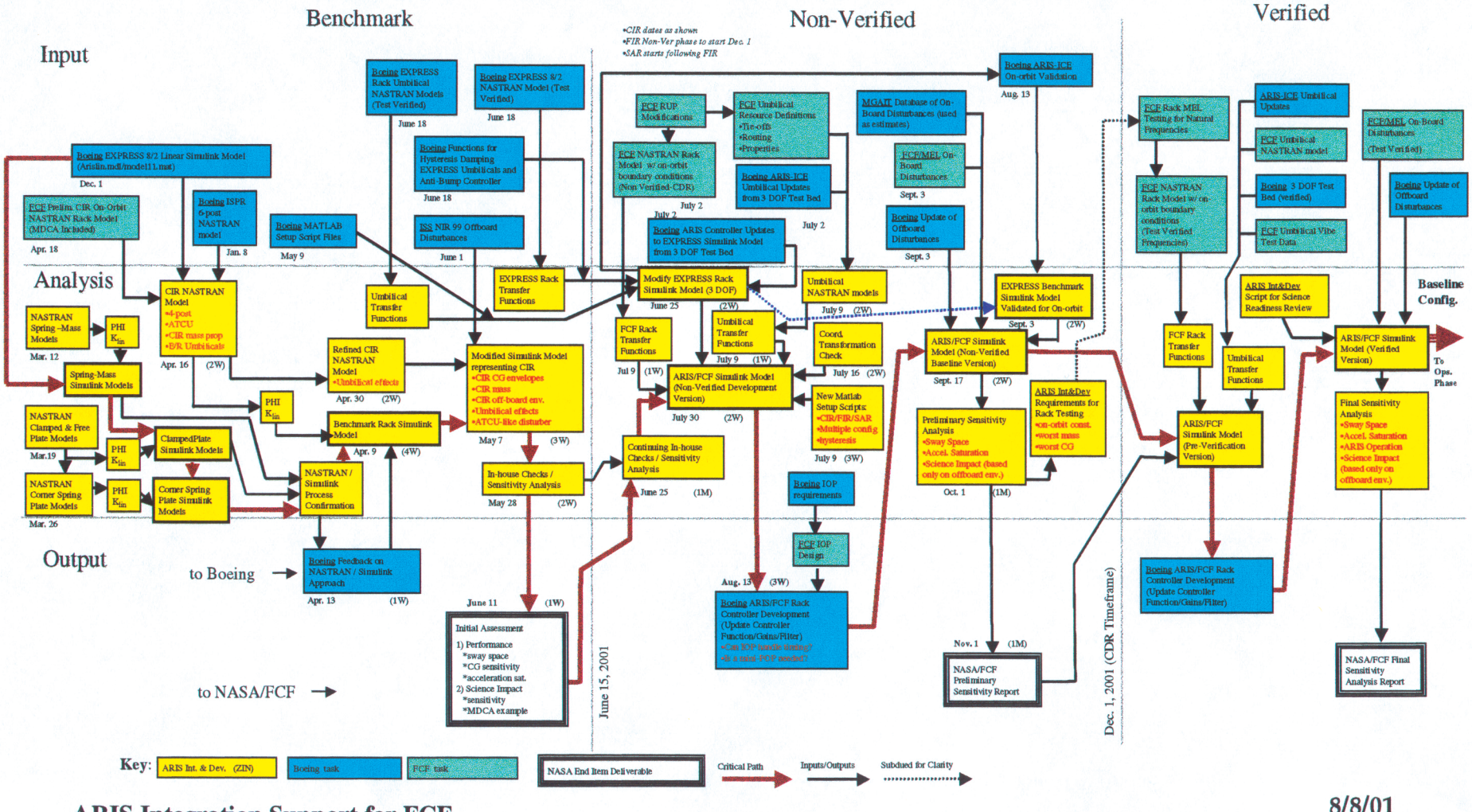

ARIS Integration Support for FCF

8/8/01

Glenn Research Center

ZIN Technologies Inc.
ARIS Integration Support

Initial Performance Analysis

- Predicted offboard loading (NIRA99 data from US Lab)
- Single onboard loading (From AAA fan disturbance data)
- Combined effects of both single onboard and predicted offboard
- Attenuation characterization
- Performance at CG and verification point
- Onboard to offboard impact
- Comparison to CIR & FIR Science Requirements Envelopes (SREDs)

Glenn Research Center

ZIN Technologies Inc.
ARIS Integration Support

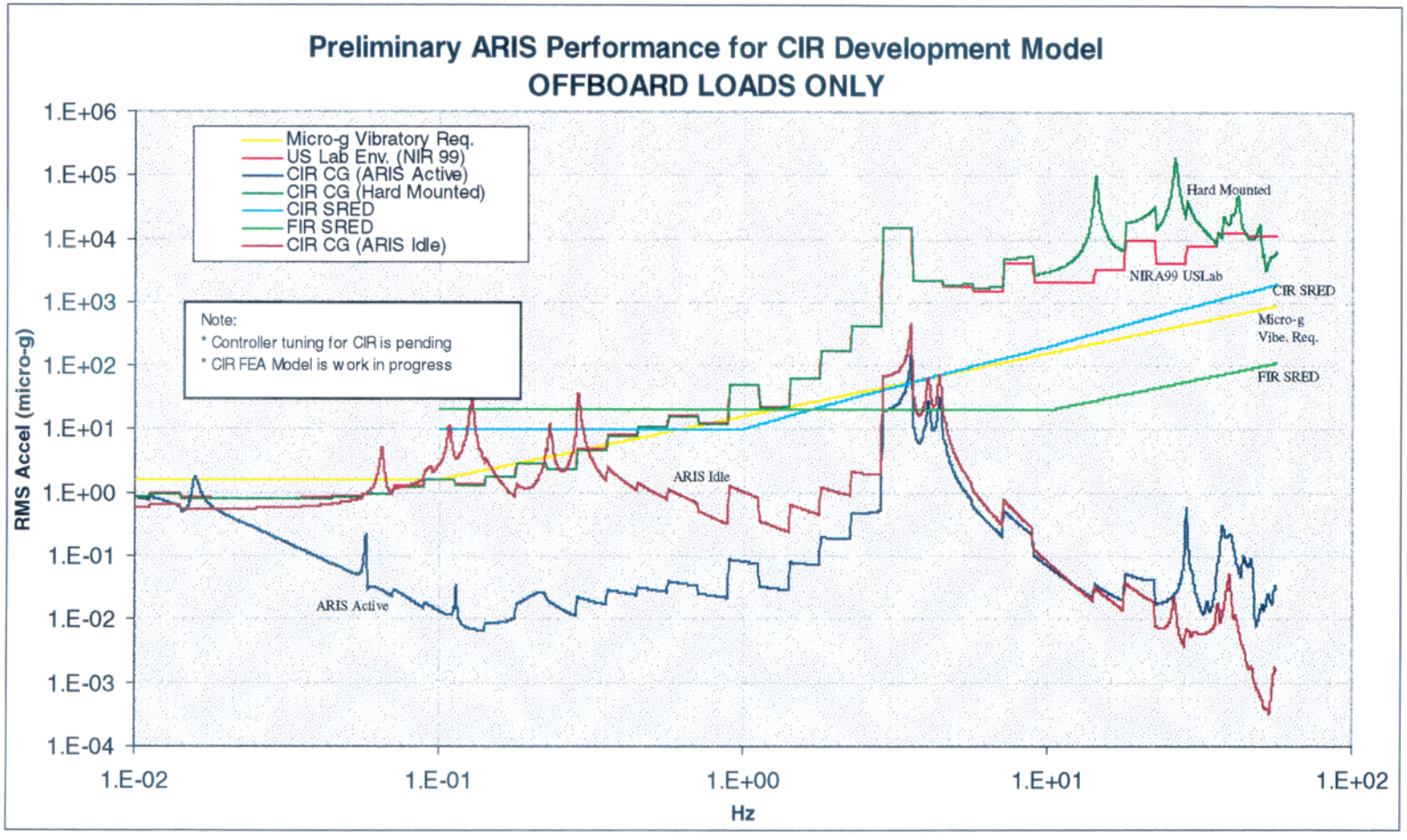

Glenn Research Center

ZIN Technologies Inc.
ARIS Integration Support

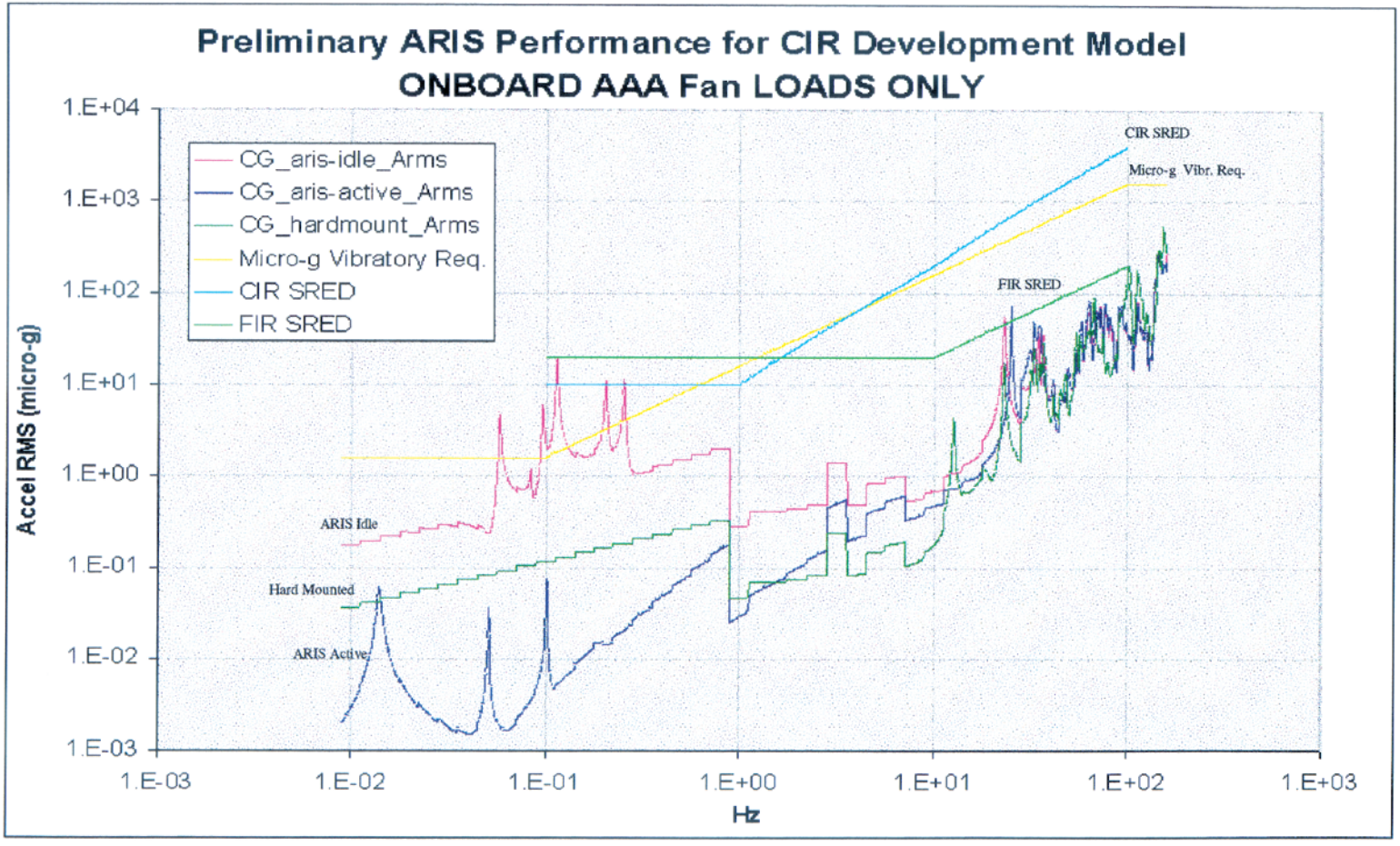

Glenn Research Center

ZIN Technologies Inc.

ARIS Integration Support

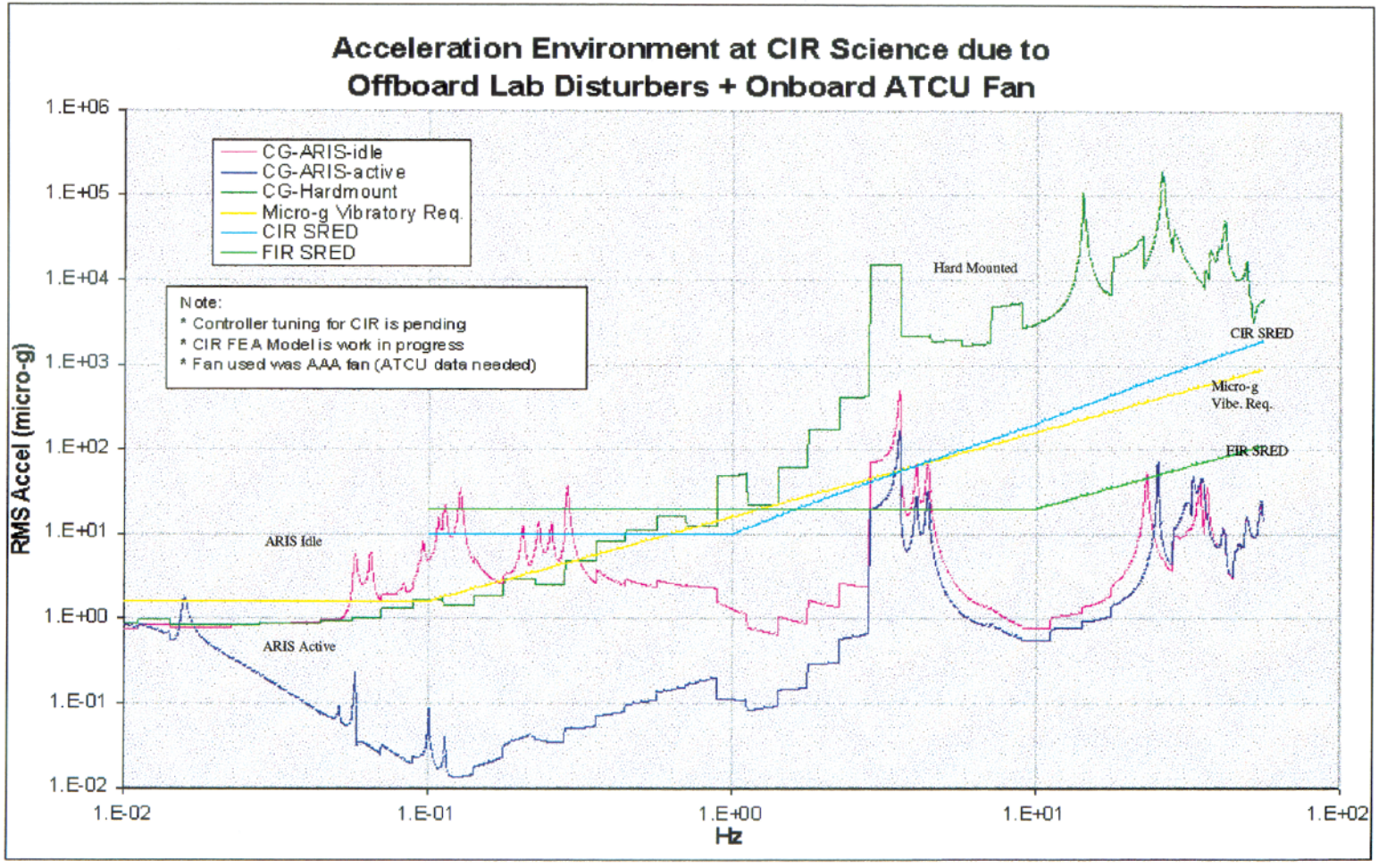

Glenn Research Center

ZIN Technologies Inc.
ARIS Integration Support

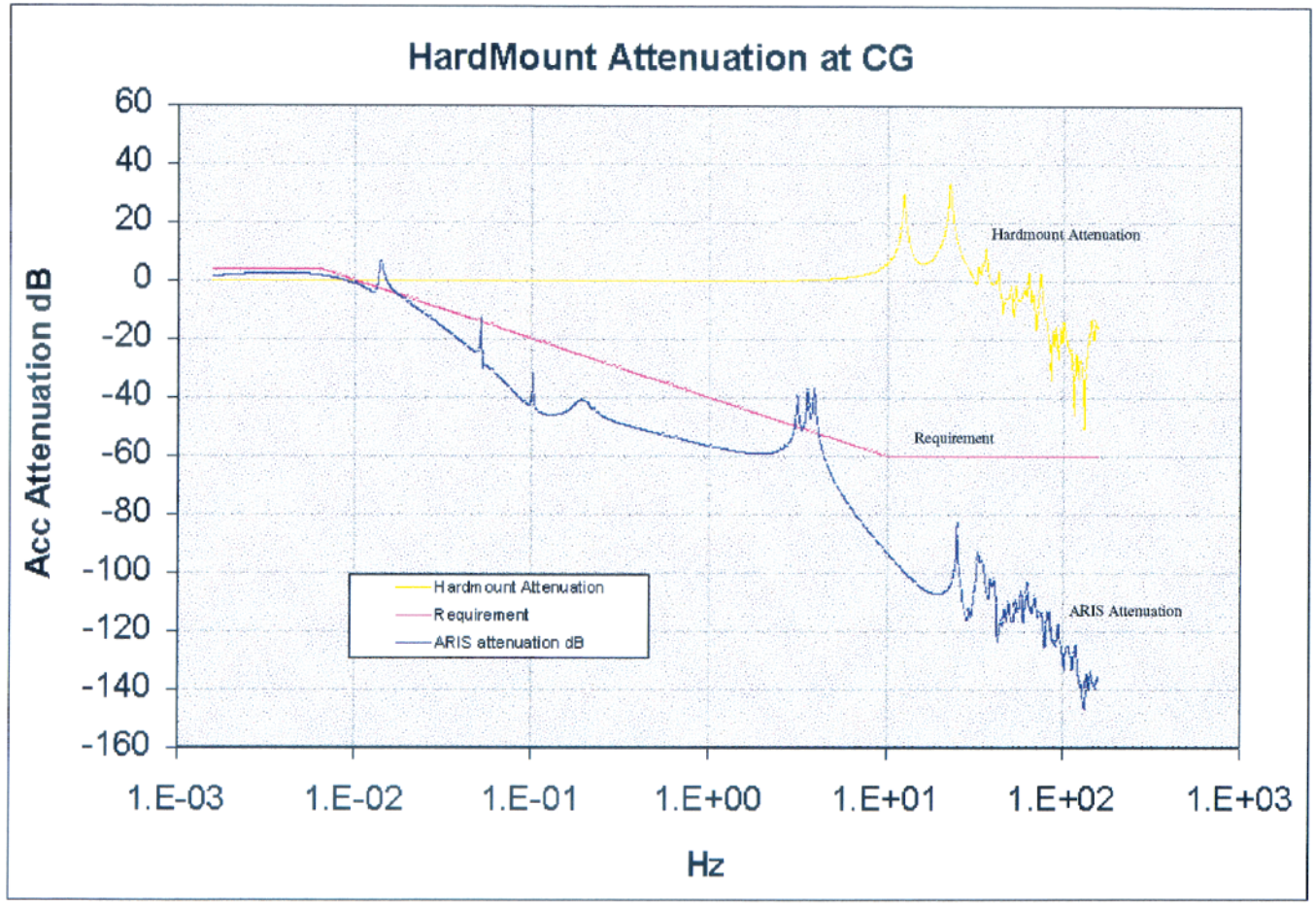

Glenn Research Center

ZIN Technologies Inc.
ARIS Integration Support

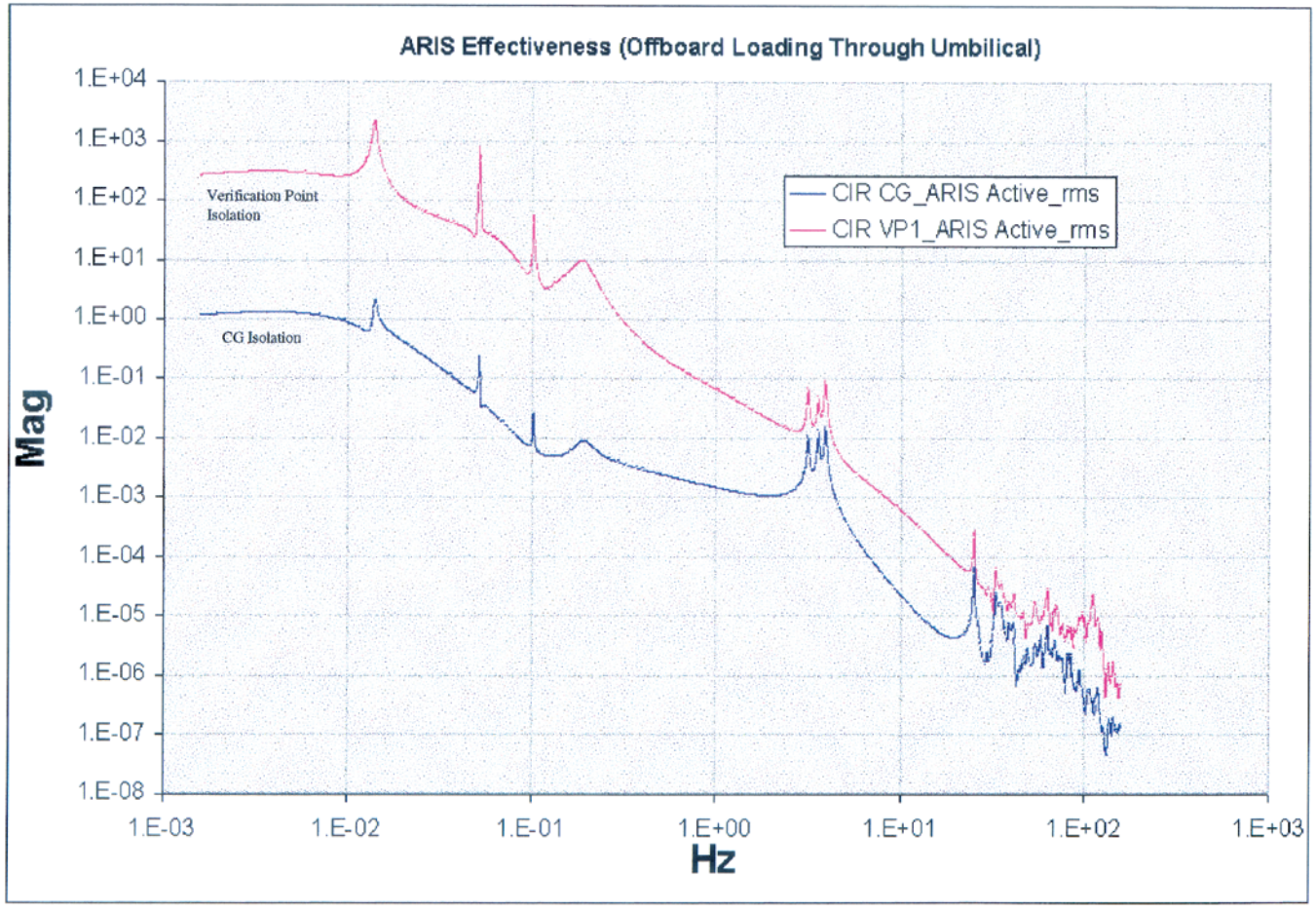

Glenn Research Center

ZIN Technologies Inc.
ARIS Integration Support

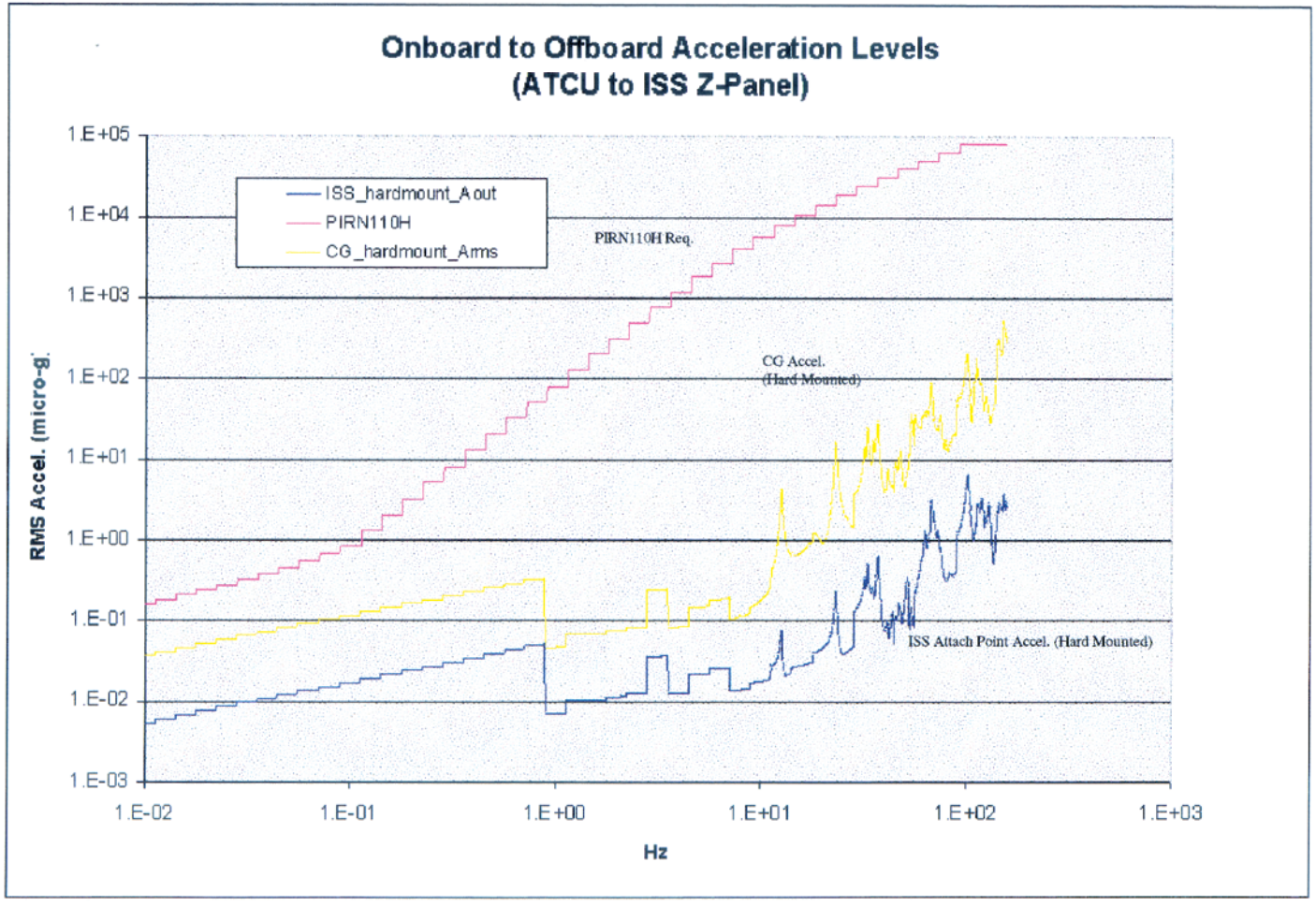

Glenn Research Center

ZIN Technologies Inc.
ARIS Integration Support

Process Verification

- Lumped Mass-Spring-Damper Model
- Square Plate with Corner Spring Model

Glenn Research Center

ZIN Technologies Inc.
ARIS Integration Support

Lumped Mass-Spring-Damper

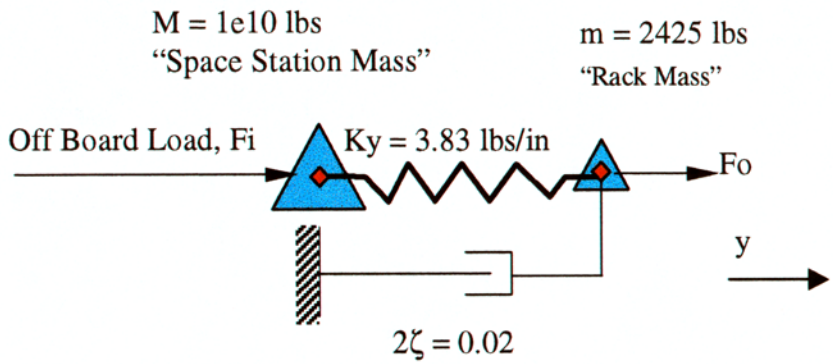

- Modeled in Simulink and NASTRAN
- Compared response with closed form solution:

$$\left|M(\omega)\right| := \frac{1}{\left[\left[1-\left(\frac{\omega}{\omega n}\right)^2\right]^2+\left(2\cdot\zeta\cdot\frac{\omega}{\omega n}\right)^2\right]^{\frac{1}{2}}}$$

Glenn Research Center

ZIN Technologies Inc.
ARIS Integration Support

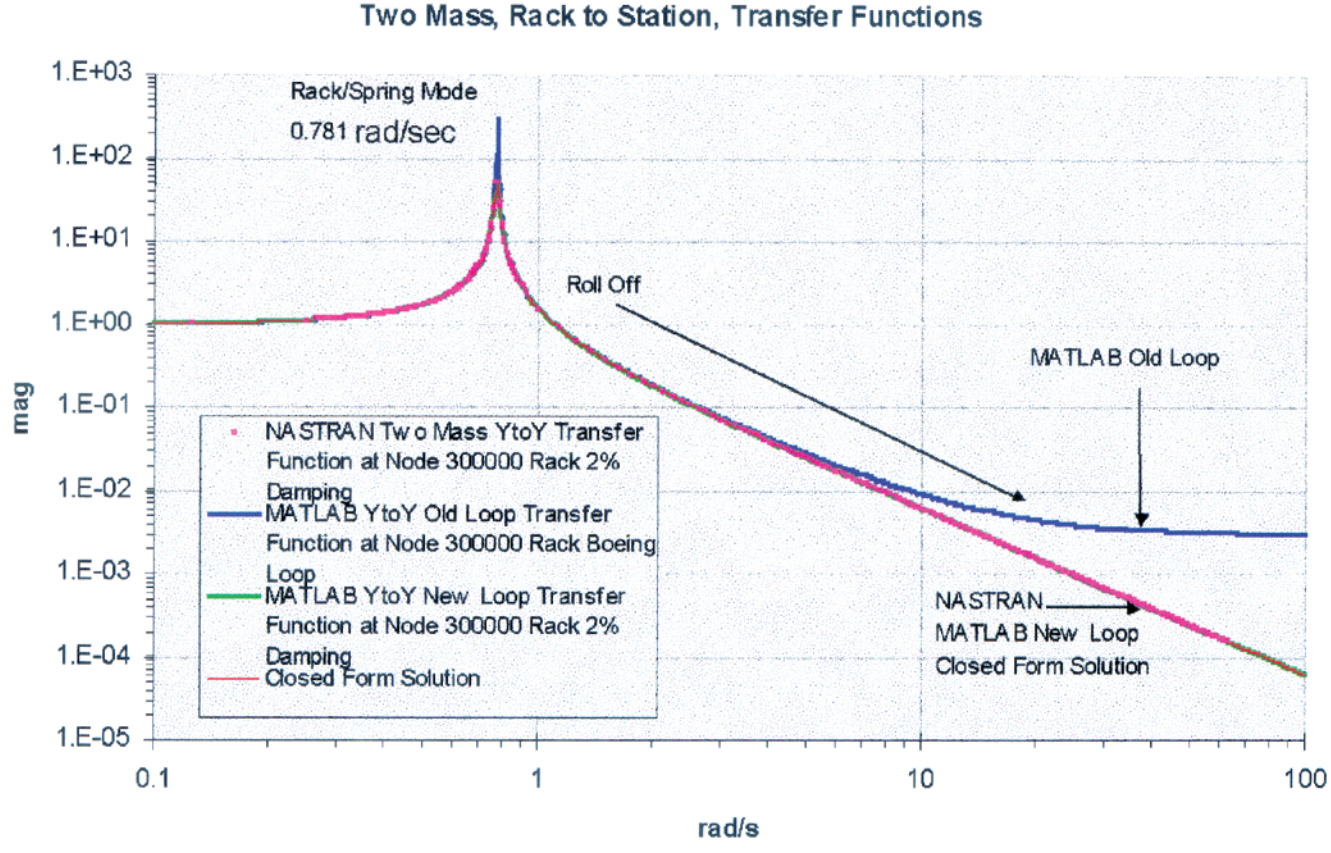

Glenn Research Center

ZIN Technologies Inc.
ARIS Integration Support

Square Plate with Springs

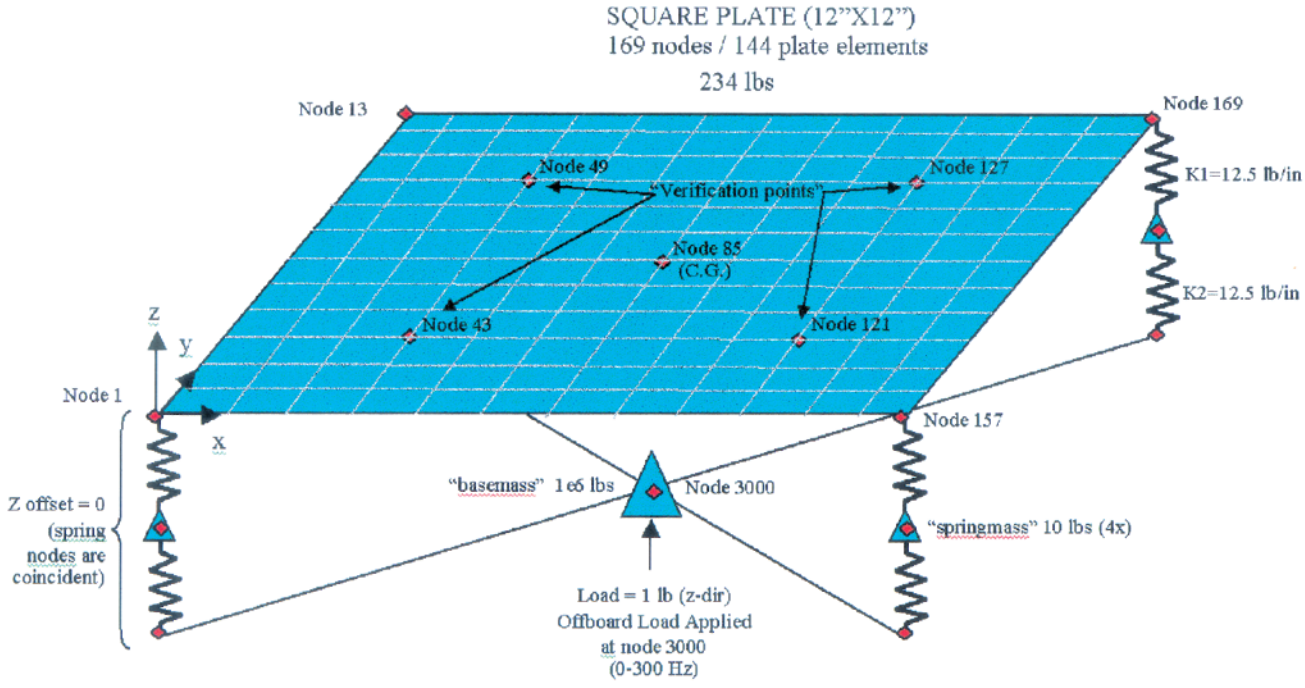

- Modeled in Simulink and NASTRAN

Glenn Research Center

ZIN Technologies Inc.
ARIS Integration Support

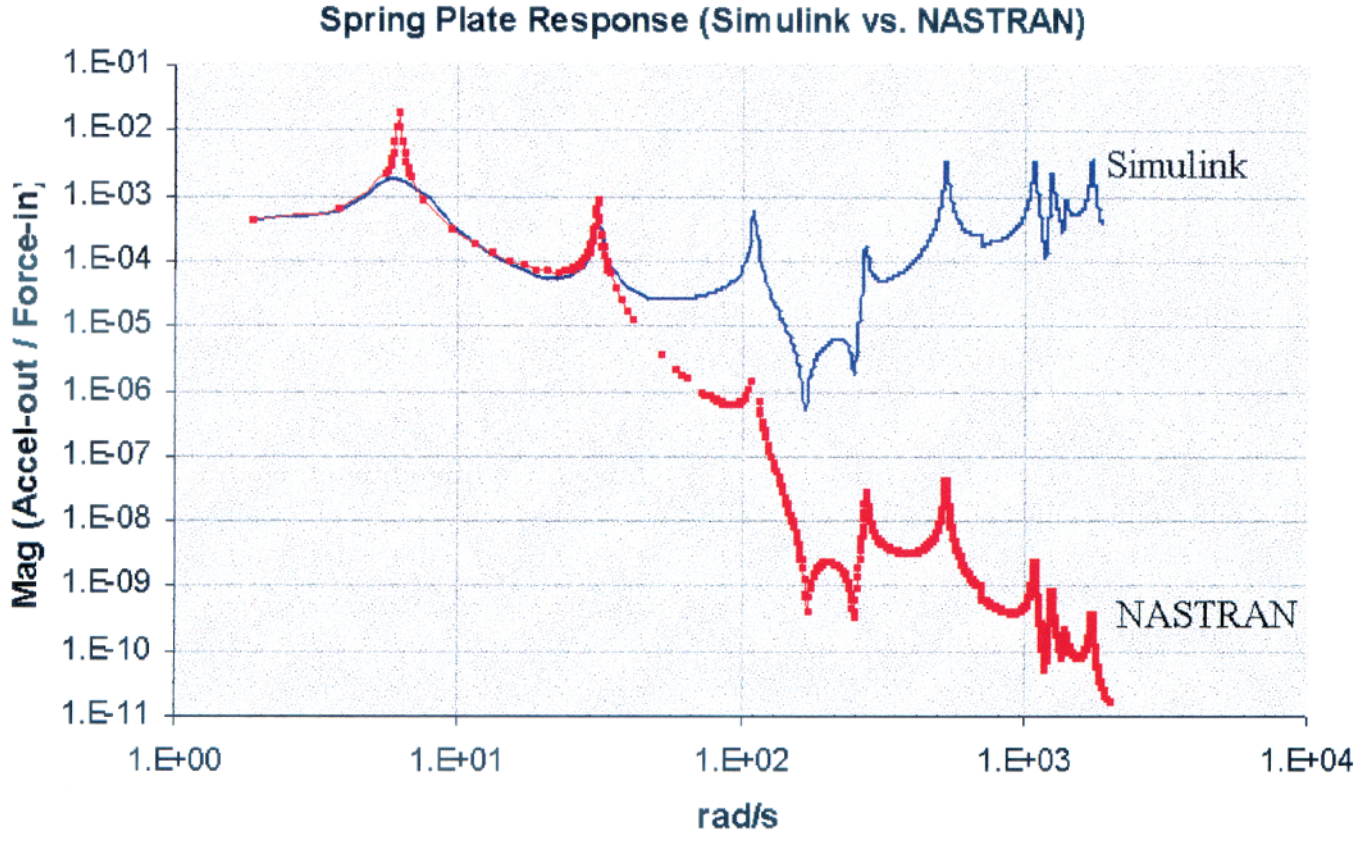

Glenn Research Center

ZIN Technologies Inc.
ARIS Integration Support

Process Modifications

- Discrepancies in Boeing Simulink model uncovered
- NASTRAN gives correct response (expected roll-off correlating with theory)
- Investigation into Simulink model shows:
  - modeling approach which treats rack, umbilical, and rigid body modes separately
  - a dynamic response loop with output coming from wrong place
- Corrections result in exact agreement with Simulink, NASTRAN, and Theory
- CIR Simulink model also verified with NASTRAN response
- Corrected version used for CIR ARIS performance analysis

Glenn Research Center

ZIN Technologies Inc.
ARIS Integration Support

ON-Orbit CIR
ISPR/ARIS NASTRAN Model

FCF Common Door FEM

Boeing ARIS ISPR FEM

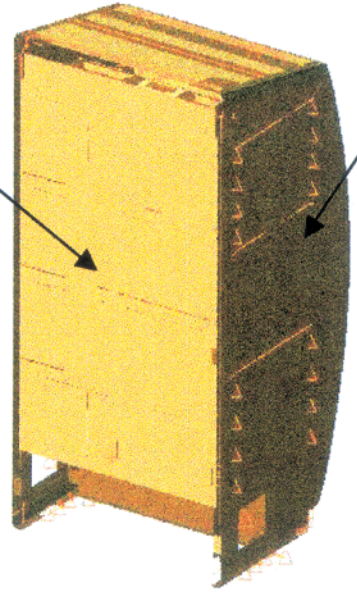

Model Components:

17,007 Nodes
102,042 DOF
18019 Elements
(Beam, Plate, Solid, Lumped Masses)
267 Property ID's
48 Material ID's

Note: Model Internals Represent the CIR FEM

NASTRAN Dynamic Analysis Run Time Statistics:

1. Modal Analysis (0 Hz to 300 Hz Range) – Eigenvectors determined for 288 Modes using three separate analytical runs (0 Hz to 100 Hz, 100 Hz to 200 Hz, 200 Hz to 300 Hz). Run time for each analysis is 1 Hour.
2. Direct Frequency/Harmonic Response Analysis (0 Hz to 50 Hz Range, first 35 Modes). Run time between 12 to 14 Hours.
3. All Analyses performed on a PC, Pentium III, 392 MB Ram, 800 MHz Processor, using MSC/NASTRAN for Windows Version 4.6.

Glenn Research Center

ZIN Technologies Inc.
ARIS Integration Support

CIR Mass Properties

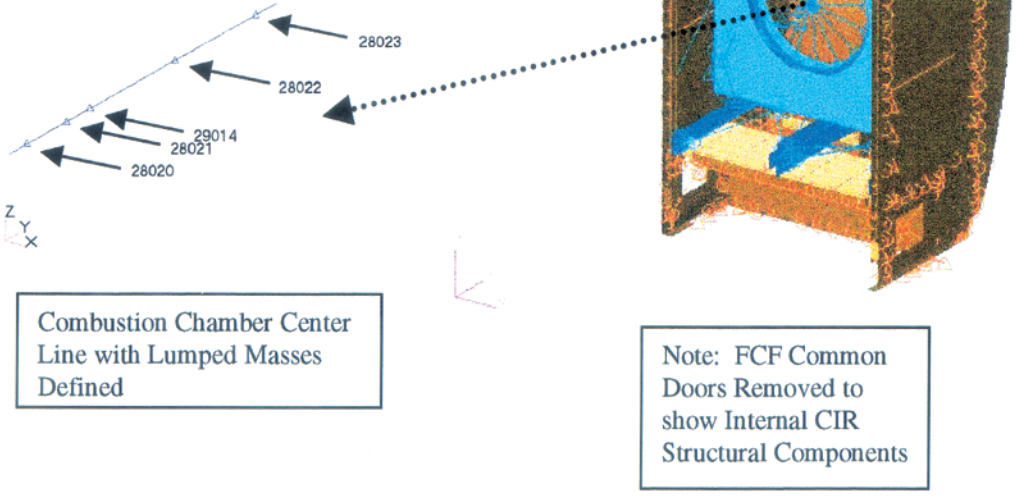

CIR Mass Properties Nominal Configuration	Value
Weight	1100 Kg (2425.9 Lbs)
Center of Gravity Based on Rack Datum	
X	18.373 in.
Y	-12.650 in.
Z	39.081 in.
Principal Moments of Inertia at CG	
I_{xx}	965896 Lbs-in^2
I_{yy}	1122746 Lbs- in^2
I_{zz}	458222 Lbs- in^2

Glenn Research Center

ZIN Technologies Inc.
ARIS Integration Support

Umbilical Model

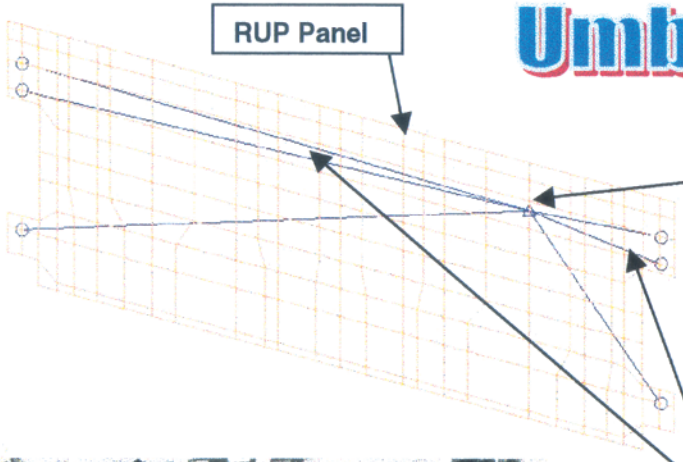

Node 300000

Six (6) RBE2's used to connect Node 300000 to the RUP/ISPR Interface

Umbilical Stiffness Represented as 6 Spring Elements:
Kx= 5.0 Lbs/in
Ky= 7.66 Lbs/in
Kz= 6.5 Lbs/in
KRx= 551.52 in-Lbs/rad
KRy= 1778.8 in-Lbs/rad
KRz= 486.0 in-Lbs/rad

6 springs

Umbilical Lumped Mass Weight=10 Lbs.

6 springs

Station Lumped Mass Weight=1E+05 Lbs. Ixx=Iyy=Izz=1E+06 Lbs-in^2

Glenn Research Center

ZIN Technologies Inc.
ARIS Integration Support

Required FEM Upgrades

- **On-Orbit configured FEA Models**
  1. On-orbit boundary conditions.
  2. Boeing ARIS ISPR FEM On-Orbit mass properties.
  3. On-Orbit science configured rack.
- **NASTRAN Model Refinements**
  1. Use of RBE3's cause singularities effecting rigid body modes. Suggest using RBE2's or CBARS.
  2. Structural model/refinement of ATCU. Need to model passive isolators (i.e., wire rope, Sorbothane® isolators, etc.).
  3. Structural model/refinement of critical locations (i.e., critical science locations, optical locations, mirrors, etc.).
- **Identify, locate, and structurally characterize FCF unique umbilicals.**

Glenn Research Center

ZIN Technologies Inc.
ARIS Integration Support

Early Evaluation of ARIS Performance Based on SAMS Sensors

- **Five SAMS SE's Utilized**
  1. SE-F02 in RTS Drawer #1 in EXPRESS Rack #1 (Non-ARIS).
  2. SE-F03 on US Lab Z-Panel below EXPRESS Rack #2.
  3. SE-F04 on US Lab Z-Panel below EXPRESS Rack #1.
  4. SE-F05 on US Lab Light Tray above EXPRESS Rack #2.
  5. SE-F06 on EXPPCS located in EXPRESS Rack #2 (ARIS).
- **Compare Microgravity Levels of Onboard Rack with Offboard Rack Locations**
- **Compare ARIS Rack with Non-ARIS Rack Microgravity Levels**
- **Compare Predicted Behavior with Actual Measured Behavior**

Glenn Research Center

ZIN Technologies Inc.
ARIS Integration Support

Location of SAMS Sensors

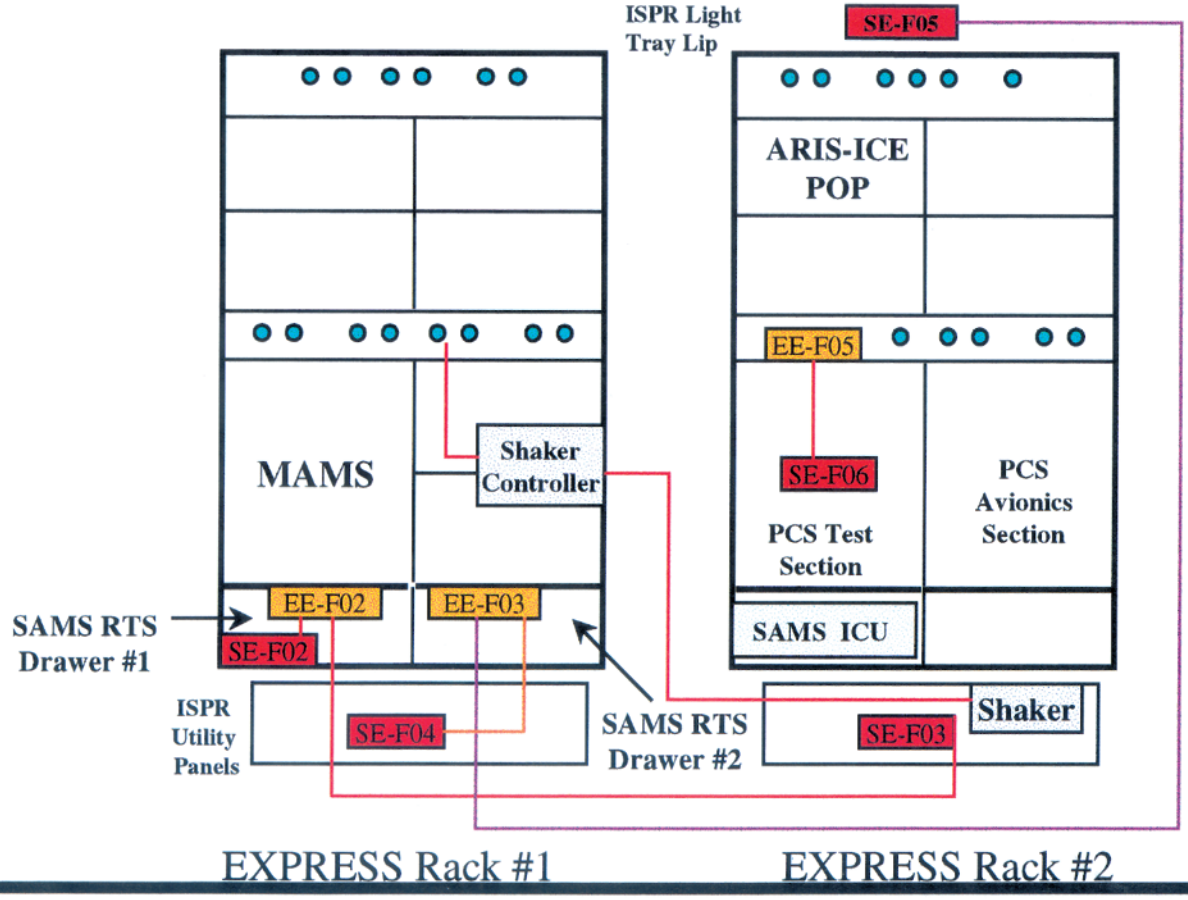

Glenn Research Center

ZIN Technologies Inc.
ARIS Integration Support

Early ARIS-ICE Data

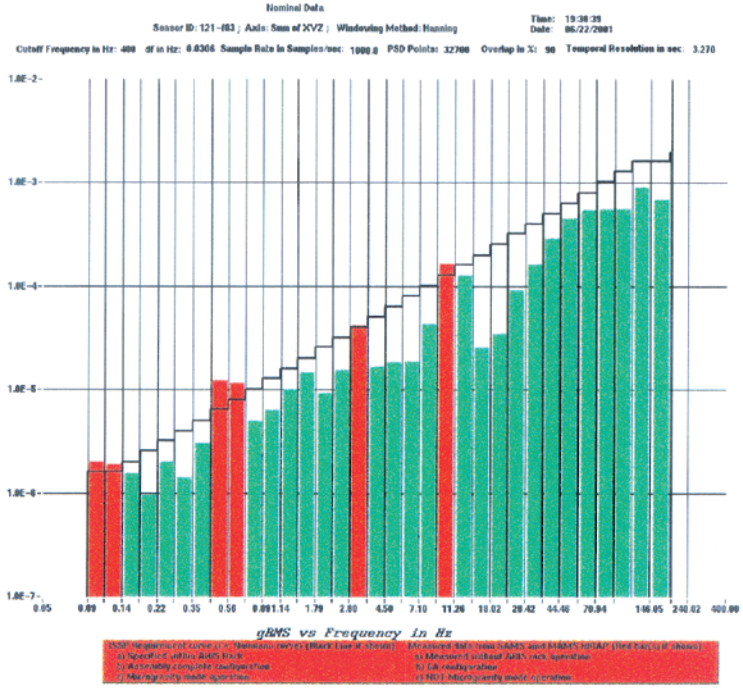

Offboard Structure

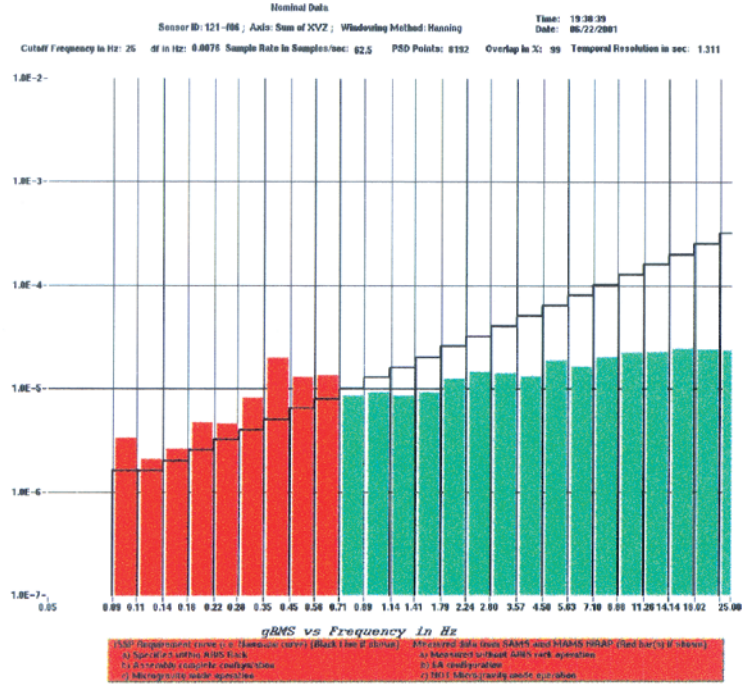

ARIS "Idle"

Glenn Research Center

ZIN Technologies Inc.
ARIS Integration Support

Early ARIS-ICE Data

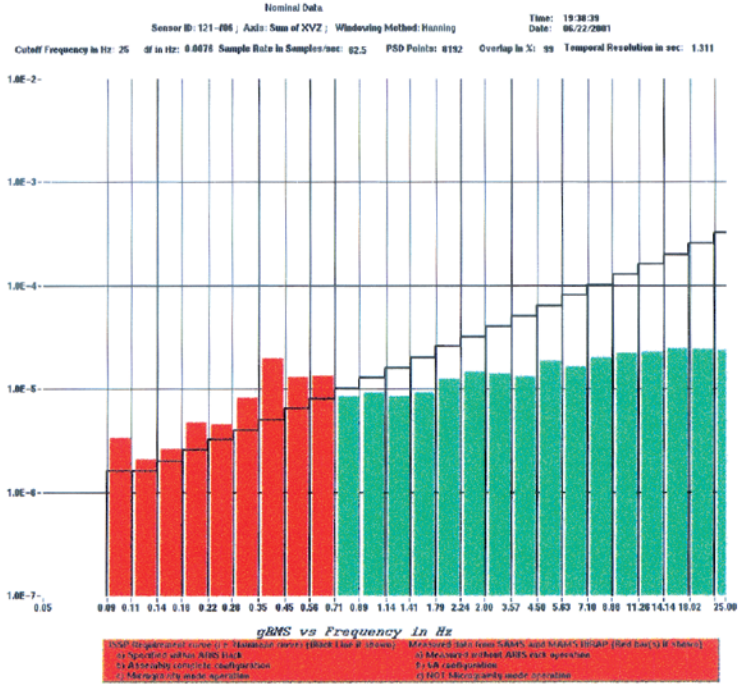

ARIS "Idle"

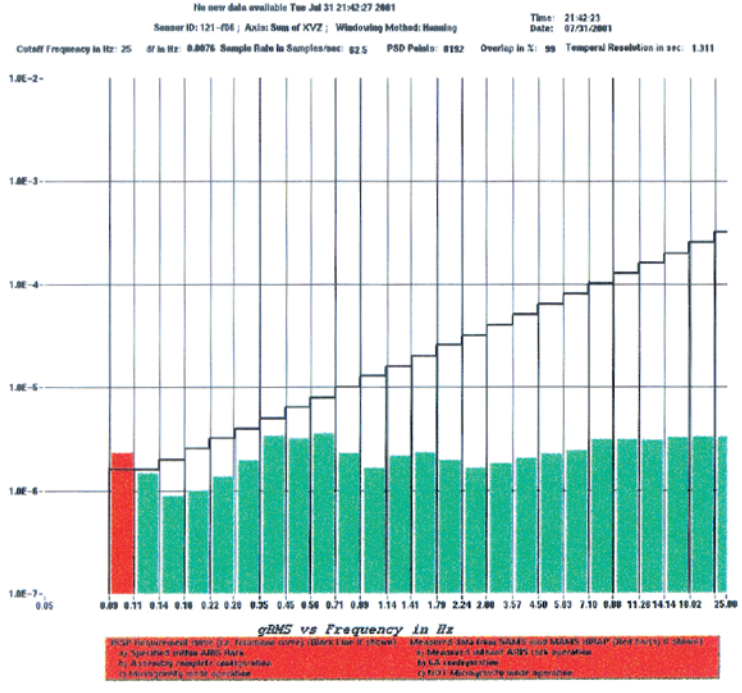

ARIS "Active?"

Glenn Research Center

ZIN Technologies Inc.
ARIS Integration Support

Ongoing Process Updates

The following data needs to be revised as process proceeds towards integration:

- Umbilical FEA Models
- NASTRAN Rack Models
- Disturber Data (ATCU etc.)
- On-orbit SAMS data (US Lab environment)
- Controller Parameters (tuning)

Light Microscopy Module: An Optical Payload in a Microgravity Environment

Tony Haecker
LMM Structural Engineer
Logicon Corporation
Cleveland, Ohio

Emphasis will be on design requirements to optical equipment in general and the LMM microscope specifically with respect to microgravity disturbances on the ISS. After a brief description of the LMM and a discussion of microgravity concerns, the Finite Element Modal results of the LMM microscope and vibration test correlation will be presented. Since ISS random and steady state vibration information has not been readily available, attendees are encouraged to participate in this data exchange.

NASA/CP—2001-211164

Light Microscopy Module (LMM)

Fluids and Combustion Facility

Tony Haecker

August 8, 2001

Presented to the MGMG Meeting

Prepared For:
National Aeronautics and Space Administration
John H. Glenn Research Center
Microgravity Science Division
Cleveland, Ohio 44135

LOGICON
A Northrop Grumman Company

Prepared By:
Logicon
Under Contract NAS3-99155
2001 Aerospace Parkway
Brook Park, Ohio 44142

NASA/CP—2001-211164

Integrated LMM/FIR Concept

The FCF FIR includes support subsystems and laboratory style diagnostics common to the specific researchers and supplements the laboratory with unique science hardware developed for each Principal Investigator (PI). The PI unique hardware customizes the FCF FIR facility in a unique laboratory configuration to perform fluid physics research effectively.

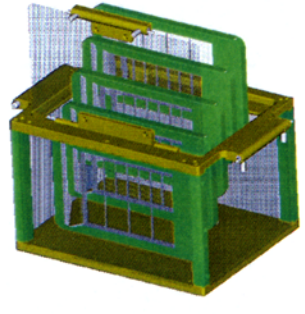

PI Specific Hardware
- PI Sample Cell with universal Sample Tray
- Specific Diagnostics
- Specific Imaging
- Fluid Containment

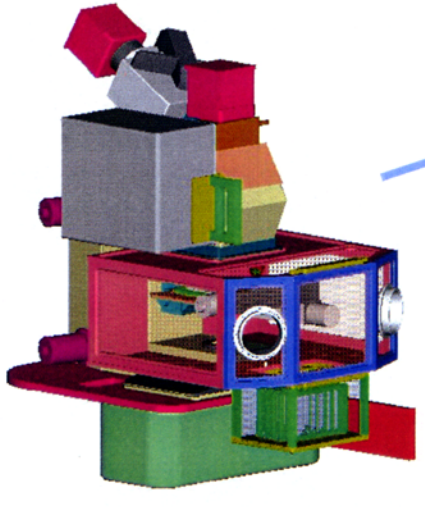

Light Microscopy Module
- Test Specific Module
- Infrastructure that uniquely meets the needs of PI fluid physics experiments
- Unique Diagnostics
- Specialized Imaging
- Fluid Containment

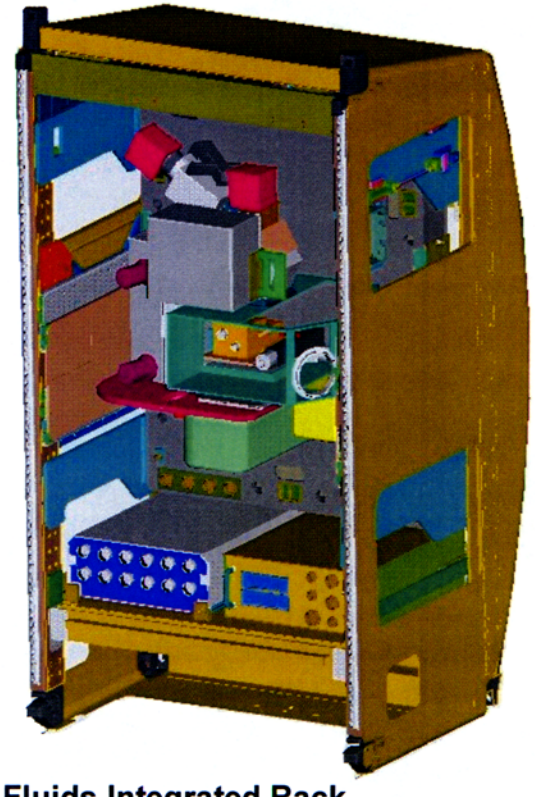

FCF Fluids Integrated Rack
- Power Supply
- Avionics/Control
- Common Illumination
- PI Integration Optics Bench
- Imaging and Frame Capture
- Fluid Diagnostics
- Environmental Control
- Data Processing
- Frangibles and Laser Light Containment

NASA/CP—2001-211164

Primary Structural Components of LMM

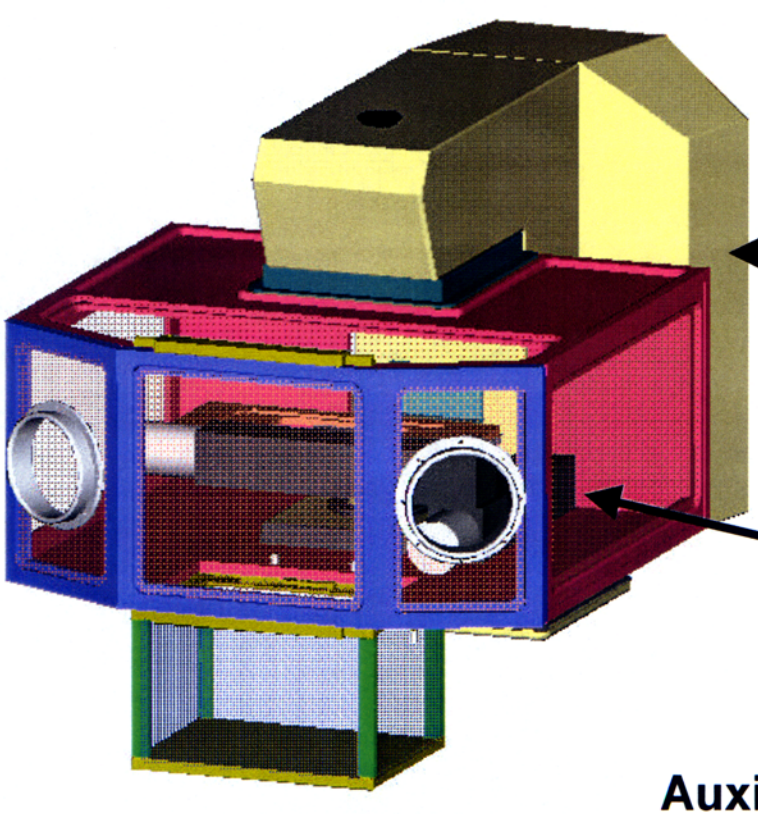

Equipment Transfer Module (ETM)

Microscope Body

Auxiliary Fluids Container (AFC)

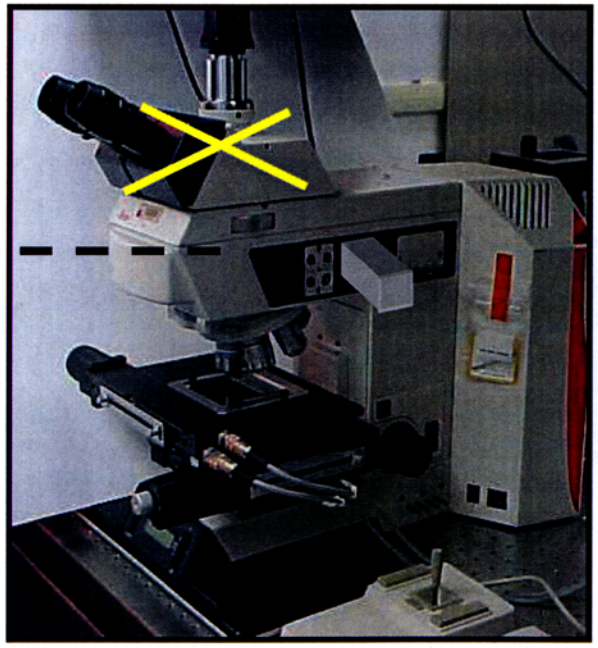

LMM is Flying a Commercial Microscope

LMM Operating Video

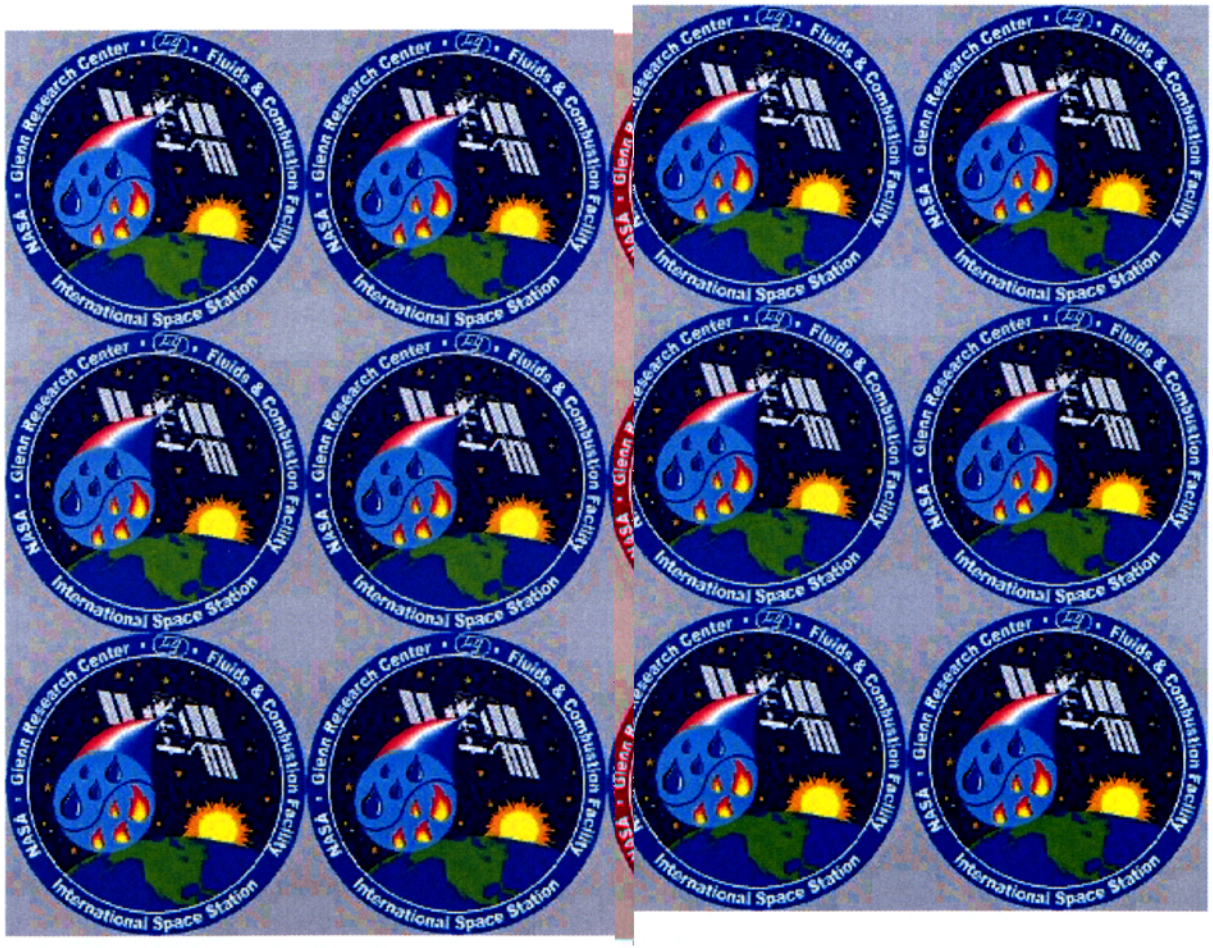

NASA/CP—2001-211164

NASA/CP—2001-211164

LMM shown in Operating Position

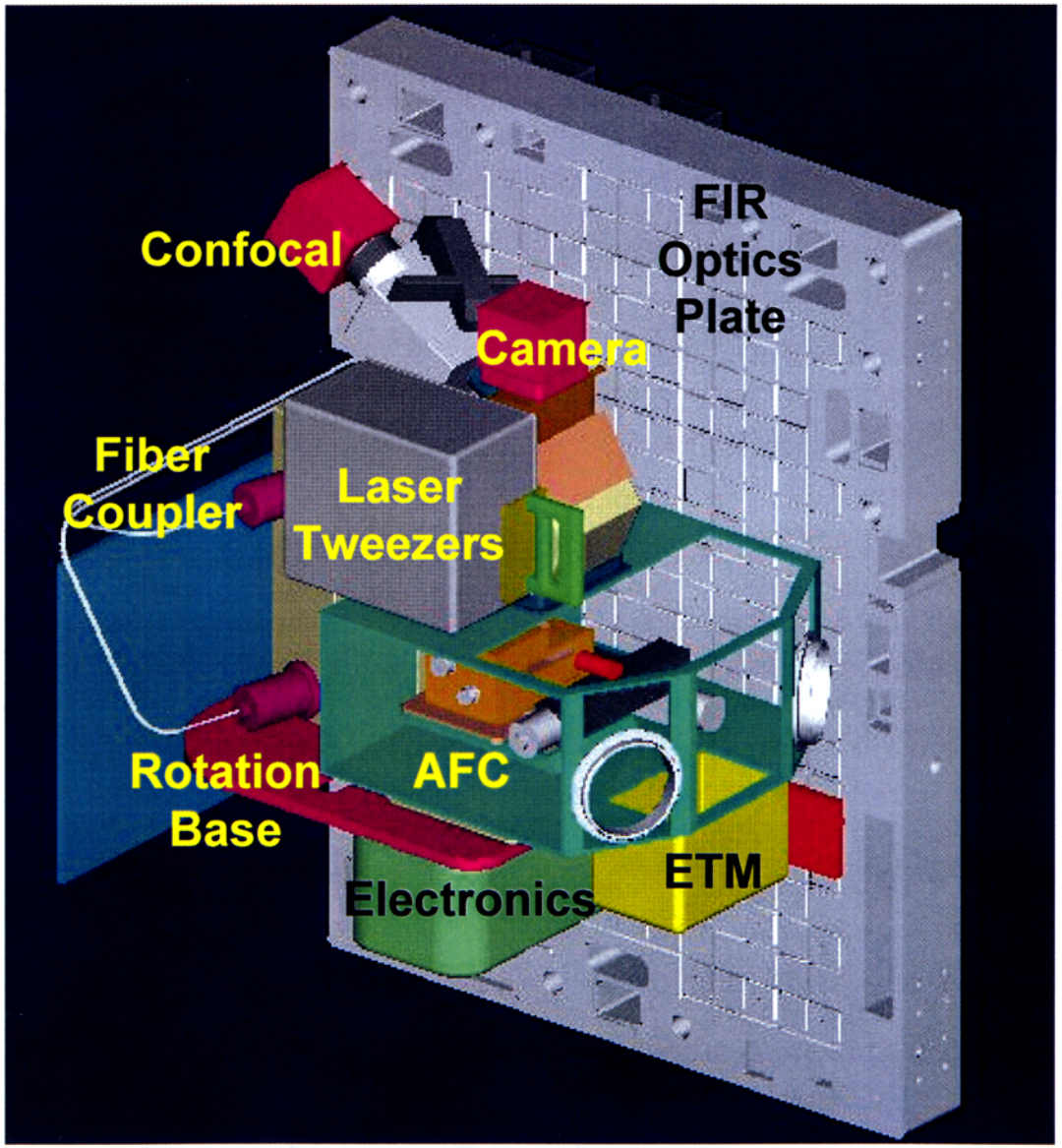

Michael Brinkmann

NASA/CP—2001-211164

LMM shown in Open Position

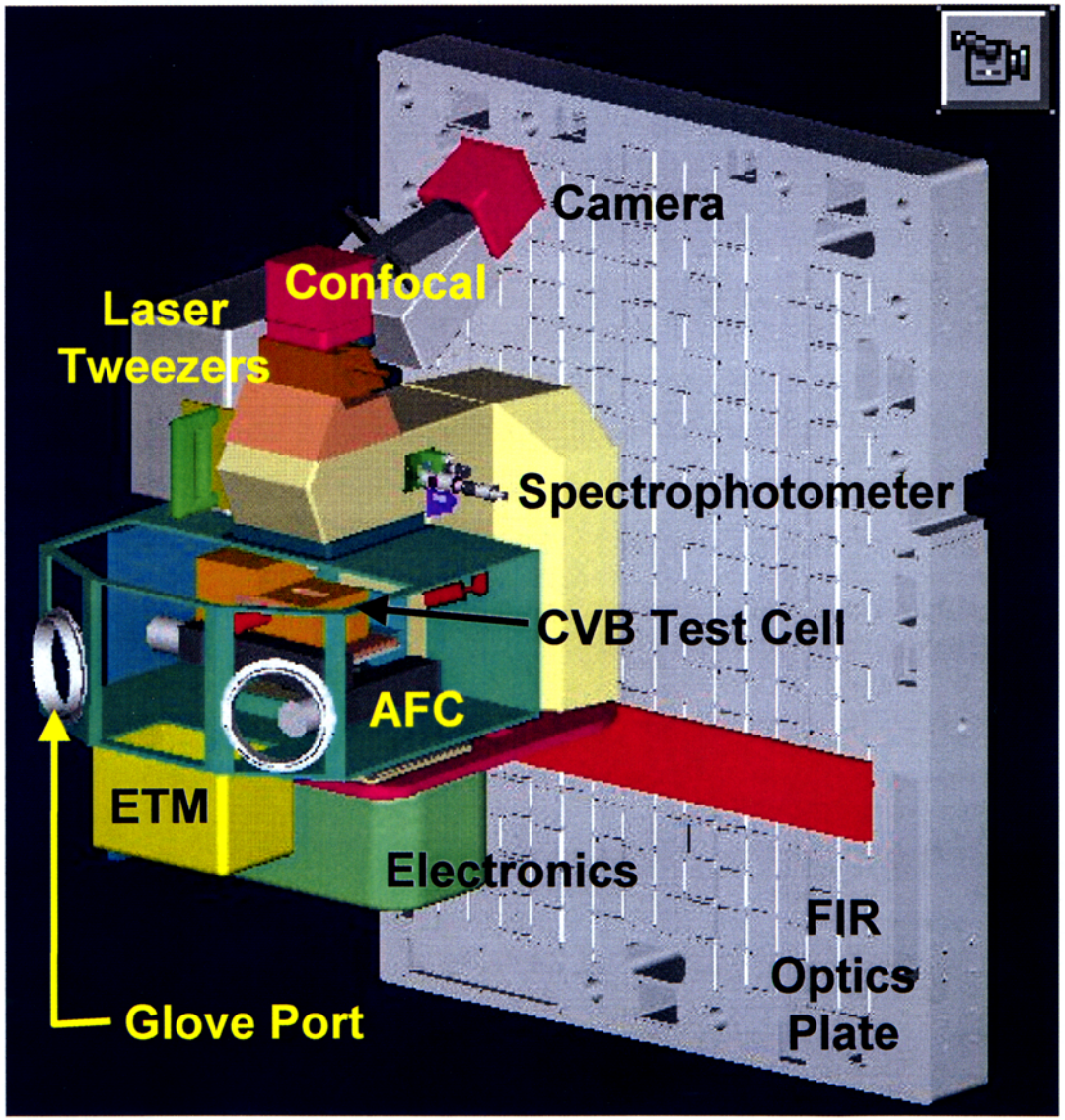

Michael Brinkmann

NASA/CP—2001-211164

Four Experiments - One Project

Interferometric measurement in a thin film

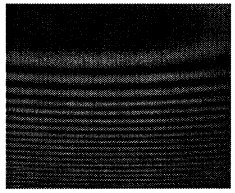

CVB: Prof. Peter C. Wayner, Jr., Rensselaer Polytechnic Institute

Objective: To determine the overall stability, the fluid flow characteristics, the average heat transfer coefficient in the evaporator, and heat conductance of the constrained vapor bubble, under microgravity conditions, as a function of vapor volume and heat flow rate.

Laser tweezers pattern with colloidal particles

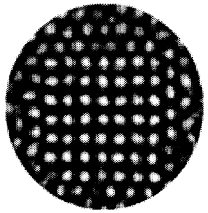

PH^{A}SE-2: Prof. Paul M. Chaikin, Princeton University

Objective: Perform investigations of hard sphere colloid growth, structure, dynamics, rheology, and phase diagram. Observe how hard sphere colloids respond to applied fields which force them into non-equilibrium conditions.

Colloidal Gel

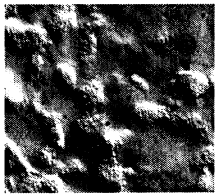

PCS-2: Prof. David A. Weitz, Harvard University

Objective: To carry out further investigation of critical fundamental problems in colloid science and to fully develop the evolving field of "colloid engineering", to create materials with novel properties using colloidal particles as precursors.

Colloidal patterning on etched substrates

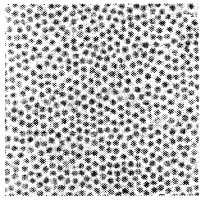

LΦCA: Prof. Arjun G. Yodh, University of Pennsylvania

Objective: To create photonic band-gap colloidal surface crystalline materials from high and low density particles in low volume fraction binary particle suspensions using entropy driven crystallization.

NASA/CP—2001-211164

Sample Images from the LMM Microscope using Standard Microscope Functions

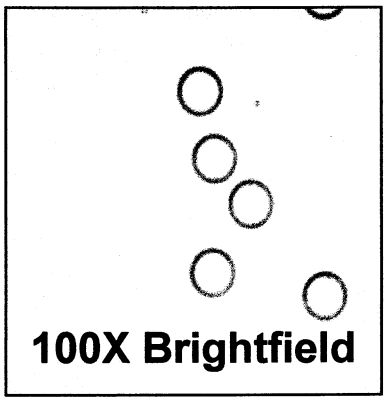

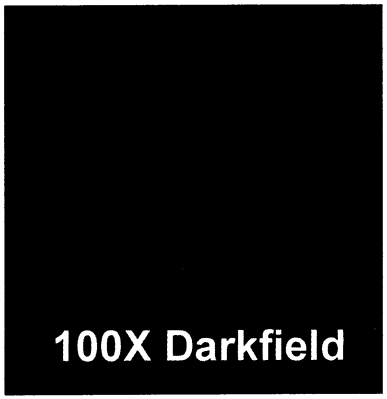

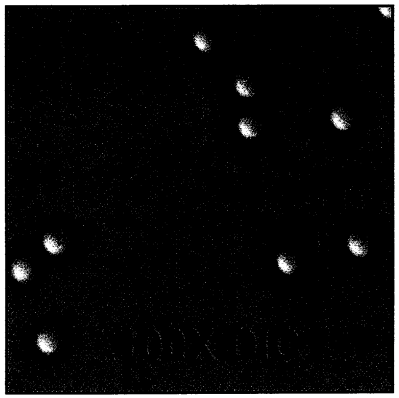

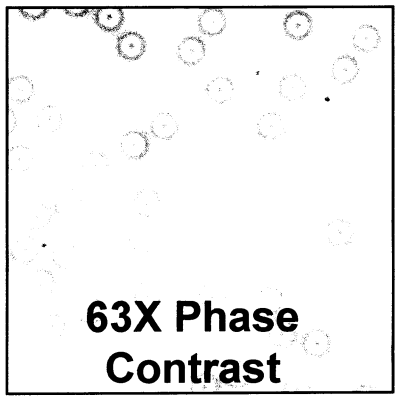

Experimental Setup

- Particle diameter: 5 micrometers
- Polystyrene spheres.
- LMM microscope images

LMM Structural Loads

Vibration Loads – Random and Steady State

- Transportation
- Shuttle – Launch and Landing in Mid-deck and MPLM
- ISS – Microgravity, Reboost and Crew Induced Loads
- Payload Induced Loads – Fans, Cameras
- Rack Induced Loads – "Good Neighbors?"
- Docking Loads
- Isolation System Loads – ARIS power on/off

Experiments require weeks of "quiet" time

"Skyline" Microgravity Profile

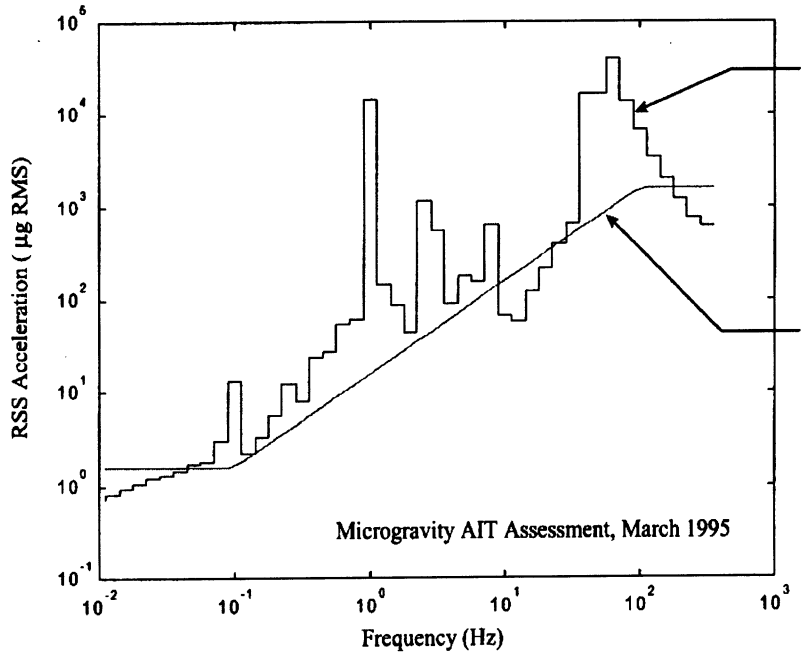

Typical ISS Environment

Typical Experiment Requirement

LMM Static Load Tests

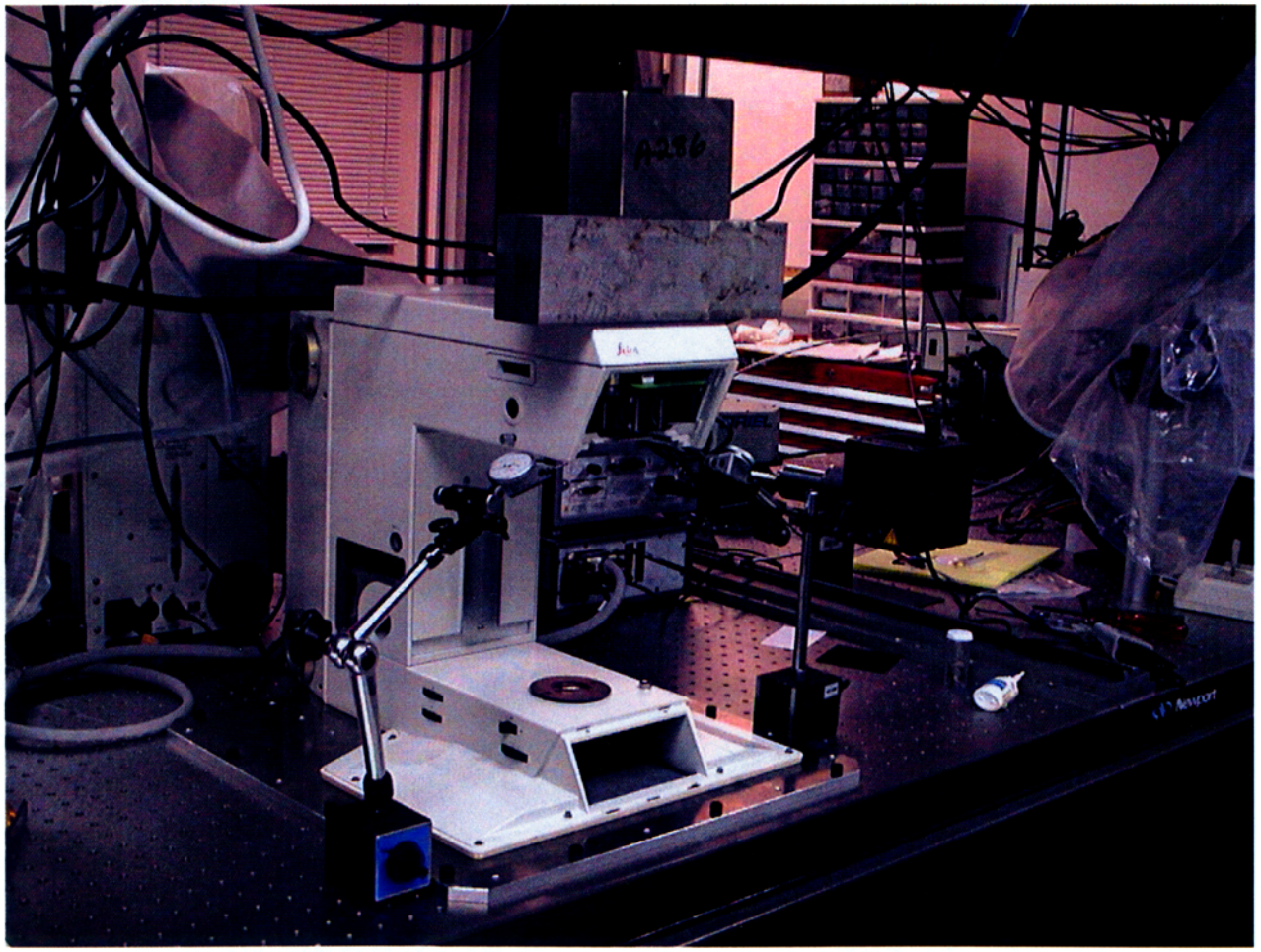

Microscope FEA Model

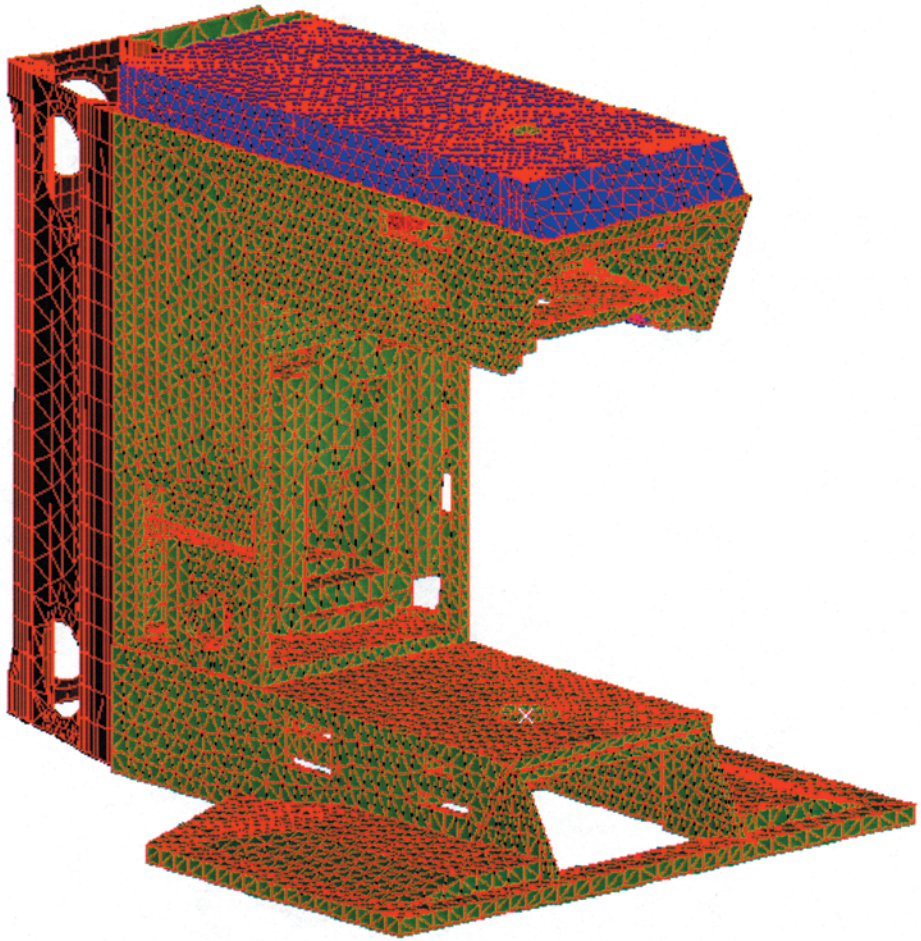

57,000 NASTRAN Elements with Lumped Masses

NASA/CP—2001-211164

FEA Static Deflection

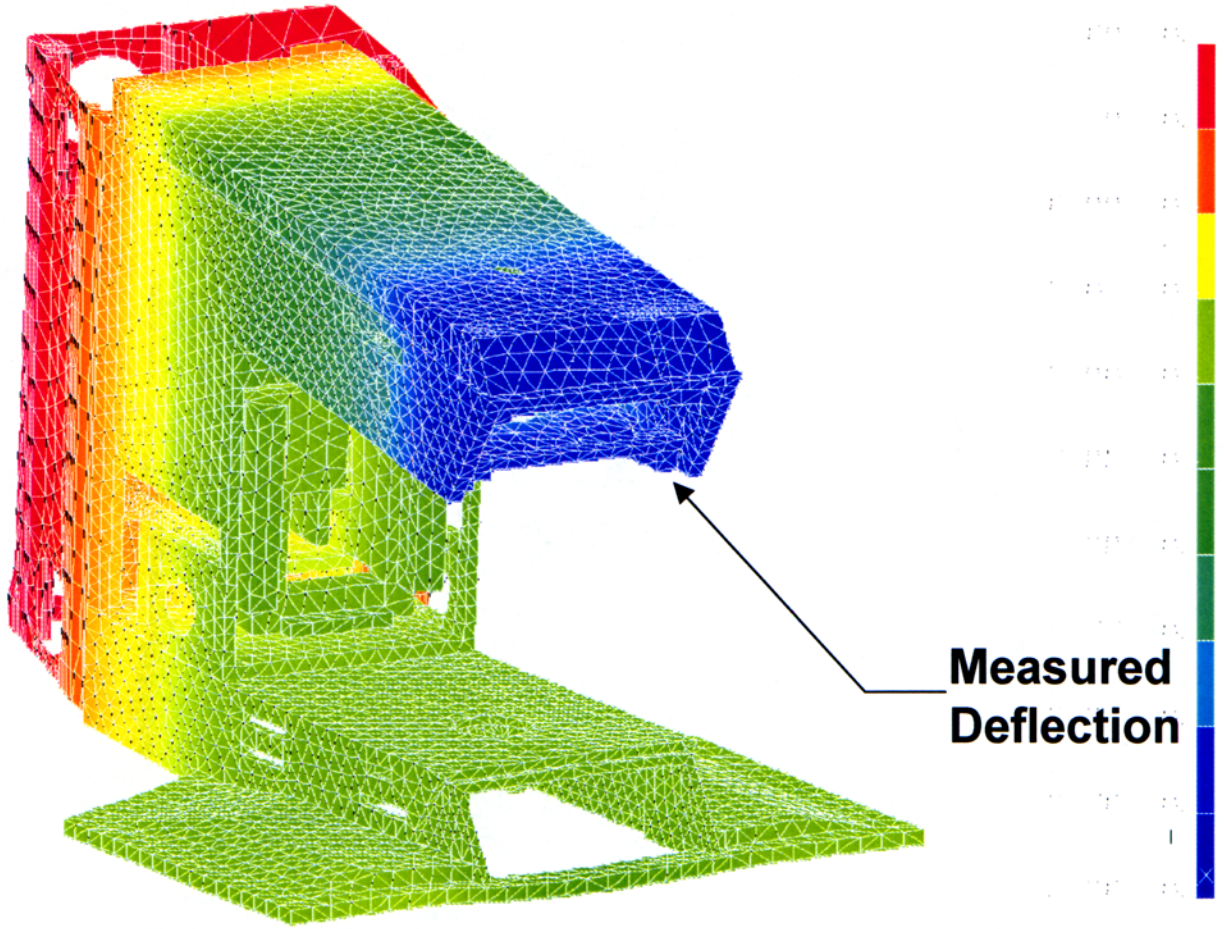

LMM Finite Element Analysis – Static

	Deflection (in.)	
Load	**FEA**	**Test**
1	0.0037	0.0035
2	0.0028	0.0027
Weight	22.7 Lb.	24.8 Lb.*

*Includes internal wiring, components and fasteners

LMM Finite Element Analysis – Dynamic

FEA Modal Analysis Results

- Mode Z – 43 Hz
- Mode X – 50 Hz
- Mode Z_2 – 80 Hz
- Mode Y_1 – 120 Hz
- Mode Y_2 – 135 Hz

FEA Mode Shapes: X – 50 Hz

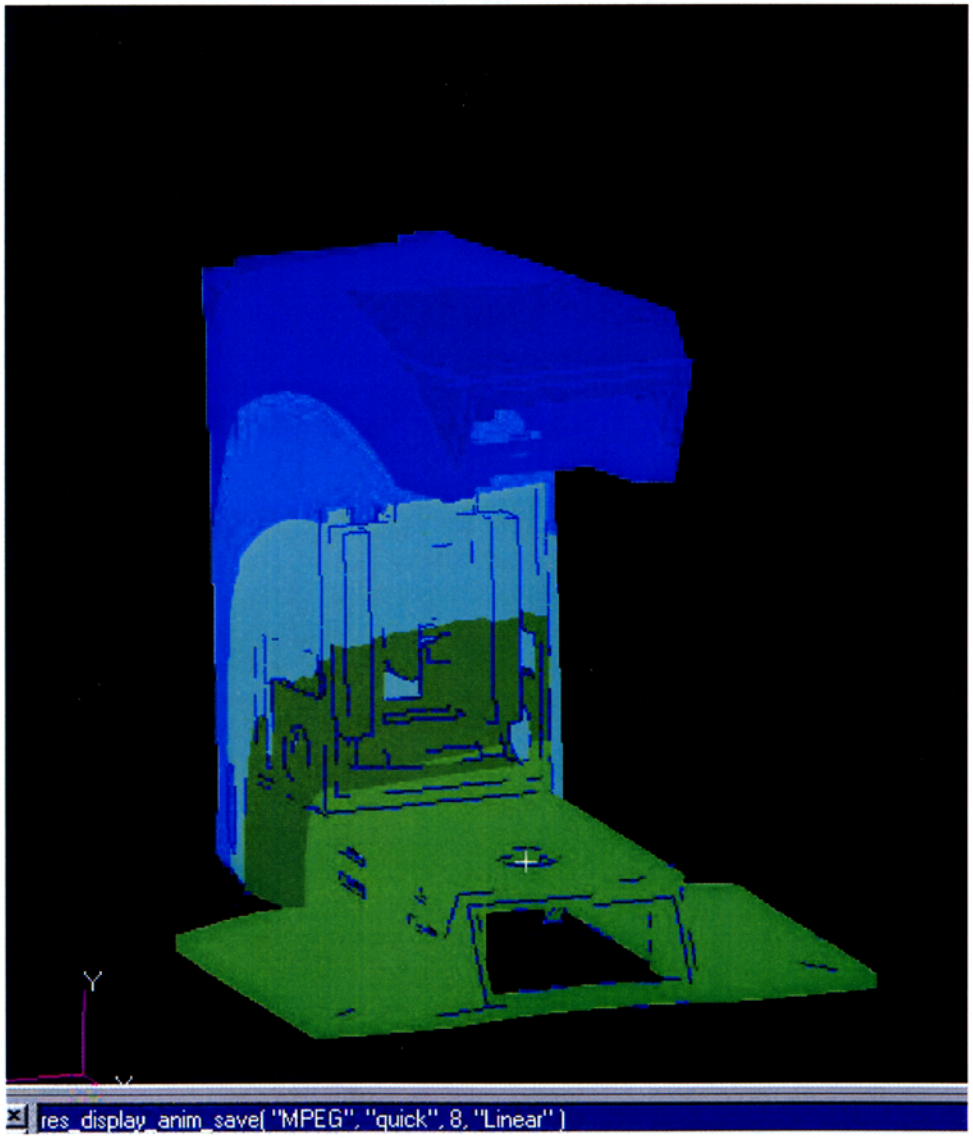

FEA Mode Shapes: Y – 135 Hz

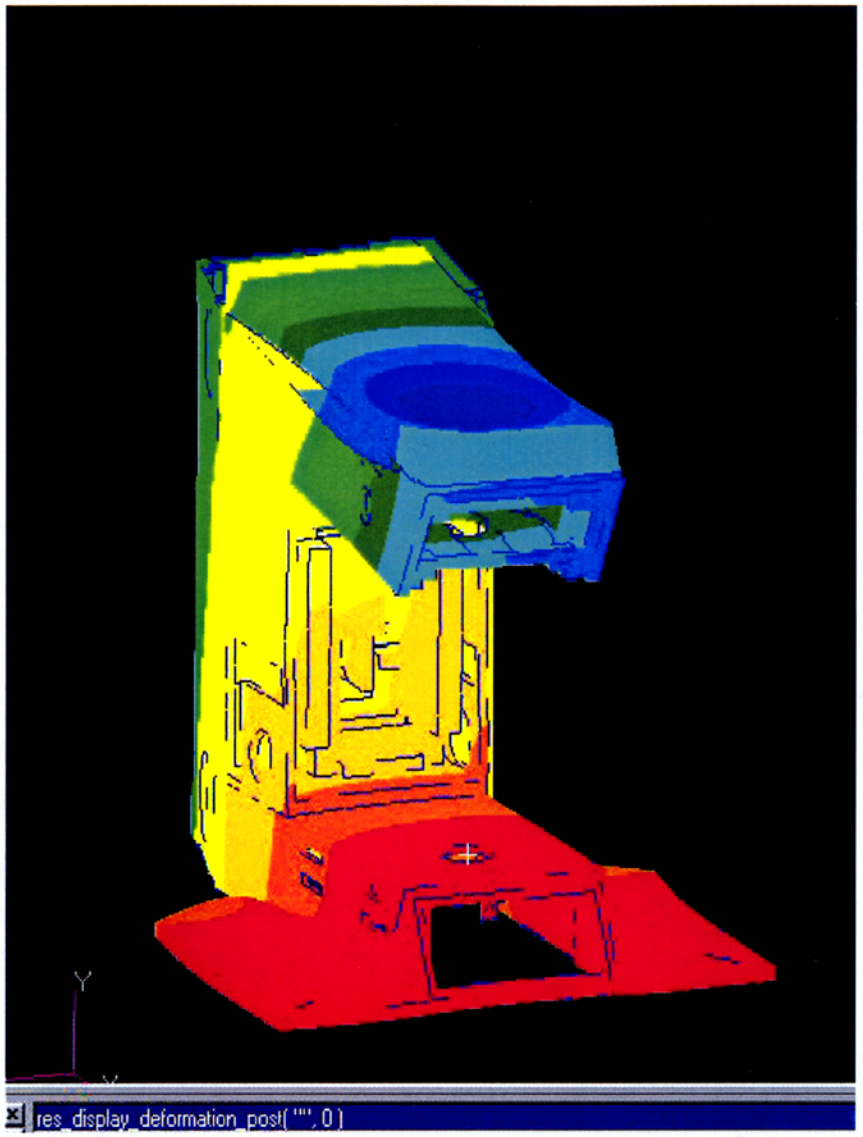

FEA Mode Shapes: Z – 43 Hz

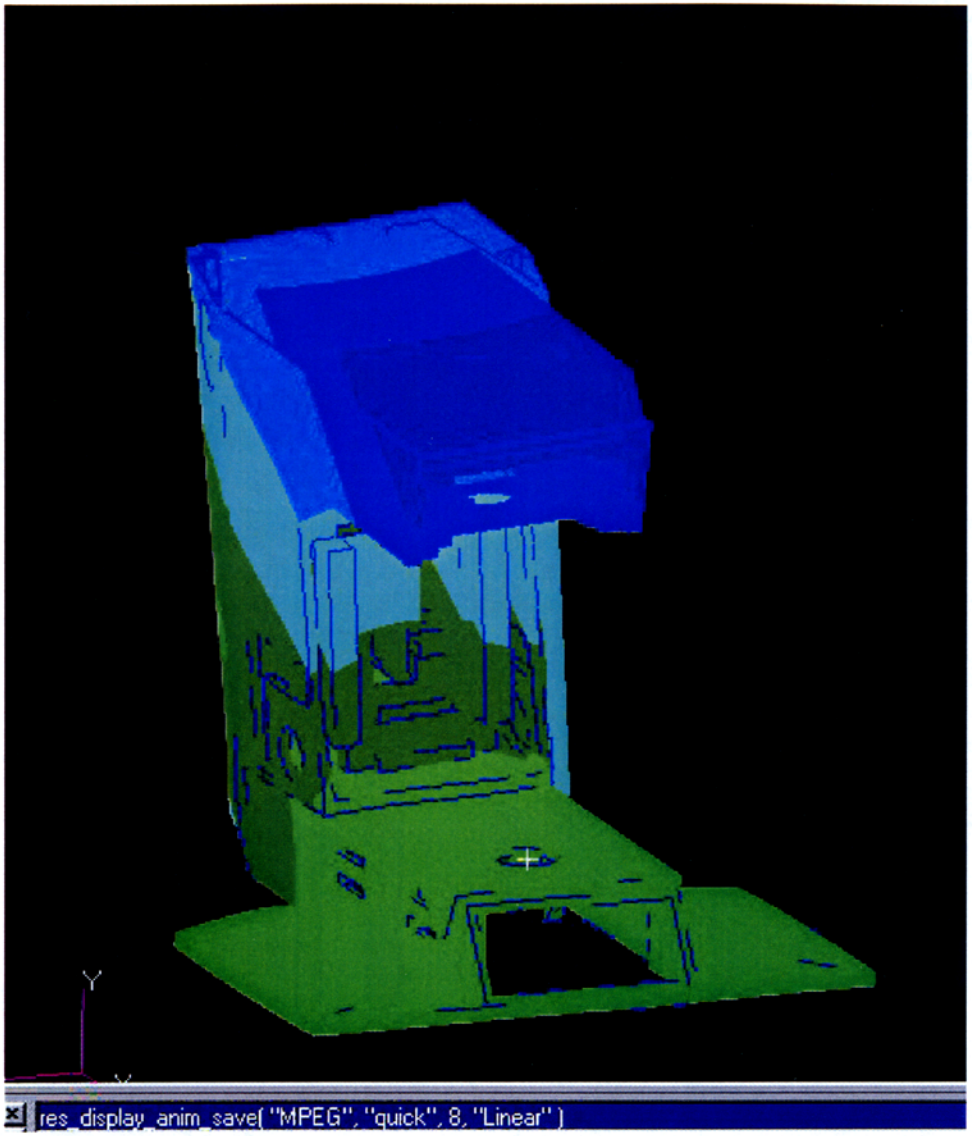

LMM Vibe Test Setup

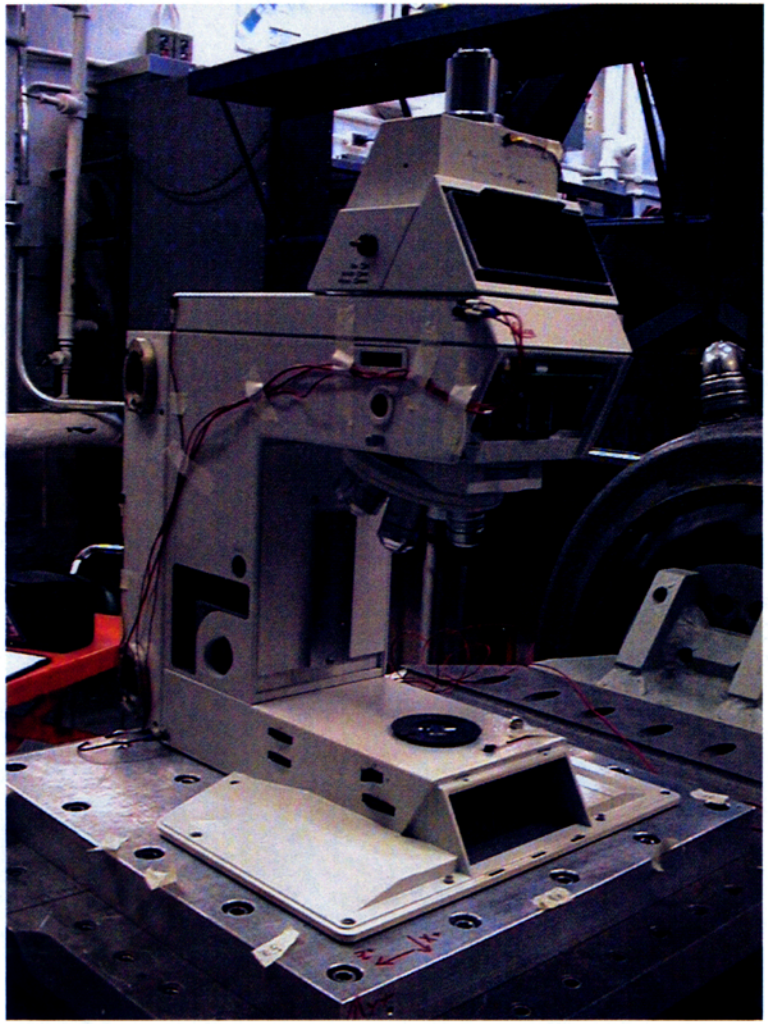

Vibe Test

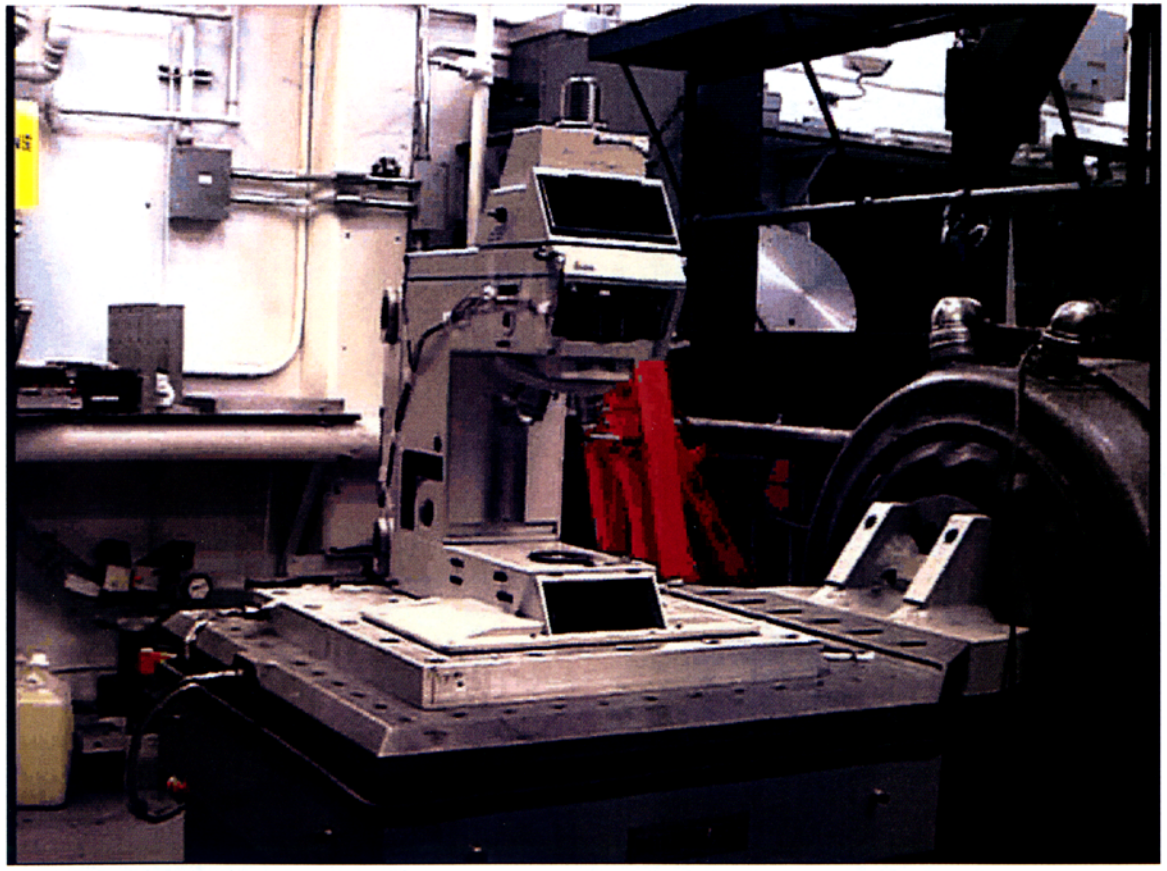

LMM Vibe Test Results

- Mode Z – 46 Hz
- Mode X – 46 Hz
- Mode Y_1 – 106 Hz
- Mode Y_2 – 142 Hz

"Z" Dir Vibe

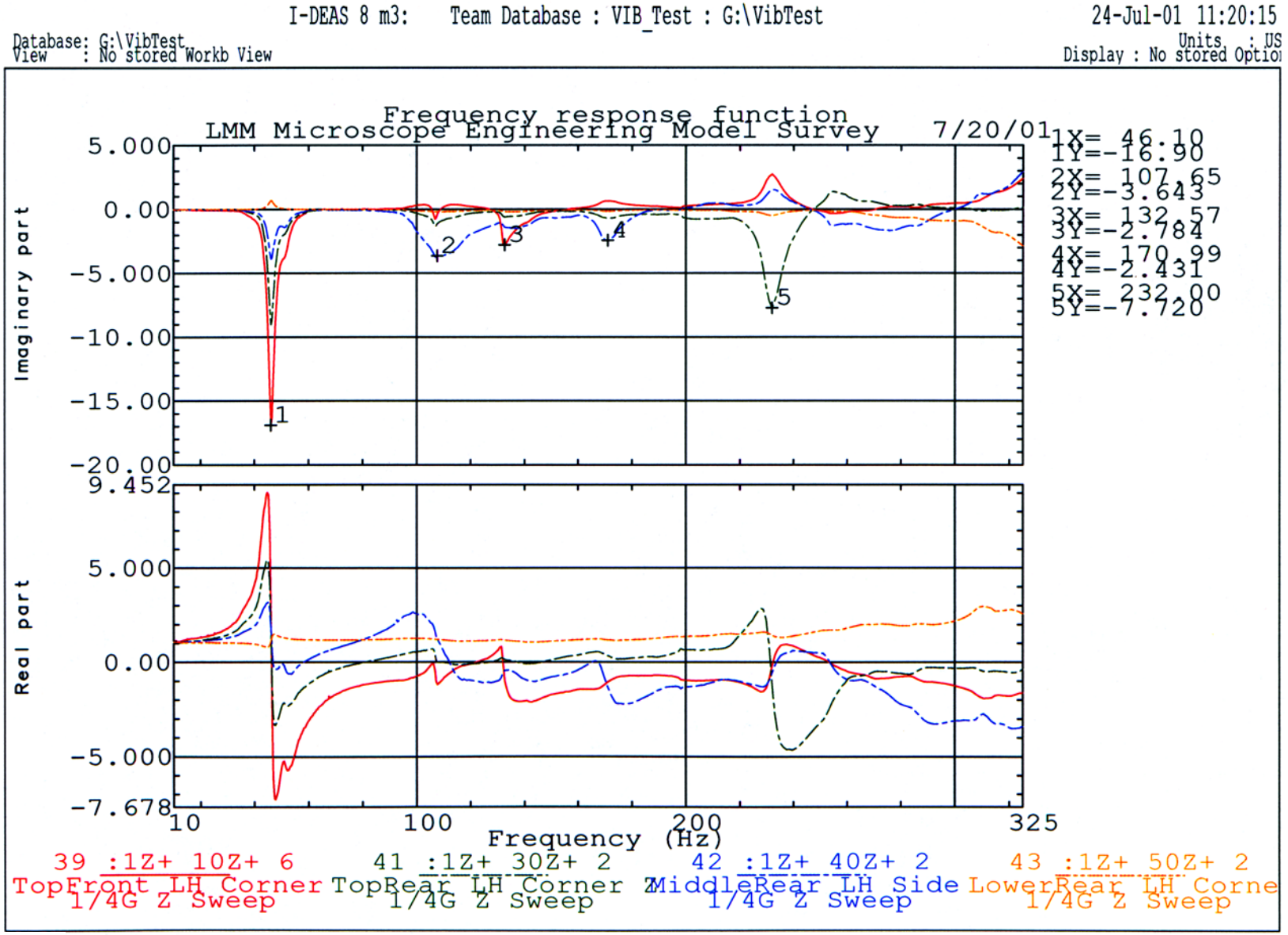
I-DEAS 8 m3: Team Database : VIB_Test : G:\VibTest
24-Jul-01 11:20:15
Database: G:\VibTest
View : No stored Workb View
Units : US
Display : No stored Optio
Frequency response function
LMM Microscope Engineering Model Survey 7/20/01
1X= 46.10
1Y=-16.90
2X= 107.65
2Y=-3.643
3X= 132.57
3Y=-2.784
4X= 170.99
4Y=-2.431
5X= 232.00
5Y=-7.720
Imaginary part
5.000
0.00
-5.000
-10.00
-15.00
-20.00
Real part
9.452
5.000
0.00
-5.000
-7.678
10
100
200
325
Frequency (Hz)
39 :1Z+ 10Z+ 6
TopFront LH Corner
1/4G Z Sweep
41 :1Z+ 30Z+ 2
TopRear LH Corner
1/4G Z Sweep
42 :1Z+ 40Z+ 2
MiddleRear LH Side
1/4G Z Sweep
43 :1Z+ 50Z+ 2
LowerRear LH Corne
1/4G Z Sweep

"X" Dir Vibe

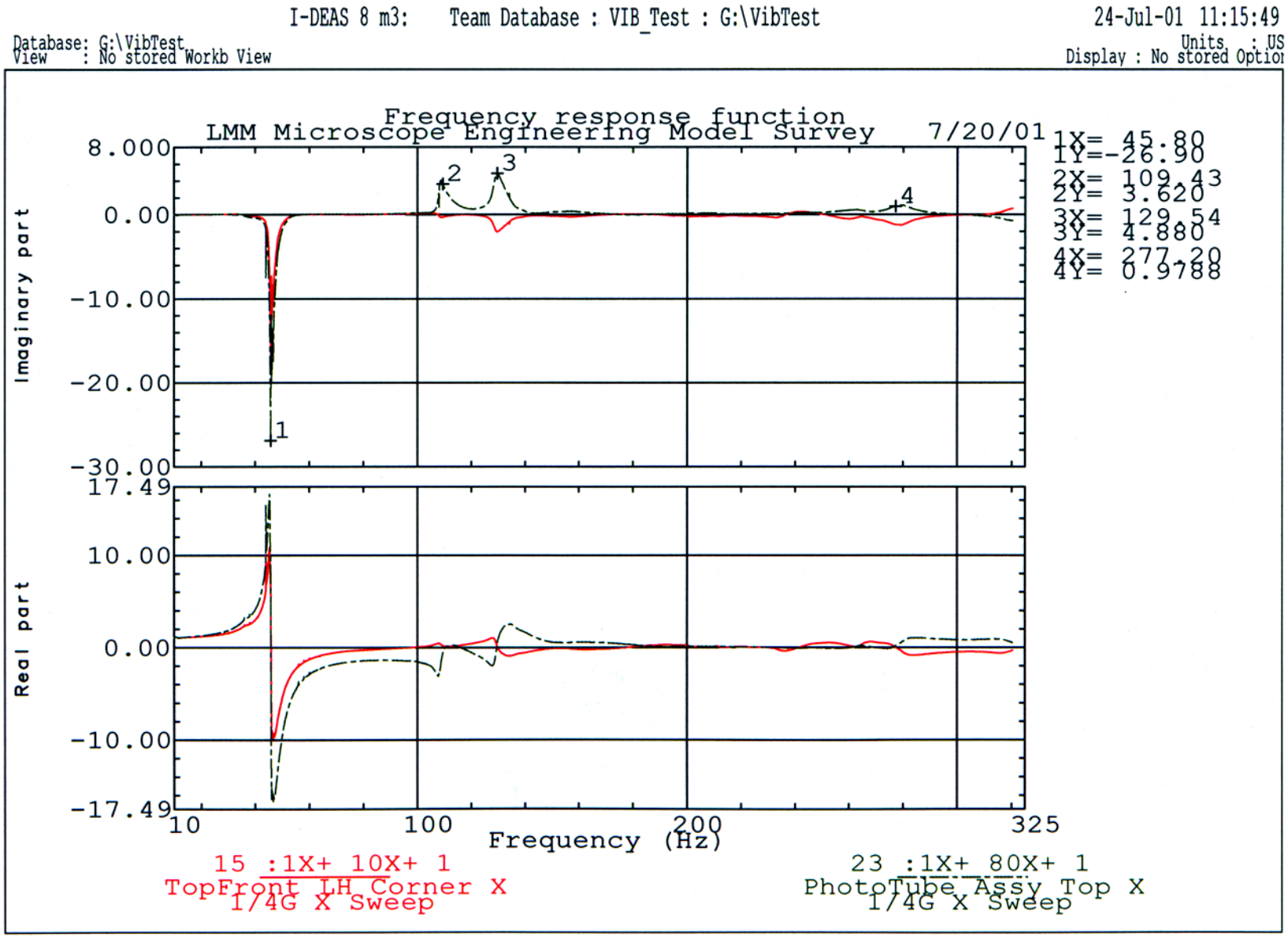
I-DEAS 8 m3: Team Database : VIB_Test : G:\VibTest
24-Jul-01 11:15:49
Database: G:\VibTest
View : No stored Workb View
Units : US
Display : No stored Optio
Frequency response function
LMM Microscope Engineering Model Survey 7/20/01
1X= 45.80
1Y=-26.90
2X= 109.43
2Y= 3.620
3X= 129.54
3Y= 4.880
4X= 277.20
4Y= 0.9788
Imaginary part
8.000
0.00
-10.00
-20.00
-30.00
Real part
17.49
10.00
0.00
-10.00
-17.49
10
100
200
325
Frequency (Hz)
15 :1X+ 10X+ 1
TopFront LH Corner X
1/4G X Sweep
23 :1X+ 80X+ 1
PhotoTube Assy Top X
1/4G X Sweep

"Y" Dir Vibe

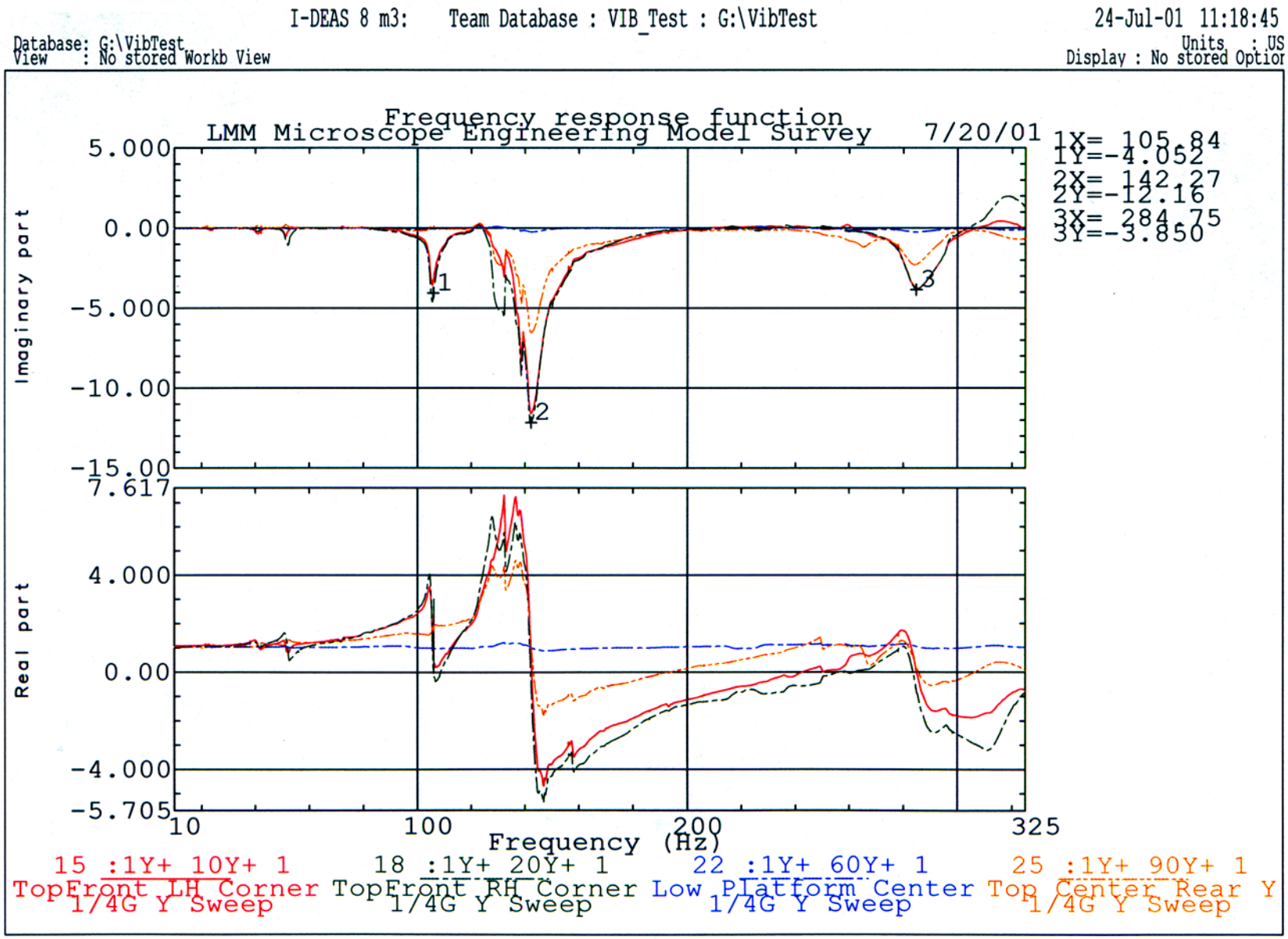
I-DEAS 8 m3: Team Database : VIB_Test : G:\VibTest
24-Jul-01 11:18:45
Database: G:\VibTest
View : No stored Workb View
Units : US
Display : No stored Optior
Frequency response function
LMM Microscope Engineering Model Survey 7/20/01
1X= 105.84
1Y=-4.052
2X= 142.27
2Y=-12.16
3X= 284.75
3Y=-3.850
Imaginary part
5.000
0.00
-5.000
-10.00
-15.00
Real part
7.617
4.000
0.00
-4.000
-5.705
10
100
200
325
Frequency (Hz)
15 :1Y+ 10Y+ 1 TopFront LH Corner 1/4G Y Sweep
18 :1Y+ 20Y+ 1 TopFront RH Corner 1/4G Y Sweep
22 :1Y+ 60Y+ 1 Low Platform Center 1/4G Y Sweep
25 :1Y+ 90Y+ 1 Top Center Rear Y 1/4G Y Sweep

FEA vs. TEST

Frequency (Hz)

MODE	FEA	TEST	DIR
1	43	46	Z
2	50	46	X
3	80	-	Z_2
4	120	106	Y_1
5	135	142	Y_2

FEA Advantages

- Rapidly Evaluate Design Changes
- “Infinite” Accelerometers and Data Points
- Guide Test Procedures
- Duplicate “Virtually” any Loading Condition without Physical Hardware - uGravity

FEA Disadvantages

- It is an approximation and assumes uniform material properties
- Does not capture geometric non-linearities
- Requires significant expertise and experience
- Must test to verify results and conclusions!!

NASA/CP—2001-211164

LMM Microscope – Issues

- How to simulate low-level disturbances during microscope imaging
- Do we fully understand the microgravity environment
- A detailed FEA model may provide microscope deflection data, but will it reveal vibrationally induced optical misalignments on a component level ?
- Determine if ARIS will be used

NASA/CP—2001-211164

Plan of Attack

- Use FEA model to "guide" tuning of microscope hardware and isolation systems
- Determine overall deflections using FEA
- Get a better understanding of microgravity and related disturbances
- Test using microgravity disturbances while imaging for final qualification

ISS Quasi-Steady Acceleration Environment

Eric Kelly
ZIN Technologies
Cleveland, Ohio

A computer will be available in the meeting room for access to the SAMS and MAMS data from the ISS. This will be a working session and a time for MGMG attendees to interact with PIMS project analysts and software engineers about data and data processing actions.

NASA/CP—2001-211164

ISS Quasi-Steady Acceleration Environment

Eric Kelly

Zin Technologies

Glenn Research Center

PIMS DATA PROCESSING BLOCK DIAGRAM

MAMS HiRAP Data Flow

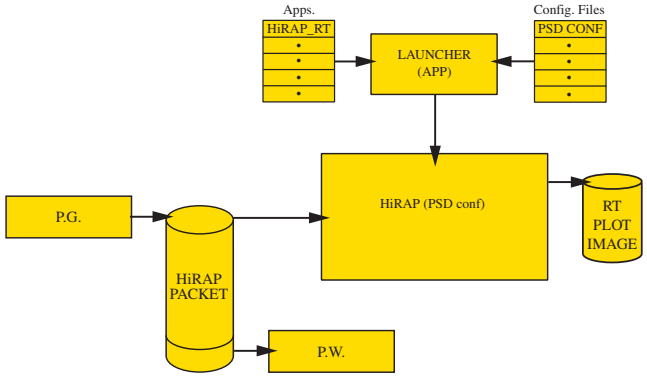

MAMS OSS Data Flow

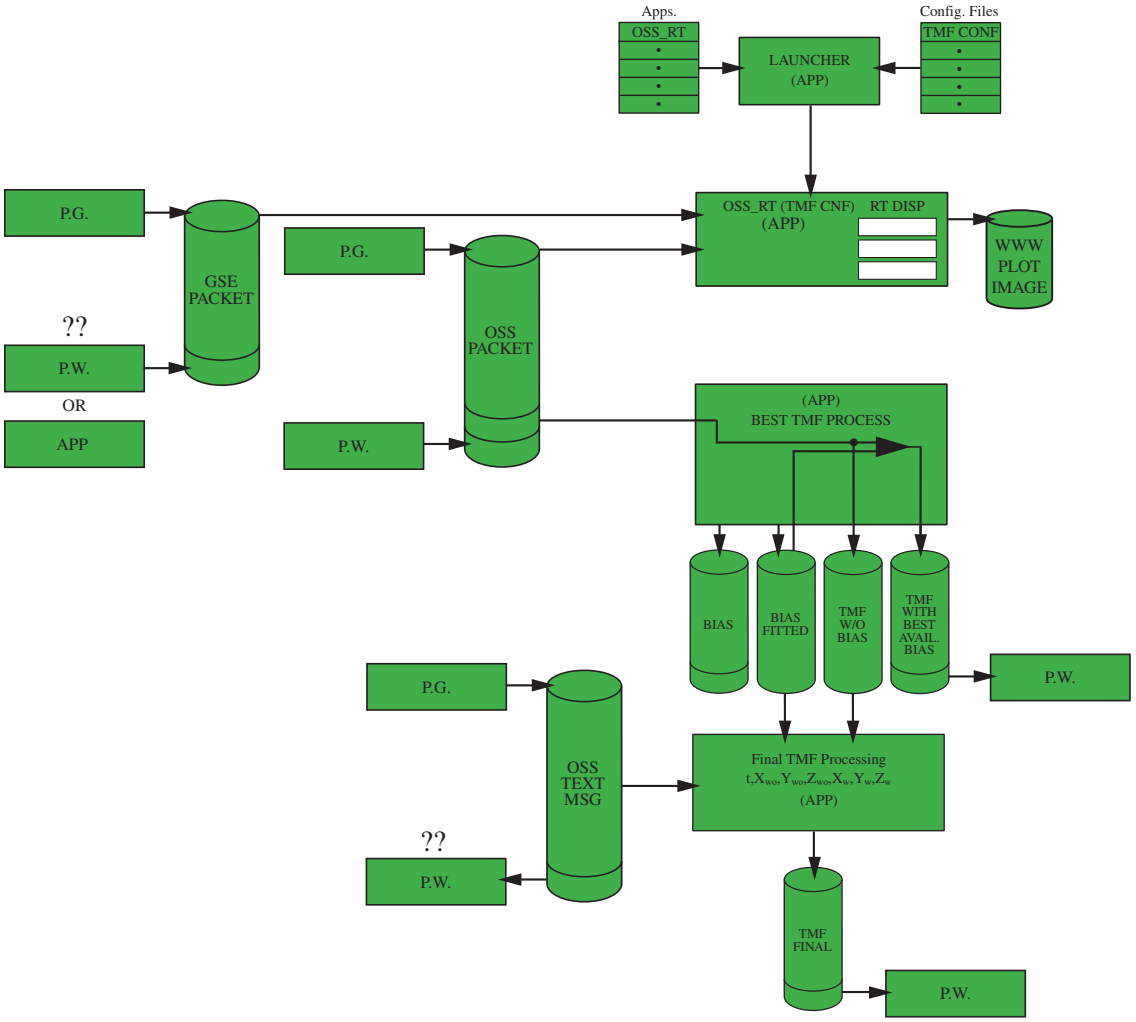

SAMS (1) Data Flow

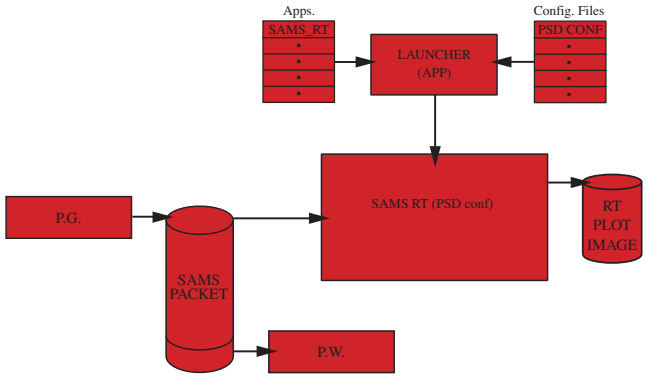

Flavors of MAMS OSS Data

- ossraw – Raw data [t x y z T s]
  - t = time in seconds,
  - [x y z] = accelerations in g’s
  - T= OSS sensor temperature
  - s = status byte
  - 10 samples / second
- Not recommended for public consumption, not trimmean filtered, not compensated for bias

MAMS Status Bits, Range C

Time			Event	Data Status								Range Status								Gimbal Status								24 bit integer
Begin	End	total		7	6	5	4	3	2	1	0	7	6	5	4	3	2	1	0	7	6	5	4	3	2	1	0	
INF	0	INF	Data Taking	1	0	0	0	1	0	0	0	0	0	1	0	1	0	1	0	0	0	1	0	0	0	1	0	8923682
0.1	50	50	Start Bias, Take data for set #1, X/Y axes	1	0	1	1	1	0	0	0	0	0	1	0	1	0	1	0	0	0	1	0	0	0	1	0	12069410
50.1	52	2	Finished set #1, delay before up ranging	1	0	1	0	1	0	0	0	0	0	1	0	1	0	1	0	0	0	1	0	0	0	1	0	11020834
52.1	54	2	Up Range to A, all 3 axes	1	0	1	0	1	0	0	0	0	0	0	0	0	0	0	0	0	0	1	0	0	0	1	0	11010082
54.1	64	10	slew outer gimbal to opposite X/Y position	1	0	1	0	1	0	0	0	0	0	0	0	0	0	0	0	0	0	1	0	1	0	0	0	11010088
64.1	68	4	slew complete, delay for sensor settling	1	0	1	0	1	0	0	0	0	0	0	0	0	0	0	0	0	0	1	0	0	0	0	1	11010081
68.1	78	10	filter settling, down ranging	1	0	1	0	1	0	0	0	0	0	1	0	1	0	1	0	0	0	1	0	0	0	0	1	11020833
78.1	128	50	Take data for set #2, all 3 axes	1	0	1	1	1	0	0	0	0	0	1	0	1	0	1	0	0	0	1	0	0	0	0	1	12069409
128.1	130	2	Finish set #2, delay before up ranging	1	0	1	0	1	0	0	0	0	0	1	0	1	0	1	0	0	0	1	0	0	0	0	1	11020833
130.1	132	2	Up Range to A, all 3 axes	1	0	1	0	1	0	0	0	0	0	0	0	0	0	0	0	0	0	1	0	0	0	0	1	11010081
132.1	142	10	slew inner gimbal to opposite X/Z position	1	0	1	0	1	0	0	0	0	0	0	0	0	0	0	0	1	0	0	0	0	0	0	1	11010177
142.1	146	4	slew complete, delay for sensor settling	1	0	1	0	1	0	0	0	0	0	0	0	0	0	0	0	0	0	0	1	0	0	0	1	11010065
146.1	156	10	filter settling, down ranging	1	0	1	0	1	0	0	0	0	0	1	0	1	0	1	0	0	0	0	1	0	0	0	1	11020817
156.1	206	50	Take data for set #3, all 3 axes	1	0	1	1	1	0	0	0	0	0	1	0	1	0	1	0	0	0	0	1	0	0	0	1	12069393
206.1	208	2	Finish set #3, delay before up ranging	1	0	1	0	1	0	0	0	0	0	1	0	1	0	1	0	0	0	0	1	0	0	0	1	11020817
208.1	210	2	Up Range to A, all 3 axes	1	0	1	0	1	0	0	0	0	0	0	0	0	0	0	0	0	0	0	1	0	0	0	1	11010065
210.1	220	10	slew outer gimbal to normal X/Z position	1	0	1	0	1	0	0	0	0	0	0	0	0	0	0	0	0	0	0	1	0	1	0	0	11010068
220.1	224	4	slew complete, delay for sensor settling	1	0	1	0	1	0	0	0	0	0	0	0	0	0	0	0	0	0	0	1	0	0	1	0	11010066
224.1	234	10	filter settling, down ranging	1	0	1	0	1	0	0	0	0	0	1	0	1	0	1	0	0	0	0	1	0	0	1	0	11020818
234.1	284	50	Take data for set #4, all 3 axes	1	0	1	1	1	0	0	0	0	0	1	0	1	0	1	0	0	0	0	1	0	0	1	0	12069394
284.1	286	2	Finish set #4, delay before up ranging	1	0	1	0	1	0	0	0	0	0	1	0	1	0	1	0	0	0	0	1	0	0	1	0	11020818
286.1	288	2	Up Range to A, all 3 axes	1	0	1	0	1	0	0	0	0	0	0	0	0	0	0	0	0	0	0	1	0	0	1	0	11010066
288.1	298	10	slew inner gimbal to start, std X/Y for data take	1	0	1	0	1	0	0	0	0	0	0	0	0	0	0	0	0	0	1	0	0	0	1	0	11010114
298.1	302	4	slew complete, delay for sensor settling	1	0	1	0	1	0	0	0	0	0	0	0	0	0	0	0	0	0	1	0	0	0	1	0	11010082
302.1	312	10	filter settling, down ranging, calib for range complete	1	0	1	0	1	0	0	0	0	0	1	0	1	0	1	0	0	0	1	0	0	0	1	0	11020834
			Error in outer gimbal	-	-	-	-	-	-	-	-	-	-	-	-	-	-	-	-	-	-	-	-	0	0	0	0	-
			Error in inner gimbal	-	-	-	-	-	-	-	-	-	-	-	-	-	-	-	-	0	0	0	0	-	-	-	-	-

1. Bits shown for bias calibration and data taking in C range.
2 .For axis range command status bit pairs: 00 = Range A, 01=Range B, 10=RangeC

Data collection mode
Capture sequence ON
Bias Calibration
Valid Data (bias only)
Filtered Data
spare
spare
spare
y axis constrainment disabled
z axis constrainment disabled
x range command status
x range command status
y range command status
y range command status
z range command status
z range command status
IG rotating from normal to opposite
IG rotating from opposite to normal
IG at normal
IG at opposite
OG rotating from normal to opposite
OG rotating from opposite to normal
OG at normal
OG at opposite

Eric Kelly
Nov. 28, 2000

Flavors of MAMS OSS Data

- ossbtmf – MAMS OSS data, [t x y z] that has been trim mean filtered and compensated for bias.
  - t = time in seconds
  - [x y z] = acceleration in g’s
  - 1 sample every 16 seconds
- PIMS recommended quasi-steady product

Flavors of MAMS OSS Data

- ossfbias , [t xm ym zm xb yb zb], Valid bias points for OSS data used in making ossbtmf, and used in offline processing with ossraw.
  - [xm ym zm] = as measured bias pts
  - [xb yb zb] = calculated bias point used in ossbtmf
- Header files of ossbtmf already include bias values used.

Summary of PIMS Acceleration Data (PAD) Archives

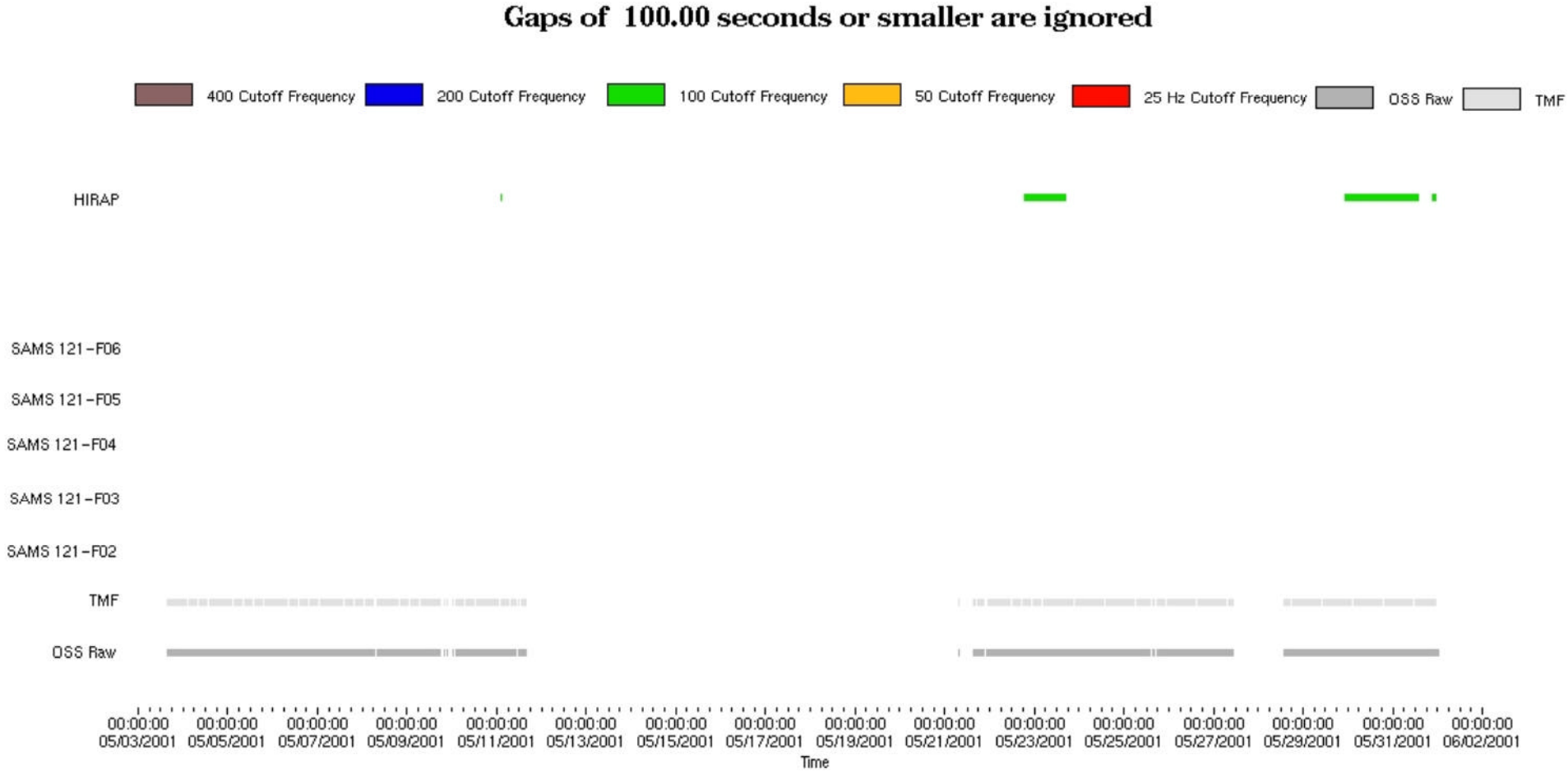
Gaps of 100.00 seconds or smaller are ignored
400 Cutoff Frequency
200 Cutoff Frequency
100 Cutoff Frequency
50 Cutoff Frequency
25 Hz Cutoff Frequency
OSS Raw
TMF
HIRAP
SAMS 121-F06
SAMS 121-F05
SAMS 121-F04
SAMS 121-F03
SAMS 121-F02
TMF
OSS Raw
00:00:00 05/03/2001
00:00:00 05/05/2001
00:00:00 05/07/2001
00:00:00 05/09/2001
00:00:00 05/11/2001
00:00:00 05/13/2001
00:00:00 05/15/2001
00:00:00 05/17/2001
00:00:00 05/19/2001
00:00:00 05/21/2001
00:00:00 05/23/2001
00:00:00 05/25/2001
00:00:00 05/27/2001
00:00:00 05/29/2001
00:00:00 05/31/2001
00:00:00 06/02/2001
Time

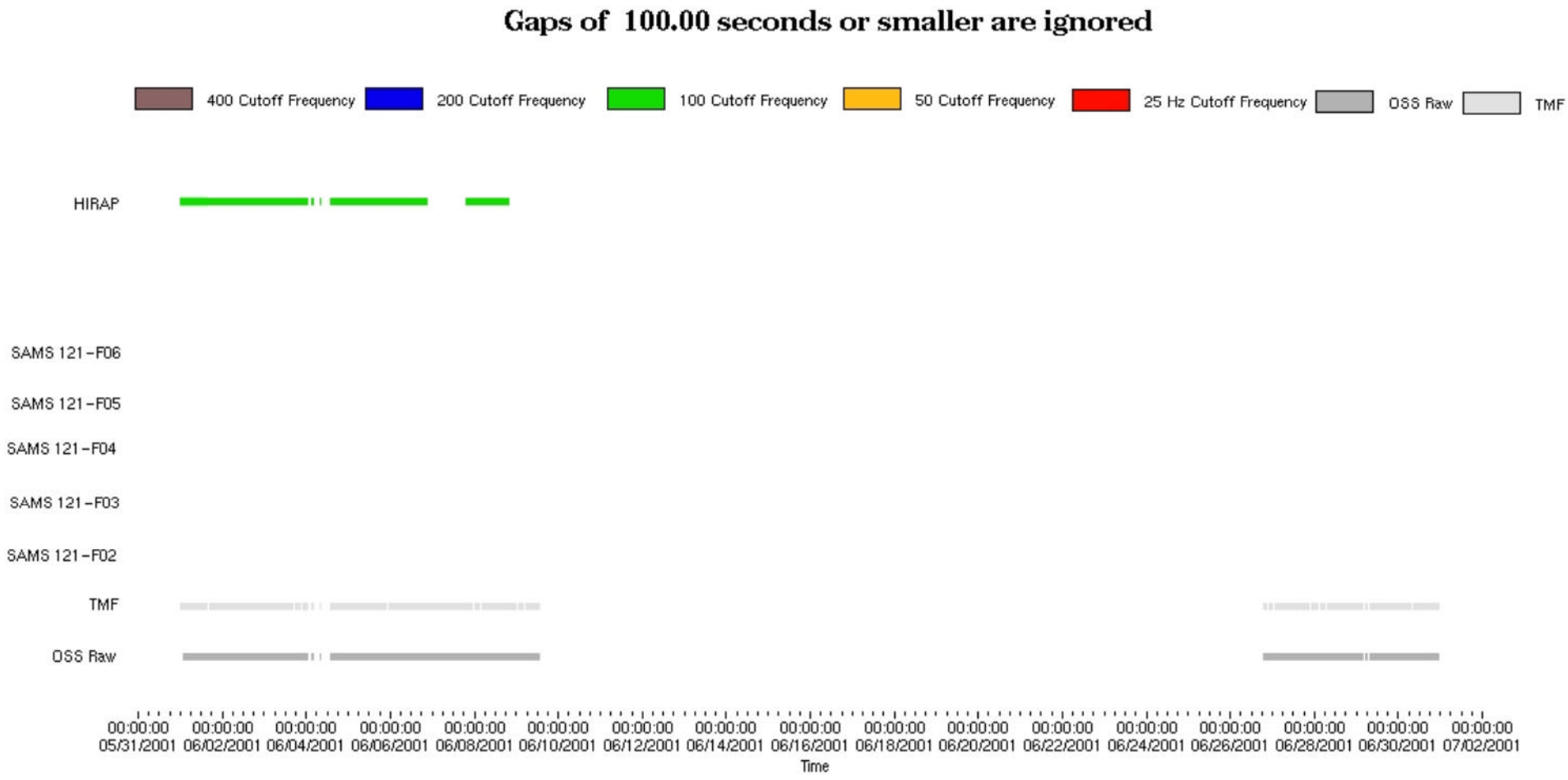
Gaps of 100.00 seconds or smaller are ignored
400 Cutoff Frequency
200 Cutoff Frequency
100 Cutoff Frequency
50 Cutoff Frequency
25 Hz Cutoff Frequency
OSS Raw
TMF
HIRAP
SAMS 121-F06
SAMS 121-F05
SAMS 121-F04
SAMS 121-F03
SAMS 121-F02
TMF
OSS Raw
00:00:00 05/31/2001
00:00:00 06/02/2001
00:00:00 06/04/2001
00:00:00 06/06/2001
00:00:00 06/08/2001
00:00:00 06/10/2001
00:00:00 06/12/2001
00:00:00 06/14/2001
00:00:00 06/16/2001
00:00:00 06/18/2001
00:00:00 06/20/2001
00:00:00 06/22/2001
00:00:00 06/24/2001
00:00:00 06/26/2001
00:00:00 06/28/2001
00:00:00 06/30/2001
00:00:00 07/02/2001
Time

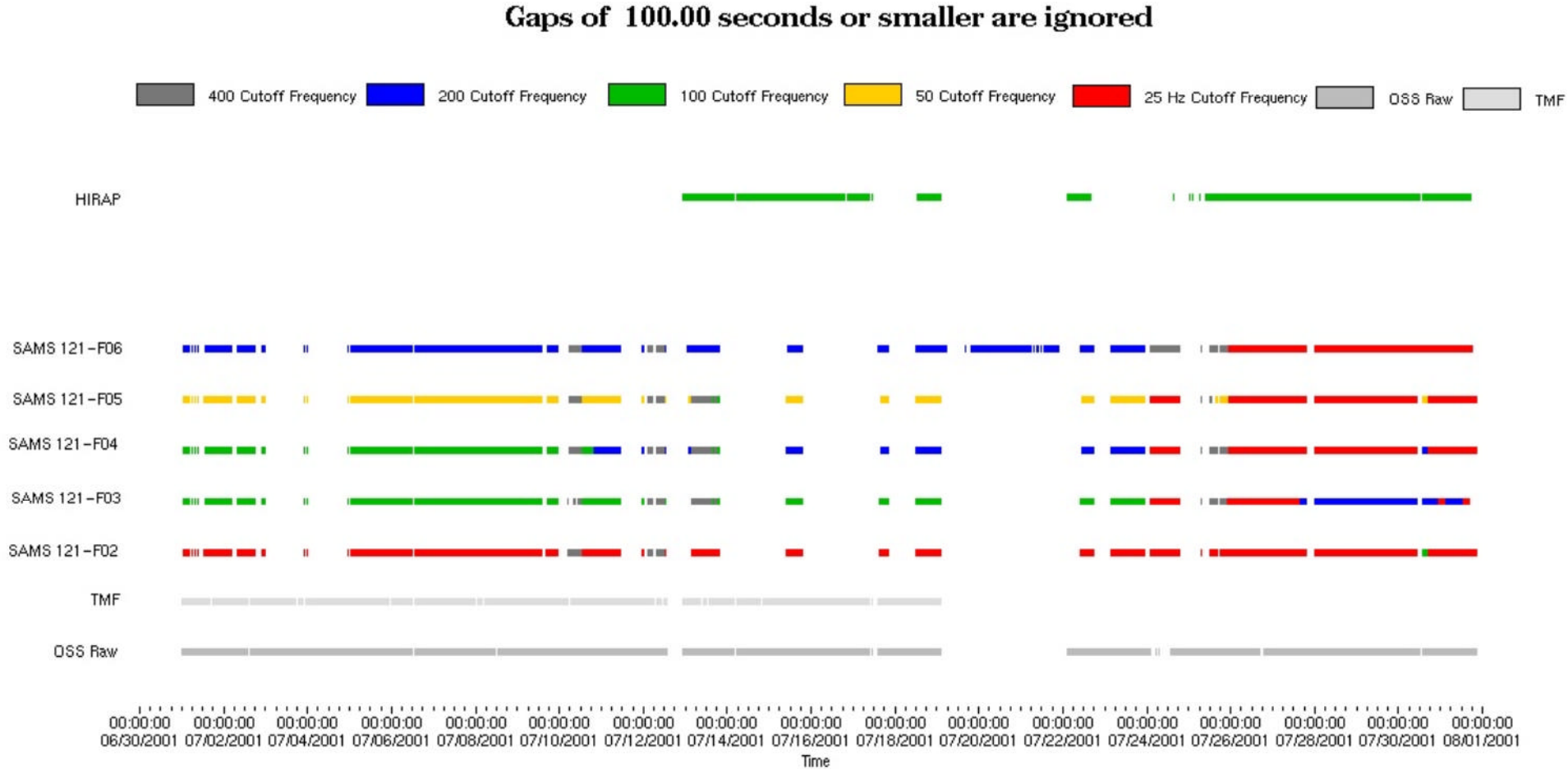
Gaps of 100.00 seconds or smaller are ignored
400 Cutoff Frequency
200 Cutoff Frequency
100 Cutoff Frequency
50 Cutoff Frequency
25 Hz Cutoff Frequency
OSS Raw
TMF
HIRAP
SAMS 121-F06
SAMS 121-F05
SAMS 121-F04
SAMS 121-F03
SAMS 121-F02
TMF
OSS Raw
00:00:00 06/30/2001
00:00:00 07/02/2001
00:00:00 07/04/2001
00:00:00 07/06/2001
00:00:00 07/08/2001
00:00:00 07/10/2001
00:00:00 07/12/2001
00:00:00 07/14/2001
00:00:00 07/16/2001
00:00:00 07/18/2001
00:00:00 07/20/2001
00:00:00 07/22/2001
00:00:00 07/24/2001
00:00:00 07/26/2001
00:00:00 07/28/2001
00:00:00 07/30/2001
00:00:00 08/01/2001
Time

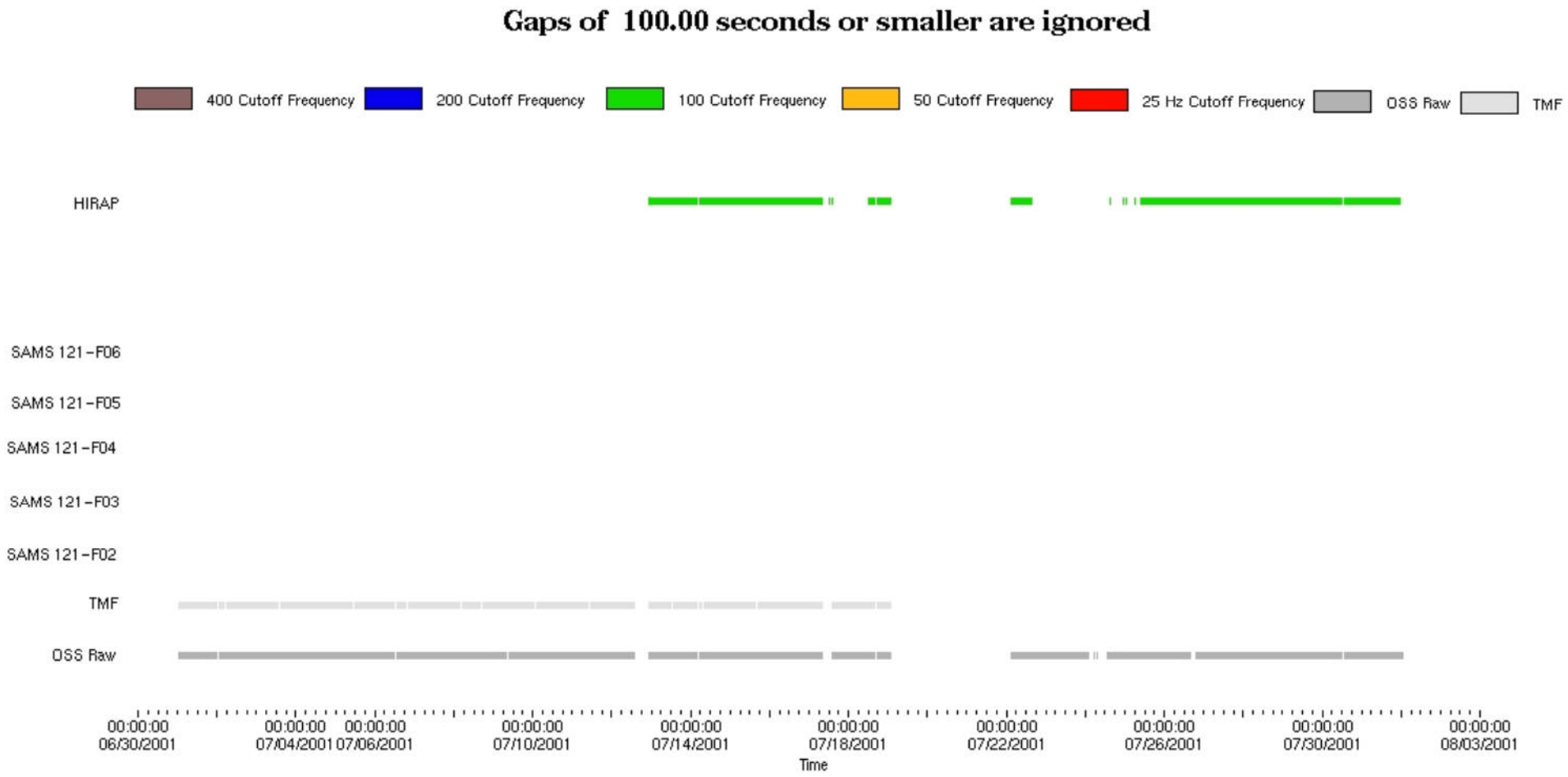
Gaps of 100.00 seconds or smaller are ignored
400 Cutoff Frequency
200 Cutoff Frequency
100 Cutoff Frequency
50 Cutoff Frequency
25 Hz Cutoff Frequency
OSS Raw
TMF
HIRAP
SAMS 121-F06
SAMS 121-F05
SAMS 121-F04
SAMS 121-F03
SAMS 121-F02
TMF
OSS Raw
00:00:00 06/30/2001
00:00:00 07/04/2001
00:00:00 07/06/2001
00:00:00 07/10/2001
00:00:00 07/14/2001
00:00:00 07/18/2001
00:00:00 07/22/2001
00:00:00 07/26/2001
00:00:00 07/30/2001
00:00:00 08/03/2001
Time

Sample Plots

- Figure 1 : OSS gimbal rotations are seen as large offsets (red line) in the ossraw data. These peaks disappear when properly compensated with A-range bias values (blue line).

- Figure 2: OSS gimbal rotations during normal bias measurements are seen in MAMS HiRAP data as large broadband spikes between 6 and 10 minutes. This plot covers the same period as in Figure 1.

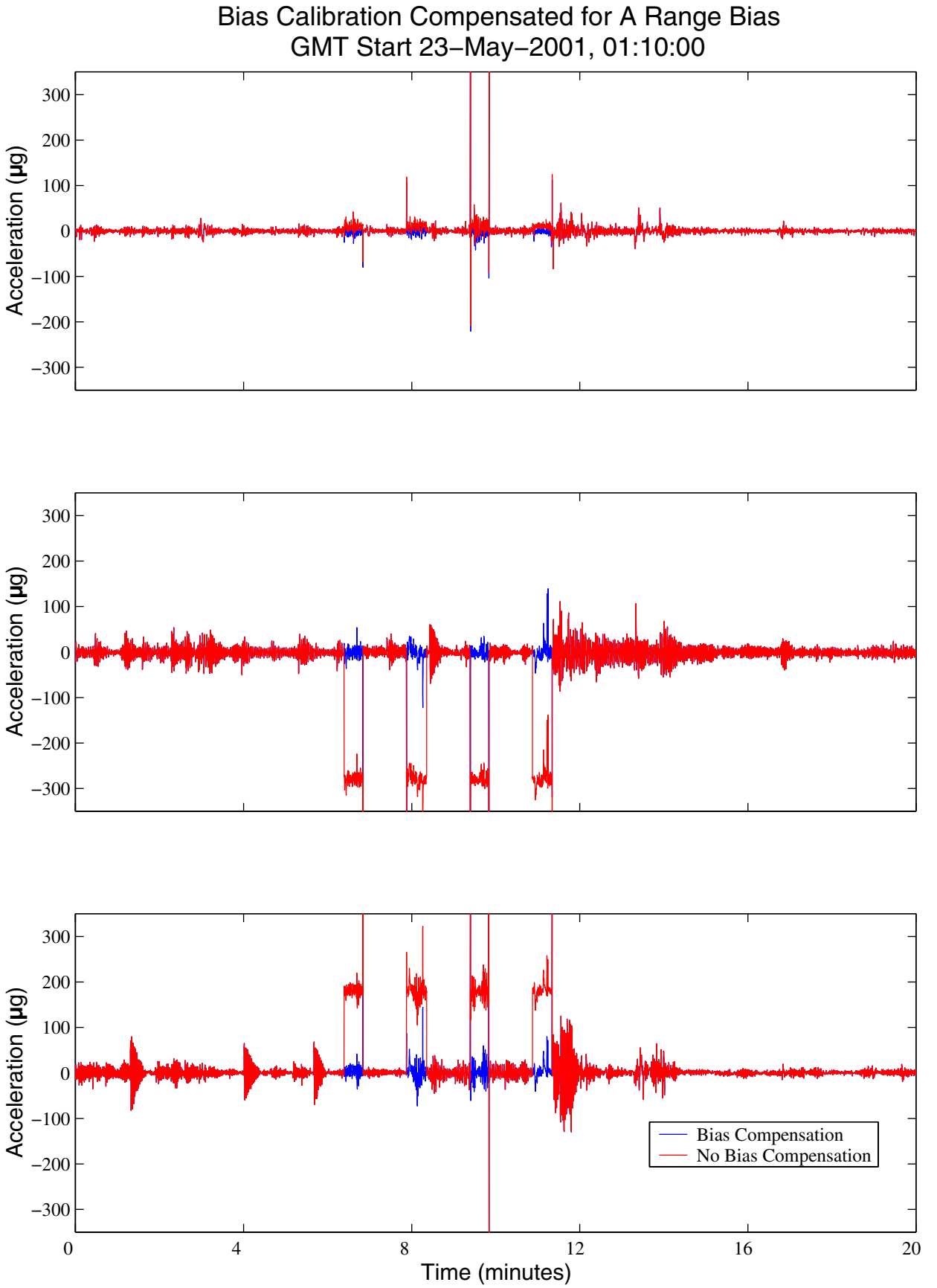
Bias Calibration Compensated for A Range Bias
GMT Start 23–May–2001, 01:10:00
Acceleration (µg)
300
200
100
0
−100
−200
−300
Acceleration (µg)
300
200
100
0
−100
−200
−300
Acceleration (µg)
300
200
100
0
−100
−200
−300
Bias Compensation
No Bias Compensation
0
4
8
12
16
20
Time (minutes)

Figure 1

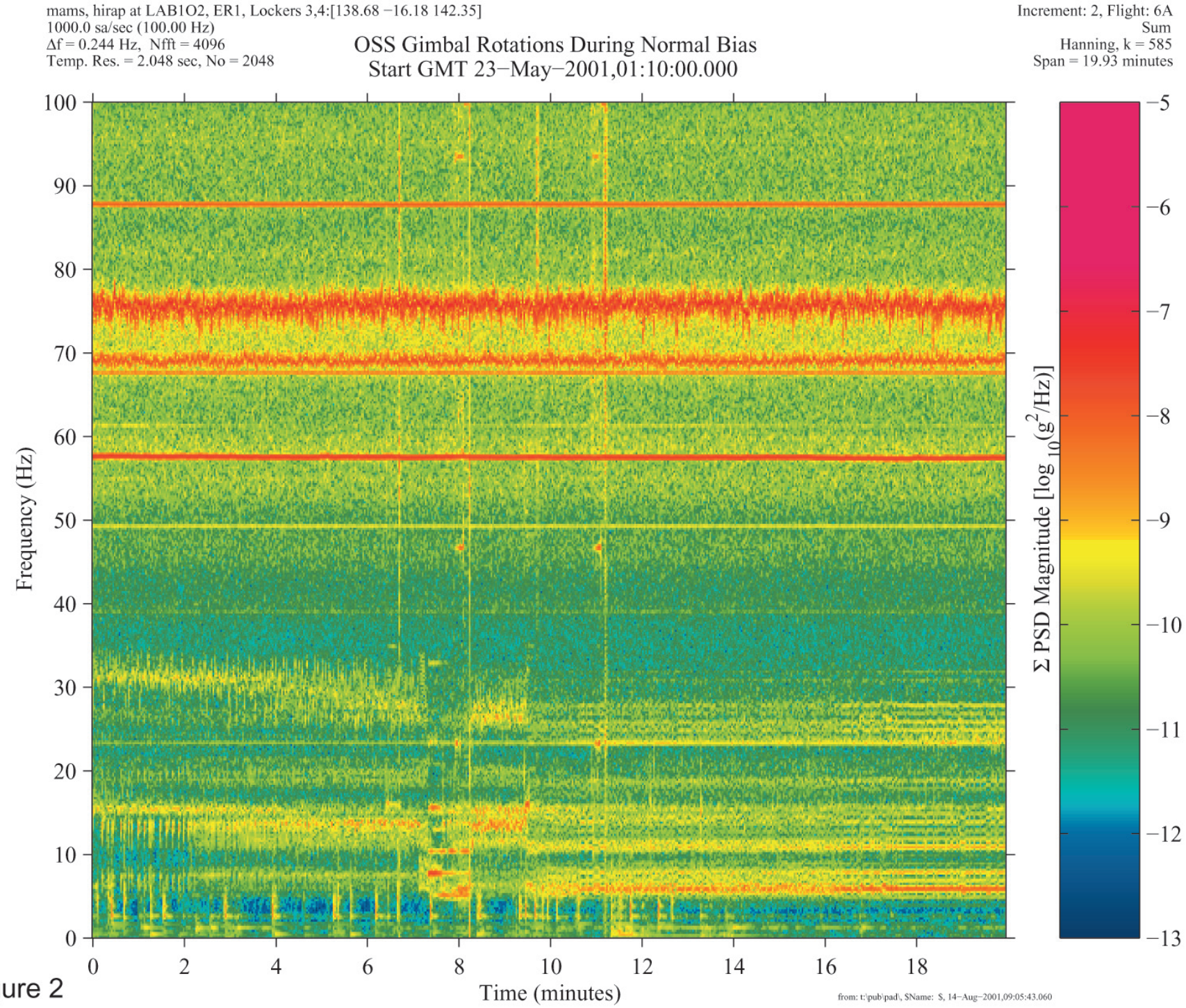
mams, hirap at LAB1O2, ER1, Lockers 3,4:[138.68 −16.18 142.35]
1000.0 sa/sec (100.00 Hz)
Δf = 0.244 Hz, Nfft = 4096
Temp. Res. = 2.048 sec, No = 2048
OSS Gimbal Rotations During Normal Bias
Start GMT 23−May−2001,01:10:00.000
Increment: 2, Flight: 6A
Sum
Hanning, k = 585
Span = 19.93 minutes
Frequency (Hz)
Time (minutes)
Σ PSD Magnitude [log10(g2/Hz)]
from: t:\pub\pad\, $Name: $, 14−Aug−2001,09:05:43.060

Figure 2

Sample Plots

- Figure 3: Three panel acceleration vs. time plot of the ISS during XPOP attitude. This was recorded during a crew sleep period.

- Figure 4: Plot showing prominent shifts in the quasi-steady acceleration levels of the OSS X and Y-axes after STS-104 docking.

Crew Sleep During XPOP Attitude

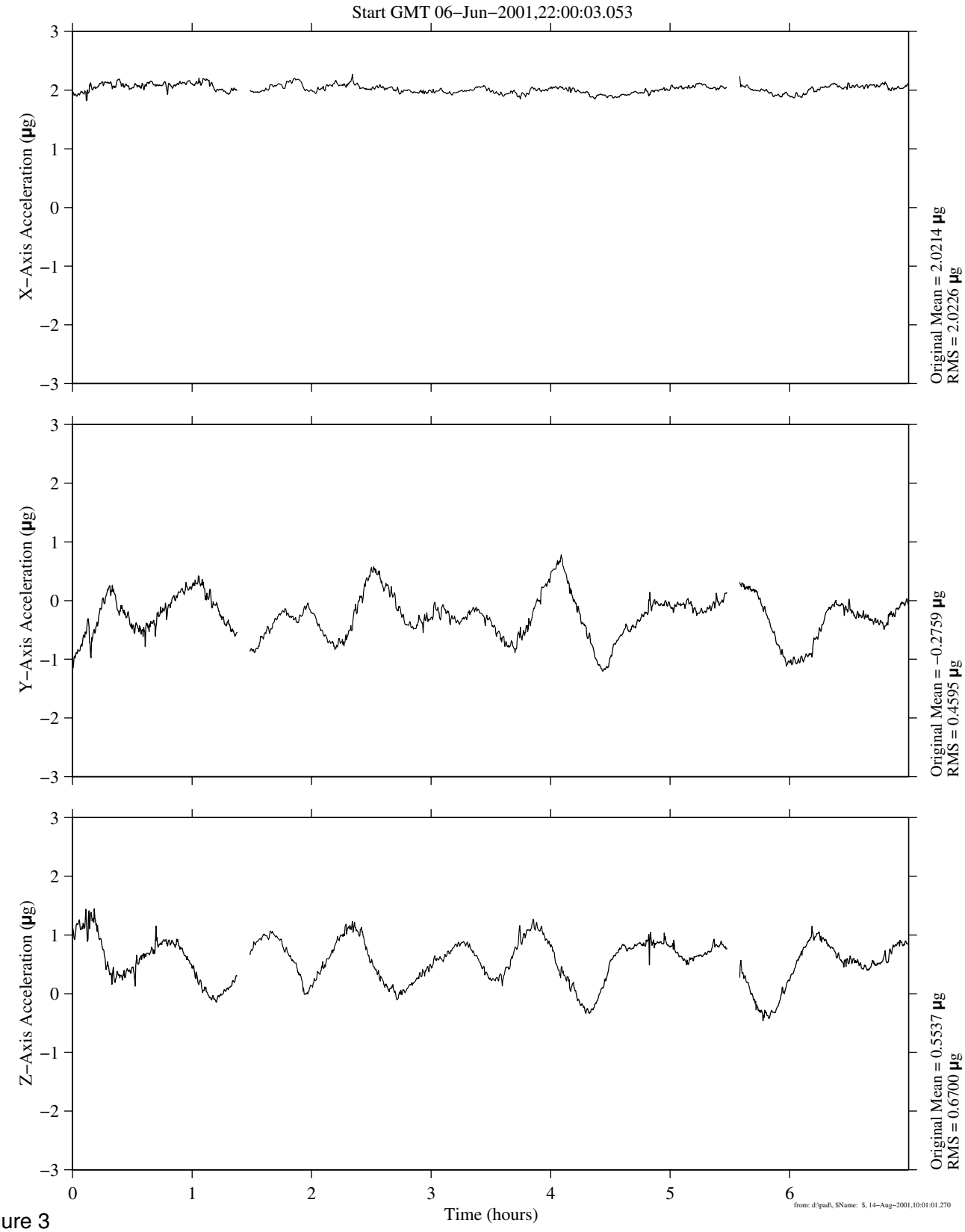

Figure 3

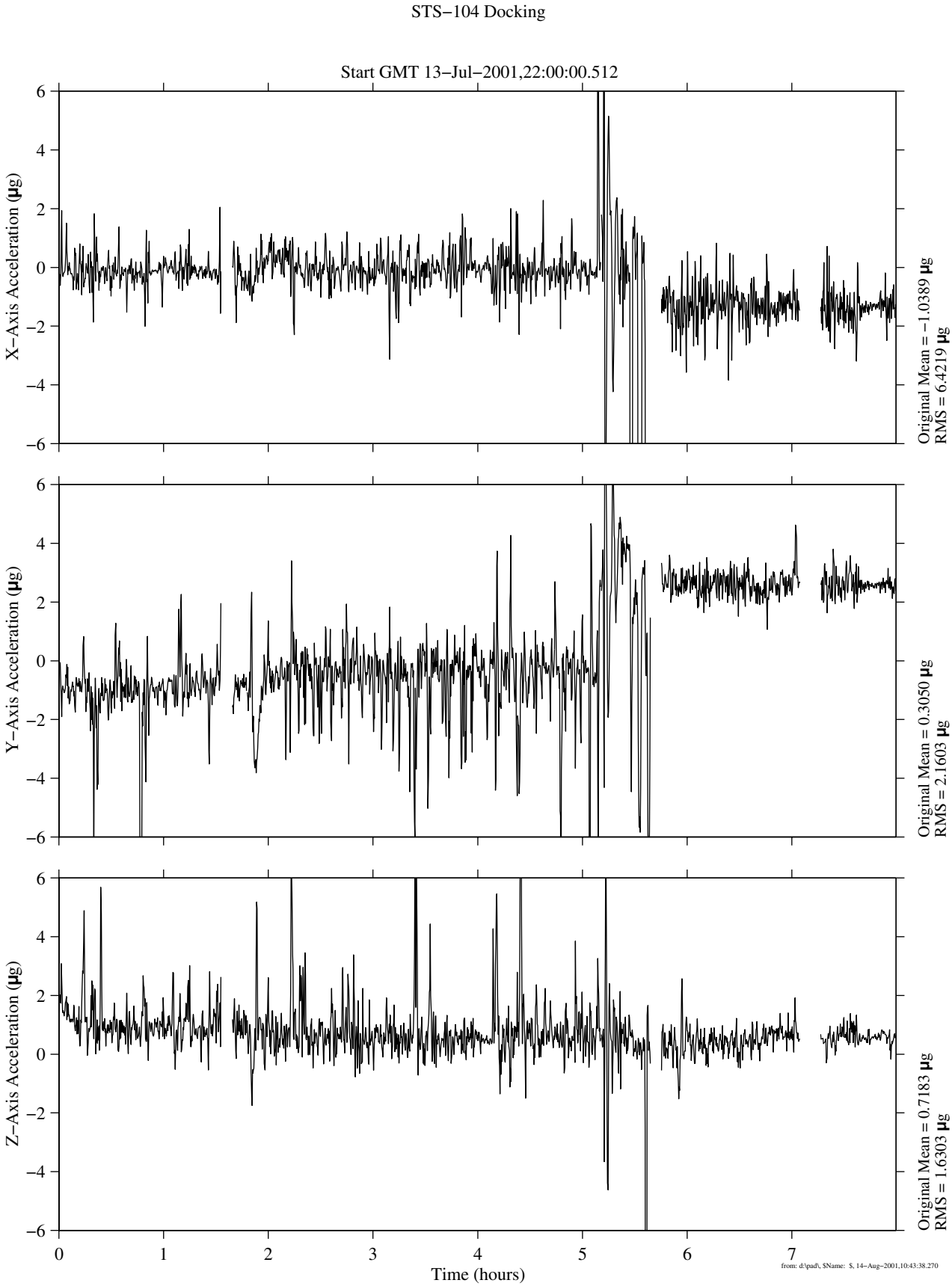
STS−104 Docking
Start GMT 13−Jul−2001,22:00:00.512
X−Axis Acceleration (µg)
Original Mean = −1.0389 µg
RMS = 6.4219 µg
Y−Axis Acceleration (µg)
Original Mean = 0.3050 µg
RMS = 2.1603 µg
Z−Axis Acceleration (µg)
Original Mean = 0.7183 µg
RMS = 1.6303 µg
Time (hours)
from: d:\pad\, $Name: $, 14−Aug−2001,10:43:38.270

Figure 4

Demonstration of microgravity outreach devices

Richard DeLombard
NASA Glenn Research Center
Cleveland, Ohio

The microgravity program has created several demonstration devices which may be used in outreach and educational events. These devices are used for NASA exhibits at technical conferences, air shows, and teachers' conferences. They are also very adaptable to presentations at schools for events such as National Engineers Week.

The Microgravity Demonstrator (a.k.a. mini-Drop Tower) was setup in the MGMG meeting room and demonstrated to the meeting attendees. The charts used by the author for talks to school classes and public groups relate a free-fall condition to orbital "weightlessness" in a manner that elementary students may understand. Aspects of changes due to free-fall are discussed and then demonstrated with the Microgravity Demonstrator. The repelling magnets demonstrated basic physics action during free-fall. A child's toy with bubbles of different density liquids illustrated surface tension forces apparent when the forces due to gravity are reduced to illustrate combustion research. The shape of a candle flame was also observed during free-fall to illustrate fluid physics research.

Other microgravity demonstration devices were also demonstrated and explained. The water-filled, holey bottle was as an effective microgravity demonstration tool with very low cost. The balloon popper was explained as another simple and low cost demonstration device.

A video of the KC-135 water balloon experiments was briefly shown to illustrate the variety of educational products (both formal and informal) which are available.

A data logger with a 3-axis accelerometer sensor was also used on the Microgravity Demonstrator to illustrate the reduction of acceleration level during free-fall.

Demonstration conducted with no presentation material.

Microgravity Emissions Laboratory (MEL) Testing of the Experiment of Physics of Colloids in Space (EXPPCS)

Anne M. McNelis
Structural Systems Dynamics Branch
NASA Glenn Research Center

The Microgravity Emissions Laboratory utilizes a 6 DOF inertial measurement system, capable of characterizing disturbances (down to 0.1 ug) of the on-orbit science environment by space-flight hardware.

Test unit operational emissions (accelerations) measured are combined with the system mass matrix to define the forces and moments at the center of gravity of the test unit.

Applying the 6 DOF forces and moments to SEA and FEM models allow payload developers a way of evaluating test component compliance to ISS PIRN- 110-H requirements.

The purpose of testing was to determine the micro gravity disturbances generated during operations of the Physics of Colloids in Space (PCS) experiment. PCS is a double locker fluids experiment installed in an EXPRESS Rack on-board the International Space Station.

NASA/CP—2001-211164

Glenn Research Center

Microgravity Emissions Laboratory (MEL) Testing of the Experiment of Physics of Colloids in Space (EXPPCS)

Prepared for 20th MGMG Conference

By

Anne M. McNelis

7735/Structural Systems Dynamics Branch

NASA Glenn Research Center

August 9, 2001

Microgravity Emissions Testing Objective

- **The Microgravity Emissions Laboratory utilizes a 6 DOF inertial measurement system, capable of characterizing disturbances (down to 0.1 μg's) of the on-orbit science environment by space-flight hardware**
- **Test unit operational emissions (accelerations) measured are combined with the system mass matrix to define the forces and moments at the CG of the test unit**
- **Applying the 6 DOF forces and moments to SEA and FEM models allow payload developers a way of evaluating test component compliance to ISS PIRN-110-H requirements**

Overview of MEL Facility

- **MEL measurements are seismic (force proportional to acceleration)**
- **Frequency range of interest is 0-312.5 Hz**
- **Main MEL system components:**
  - **Zero rate spring mechanism (ZSRM) and CSA pneumatic suspension system that reduces vertical frequencies to 0.3 Hz**
  - **34 ft pendulum braided vectran cable that reduces lateral frequencies to 0.18 Hz**
  - **98.24 lb “mushroom” #2 platform for attachment to test unit (1st natural frequency of 380 Hz)**
  - **10 QA-700 servo control accelerometers (3 measurements in X direction, 3 in Y direction and 4 in Z direction)**
  - **Total suspension capacity of MEL is 750 lbs**

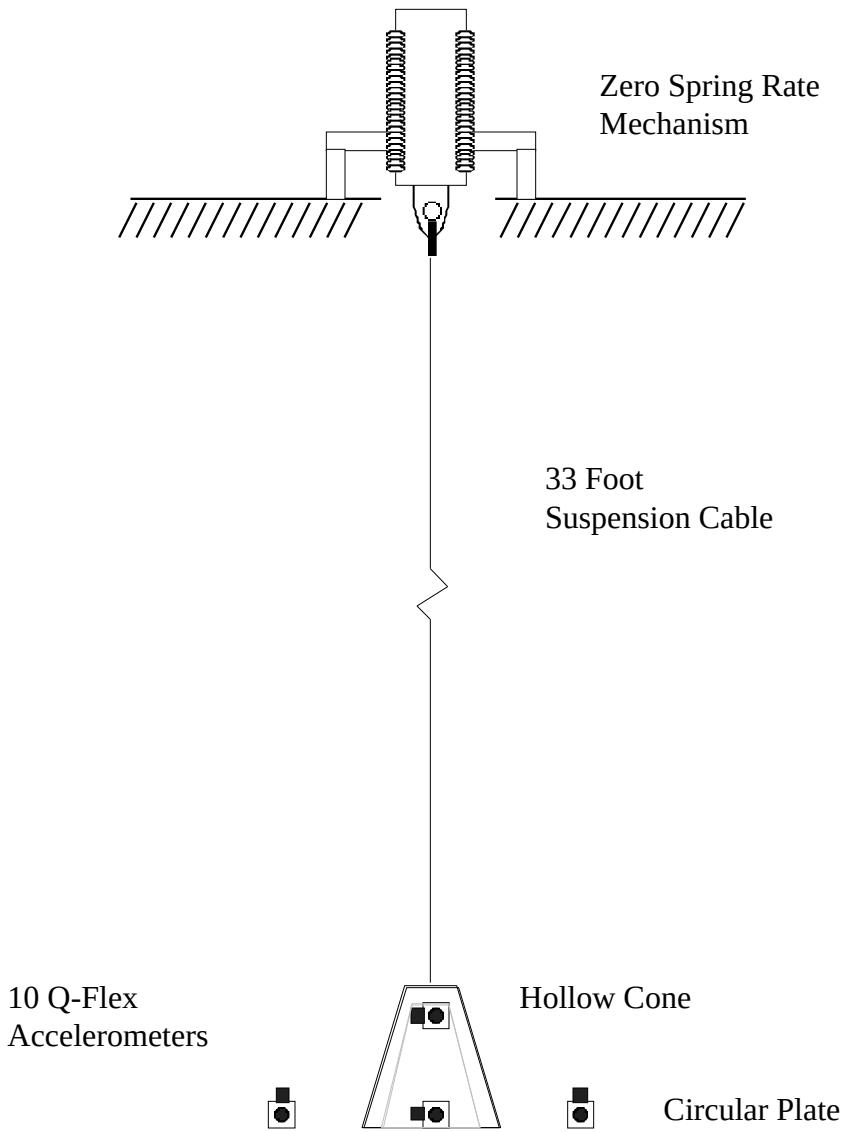
Zero Spring Rate
Mechanism
33 Foot
Suspension Cable
10 Q-Flex
Accelerometers
Hollow Cone
Circular Plate

General Products of MEL Test Reporting

MEL Test Products to date using GRC Methodology Including:

- **Mass of unit under test**
- **Mass moment of inertia in 3 axes for combined test article**
- **Force and Moment at CG of test unit or unit's interface upon request.**
  - **Narrowband and 1/3 octave**
- **PSDs at CG of test unit upon request**
  - **Narrowband and 1/3 octave**
- **Response acceleration spectral characteristics as requested**
- **Ambient/Noise floor documented**

PCS MEL Testing

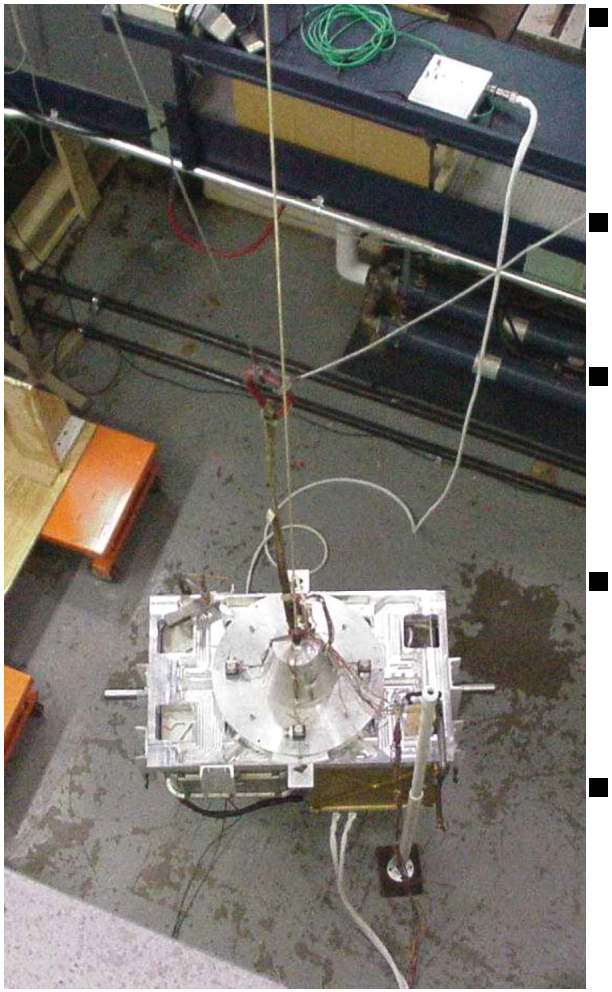

- **Purpose of testing was to determine the microgravity disturbances generated during operations of the Physics of Colloids in Space (PCS) experiment.**
- **PCS is a double locker fluids experiment installed in an Express Rack aboard the International Space Station.**
- **The disturbances were processed into six degree of freedom forces and moments about the center of gravity of the test article assembly.**
- **Additionally, two axes of acceleration measurements, recorded at the SAMS II sensor location on the front cover of the Experiment Package were acquired.**
- **The measurements were conducted using the Microgravity Emissions Laboratory (MEL) at NASA Glenn Research Center on May 4 and 5, 2000.**

PCS MEL Testing

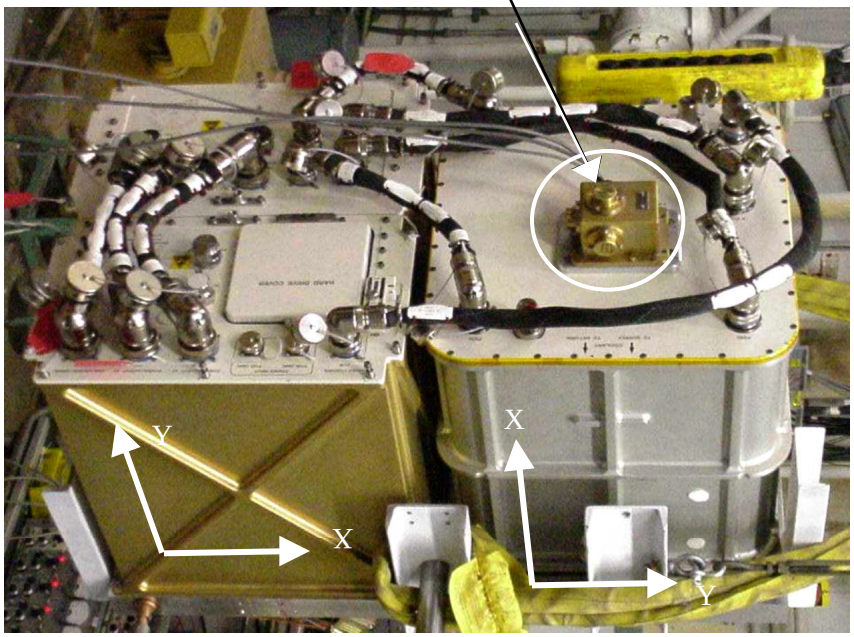

- Science investigation on sample cells is conducted in the Test section
- The Test section is designed to contain the individual sample cells for mixing, testing, and optical analyses
- The primary disturbance source is the sample cell handling and operation mechanisms
- The Avionics section serves as the control and power center for the Test section.

PCS MEL Testing

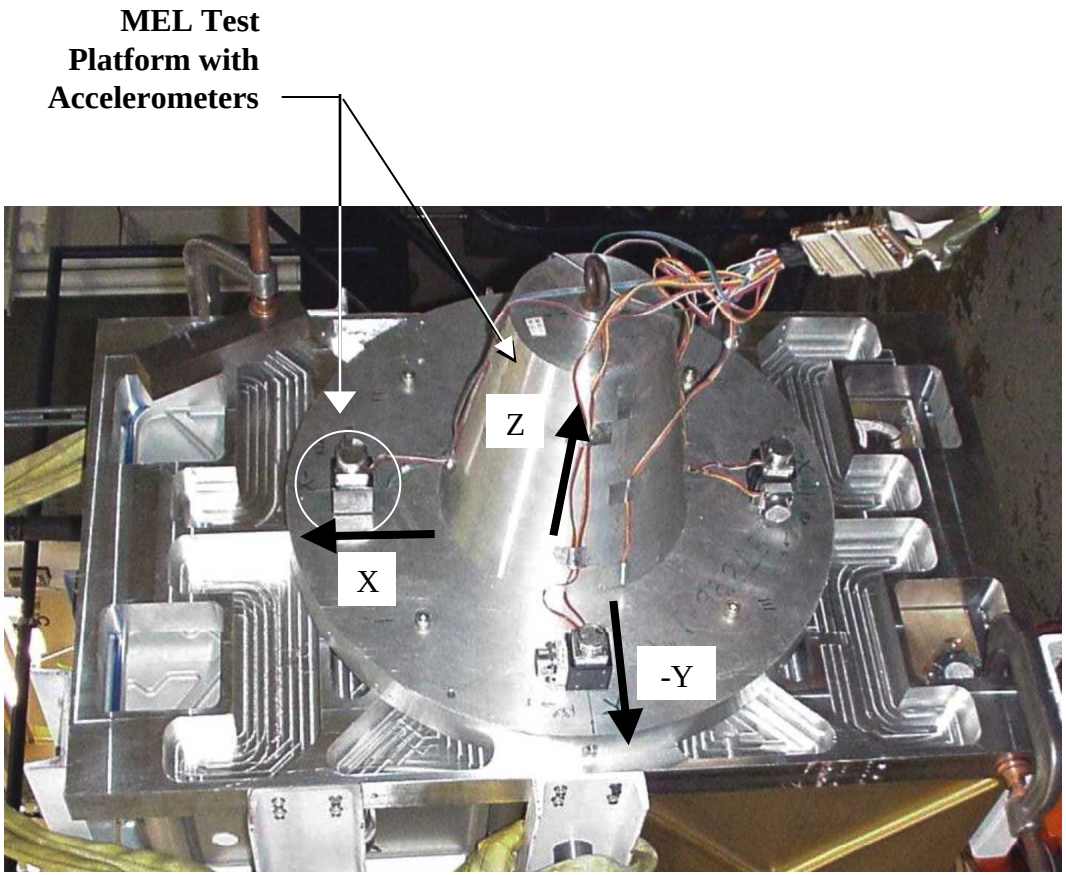

MEL Axes Designations Shown

PCS MEL Testing

- **Inertial response forces from eight fundamental PCS operations were measured.**

- **MEL data presented:**
  - **Sedimentation Mix**
  - **Rheology**
  - **Hard Drive and Fan operations**

PCS MEL Testing
Sedimentation Mix Operation

- **Sedimentation mix operations are conducted in the test section of the PCS experiment**
- **The Mix/Melt operation will be performed up to 20 times on-orbit with the longest period of operation of 5 hours in a given day (restriction due to acoustic noise emissions).**
- **Most Mix/Melt operations will be on the order of 5 minutes with the initial Sedimentation Mixes to eliminate sedimentation taking up to 30 minutes each.**
- **The operation is performed to eliminate sedimentation and aggregation of particles and to disperse the solid particles throughout the fluid**
- **This operation consists of quickly oscillating the sample cell via a DC motor and belt system. The mode of this operation is repeated quick acceleration and deceleration of the sample cell**
- **The MEL test operating condition for sedimentation mix was run as a steady state condition for a duration of 360 seconds.**

PCS MEL Testing
Rheology Operation

- **Rheology operations are conducted in the test section of the PCS experiment and is performed on each sample cell when the sample has reached its final state.**

- **There is about 24 hours of Rheology operation planned for each of eight colloid samples and is performed at several different frequencies and amplitudes for each sample cell.**

- **The frequency range of operation is 0 to 20 Hz, and the amplitude range is 0.5 degrees to 1.5 degrees**

- **The same motor and belt system used to perform the Sedimentation Mix is used for Rheology.**

- **The MEL test operating condition for Rheology was run as a 20 Hz steady state condition for a duration of 360 seconds.**

PCS MEL Testing
Fan and Hard Drive Operation

- **The Avionics section's potential disturbance source are the cooling fans and hard drive storage operations.**

- **The fan and hard drive operations perform two core functions whenever powered:**
  - **To circulate the EXPRESS Rack AAA air within Avionics Section's drawer assemblies**
  - **To take health and system status data and transmit it to the EXPRESS Rack.**

- **The MEL test operating condition for Fan and Hard Drive with Ethernet Connection was run as a steady state condition for a duration of 360 seconds.**

MEL FORCES AND MOMENTS

- **MEL Test Platform unit operational emissions (accelerations) measured are combined with the system mass matrix to define the forces and moments at the CG of the test unit**

- **The Forces and Moments calculated at the center of gravity for the PCS experiment were provided to program integrators to evaluate ISS requirements**

MEL/FLIGHT SAMS Sensor Location Comparison

- **Future plan to compare Operations measurements at the SAMSII Sensor Location for MEL and Flight**
  - **Rheology**
  - **Sedimentation Mix**
  - **Ambient**

- **Included is a comparison of the background measurement from Flight as compared to MEL at the SAMS location**

MEL Facility Web Presence

- Microgravity Emissions Laboratory Testing URL:

http://www.grc.nasa.gov/WWW/MEL

  - **Web site test request form**
  - **Testing schedule for MEL**
  - **Sample disturber data**
  - **Overview slides of MEL capabilities**

  - Contact Anne McNelis at 216-433-8880

Working Session for AAA Fan Retesting

Thomas Goodnight, NASA Glenn Research Center, Cleveland, Ohio
Mark McNelis, NASA Glenn Research Center, Cleveland, Ohio
Roy Christoffersen, SAIC / Code OZ, NASA Johnson Space Center, Houston, Texas

Several years ago, the ISS Avionics Air Assembly fan was tested at NASA Langley Research Center in the original configuration of the Microgravity Emissions Laboratory. The Microgravity Emissions Laboratory has been moved to NASA Glenn Research Center.

This working session will cover the technical and programmatic aspects of using the Microgravity Emissions Laboratory (MEL) to test payload sub-systems that are microgravity disturbers. The session will focus on testing of the ISS Avionics Air Assembly fan. Capability of the MEL will be reviewed and ISS Program requirements for utilizing the MEL will be discussed.

Discussion points:

* AAA fans are used for all EXPRESS racks
* AAA fans may pose ARIS saturation issue
* AAA fan is a high speed centrifugal blower, which may have "beating" phenomenon well below rotational rates
* There is a difficulty in characterizing the AAA fan directly due to high rotational rate at or above 25,0000 r.p.m. (416 Hz)
* PIMS may be able to correlate turbulence or other ancillary effects to fan operation
* A possible SDTO was suggested for AAA fan characterization

Outcome:

The NASA GRC Microgravity Emissions Lab will provide Rodney Rocha (NASA JSC) a draft AAA test plan in which the test matrix and test configuration will be defined.

No presentation material utilized in this discussion.

The Iterative Biological Crystallization Project

Scott Spearing
Morgan Research
4811 A Bradford Drive
Huntsville, Alabama 35805

The Iterative Biological Crystallization (IBC) project was initiated in response to a report from the National Research Council (NRC) issued in March 2000. The report recommended that biotechnology payloads provide state of the art hardware that supports near real time interaction between the investigator and the payload. The IBC team is simultaneously investigating several concepts designed to mix and dispense solutions into growth cells for macromolecular crystallization onboard the International Space Station. The growth cells will be incubated in a thermally controlled environment wherein an imaging system resides. All of these functionalities will be performed in an automated fashion via instructions sent from the PI. Of the concepts mentioned for mixing and dispensing, the one utilizing lab-on-a-chip appears to be the most appealing. An EXPRESS rack is the current choice for integration. Both the science and engineering teams are currently performing trade studies and, developing for assessment, these concepts.

National Aeronautics and
Space Administration
Marshall Space Flight Center

ITERATIVE BIOLOGICAL CRYSTALLIZATION (IBC)

Scott Spearing
IBC Lead Systems Engineer
Morgan Research Corporation

Micro**G**ravity **M**easurements **G**roup
Meeting

NASA Glenn Research Center
Cleveland, Ohio
August 9, 2001

National Aeronautics and Space Administration
Marshall Space Flight Center

ITERATIVE BIOLOGICAL CRYSTALLIZATION
PURPOSE OF IBC

IBC is to establish the capability aboard ISS that will enable an iterative aspect into macromolecular crystallization in a microgravity environment.

- **In response to the following paraphrased comments/recommendations from the National Research Council Report, March 1, 2000 (http://www.nas/edu/ssb/btfmenu.htm);**
  - **Investigate structures with biological importance, (p. 18)**
  - **Reduce weight & volume limitations imposed by logistics resupply capabilities, (p. 10)**
  - **Increase sample throughput capability, (p. 15)**
  - **Advance technical innovations in automation, (p. 24)**
  - **Provide state-of-the-art facilities on ISS, (p. 24)**
  - **Increase user control over samples, equipment, and procedures, (p. 25)**
  - **Provide for ground investigators abilities to interact with their experiment in real time, (p. 25)**
  - **And provide sample recovery of successful biological crystal growth experiments. (p. 25)**

National Aeronautics and
Space Administration
Marshall Space Flight Center

ITERATIVE BIOLOGICAL CRYSTALLIZATION
GOALS OF IBC

IBC will use automated systems, receive instructions from PIs, and prepare sample solutions accordingly. These solutions are to be placed into growth cells, incubated, and remotely observed for results. Selected crystals will be harvested and/or returned to Earth for further study.

This will be performed while accommodating the following;

- **Minimum of 1500 samples processed for 10 PIs during a 105 day increment,**
- **"Wet Bar" allows 8 solutions per PI,**
- **Minimize the amount of solution and sample material needed,**
- **Accommodate vapor diffusion, batch, and liquid-liquid diffusion growth techniques,**
- **Near real time imaging to assess crystallization,**
- **Ability to alter and maintain defined growth conditions,**
- **Remote control of automated mixing/dispensing,**
- **And minimize the inclusion/formation of bubbles in and around sample solutions.**

National Aeronautics and Space Administration
Marshall Space Flight Center

ITERATIVE BIOLOGICAL CRYSTALLIZATION
ITERATIONS ARE IMPORTANT

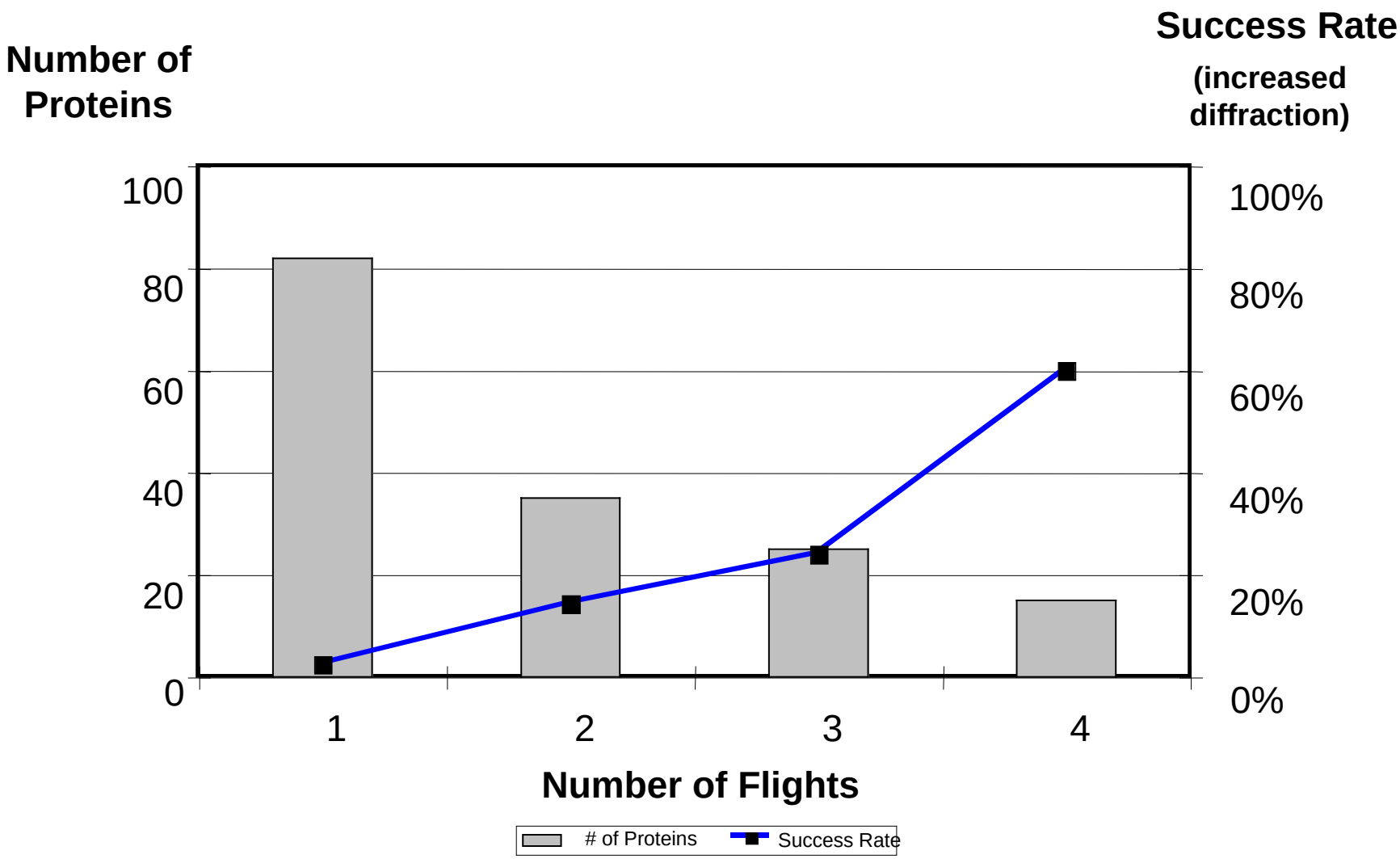

National Aeronautics and Space Administration
Marshall Space Flight Center

ITERATIVE BIOLOGICAL CRYSTALLIZATION
EXPRESS rack concept for IBC

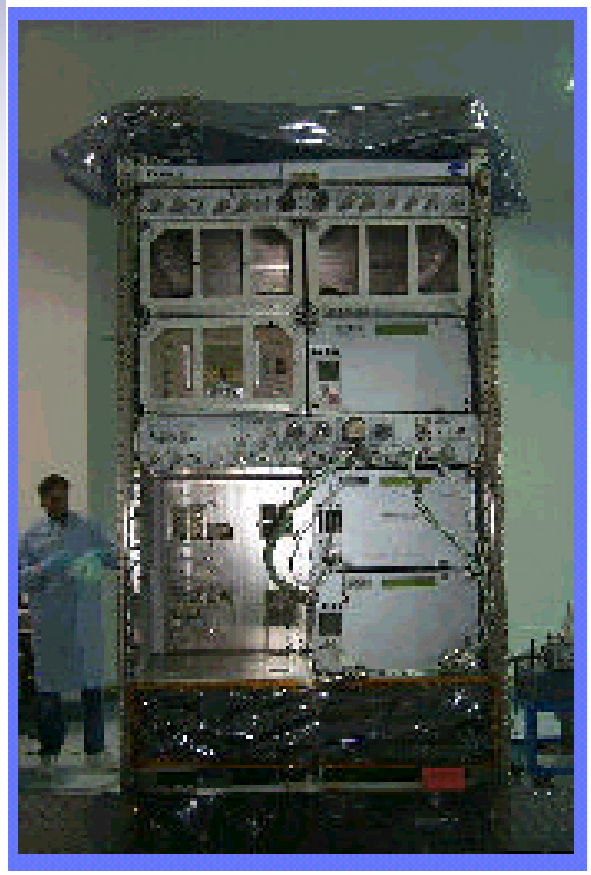

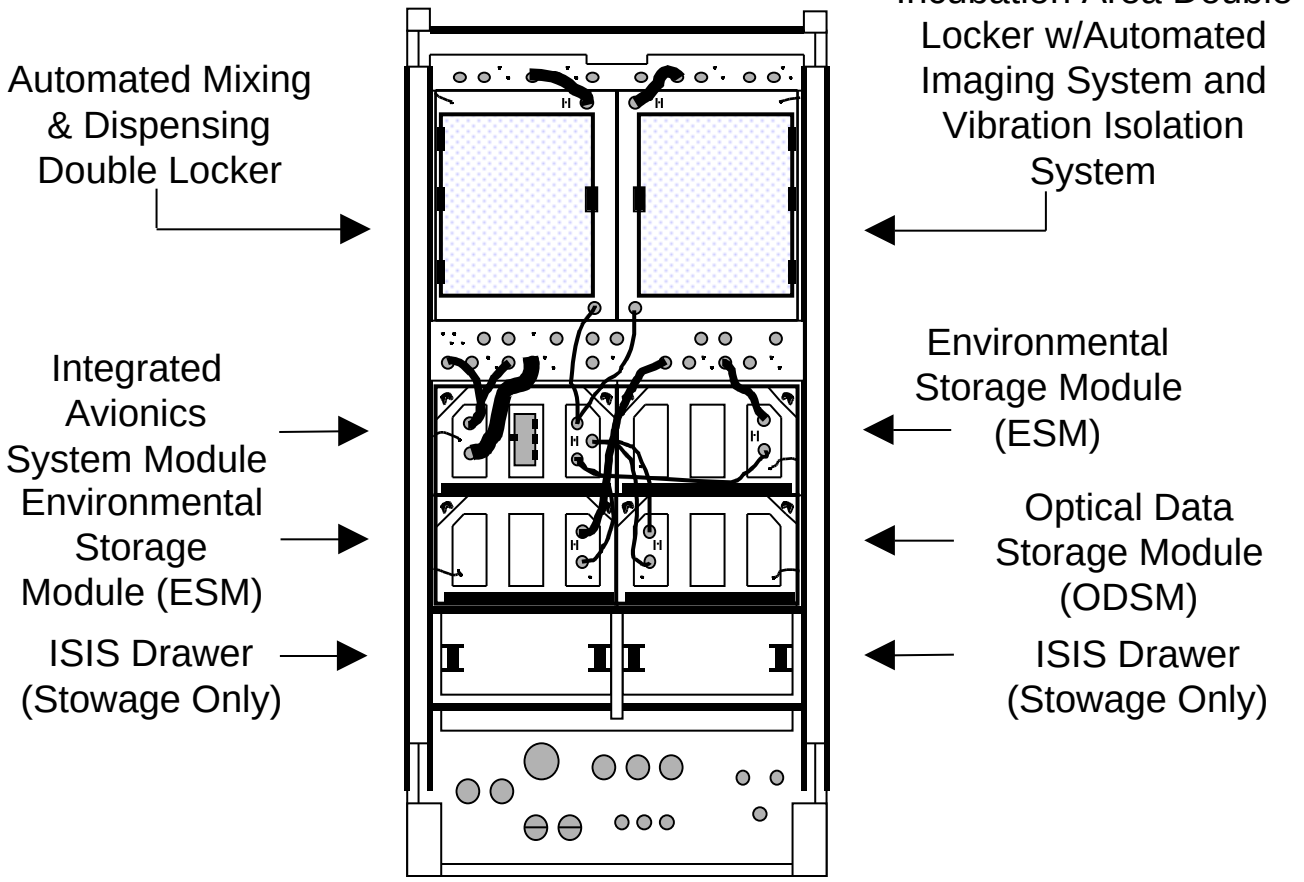

National Aeronautics and
Space Administration
Marshall Space Flight Center

ITERATIVE BIOLOGICAL CRYSTALLIZATION
VIBRATION ISOLATION REQUIREMENTS

• The strategy for assessing IBC's vibration isolation requirements entails the following

– Assess the background noise that is currently present onboard ISS

– Assess the vibration isolation platforms and their capabilities

– Estimate the frequency ranges that may adversely affect IBC with some rough order of magnitude estimates

– Perform ground-based experimental studies to determine what if any affects known disturbances have on crystal quality

National Aeronautics and
Space Administration
Marshall Space Flight Center

ITERATIVE BIOLOGICAL CRYSTALLIZATION

Phase I LabChip® investigations with Caliper

- Determine fluid flow capabilities through micron size channels,
- Determine proper fluid mixing of solutions,
- Demonstrate crystals can grow in smaller solution quantities,
- Determine if crystals of viable size can be grown (x-ray diffraction),
- Establish “chip technology” is suitable for crystal growth investigation,
- Determine potential advancements for chip design to enhance IBC capabilities.

National Aeronautics and Space Administration
Marshall Space Flight Center

ITERATIVE BIOLOGICAL CRYSTALLIZATION

Lab-on-a-Chip preliminary results

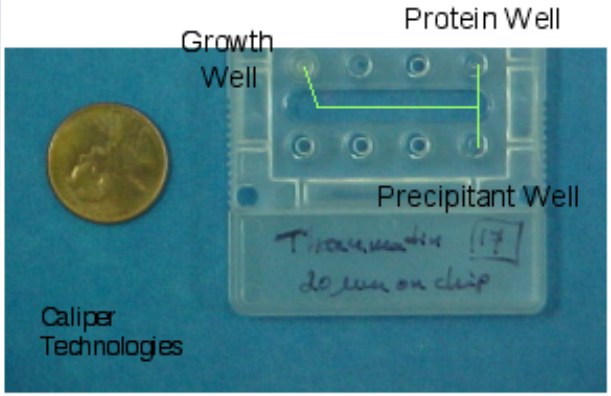

Crystal Growth In Well

Crystal Growth In Channel

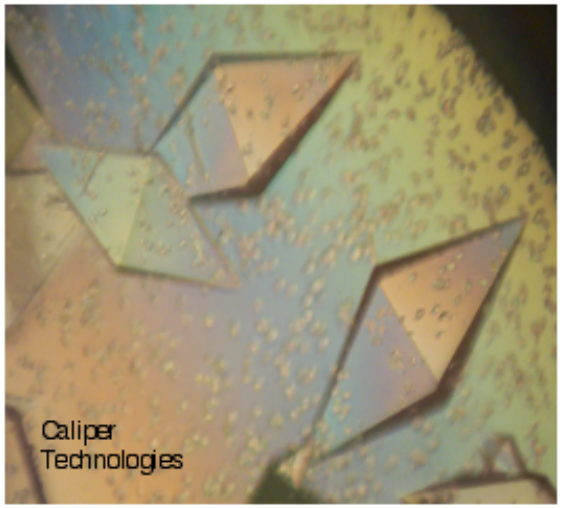

Thaumatin Crystals – 300µm

X-Ray Diffraction Analysis

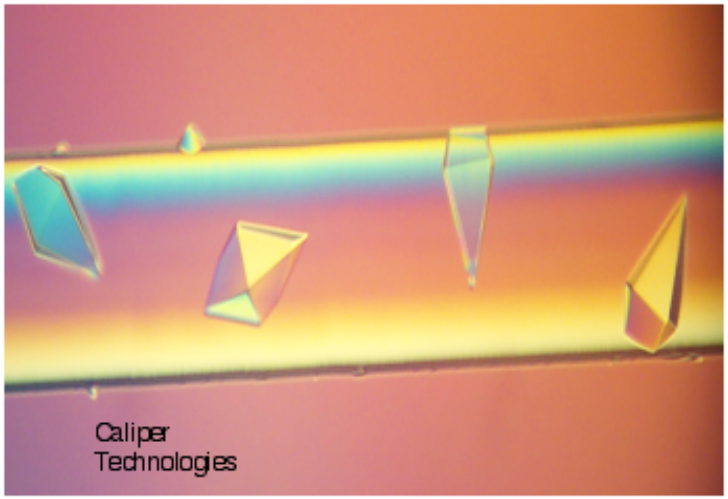

Thaumatin Crystals – 100µm in length

Comparable Quality To Existing Crystal Growth Methods

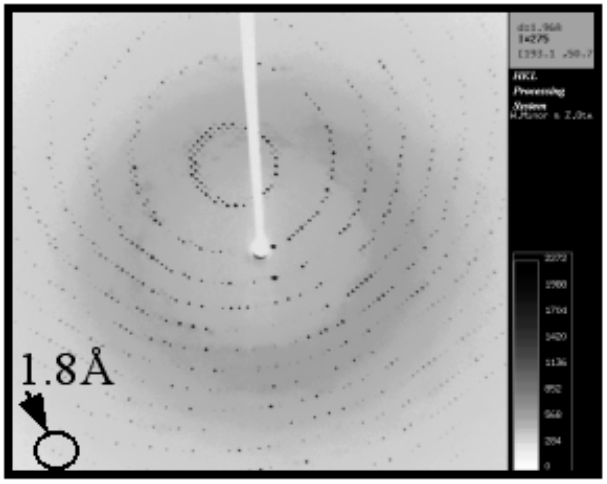

Microgravity Vibration Isolation Systems that the Canadian Space Agency is developing for ISS

Bjarni Tryggvason
Canadian Space Agency
6767 Route de l'Aeroport
St. Hubert, Quebec J3Y8Y9
CANADA

The development status of several vibration isolation systems for ISS was briefly described.

This was impromptu presentation at the MGMG and therefore no presentation material was prepared for the minutes.

Presentation not available at time of printing.

Preliminary Review of Microgravity Environment in Russian Segment of ISS

E. V. Babkin, Rocket and Space Corporation Energiya
M. Yu. Belyaev, Rocket and Space Corporation Energiya
A. Yu. Kaleri, Rocket and Space Corporation Energiya
V. M. Stazhkov, Rocket and Space Corporation Energiya
O. N. Volkov, Rocket and Space Corporation Energiya
V. V. Sazonov, Keldysh Institute of Applied Mathematics, RAS

The paper presents the first results of determination of residual accelerations in Russian Segment of ISS in spring and summer 2001. A quasi-steady acceleration component was determined using telemetry information about the station attitude motion. The information contains values of the station angular rates and the quaternion of the station attitude with respect to an inertial coordinate system at some instants. Basing on the information, we reconstruct the station motion and calculate the acceleration at any given point on its board as a function of time. As a rule, telemetry information, having at hand, allowed us to calculate acceleration during an orbital periods.

The main part of this approach is the reconstruction of the station attitude motion. We have a few various techniques for solving this problem, which differ by used mathematical models of the station attitude motion and types of processed telemetry information. A vibrational acceleration component was measured by several three-axis accelerometers IMU-128. They measure accelerations with magnitude more then 0.001 m/s in the frequency range up to 20 Hz. Although, the accelerometers IMU-128 are not very sensitive, they are able to measure typical accelerations caused by operation of onboard equipment.

Note:

This paper was submitted in preparation for the meeting, but the paper was not presented at the MGMG meeting.

PRELIMINARY REVIEW OF MICROGRAVITY ENVIRONMENT IN RUSSIAN SEGMENT OF ISS

E.V.Babkin, M.Yu.Belyaev, A.Yu.Kaleri, V.M.Stazhkov, O.N.Volkov
(Rocket and Space Corporation Energiya)

V.V.Sazonov
(Keldysh Institute of Applied Mathematics, RAS)

The paper presents the first results of determination of residual accelerations in Russian Segment of ISS in spring and summer 2001. A quasi-steady acceleration component was determined using telemetry information about the station attitude motion. The information contains values of the station angular rates and the quaternion of the station attitude with respect to an inertial coordinate system at some instants. Basing on the information, we reconstruct the station motion and calculate the acceleration at any given point on its board as a function of time. As a rule, telemetry information, having at hand, allowed us to calculate acceleration during an orbital periods. The main part of this approach is the reconstruction of the station attitude motion. We have a few various techniques for solving this problem, which differ by used mathematical models of the station attitude motion and types of processed telemetry information. A vibrational acceleration component was measured by several three-axis accelerometers IMU-128. They measure accelerations with magnitude more then 0.001 m/s^2 in the frequency range up to 20 Hz. Although, the accelerometers IMU-128 are not very sensitive, they are able to measure typical accelerations caused by operation of onboard equipment.

1. Determination of a quasi-steady component in residual accelerations by telemetry information

Since ISS and Service Module (SM) were mated, the station performed its flight being almost continuously in oriented mode. Mainly, it maintained invariable attitude either in the orbital coordinate system or in the absolute space. The ISS attitude control system operated continuously on that reason, and the computer of SM contained the complete information about the station attitude motion. The information contains values of the station angular rates and the quaternion of the station attitude with respect to an inertial coordinate system. These values are given at some instants. There are two possibilities. First, the data are given with a time step about 1.5 s during a short interval (≤ 10 min) when the station passes over a ground receiving station and the data are transmitted from the computer immediately. Second, the data are given with a time step about 1.5 min during an orbital period, if the data are stored on board and transmitted to the ground under suitable conditions.

The long time intervals containing scarce data are most convenient for calculating of a quasi-steady acceleration component.

The most valuable kind of telemetry data is the quaternion values. They are most exact and sufficient for solving the problem [1]. The values of the station angular rates are not exact especially for slow motions [1, 2]. Those data were used for testing. There are another kinds of data in the telemetry information, but their employment requires using rather complicated mathematical models. Here we present the results obtained in the framework of simple models based on kinematical equations of an attitude motion [1].

The simple formula is known for calculating a quasi-steady component in residual accelerations on board an Earth artificial satellite. Let a satellite be a rigid body and a point P be fixed with its frame. We assume only the atmosphere drag is significant among nongravitational actions upon the satellite. Then the residual acceleration $\mathbf{n}$ at the P is expressed by the formula [3]

$$\mathbf{n} = \mathbf{r} \times \frac{d\dot{\mathbf{u}}}{dt} + (\dot{\mathbf{u}} \times \mathbf{r}) \times \dot{\mathbf{u}} + \frac{\mu_e}{|\mathbf{R}|^3}\left[\frac{3(\mathbf{R}\cdot\mathbf{r})\mathbf{R}}{|\mathbf{R}|^2} - \mathbf{r}\right] + c\rho\,|\mathbf{v}|\,\mathbf{v} \,. \qquad (1)$$

Here $\mathbf{r}$ is the radius vector of the point P with respect to the satellite center of mass, $\mathbf{R}$ and $\mathbf{v}$ are the geocentric radius vector of this center of mass and its velocity with respect to the Earth surface, $\dot{\mathbf{u}}$ is the absolute angular rate of the satellite, t is time, μ_e is the Earth gravitational parameter, c is the satellite ballistic coefficient, ρ is the density of the aerodynamic flow incoming the satellite. Formula (1) gives an approximate expression for the difference between the strength of the gravitational field at the point P and the absolute acceleration of that point. If we reconstruct a real satellite motion basing on some information about it, then we can calculate an actual residual acceleration at the point P as a function of time. For a large satellite, this approach can give only a quasi-steady acceleration component because such a satellite is not a rigid body and information about its attitude does not have sufficient resolution in time. This approach is very convenient in the case, when $\dot{\mathbf{u}}$ and $d\dot{\mathbf{u}}/dt$ must be known in addition to $\mathbf{n}$ [3].

The calculation scheme is as follows. Let the instants with the values of the attitude quaternion be sufficiently dense in a time interval – with the step about 1.5 min in our case. These values are smoothed by a quaternion function of time, which has a continuous second derivative. We determine $\dot{\mathbf{u}}$ and $d\dot{\mathbf{u}}/dt$ by differentiating this function and obtain the approximation of the attitude motion of the station. The motion of its center of mass is assumed to be Keplerian. The elements of that motion are known from processing the trajectory measurements. The knowledge of the motion of the station center of mass and the station attitude motion allows one to calculate the first three terms in formula (1). The calculation of the fourth term requires the specification of the ways of calculation of ρ and c. The first of these quantities is calculated according to the model of the atmosphere [4], the second one is assumed to be constant and is known from processing the trajectory measurements.

The quaternion above defines the station attitude with respect to the inertial coordinate system $EY_1Y_2Y_3$, which is right-hand one and related to the Earth equator. The point E is the Earth center, the axis EY_1 is directed to the vernal equinox of epoch 2000.0, the axis EY_3 is directed to the corresponding north celestial pole. When we say about the station attitude, we have in mind the attitude of the structural coordinate system $Oy_1y_2y_3$, which is rigidly coupled with the station body. This system is right-hand one too. The origin of this system is located at the station center of mass, the axis Oy_1 is parallel to the longitudinal axis of SM and directed from its transition bay to its equipment bay, the axis Oy_2 is perpendicular to the rotation axis of the SM solar batteries. We specify the attitude of the system $Oy_1y_2y_3$ with respect to the system $EY_1Y_2Y_3$ by the quaternion $Q=(q_0, q_1, q_2, q_3)$, which has unit norm: $q_0^2+q_1^2+q_2^2+q_3^2=1$. We designate the transition matrix from the coordinate system $Oy_1y_2y_3$ to the system $EY_1Y_2Y_3$ as $\|a_{ij}\|_{i,j=1}^3$, where a_{ij} is the cosine of the angle between the axes EY_i and Oy_j. The elements of this matrix are expressed in terms of components of Q by means of the known formulas

$$a_{11}=q_0^2+q_1^2-q_2^2-q_3^2,\quad a_{12}=2(q_1q_2-q_0q_3),\quad a_{21}=2(q_1q_2+q_0q_3),\ldots$$

Below, the components of vectors and the coordinates of points are referred to the system $Oy_1y_2y_3$.

Telemetry information is covers a time interval of the length about an orbital period and contains the sequence of instants and quaternions

$$t_k,\quad Q_k=\left(q_0^{(k)}, q_1^{(k)}, q_2^{(k)}, q_3^{(k)}\right)\quad (k=0,1,\ldots,N). \tag{2}$$

Here, $t_0<t_1<\ldots<t_N$, Q_k is the quaternion Q calculated for the instant t_k. As a rule, $t_{k+1}-t_k=1-1.5$ min, $N<100$. The quaternion specifying the station attitude is defined within its sign. The signs of Q_k and the instant t_0 in (2) are chosen from the conditions

$$q_0^{(0)}>0,\quad \sum_{i=0}^{3} q_i^{(k-1)}q_i^{(k)}>0\quad (k=1,2,\ldots,N).$$

We have two ways for smoothing sequence (2). In *the first way,* smoothing is fulfilled componentwise basing on the solution of the following problem. Let the approximate values $x_k\approx f(t_k)$ of some smooth function $f(t)$ be known at the points t_k $(k=0,1,2,\ldots,N)$, $t_k<t_{k+1}$. It is required to reconstruct this function in the segment $t_0\le t\le t_N$.

The determination of $f(t)$ assuming that this function is twice continuously differentiable is reduced in [5] to the solution of the variational problem

$$\int_{t_0}^{t_N} [d^2 f(t)/dt^2]^2 dt \to \min , \qquad \sum_{k=0}^{N} [x_k - f(t_k)]^2 \le S . \qquad (3)$$

Here, S is prescribed positive number. The solution to problem (3) is a cubic spline. In [5], an Algol-60 code is given for calculating the coefficients of this spline from the values of S, t_k, x_k $(k = 0,1,2,...,N)$. We use that code rewritten in Turbo Pascal.

The norm of a quaternion function generated by the splines, which smooth the components of quaternions (2) is no longer equal to unity, but insignificantly differs from it. This quaternion function is normed to unity and used for describing rotation of the system $Oy_1y_2y_3$ with respect to the system $EY_1Y_2Y_3$ in the segment $t_0 \le t \le t_N$. The projections of the absolute angular rate $\boldsymbol{\omega}$ of the system $Oy_1y_2y_3$ onto its own axes are determined using the derivative of this function and the kinematic equations

$$\omega_1 = 2\left(q_0 \frac{dq_1}{dt} - q_1 \frac{dq_0}{dt} + q_3 \frac{dq_2}{dt} - q_2 \frac{dq_3}{dt} \right),$$
$$\omega_2 = 2\left(q_0 \frac{dq_2}{dt} - q_2 \frac{dq_0}{dt} + q_1 \frac{dq_3}{dt} - q_3 \frac{dq_1}{dt} \right),$$
$$\omega_3 = 2\left(q_0 \frac{dq_3}{dt} - q_3 \frac{dq_0}{dt} + q_2 \frac{dq_1}{dt} - q_1 \frac{dq_2}{dt} \right).$$

We determine $d\omega_i / dt$ $(i = 1,2,3)$ by differentiation of these equations with respect to time and substitution of the first and second derivatives of the normed quaternion function into deduced expressions. Now, everything is ready for calculating the residual acceleration on formula (1).

The second way of smoothing sequence (2), as well as the first one, consists in solving the variational problem. But now, the problem has clear kinematic sense. We write kinematic equations of the station attitude motion in the form

$$2\frac{dq_0}{dt} + \omega_1 q_1 + \omega_2 q_2 + \omega_3 q_3 = 0 , \quad 2\frac{dq_1}{dt} + \omega_2 q_3 - \omega_3 q_2 - \omega_1 q_0 = 0 ,$$
$$2\frac{dq_2}{dt} + \omega_3 q_1 - \omega_1 q_3 - \omega_2 q_0 = 0 , \quad 2\frac{dq_3}{dt} + \omega_1 q_2 - \omega_2 q_1 - \omega_3 q_0 = 0 , \qquad (4)$$
$$\frac{d\omega_1}{dt} = u_1 , \quad \frac{d\omega_2}{dt} = u_2 , \quad \frac{d\omega_3}{dt} = u_3 .$$

Here, the angular accelerations u_i are unknown functions of time. They have to be determined on the segment $t_0 \le t \le t_N$ to minimize the functional

$$J = \Phi + \frac{\lambda}{2} \int_{t_0}^{t_N} [u_1^2(t) + u_2^2(t) + u_3^2(t)]^2 dt , \qquad \Phi = \sum_{k=0}^{N} \sum_{i=0}^{4} [q_i^{(k)} - q_i(t_k)]^2 . \qquad (5)$$

Here, λ is a positive parameter.

Functional (5) has the following sense. For the quaternion function $Q(t)$, which satisfies equations (6) and smoothes data (2), the relations $Q(t_k) \approx Q_k$ $(k = 0,1,2,...,N)$ take place. The locations of the stations specified by the quaternions $Q(t_k)$ and Q_k are close, therefore it may be assumed that the location Q_k is generated from the location $Q(t_k)$ by an infinitesimal rotation with the vector $\grave{\mathbf{e}}_k = \left(\theta_1^{(k)}, \theta_2^{(k)}, \theta_3^{(k)}\right)$. This fact is expressed in terms of the relations

$$q_0^{(k)} \approx q_0(t_k) - \frac{1}{2}\left[q_1(t_k)\theta_1^{(k)} + q_2(t_k)\theta_2^{(k)} + q_3(t_k)\theta_3^{(k)}\right],$$

$$q_1^{(k)} \approx q_1(t_k) + \frac{1}{2}\left[q_2(t_k)\theta_3^{(k)} - q_3(t_k)\theta_2^{(k)} + q_0(t_k)\theta_1^{(k)}\right],$$

$$q_2^{(k)} \approx q_2(t_k) + \frac{1}{2}\left[q_3(t_k)\theta_1^{(k)} - q_1(t_k)\theta_3^{(k)} + q_0(t_k)\theta_2^{(k)}\right],$$

$$q_3^{(k)} \approx q_3(t_k) + \frac{1}{2}\left[q_1(t_k)\theta_2^{(k)} - q_2(t_k)\theta_1^{(k)} + q_0(t_k)\theta_3^{(k)}\right],$$

by means of which Φ in (5) can be transformed to the form

$$\Phi \approx \frac{1}{4}\sum_{k=0}^{N} |\grave{\mathbf{e}}_k|^2 .$$

Hence, Φ characterizes the proximity of the calculated and actual motions of the station. The last formula also substantiates the first way considered above.

The second term in the right-hand side of the formula for J is a penalty for large angular accelerations of the station, which can arise under exact approximation. Therefore, functional (5) is compromise. This functional is similar to the functional, which appears in solving isoperimetric variational problem (3) by the method of Lagrange multipliers [5]. In [5], the Lagrange multiplier, similar to λ in (5), is chosen to satisfy the second (isoperimetric) condition (3). In numerical solving the new variational problem, λ is a variable parameter. We decrease it while Φ decreases [1]. The solution of the problem, corresponding to the minimal value of Φ, is considered to be an approximation of the station actual motion.

Fig. 1 – 4 present examples of the reconstruction of the station attitude motion by data (2) and calculation, basing on the reconstruction, the quasi-steady component in the residual acceleration. The right-hand plots in fig. 1, 3 illustrate smoothing the telemetry data (they are designated by marks) by solutions of equations (4) (solid lines) in the framework of the second way; the left-hand plots present the quasi-steady acceleration component $\mathbf{n} = (n_1, n_2, n_3)$ at the point $P =$ (5 m, 2 m, 0). Some details of the reconstructed attitude motion are shown in fig. 2, 4. Here, the left-hand plots present Krylov's angles which specify attitude of the system $Oy_1y_2y_3$ with respect to the system $EY_1Y_2Y_3$ (fig. 2) or the orbital coordinate system $OX_1X_2X_3$ (fig. 4, the axes OX_3 and OX_2 are directed along the vectors $\mathbf{R}$ and $\mathbf{R} \times d\mathbf{R}/dt$ respectively). The solid lines present the results of smoothing, the marks indicate the

results obtained from data (2). The way of the definition of the angles is not significant in this case. The ranges of variation of the angles are only important. These ranges characterize errors in maintaining the attitude of the station. The plots in the middle of the fig. 2, 4 illustrate the station angular rates. Here, the solid lines present solutions of equations (4), the marks indicate telemetry data. The right-hand plots in fig. 2, 4 present the station angular accelerations – the functions u_1, u_2, u_3 in (4), horizontal lines indicate zero.

Figures illustrate the motions of the station when the gyrodines maintained its invariable attitude with respect to the absolute space (fig. 1, 2) or the orbital coordinate system (fig. 2, 4). There were sufficiently soft motions – the attitude control jets were not turned on during them. We give the example of another situation for comparison.

Fig. 5, 6 illustrate maintaining the invariable attitude of the station in the absolute space by the control jets. These figures are analogous to fig. 1 – 4, but they obtained in the first way, and the orientation of the system $Oy_1y_2y_3$ with respect to the system $EY_1Y_2Y_3$ is specified by another angles. Peaks on the plots of residual accelerations became more sharp (fig. 5), but the acceleration level did not change in large. Fig. 7 shows the results of reconstruction of the station attitude motion by the same telemetry information using the dynamical model. The plots in fig. 7 are analogous to the plots in the right-hand and middle parts of fig. 6. Comparing the analogous plots, we see worse accuracy of data approximation in the case when the dynamical model was used. The errors are not so large as it seems at first sight. They do not exceed a few tens of a degree. Besides, we have to take into account the following case. In the first way, the total error of data approximation is characterized by parameter S in (3). Its value can be taken arbitrary and we took $S = 0$ when fig. 5, 6 were drawn.

The main distinction in fig. 6 and 7 consists in the plots of angular rates. The vertical segments on those plots in fig. 7 are instantaneous jumps of the angular rates caused by operation of the control jets. In the dynamical model, this operation is simulated as a sequence of shocks, so infinitely large angular accelerations (like delta-functions) correspond to those jumps in the angular rates. In fact, the station undergoes finite but very large disturbances when the control jets operate. The absolute values of the angular accelerations can reach then about 0.0006 s^{-2}. If we would calculate more exactly, then we obtain peaks on the acceleration plots in 500 – 1000 times greater than we have in fig. 5. When we apply the techniques above to data (2) at hand, we spread shocks with duration about 0.1 s over time intervals of about 1.5 min. As a result, peaks on the plots of residual and angular accelerations decrease.

We made one more error when calculated accelerations in fig. 5. The control jets operate by bundles and some bundles are not balanced. They do not produce a net torque (a force couples) but both a torque and a force. Such forces have a shock

character and can modify peaks above. This drawback cannot be eliminated in the ways above but it only alters the previous error.

The last example demonstrates obstacles in determination of residual accelerations by indirect information. It shows insufficiency of the techniques [1] for determination of residual accelerations in considered situation. Such motions have to be treated in the framework of more complicated models, which are developed now. On the other hand, we cannot consider residual accelerations obtained during such motions as quasi-steady ones (see discussion of this problem in [1]).

2. Measurements of vibrational residual accelerations by means of accelerometers IMU-128

A vibrational component of residual accelerations in Russian segment of ISS were measured by means of three-axis accelerometers IMU-128. A single-axis sensor of this accelerometer is a pendulum in an electromagnetic suspension. There are five such accelerometers in FGB and five in SM. The basic characteristics of this device are as follows

Amplitude range of measured accelerations – $0.01 - 0.0001$ m/s^2 ,
Frequency range of measured accelerations – $0.01 - 20$ Hz,
Sensitivity threshold – 0.00002 m/s^2 ,
Sample rate – 50 readings/s .

To increase measurement accuracy in the region of small amplitudes, the measurements of each single-axis sensor transmitted on two telemetry channels. One of them (rough) is used for transmission of data in the full range of amplitudes up to 0.01 m/s^2 , the other (fine) is used for transmission of data in the range of amplitudes which are not more than 0.001 m/s^2 . The fine channels did not operate for all accelerometers because of zero drifts. The rough channels operated for 4 single-axis sensors of different accelerometers in FGB and for 4 such sensors in SM.

The obtained data make up the segments of time series with the length of a few minutes. The analysis of the data consisted in solving two problems: 1) the search for cyclic trends, 2) estimating the spectral density of the residue series which was obtained by eliminating significant cyclic trends from the original series. Below we describe the methods for solving these problems. More detailed description of these methods one can find in [6 – 8].

Finding cyclic trends and estimating spectral density of residue series. Such study was carried out only for such segments of data series which, judging from their plots, can be considered stationary. According to the mechanical nature of the selected data, these segments have to contain only cyclic trends, i.e. the trends expressed as linear combinations of several harmonics with incommensurable, in general case, frequencies.

Cyclic trends cause jumps in the spectral function of a series. If such trends are eliminated, the spectral function of the residue series can be considered to be

absolutely continuos, and instead of this function on can consider its derivative, the spectral density. The search for cyclic trends was carried out using the analysis of the periodogram of a series [6,7].

Let $N = 2N_1$ be a natural even number, n_k $(k = 0,1,...,N-1)$ are measurement data of any component of acceleration obtained at the instants $t_k = t_0 + kh$, $h > 0$. The function $I(f)$, considered on the segment $0 \le f \le F$, $F = 1/2h$ and defined by relations

$$I(f) = \frac{1}{N}\left|\sum_{k=0}^{N-1}(n_k - \bar{n})\exp\left(-\frac{\pi k f}{F}\sqrt{-1}\right)\right|^2, \qquad \bar{n} = \frac{1}{N}\sum_{k=0}^{N-1} n_k ,$$

is called a periodogram. Here, f is the trial frequency and F is the Nyquist frequency. If instants t_k are expressed in seconds, f and F are measured in hertzes. In our case, $h = 0.02$ s and $F = 25$ Hz.

Let the segment of series under investigation contain a cyclic trend $n = \alpha_0 + \alpha\cos 2\pi\nu t + \beta\sin 2\pi\nu t$, where α_0, α, β, ν are parameters and $0 < \nu < F$. Then $\bar{n} \approx \alpha_0$, the periodogram has a maximum at the point $f = \lambda \approx \nu$ and $\alpha^2 + \beta^2 \approx 4I(\lambda)/N$. In the general case, the accuracy of written approximate relations increases with increasing N. Thus, the search for cyclic trends is reduced to the search for maxima of $I(f)$.

The periodogram is usually a sawtooth function with a lot of local maxima. Distances between its neighboring maxima are $\Delta f \approx 1/Nh$. Searching for cyclic trends, one should choose only significant maxima of the periodogram, which essentially exceed mean level of its maxima. In order to search for significant maxima, we applied the Schuster criterion [6,7]. The rule of its application consists in the following. The measurement data are subjected to the discrete Fourier transform

$$Y_m = \frac{1}{N}\sum_{k=0}^{N-1} n_k \exp\left(-\frac{2\pi k m}{N}\sqrt{-1}\right) \qquad (m = 0,1,...,N-1) .$$

The relations take place (recall that $N = 2N_1$)

$$I(f_m) = N|Y_m|^2, \quad f_m = \frac{mF}{N_1} \quad (m = 1,2,...,N_1 - 1) .$$

They allow one to reduce a search for significant maxima of the periodogram to a study of the quantities $|Y_m|^2$. Namely, local maxima of the sequence $y_m = |Y_m|^2$ $(m = 1,2,...,N_1 - 1)$ are found, i. e., the elements y_k, satisfying the inequalities $y_{k-1} < y_k$, $y_k \ge y_{k+1}$. The local maximum y_k is considered significant, if

$$\frac{(N-2)y_k}{2\sum_{m=1}^{N_1-1} y_m} > \ln\frac{N-2}{2q},$$

where q is the probability of making error which is admissible for a researcher. In our work we took $q = 0.02$. The last inequality represents an asymptotics of the Schuster criterion at $N >> 1$, $q << 1$. The estimate of a frequency of the cyclic trend, corresponding to the significant local maximum y_k, was calculated by the formula

$$\lambda = \frac{F}{N}\left(2k + \frac{y_{k+1} - y_{k-1}}{2y_k - y_{k+1} - y_k}\right).$$

This formula defines the abscissa of the vertex of a quadratic parabola, which passes through the points (f_{k-1}, y_{k-1}), (f_k, y_k) and (f_{k+1}, y_{k+1}). Then, the found estimate was refined in constructing the best, in the sense of the least squares method, approximation of the measurement data by the expression $n = \alpha_0 + \alpha\cos 2\pi\nu t + \beta\sin 2\pi\nu t$. The parameters λ, α_0, α and β were found by the Gauss-Newton method – the problem is nonlinear in λ.

When the frequencies λ_k $(k = 1,2,...,M; M << N)$ were determined by the technique above, the trend, corresponding to them, was searched for in the form

$$n = \alpha_0 + \sum_{k=1}^{M}(\cos 2\pi\lambda_k t + \sin 2\pi\lambda_k t). \qquad (6)$$

The parameters $\alpha_0, \alpha_k, \beta_k$ $(k = 1,2,...,M)$ were determined by the least squares method from the condition of the best approximation of the data by expression (6).

After eliminating cyclic trends from the data, we carried out the spectral analysis of the series of residues. This series can be considered as a series with continuos spectrum, and its spectral density is to be estimated. To obtain an estimate of this spectral density we used discrete Fourier transform. Let the sequences x_k and X_k $(k = 0,1,...,N-1)$ represent a residue series and its discrete Fourier transform, respectively. The following relation (Parseval equality) is valid

$$\sum_{k=0}^{N-1} x_k^2 = N\sum_{m=0}^{N-1} |X_m|^2 .$$

The periodogram of the residue series at points f_m is equal to $N|X_m|^2$, and the quantities $N|X_m|^2 / F$ $(m = 1,2,...,N_1 - 1)$ could be considered as estimates for values of the spectral density at those points. However, these estimates are inconsistent. In order to obtain a consistent estimate of the spectral density, it is necessary to divide the segment $0 \le f \le F$ in several subsegments and to perform averaging of the above quantities over them. The found average quantities can be used for approximate estimates of the spectral density on corresponding subsegments. As a result, the spectral density is estimated by a piecewise constant function. Namely, let the natural number L be a divisor of the number N_1 : $N_1 = KL$. We divided the segment $0 \le f \le F$ in K subsegments with identical length, and on the

subsegment $Fl/K < f < F(l+1)/K \quad (l = 0,1,...,K-1)$ we estimated the spectral density $p(f)$ of the residue series by the constant

$$p_l = \frac{1}{L} \sum_{m=Ll}^{L(l+1)-1} |X_m|^2 .$$

By virtue of the Parseval equality, the found estimate $\hat{p}(f)$ of the spectral density satisfies the relation

$$\frac{1}{N} \sum_{k=0}^{N-1} x_k^2 = \frac{F}{K} \sum_{l=0}^{K-1} p_l = \int_0^F \hat{p}(f)\, df .$$

To improve this estimate by decreasing leakage, we made the following transformations. First, before calculating the discrete Fourier transform, the terms of the residue series were multiplied by values of a window function: $w_k x_k \to x_k$ $(k = 0,1,...,N-1)$. Then, to compensate a loss of signal power occurring in this case, the right hand side of the formula determining p_l is divided by

$$\frac{1}{N} \sum_{k=0}^{N-1} w_k^2 .$$

We used the Hann window function [6 – 8]

$$w_k = \frac{1}{2}\left[1 + \cos\frac{\pi(N-k)}{N}\right].$$

The plots of the spectral density estimate $\hat{p}(f)$ give no pictorial presentation of the frequency distribution of amplitudes of residual accelerations. Instead of these plots, the plots of the function $\hat{A}(f) = \sqrt{F\hat{p}(f)/N}$ were constructed. The function $\hat{A}(f)$ is also piecewise constant. Its value on each segment of constancy represents the root mean square (on this segment of frequencies) amplitude of oscillations with continuous spectrum.

Measurements of residual accelerations in FGB along the axis Oy_1 and their amplitude spectra are presented in fig. 8, 9. Here, the top panels contain the plots of measurement data. The plots are broken lines, whose vertexes have ordinates equal to measurement data (with eliminated mean values) and abscissas formed a uniform grid with the step of 0.02 s. The second from above plots present the function $A(f) = \sqrt{4I(f)/N}$. These plots were constructed at $N = 2048$ for the data whose initial segments are presented in the tops of the figures. The plots of $A(f)$ are also broken lines with vertexes at the points $f = f_m$, $A(f_m) = 2\sqrt{y_m}$ $(m = 1,2,...,N_1)$. The use of the function $A(f)$ instead of $I(f)$ is convenient because of the values of $A(f)$ at its significant maxima are the estimates of amplitudes of cyclic trends. A drawback of the function $A(f)$ is that its significant maxima are less pronounced than significant maxima of the periodogram.

The analysis of those maxima and subsequent search for cyclic trends by the least squares method led to the following frequencies λ_k (in Hz) and amplitudes $A_k = \sqrt{\alpha_k^2 + \beta_k^2}$ (in 0.001 m/s^2): $\lambda_1 = 0.09$, $A_1 = 4.9$, $\lambda_2 = 9.03$, $A_2 = 1.1$, $\lambda_3 = 12.03$, $A_3 = 0.8$, $\lambda_4 = 12.22$, $A_4 = 1.2$ in the case of data presented in fig. 8; $\lambda_1 = 0.30$, $A_1 = 6.0$, $\lambda_2 = 8.48$, $A_2 = 0.9$, $\lambda_3 = 11.82$, $A_3 = 0.8$, $\lambda_4 = 12.42$, $A_4 = 1.4$ in the case of data presented in fig. 9. Both trends with the frequencies λ_1 could be caused by elastic oscillations of the station body or crew activities. The other trends were caused by operation of on board systems.

The third (central) plots in fig. 8, 9 illustrate the residue series obtained after elimination of cyclic trends from the data segment presented on the corresponding top plots. The fourth plots in the figures are plots of the function $A(f)$ for the residue series. These plots are also constructed for $N = 2048$. The fifth (bottom) plots present the function $\hat{A}(f)$ connected with an estimate of the spectral density of the residue series. The last plots were constructed at $L = 16$.

As one can see from fig. 8, the periodogram has maxima near the frequency $f \approx 25$ Hz. The accelerometer IMU-128 has the resonance at this frequency, and its amplitude characteristic differs from unity essentially when $f > 20$ Hz. We eliminated the cyclic trend with that frequency from original data, but it has no sense in the analysis of the microgravity environment on ISS.

Measurements of residual accelerations in SM along the axes Oy_1, Oy_2, Oy_3 and their amplitude spectra are presented in fig. 10 – 12. These figures are analogous to fig. 8, 9 and they were constructed in exactly that manner. The measurements were carried out when the compressor of the SM system for the moisture condensation and some other systems were turned off. So, the rather soft results were obtained. The frequencies and the amplitudes of the cyclic trends in these data are: $\lambda_1 = 0.16$, $A_1 = 0.38$, $\lambda_2 = 0.28$, $A_2 = 0.37$, $\lambda_3 = 0.44$, $A_3 = 0.35$ in the case of data presented in fig. 10; $\lambda_1 = 0.16$, $A_1 = 0.40$, $\lambda_2 = 1.06$, $A_2 = 0.24$, $\lambda_3 = 2.31$, $A_3 = 0.29$ in the case of data presented in fig. 11; $\lambda_1 = 0.08$, $A_1 = 0.35$, $\lambda_2 = 0.42$, $A_2 = 0.36$, $\lambda_3 = 0.63$, $A_3 = 0.53$ in the case of data presented in fig. 12. Here, we use the same units of measurements for λ_k and A_k as in the case above. The found trends are insignificant. Their elimination did not influence on the spectrum of data (compare the plots of the functions $A(f)$ and $A'(f)$ in figures). That is the residual accelerations in SM had a continuous spectrum that time. The accelerations with such a spectrum could be caused by elastic oscillations of the station body and crew activities.

References

1. V.V. Sazonov, my. Belyaev, N.I. Efimov, V.M. Stazhkov, E.V. Babkin. Determination of the quasistatic component of microaccelerations at the Mir station. Cosmic research, 2001, vol. 39, No. 2, pp. 126 – 136.
2. E.V. Babkin, M.Yu. Belyaev, N.I. Efimov, V.V. Sazonov, V.M. Stazhkov. Uncontrollable rotational motion of the Mir orbital station. Cosmic research, 2001, vol. 39, No. 1, pp. 23 – 37.
3. V.V. Sazonov, M.M. Komarov, V.I. Polezhaev, S.A. Nikitin, M.K. Ermakov, V.M. Stazhkov, S.G. Zykov, S.B. Ryabukha, J. Acevedo, E. Liberman. Microaccelerations onboard the Mir orbital station and prompt analysis of gravitational sensitivity of convective processes of heat and mass transfer. Cosmic research, 1999, vol. 37, No. 1, pp. 80 – 94.
4. GOST (State Standart) 22721-77: Models of the upper atmosphere for ballistic calculations, 1977, Moscow: Izd. Standartov, 1978.
5. C.H. Reinsch. Smoothing by spline functions. Numerische mathematik, 1975, B. 24, No. 5, S. 383-393.
6. E.J. Hannan. Time series analysis. London: Methuen & Co Ltd., New York: John Wiley & Sons, 1960.
1. V. Yu. Terebizh. Time series analysis in astrophysics. åoscow: Nauka, 1992.
2. R.K. Otnes, L. Enochson. Applied time series analysis. Vol. 1. Basic techniques. New York: A Wiley-Interscience Publication, John Wiley & Sons, 1978.

REPORT DOCUMENTATION PAGE

Form Approved
OMB No. 0704-0188

1. AGENCY USE ONLY (*Leave blank*)	2. REPORT DATE	3. REPORT TYPE AND DATES COVERED
	December 2001	Conference Publication

4. TITLE AND SUBTITLE

Twentieth International Microgravity Measurements Group Meeting

5. FUNDING NUMBERS

WU–398–95–0G–00

6. AUTHOR(S)

Richard DeLombard, compiler

7. PERFORMING ORGANIZATION NAME(S) AND ADDRESS(ES)

National Aeronautics and Space Administration
John H. Glenn Research Center at Lewis Field
Cleveland, Ohio 44135–3191

8. PERFORMING ORGANIZATION REPORT NUMBER

E–13023

9. SPONSORING/MONITORING AGENCY NAME(S) AND ADDRESS(ES)

National Aeronautics and Space Administration
Washington, DC 20546–0001

10. SPONSORING/MONITORING AGENCY REPORT NUMBER

NASA CP—2001-211164

11. SUPPLEMENTARY NOTES

Abstracts and viewgraphs of a conference sponsored by the Microgravity Science Division, NASA Glenn Research Center and held at the Sheraton Airport Hotel, Cleveland, Ohio, August 7–9, 2001. Responsible person, Richard DeLombard, organization code 6727, 216–433–5285.

12a. DISTRIBUTION/AVAILABILITY STATEMENT

Unclassified - Unlimited
Subject Categories: 19, 18, and 35 Distribution: Nonstandard

This publication is available from the NASA Center for AeroSpace Information, 301–621–0390.

12b. DISTRIBUTION CODE

13. ABSTRACT ***(Maximum 200 words)***

The International Microgravity Measurements Group annual meetings provide a forum for an exchange of information and ideas about various aspects of microgravity acceleration research in international microgravity research programs. These meetings are sponsored by the PI Microgravity Services (PIMS) project at the NASA Glenn Research Center. The twentieth MGMG meeting was held 7–9 August 2001 at the Hilton Garden Inn Hotel in Cleveland, Ohio. The 35 attendees represented NASA, other space agencies, universities, and commercial companies; eight of the attendees were international representatives from Canada, Germany, Italy, Japan, and Russia. Seventeen presentations were made on a variety of microgravity environment topics including the International Space Station (ISS), acceleration measurement and analysis results, science effects from microgravity accelerations, vibration isolation, free flyer satellites, ground testing, and microgravity outreach. Two working sessions were included in which a demonstration of ISS acceleration data processing and analyses were performed with audience participation. Contained within the minutes is the conference agenda which indicates each speaker, the title of their presentation, and the actual time of their presentation. The minutes also include the charts for each presentation which indicate the author's name(s) and affiliation. In some cases, a separate written report was submitted and has been included here.

14. SUBJECT TERMS

Microgravity; Instrumentation; International Space Station; Acceleration measurement

15. NUMBER OF PAGES

295

16. PRICE CODE

17. SECURITY CLASSIFICATION OF REPORT	18. SECURITY CLASSIFICATION OF THIS PAGE	19. SECURITY CLASSIFICATION OF ABSTRACT	20. LIMITATION OF ABSTRACT
Unclassified	Unclassified	Unclassified	